

ROLE OF UHRF1 AND HISTONE H3 UBIQUITINATION IN CHROMATIN RE-ESTABLISHMENT DURING DNA REPLICATION

by

CYNTIA FERNANDEZ CUESTA

A thesis submitted to the University of Birmingham for the degree of DOCTOR OF PHILOSOPHY

Institute of Cancer and Genomic Sciences

School of Cancer Sciences

College of Medical and Dental Sciences

University of Birmingham

December 2023

UNIVERSITY OF
BIRMINGHAM

University of Birmingham Research Archive

e-theses repository

This unpublished thesis/dissertation is copyright of the author and/or third parties. The intellectual property rights of the author or third parties in respect of this work are as defined by The Copyright Designs and Patents Act 1988 or as modified by any successor legislation.

Any use made of information contained in this thesis/dissertation must be in accordance with that legislation and must be properly acknowledged. Further distribution or reproduction in any format is prohibited without the permission of the copyright holder.

ABSTRACT

Chromatin re-establishment after DNA replication consists of nucleosome re-assembly and restoration of epigenetics marks in both daughter strands. These marks comprise DNA methylation and post-translational modifications of histones that regulate chromatin conformation and gene expression. Unrepaired errors during these processes result in genomic instability that leads to diseases such as cancer.

The E3 ubiquitin ligase Uhrf1 is an epigenetic regulator considered an oncogene for its ability to promote cell proliferation. This protein mediates DNA methylation maintenance by ubiquitinating histone H3 and Paf15 and subsequently recruiting DNA methyl transferase Dnmt1 to hemi-methylated sites. Although the role of Uhrf1 in recruiting Dnmt1 is clear, there are still many unresolved questions about the mechanism itself and how it is coordinated with other processes taking place at the same time, such as chromatin assembly and remodelling. This PhD project focuses on understanding the roles of Uhrf1 and histone H3 ubiquitination in DNA methylation maintenance and chromatin re-establishment during DNA replication.

Using *Xenopus laevis* egg extract as a model system, I have confirmed the role of Uhrf1 in mediating the dual mono-ubiquitination of histone H3 and Paf15 and recruiting Dnmt1 through ubiquitination. Importantly, this study has revealed that Uhrf1 also recruits Lig1 to replicating chromatin and its absence impairs the binding of Fen1 and CAF1. Finally, I have identified novel interacting partners of Uhrf1 during DNA replication. All these findings suggest that Uhrf1 plays a central and multifaceted role in chromatin-re-establishment, coordinating DNA methylation with DNA replication and nucleosome assembly.

DEDICATION

To my family, for their endless love, support and joy of living…

Specially to my grandmother, Lola, for being an inspiration of hard-work, strength and love,

and to Jairo y Estrella, for showing me to view life through the eyes of a child



ACKNOWLEDGEMENTS

To begin with, my deepest gratitude goes to my supervisor, Prof Aga Gambus, for her massive support and guidance throughout the PhD journey. I am particularly thankful to her for believing in my potential and giving me the opportunity to join her lab, initially as a summer student and later as a PhD student. This has made me grow academically but also has enriched my life experiences. Her deep passion and curiosity for science, along with her unique ability to make complex and stressful situations more manageable and enjoyable, has been an inspiration for me. I will forever be grateful for all she has taught me, personally and professionally. Finally, I would like to thank her for always being there in the challenging times, particularly during the COVID pandemic when I was far from my family.

I also want to thank everyone in the lab for being extremely friendly and supportive; I could not have asked for better colleagues. Firstly, I would like to make a special mention to my friend Sara, not only because she put me in contact with Aga and brought me to the world of research, but also for her mentorship during every step of my research path and for being an example for me to follow. I am also immensely grateful to the other Spaniard Joaquin for the valuable advice and lessons that were extremely useful for my PhD. Additionally, I would like to thank Becky and Divya, with whom I have shared my journey in the Gambus lab from the beginning. Thanks for always being so nice, patient and supportive with me; it meant a lot to me, especially in the hard times. And to the rest of the members of the lab, Paolo, Nev, Georgia, Alicja, Angeliki, Abi, Shaun, Zeynep, Sharmi, Chongluan and Chaoyu, for making the days much funnier and for creating the perfect work environment and team. It has been a privilege to work alongside such friendly and talented people.

From the institute, I would like to say a special thanks to Cristina and Martina. You both have been like family to me. All the deep conversations with Cristina during the lunch breaks were really helpful in disconnecting from work and made me feel always supported. Out from work, she has also shown me the meaning of an unconditional friendship. I am also immensely thankful for sharing the PhD experience with my friend Martina. Her warm and funny personality brought light to my days and made me feel at home.

Out from the work environment, I want to thank all the special people I met in Birmingham, for making my years abroad much funnier and easier. Firstly, I would like to thank Valter for being the best "compagno di viaggio" I could have asked for. His endless support gave me strength in the most difficult time of the PhD and during the writing period. I would also like to give a special mention to Asier. We met during the MIBTP training and shared our PhD journey together. Thank you for always being there, ready for a beer, a hug or a joke, and being a warm refuge in the cold UK. Finally, I want to express my gratitude to Tom and everyone from the "yellow submarine" group. You have been such good friends that I will feel forever lucky and thankful for all the experiences we have had together in Birmingham.

Finalmente, me gustaría agradecer a mi familia por estar siempre presente desde la distancia y porque sin ellos no hubiera llegado hasta aquí. Gracias a mis padres, por empujarme a creer en mi y a luchar por mis sueños. Siempre os estaré agradecida por todo el apoyo moral y económico. A mis hermanos, por estar ahí en todo momento para hacerme disfrutar de la vida y olvidar las preocupaciones del trabajo. Gracias al resto de mi familia, en especial mis tías, por confiar siempre en mi y hacerme llegar vuestro amor y apoyo, incluso estando lejos. Sin todos vosotros esta tesis doctoral no hubiera sido possible.

TABLE OF CONTENTS

1. INTRODUCTION……..……..…….……..……..…..1

1.1. Eukaryotic DNA replication overview…….……...……..……..…1

1.1.1. Initiation…….3

1.1.2. Elongation……..……..…..…..…..4

1.1.2.1. Okazaki fragment maturation……...…..…….…….....….6

1.1.3. Termination……..……..……..…..….9

1.2. Chromatin replication……...…….……..…11

1.2.1. Chromatin as carrier of epigenetic information……..…..…….……11

1.2.2. DNA replication-coupled nucleosome assembly…...……..…….……...15

1.2.2.1. Parental histone recycling…...……..…….……....15

1.2.2.2. New histones supply……...……..…….……....18

1.2.3. Epigenome maintenance…...……...……....23

1.2.3.1. Nucleosome positioning…...……..…….…….....23

1.2.3.2. Histone PTMs maintenance…...……..……..……....23

1.2.3.3. Restoration of the DNA methylation pattern.…….……...26

1.3. DNA methylation maintenance.……..……...……..…27

1.3.1. DNA methylation importance……...……..…..……..…27

1.3.2. Mechanism of DNA methylation maintenance……...…...……..……..…29

1.3.3. DNA methylation in the context of chromatin replication.....……..……...…31

1.3.4. Kinetics of the restoration of the methylation pattern……..…..….33

1.4. E3 ligase Uhrf1……..……...……..……..……..35

1.4.1. Structure and enzymatic activity……...……..…..……35

1.4.2. Conformational regulation of Uhrf1…….....……..…..……38

1.4.3. Role of Uhrf1 in DNA methylation maintenance....……..…..….39

1.4.3.1. Interaction between Dnmt1 and Uhrf1……..……....….40

1.4.3.2. Uhrf1 mediated histone H3 ubiquitination as a platform for Dnmt1 recruitment……..…..…..41

1.4.3.3. Uhrf1 mediated Paf15 ubiquitination as a platform for Dnmt1 recruitment……...……..42

1.4.3.4. Uhrf1 recruitment to chromatin……..…..44

1.4.3.5. Other factors involved in DNA methylation maintenance……...……..…...45

1.4.4. Other roles of Uhrf1 in DNA replication: translesion DNA synthesis……...47

1.4.5. Role of Uhrf1 in DNA damage response…….……47

1.4.6. Role of Uhrf1 in gene expression……49
1.4.7. Importance of studying Uhrf1: role as a tumour promoter……50
1.4.7.1. Uhrf1 promotes cell proliferation……50
1.4.7.2. Other roles of Uhrf1 in tumorigenesis ……51
1.4.8. Regulation of Uhrf1 levels……52
1.5. *Xenopus laevis* egg extract as a model system……54
1.6. Aims……55
2. MATERIALS AND METHODS……57
2.1. Tables……57
2.2. Working with mouse sperm……60
2.2.1. Preparation of mouse sperm nuclei……61
2.3. Working with *Xenopus laevis* egg extract……61
2.3.1. Preparation of metaphase II arrested *Xenopus laevis* egg extract……61
2.3.2. Use of *Xenopus laevis* egg extract……63
2.3.3. Activation of *Xenopus leavis* egg extract……63
2.3.4. Chromatin Isolation……63
2.3.5. TCA assay……64
2.3.6. Testing nuclear assembly under the microscope……66
2.3.7. Protein release from replicating chromatin ……67
2.3.8. Small-scale immunoprecipitation (IP) from extract (Uhrf1, Dnmt1, Lig1, Fen1, Paf15 and RPA) ……68
2.3.9. Pull-down of GST-Uhrf1 from Xenopus egg extract……69
2.3.10. Coupling antibodies to beads……70
2.3.11. Small-scale Immunoprecipitation (IP) from chromatin (Uhrf1 and RPA)……73
2.3.12. Large-scale IP of Uhrf1 for mass spectrometry analysis……75
2.3.13. Immunodepletion of Uhrf1, Lig1 and Paf15……76
2.4. *In vitro* Assays……77
2.4.1. In vitro Ubiquitination Assay……77
2.5. Working with DNA……78
2.5.1. Polymerase chain reaction (PCR) of xUhrf1 to prepare it for cloning……78
2.5.2. Cloning of Uhrf1……78
2.5.3. Cloning of Dnmt1……79
2.5.4. Agarose gel electrophoresis……80
2.6. Working with bacteria……81
2.6.1. Transformation……81

2.6.2. Plasmid purification……..……..……81
2.6.3. Testing expression of recombinant proteins…….....…81
2.6.4. Testing solubility……..…….……...82
2.6.5. Protein expression and purification…….…83
2.6.6. Antibody purification……...……...88
2.7. General procedures…….……..…….……..…..…90
2.7.1. SDS-PAGE (Sodium Dodecyl Sulphate Poly Acrylamide Gel Electrophoresis).90
2.7.2. Coomassie staining……..…..…….…….90
2.7.3. Western blotting or immunoblotting…….…..……..…90
2.7.4. Preparation of gels for mass spectrometry (MS) ……..…91
2.7.5. Bradford Assay……...…….…….……91
2.8. Computational analysis……..92
2.8.1. Quantifications using ImageJ…….…….…….……92
2.8.2. Alpha Fold Modelling…….…….……....93
3. RESULTS…...……...…..…….…….……..…...94
3.1. Histone H3 is di-mono-ubiquitinated during DNA replication…….…..……94
3.1.1. Introduction……..……...…….……..…..…….…...94
3.1.2. Results…….…….……...……...……...…..……....97
3.1.2.1. Histone H3 ubiquitination characterization……...……97
3.1.2.2. Recombinant histone H3 recapitulates endogenous histone H3 ubiquitination…….……..……99
3.1.2.3. The impairment of histone H3 ubiquitination by using histone H3 mutant does not affect Dnmt1 recruitment…….…….…….……..101
3.1.2.4. Using mouse sperm to incorporate rH3 wild type and mutants more efficiently…….……...……..105
3.1.3. Discussion…….……..……...……....…….……113
3.2. Uhrf1 as the E3 ubiquitin ligase responsible of histone H3 ubiquitination…….…..118
3.2.1. Introduction……..…….…….……...…118
3.2.2. Results…….…….……...……...……..119
3.2.2.1. Uhrf1 immunodepletion inhibits histone H3 ubiquitination and Dnmt1 recruitment…….…….…...119
3.2.2.2. The removal of Uhrf1 also impaired Lig1, Fen1 and CAF1 recruitment……..…124
3.2.2.3. Uhrf1 mediates histone H3 ubiquitination and Dnmt1 and Lig1 recruitment... ……131
3.2.2.4. Lig1 removal does not impair Uhrf1 recruitment……140
3.2.3. Discussion…….……...……...……...…..……142

3.3. Deciphering the mechanism of Dnmt1, Lig1, Fen1 and CAF1 recruitment through Uhrf1……..…..150

3.3.1. Introduction……..……...…….……..…..…….……...…150

3.3.2. Results…….……...……...…..……..….152

3.3.2.1. Investigating which phenotypes are regulated by Uhrf1-mediated Paf15 ubiquitination…….……...……..…152

3.3.2.2. Uhrf1 as a scaffold protein…….....158

3.3.2.3. Analysing which phenotypes are regulated by ubiquitination.……...165

3.3.3. Discussion…….……...……...…….……169

4. DISCUSSION..……..…..……..……..……..…..176

5. LIST OF ABBREVIATIONS..……..……..……..……...…..190

6. REFERENCES..……..……..……..……..……..……...….195

7. APPENDIX..……..……..……...…...……..……..……..…….....213

1. INTRODUCTION

1.1. Eukaryotic DNA replication overview

Accurate genome duplication is an essential process for cell division as it allows faithful maintenance of the genetic information through generations. DNA replication is a semiconservative process in which two daughter DNA strands are synthesised from parental templates, resulting in identical DNA molecules, each containing a new and an old strand (1,2). While the basic mechanism is evolutionarily conserved, the complexity of the replication machinery and its regulation is higher in more complex organisms with larger genomes. Due to its importance, this process must be highly regulated and coordinated with other cellular processes within the cell cycle, like DNA transcription. This ensures that all of the DNA replicates accurately during S phase and just once per cell cycle (3). Errors in DNA replication that are not efficiently repaired lead to genomic instability that causes cancer, genetic diseases and premature ageing (4,5). To avoid such DNA instability, cells have evolved multiple systems of DNA repair (6).

DNA replication initiates from DNA loci called replication origins, where replicative helicases are activated and initiate the DNA unwinding. In bacteria, only one origin of replication is formed to initiate replication of the circular chromosome. Due to the greater size of eukaryotic chromosomes, replication starts from multiple replication origins (hundreds in yeasts and tens of thousands in mammalian cells) to ensure that the entire DNA is duplicated before mitosis. These replication origins in bacteria and in budding yeast are highly conserved sequences that share consensus DNA sequence elements. However, in higher eukaryotes origins are not defined by consensus sequence elements. Instead, they are determined by some DNA and chromatin features, such as: CpG islands (explained below) and AT enriched regions,

transcription start sites, G4 motifs structures and histones' epigenetic marks and variants. These generate an open chromatin structure that enables DNA accessibility (7–9).

After origin recognition, helicase assembly and activation, two replication forks are started from each origin forming a replication bubble. Forks then move along the DNA in opposite directions replicating each strand as they go. DNA replication terminates when two forks coming from neighbouring origins meet. In general, DNA replication can be divided into three stages: initiation, elongation and termination (Figure 1). To prevent re-replication or under-replication of DNA, initiation is divided into two non-overlapping sub-stages: origin licensing and firing (10).

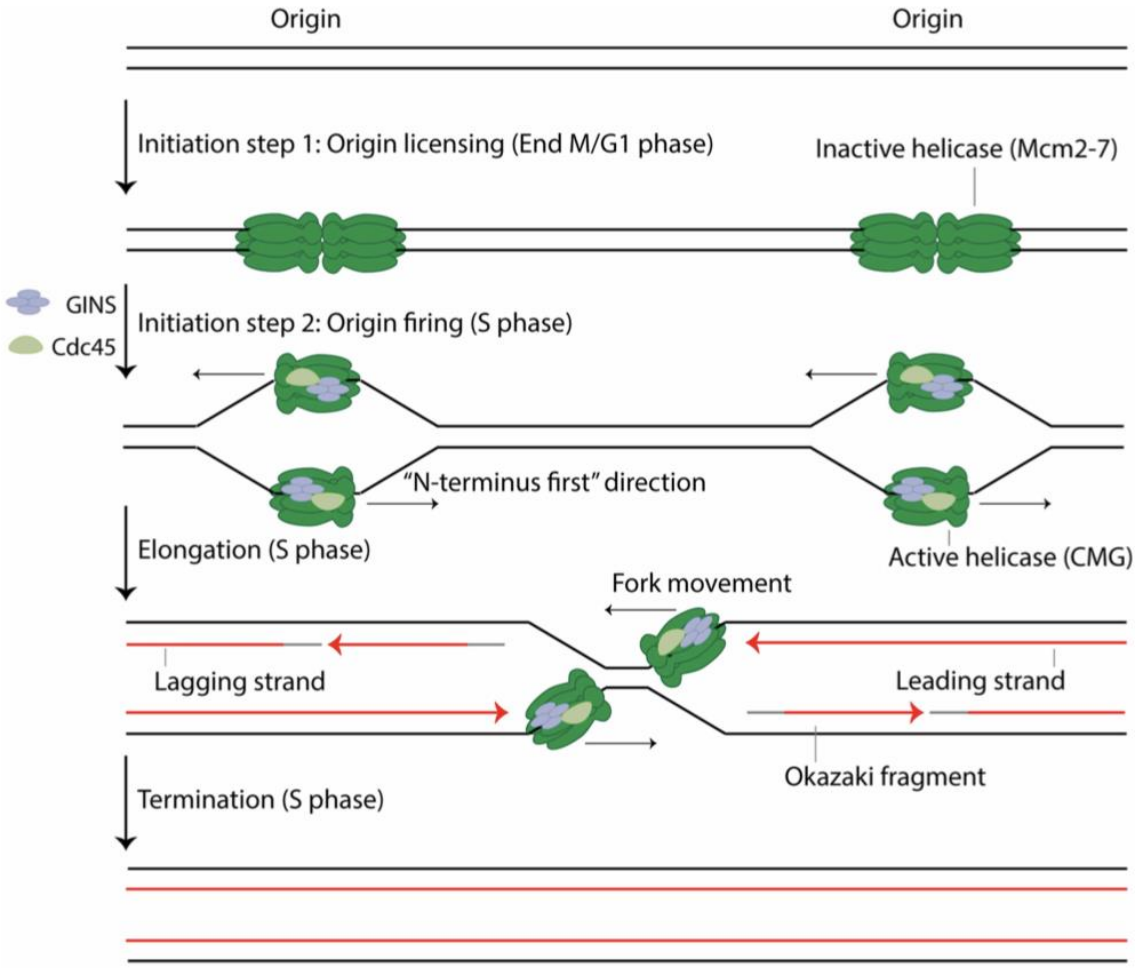


Figure 1. Model of eukaryotic DNA replication. After origin recognition, inactive Mcm2-7 helicases are loaded onto DNA, which is then activated by the recruitment of GINS and Cdc45 (CMG complex). The CMG complex unwinds the DNA and the replication machinery assembles around the helicase forming two replication forks that move along the DNA in opposite directions replicating each strand. DNA replication termination occurs when two forks coming from neighbouring origins meet (11).

1.1.1. Initiation

The first stage of DNA replication takes place in two steps occurring in different phases of the cell cycle: the loading of the helicase core in G1 phase (origin licencing), followed by its subsequent activation in S phase (origin firing).

Origin licensing: consists of the recruitment of a double hexamer of the Minichromosome Maintenance 2-7 (Mcm2-7) protein complex to each DNA origin to form a pre-replicative complex (pre-RC). This process takes place from late M phase through to G1 phase, when the decrease in the activity of Cyclin Dependent Kinases (CDKs) allows origin licensing (12). Loading of the pre-RC is mediated by the Origin Recognition Complex (ORC), which recognises the replication origin, as well as its cofactors Cdc6 and Cdt1. Mcm2-7 will remain stably bound to the DNA to form the core of the replicative helicase throughout S phase. Hundreds of thousands of Mcm2-7 hexamers are recruited onto DNA as head-to-head double hexamers, but only a subset of them (5-10% in *Xenopus laevis)* will become active. The rest will remain as "dormant origins" and will be activated only in situations of replication stress (7,13).

Origin firing: consists of the formation of two active helicases or CMG complexes. This step occurs in S phase, where S phase kinases recruit Cdc45 and GINS complex (Psf1, Psf2, Psf3 and Sld5) to the Mcm2-7 hexamer to form the CMG complex (Cdc45, Mcm2-7 and GINS), but also block Mcm2-7 re-loading by inhibition of origin licensing factors ORC, Cdc6 and Cdt1. This mechanism prevents re-replication of already duplicated DNA and ensures once-per-cell-cycle replication. However, as origin licensing is inhibited in S phase there could be a risk of under replication if replication forks became stalled. This is resolved by the overloading of Mcm2-7 complexes in M-G1 phases, to ensure full DNA replication (10,14). The process of CMG formation starts with the DDK-mediated phosphorylation of both Mcm2-7 hexamers and

subsequent recruitment of Treslin/MTBP (Sld3/Sld7 in yeast) and Cdc45. CDK-mediated phosphorylation of Sld3/Sld2 then promotes recruitment of the Donson/TopBP1/GINS/Pol ε complex (Sld2, Dpb11, GINS and DNA Polε in yeast) (15), ultimately leading to the stable association of Cdc45 and GINS with the Mcm complexes and the formation of two CMGs at each origin (16–19). After CMG assembly, the DNA is unwound, leaving each CMG helicase encircling a leading ssDNA strand, and two replication forks are established. In yeast, this step of transforming one Mcm2-7 double hexamer encircling dsDNA into two single hexamers surrounding ssDNA requires Mcm10 (20). Importantly, origins do not fire simultaneously across the genome. They are activated at different times during S phase, following a strict replication timing programme (13).

1.1.2. Elongation

After replication fork establishment, forks move in opposite directions through chromatin replicating the DNA. The active helicases move away from each other unwinding dsDNA in the 3'-5' direction using energy from the hydrolysis of ATP (21). The resulting ssDNA is then stabilised by the binding of the ssDNA binding protein RPA (Replication Protein A) (22). The helicase or CMG complex acts as the organising centre of each of these replication forks, with many regulatory proteins binding to it to carry out their functions, forming the replisome (23).

Once ssDNA is exposed, it can act as a template for DNA synthesis by DNA polymerases. DNA polymerases, however, cannot initiate DNA synthesis, they can only extend existing chains. They need therefore a primer sequence, synthesised by the eukaryotic Pol α-primase, which binds to the CMG complex through the homotrimer of Ctf4 (Chromosome transmission fidelity 4) (24). Pol α is a heterotetrameric complex that contains primase and polymerase activity. The primase subunit generates a short RNA primer (~10 nucleotides) that provides a 3'-OH end for

extension by the polymerase subunit, which adds 20-30 dNTPs. This results in an RNA-DNA hybrid primer that is elongated by the high processivity DNA polymerases Pol δ or Pol ε (25).

As the DNA molecule is an antiparallel double strand and polymerases synthesise DNA in a 5'-3' direction, DNA replication is semi-discontinuous. This means that the strand replicated in the direction of the fork, the leading strand, is synthesised continuously, while the strand replicated in the opposite direction, the lagging strand, is copied discontinuously, forming Okazaki fragments (21). Studies in yeast have supported this eukaryotic model, confirming that Pol ε replicates the leading strand and Pol δ synthesises the lagging strand (26–28). Both of these polymerases associate with a homo-trimeric eukaryotic clamp PCNA (Proliferating Cell Nuclear Antigen), which enhances their processivity, especially for Pol δ. The clamp loader RFC recruits PCNA to the primer-template junctions in an ATP-dependent manner. Once loaded, PCNA serves as a platform for many factors to interact with the replication fork (29).

The leading strand is continuously synthesised by Pol ε, which is recruited by the binding with the Psf1 subunit of GINS (30). Yeeles *et al* (2017) showed that Pol δ carries out leading strand replication in situations where this strand remains uncoupled, such as initiation of leading strand synthesis (before handing over to Pol ε) and replication stress (27). On the lagging strand, Pol δ mediates the discontinued synthesis of short DNA sequences, known as Okazaki fragments. These fragments are later processed as the RNA primers are removed and the fragments are ligated together to form the continuous lagging-strand DNA. This transformation is called Okazaki fragment maturation (OFM) and requires a highly synchronized sequence of enzymatic reactions, executed by an ensemble of polymerases, nucleases, and DNA ligases (31–33).

1.1.2.1. Okazaki fragment maturation

During lagging strand synthesis, Pol δ elongates RNA-DNA primers synthesized by Pol α until it reaches the 5'-end of the previous Okazaki fragment (Figure 2). However, upon reaching the previous Okazaki fragment, Pol δ replicates further, displacing the RNA primer (originally synthesised by Pol α) and forming a 5'-flap which is then removed by the endonuclease Fen1 (Flap endonuclease 1). This leaves a nick between Okazaki fragments that is ligated by DNA ligase I (Lig1). Sometimes, Pol δ generates a longer 5'-flap because of the binding of Pif1, which is there to prevent the formation of DNA-RNA secondary structures. This longer flap is stabilised by the binding of RPA, affecting accessibility of Fen1. In these cases, Dna2 acts to first remove RPA and then creates a shorter flap by its 5'-3' endonuclease activity allowing then the activity of Fen1 (25,34). Once Okazaki fragments are ligated, PCNA is unloaded by the activity of ATAD5-RLC (Elg1-RLC in *Saccharomyces cerevisiae*) to be recycled at the next primer-template junction (35,36).

The absence of Lig1 generates un-ligated Okazaki fragments and causes an accumulation of PCNA and Fen1 on chromatin, as these proteins require completion of OFM to be unloaded (36,37). In this situation, DNA ligase 3 (Lig3) can act to ligate the nicks and allow unloading of PCNA/Fen1 from chromatin. Kumamoto et al. (2021) showed that when Lig1 is not present, PARP1/HPF1 proteins mediate ADP-ribosylation of histone H3 which promotes the recruitment of Lig3/XRCC1 complex, acting as a backup mechanism for ligation of Okazaki fragments (37). This mechanism prevents the generation of un-ligated Okazaki fragments and incomplete DNA replication that would lead to DNA damage and cell death.

As described, efficient completion of the OFM involves the sequential and coordinated action of Pol δ, Dna2, Fen1 and Lig1, but also relies on the histone chaperone CAF1. As such, cells have evolved a mechanism to recruit these proteins to the replication site and then release them,

allowing the next enzyme in line to act. It is the interaction of these proteins with PCNA that is crucial for bringing these enzymes to the replication site (33). The trimeric structure allows PCNA to bind three ligands simultaneously, thus coordinating OFM. Post-translational modifications (PTMs) of these proteins is a key aspect that regulates this process. It is known, for example, that the binding and dissociation of Fen1 with PCNA is tightly regulated by different modifications: methylation, phosphorylation, SUMOylation and ubiquitination (38,39). Arginine methylation of Fen1 facilitates its binding with PCNA. Once Fen1 cleaves the flap, an arginine demethylase (JMJD1B) demethylates Fen1 allowing CDK1 to phosphorylate it, prompting its release from PCNA. Phosphorylated Fen1 is then subjected to SUMOylation and ubiquitination, leading to its proteosomal degradation. This detachment from PCNA and degradation make way for Lig1 to bind PCNA and seal the nicks (33). In addition, PCNA ubiquitination during S phase has been shown to promote efficient OFM and CAF1 mediated nucleosome assembly (40). These findings give a better understanding of how the process of OFM could be regulated.

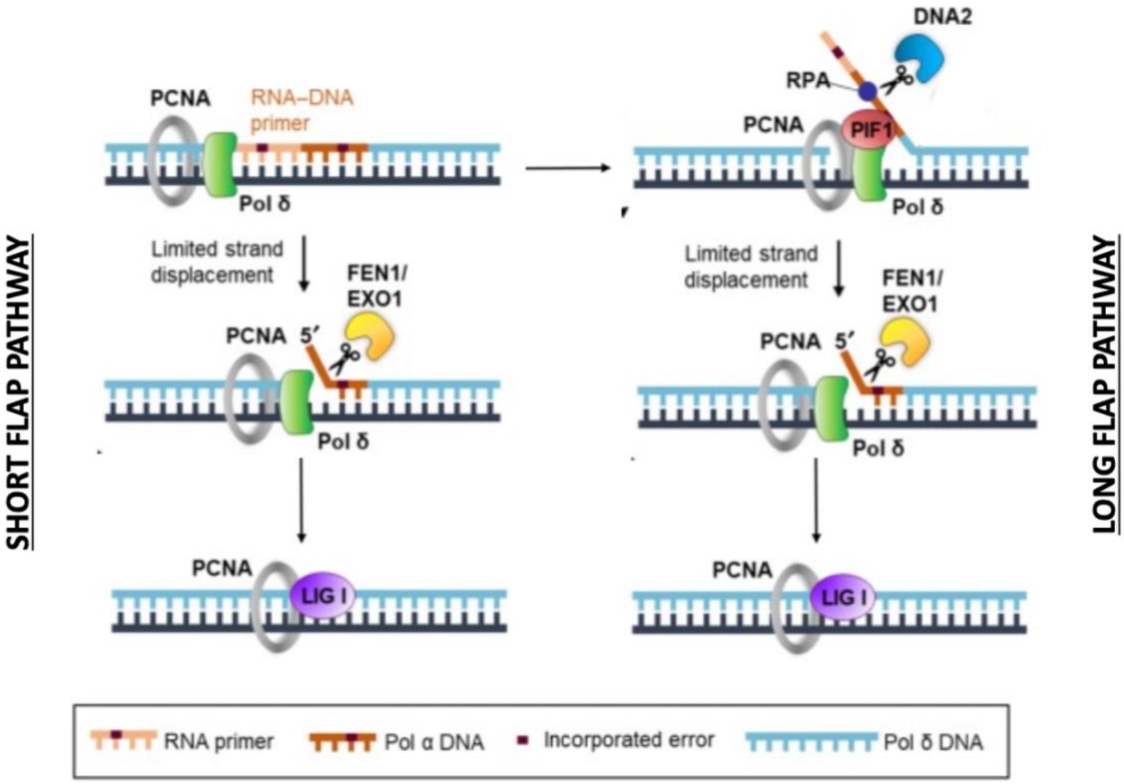


Figure 2. Okazaki fragment maturation process. On the lagging strand, Pol δ extends primers created by Pol α until it encounters the 5'-end of the preceding Okazaki fragment. When it does, Pol δ continues to replicate through the RNA primer, generating a 5'-flap. This flap is cut by Fen1, leaving a gap between Okazaki fragments. DNA ligase I (Lig1) then seals the nick. In some situations, the 5'-flap becomes longer due to the action of the Pif1 protein, which inhibits the formation of secondary structures between DNA and RNA. The binding of the RPA protein is then needed to stabilize the generation of ssDNA. This makes it more challenging for Fen1 to access the flap. In such cases, Dna2 acts to displace RPA and shorten the flap through its 5'-3' endonuclease activity. This creates a flap appropriate for the subsequent removal by Fen1. (33)

Finally, the supercoiling generated by the unwinding of the dsDNA during DNA elongation is relaxed by topoisomerase I, which cuts one strand, and topoisomerase II, which cuts both strands, allowing DNA topology maintenance (41).

1.1.3. Termination

DNA replication finishes when replication forks coming from neighbouring origins converge. This phase of replication consists of completion of DNA synthesis between the two forks, replisome disassembly and resolution of resulted DNA sister chromatids. This step of replication is relatively less well understood in comparison to initiation and elongation. However, great progress in DNA termination knowledge has been made in the last decade (11).

Replication termination takes place on average midway between two neighbouring fired origins (9). When converging forks are getting close to each other the un-replicated DNA between them accumulates supercoils, but there is not enough space for Topoisomerase I to release the torsional tension in the DNA. Instead, pre-catenanes are formed by rotation of the entire replication fork to release topological stress. When converging helicases meet, they pass each other on opposite leading strands and DNA synthesis continues until polymerases reach the downstream last Okazaki fragment of the met lagging strand. This Okazaki fragment is possibly processed by Pol δ, generating a flap which is cleaved by Fen1, and ligated, as described above (42). At this stage, the CMG helicase changes from encircling ssDNA to once-again encircling dsDNA of the last Okazaki fragment and from here, replisome disassembly occurs.

Using *Saccharomyces cerevisiae* and *Xenopus laevis* egg extract, Karim Labib's and our laboratory showed that Mcm7 polyubiquitination with K48-linked ubiquitin chains leads to helicase unloading (43,44). This ubiquitination is driven by the E3 ubiquitin ligase SCF^{Dia2} in yeast (44) and $Cul2^{LRR1}$ in *Xenopus*, *Caenorhabditis elegans* embryos and mouse embryonic stem cells (45,46). The ubiquitinated helicase disassembly is performed by the activity of the ubiquitin-selective segregase p97, also known as VCP and Cdc48, and requires the p97 cofactor Ubxn7 (47–49). It has been recently shown that this mechanism of replisome disassembly is also conserved in human cells and also requires Cullin2, LRR1 and p97 for the unloading of

the replisome (50,51). If unloading of the helicase in S phase is not successful, there is evidence of a mitotic backup pathway of replisome disassembly in worms, frogs, mice and humans that acts instead. This mitotic CMG helicase unloading still requires Mcm7 polyubiquitination but instead uses K6 and K63-linked ubiquitin chains, created by TRAIP ubiquitin ligase and the activity of p97 segregase (11,46,52). In *C. elegans*, this backup pathway also requires the p97 cofactor UBXN-3 (FAF1 in humans) and the SUMO protease UPL-4 (45). However, until recently, it was unclear how E3 ligases could distinguish between terminated and ongoing replisomes during S phase. Using cryo-electron microscopy, the structures of the replisome–E3 ligase complex was solved in yeast and humans. Strikingly, both Dia2 and LRR1 leucine reach repeat domains (LRR) attach to the same area within the CMG: the Mcm3 and Mcm5 zinc-fingers. This interaction platform, essential for replisome disassembly, is blocked by the excluded lagging DNA strand at replication forks, explaining the delay in CMG ubiquitylation until termination when the lagging strand is no longer present (53).

The termination of DNA replication ends by removal of catenates formed (decatenation) by topoisomerase II (42). Inactive Mcm2-7 complexes are also removed from chromatin during S phase. It could happen throughout elongation, when active helicases collide with them, or at the termination point, where they would be pushed together by converging replication forks (54). However, the mechanism of their disassembly remains unknown.

1.2. Chromatin replication

In eukaryotic cells, DNA is greatly packed to fit in the nucleus. It associates with different proteins, mainly histones, to form a highly regulated macromolecular complex called chromatin. The structure of the chromatin organises DNA and controls processes such as mitosis, DNA replication, transcription and repair. Epigenetic marks comprise post-translational modifications (PTMs) of histones tails and DNA methylation, that control chromatin accessibility and, therefore, the recruitment of effector proteins to regulate gene activity. Many of these epigenetic marks are heritable and are responsible for cell identity, regulating transcriptional programmes during development. As the carrier of genetic and epigenetic information, chromatin needs to be faithfully duplicated to ensure genome stability.

1.2.1. Chromatin as carrier of epigenetic information

The basic structural unit of chromatin is the nucleosome. It is composed of two turns of DNA (~149 bp) wrapped around a histone octamer consisting of a H3-H4 tetramer and two H2A-H2B dimers (Figure 3). Nucleosome cores are separated by linker DNA and are associated with histone H1. This level of chromatin compaction is often referred to as “beads on a string”. Eukaryotic DNA is further packaged into a more compacted structure with the highest compaction reached during mitosis to allow for chromosome segregation (55).

The post-translational modification of these histones and the methylation of the DNA are known as epigenetics marks which control chromatin conformation and accessibility:

- Histone post-translational modifications. Histones are subjected to a wide variety of post-translational modifications (PTMs) on their flexible N-terminal or C-terminal tails, for example: methylation, acetylation, phosphorylation, ubiquitination, sumoylation, biotinylation, and ADP-ribosylation. These modifications often act like signals for the recruitment of

chromatin remodelling complexes or transcription factors (56). Although less frequent than in the tails, histones can also be modified within the globular histone core, directly impacting the stability and dynamic of the nucleosome (57). All these histones PTMs affect inter and intra-nucleosomal interactions and the binding with DNA and histone interacting proteins, affecting overall chromatin structure and function. Histone H3 ubiquitination is the focus of this project and specifically, mono-ubiquitination of lysines K14/18/23/27 has been shown to regulate DNA methylation maintenance during DNA replication (58–60). However, other ubiquitinated residues in histone H3 have also been identified such us K36/37/121/122/125 (61). Ubiquitination involves the attachment of a small 76 amino acid protein called ubiquitin to a lysine residue on proteins, or on ubiquitin itself, generating various types of poly-ubiquitin chains. This modification is performed by a cascade of three enzymes: E1 activating enzyme, which binds and activates ubiquitin before it is then transferred to a E2 conjugating enzyme, and finally to the E3 ligase enzyme, which facilitates the transfer of ubiquitin from the E2 to the substrate (62). Histones are one of the most frequently mono-ubiquitinated proteins.

- DNA methylation: cytosine and adenine residues of DNA can be modified by the addition of a methyl group, with 5-methylcytosine being the most abundant form in higher eukaryotes. This modification occurs mainly on cytosines preceding a guanine nucleotide (CpG dinucleotides) by DNA methyltransferases (Dnmts). The majority (75%) of CpG sites are methylated in mammals, which generally leads to silencing of gene expression. However, there are CpG-rich regions (from 500 bp and more than 55% of G + C content) mainly within promoters that are unmethylated known as CpG islands, which are correlated with accessible chromatin and transcriptional activation. DNA methylation works together with histone modifications to control gene expression and maintain cell identity (63,64).

Generally, histone modifications and DNA methylation change chromatin conformation and promote the recruitment of effectors that recognise specific modifications and regulate transcriptional activity (63). For instance, an active chromatin state is enriched for H3K27ac and H3K4me3 histones marks and unmethylated DNA that both favour transcription factor (TF) binding and gene expression, while a repressive state is characterized by H3K27me3 and H3K9me3 histone marks and DNA hypermethylation of promoters leading to a more compact and silenced state (65). Finally, histone variants and miRNAs further control gene activity and cooperate with other epigenetic marks forming a complex epigenetic network (66). Defects in the chromatin replication process can generate alterations in the epigenetic information, leading to several diseases. In cancer, there is a general hypomethylation of DNA that induces genome instability and transcription of oncogenes, as well as specific hypermethylation of CpG islands in promoters of tumour suppressor genes that lead to silencing (64,65). Therefore, accurate propagation of the epigenome during DNA replication is essential to maintain genome integrity.

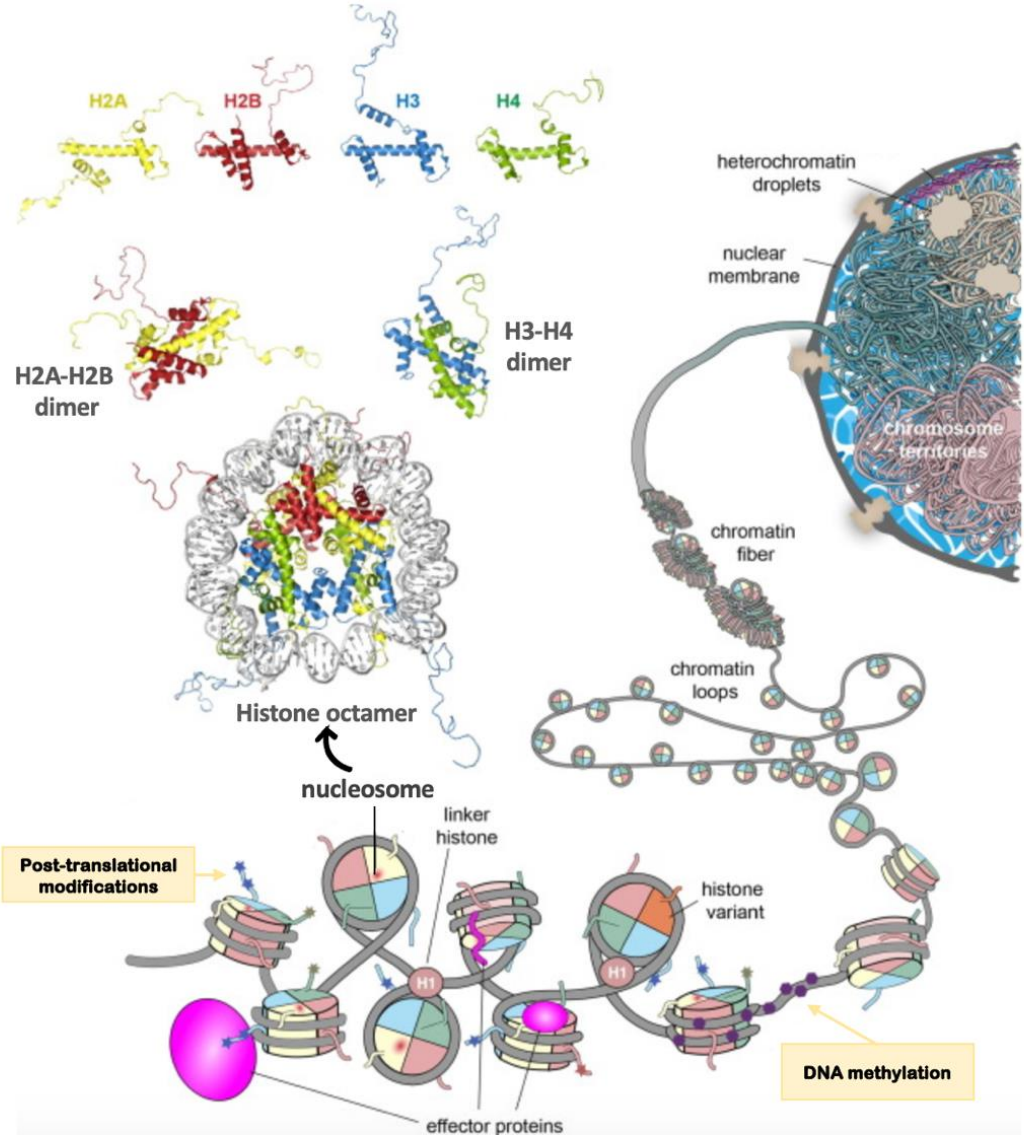


Figure 3. Chromatin structure. DNA is tightly package in the nucleus by the association with histones to form the nucleosomes, the basic unit of chromatin. The nucleosome consists of a histone octamer, formed by the association of two H2A-H2B dimers and a H3-H4 tetramer, wrapped by two turns of DNA. The post-translational modifications of histones and DNA methylation comprise the epigenetic marks, which regulate chromatin conformation, accessibility and activity. Adapted from (55)

During the DNA replication process, not only does the DNA need to be duplicated, but also chromatin needs to be accurately re-established. Chromatin re-establishment consists of the re-assembly of the nucleosomes and the restoration of the epigenetics marks in both daughter strands.

1.2.2. DNA replication-coupled nucleosome assembly

Replication-coupled (RC) nucleosome assembly is the first step in epigenetic information transfer. During DNA replication, nucleosomes must be disassembled from DNA ahead of the replication fork, for the replisome to be able to progress, and then re-assembled behind the fork. This nucleosome remodelling is tightly coordinated with DNA replication by the cooperation between histone chaperones and replisome components (Figure 4). Nucleosome disruption is promoted by its destabilization, as a result of a collision with the helicase or the topological stress created ahead of the replication fork. Parental histones are recycled to both daughter strands. However, the generation of two copies of DNA makes necessary the supply of newly synthesized histones. Parental and new histones are mixed and assembled, followed by the restoration of the epigenetic marks (67–69).

1.2.2.1. Parental histone recycling

Recycling of parental histones is important as they carry the PTMs that regulate genome activity and give identity to cells. They maintain their PTMs throughout chromatin assembly and the maturation processes to ensure PTM inheritance. Most studies support the model in which parental H3-H4 histones dissociate from the nucleosome and are randomly transferred to the two daughter DNA molecules as tetramers, being rapidly associated with two H2A-H2B dimers (70,71). The recycling of H2A-H2B is less clear because of their dynamic behaviour, but it has been recently shown in mouse embryonic stem cells (mESCs) that they are recycled similarly to H3-H4 (72). Parental histones can be removed from DNA and directly transferred by the cooperative actions of the replisome and chaperones; otherwise, they remain assembled and slide ahead of the replication fork, promoting replication fork slowing/stalling, which depends on a free pool of histones (73). When old histones are dissociated from DNA, they remain close

to the replisome and to their original location (within 400 bp) (74). Parental H3-H4 recycling pathways differ between leading and lagging strands (Figure 4).

Lagging strand. The Mcm2-Ctf4-Polα complex mediates parental histone recycling to the lagging strand (75,76). Mcm2 has an N-terminal histone-binding domain (HBD) that can bind H3-H4 tetramers, acting as a chaperone, and directly regulates parental histone segregation to sister chromatids. The mutation of HBD on Mcm2 leads to an increase in the distribution of parental histones to the leading strand in mESCs, demonstrating that Mcm2 promotes histone H3-H4 recycling specifically to the lagging strand (69,77). This leading strand bias of old H3-H4 also occurs when inhibiting the interaction between Polα and Ctf4 in yeast (76), demonstrating conservation of this Mcm2-Ctf4-Polα pathway. Mcm2 forms co-chaperone complexes with histone chaperones Asf1 and FACT, to which Mcm2 may transfer histones for deposition. It has been shown that the interaction of Mcm2 with both chaperones is bridged by H3-H4. Moreover, both Asf1 and FACT are essential for DNA unwinding and fork progression, probably by promoting nucleosome removal (78–80). FACT (Spt16/SSRP1 complex) is involved in disassembly and assembly of both parental and new H3-H4 tetramers and H2A-H2B dimers. Interestingly, this chaperone can form a complex with a H3-H4 tetramer together with H2A-H2B dimers and its subunits can interact independently or simultaneously with DNA, H2A-H2B and H3-H4, suggesting that FACT could coordinate H3-H4 and H2A-H2B recycling (69,71,81). FACT also interacts with other replisome components such as RPA and Polα (82,83), which are enriched at the lagging strand. On the other hand, the histone chaperone Asf1 binds H3-H4 dimers and prevents their tetramerization but is not able to split the tetramer by itself, suggesting a requirement of other factors or PTMs (84). In addition to its interaction with Mcm2, Asf1 binds the clamp loader RFC, which recruits Asf1 to the primer-template junctions (85). As PCNA loading is increased at lagging strands because of Okazaki fragment synthesis, Asf1 could use this binding to RFC to be directed to the replicated lagging strand

DNA. It is likely that Asf1 contributes to H3-H4 recycling to the lagging strand by collaborating with Mcm2 in H3-H4 disassembly and with RFC in the re-assembly (69).

Leading strand. The recycling of parental histones to the leading strand is regulated by Polε as it has been shown that Polε has a histone chaperone role. The regulatory subunits POLE3/POLE4 (Dpb3/Dpb4 in yeast) of Polε bind parental and new H3-H4 dimers and tetramers directly, with a preference for the tetrameric form and promoting tetramer formation (69). Budding yeast lacking Dpb3-Dpb4 exhibit an increase in parental transfer of H3-H4 tetramers to the lagging strand, confirming the role of Polε in the recycling of parental histones to the leading strand (86). Similarly, mammalian cells lacking POLE3/POLE4 accumulate RPA and PCNA on chromatin due to the shortage of nucleosomes (69). POLE3-POLE4 could recycle H3-H4 tetramers independently of Mcm2-Asf1 pathway or collaborate downstream with Asf1, which binds H3-H4 dimers, in the re-assembly at the leading strand. The same group also suggested that Polε could coordinate new and parental deposition pathways (87).

Parental histone H2A-H2B recycling. The mechanism of H2A-H2B dimer recycling has remained poorly understood due to the fact that, while the H3-H4 tetramer binds stably acting as a firm core, H2A-H2B dimers are highly dynamic and exchanged in the active regions soon after re-assembly to allow gene expression (88). Using chromatin occupancy after replication (ChOR-seq), Flury and co-workers have shown that the recycling of H2A-H2B is also symmetrical between both daughter strands and follows a mechanism that is similar but independent of H3-H4 recycling, involving the lagging strand polymerase POLA1. They show that H2A-H2B PTMs are restored immediately after replication, with comparable timing to the restoration of transcription (72). As mentioned, the chaperone mediating the disassembly and assembly of parental H2A-H2B dimers is FACT, which coordinates this with H3-H4 tetramer recycling.

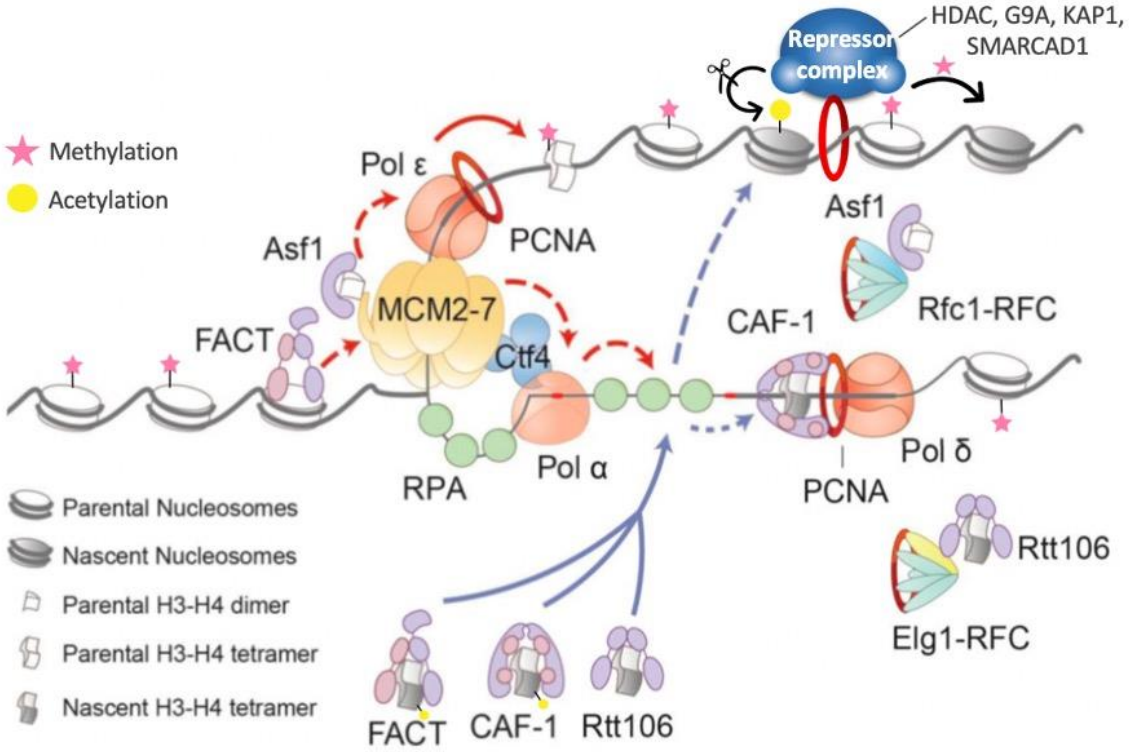


Figure 4. DNA replication-coupled nucleosome assembly and PTM restoration. Parental histones are recycled with their PTMs by the cooperation between histones chaperones (FACT and Asf1) and replisome components. In the leading strand, Pol ε mediates recycling while Mcm2-Ctf4-Pol α promotes the transfer in the lagging strand. Newly synthesised histones are delivered by a network of chaperones that ends in CAF1, FACT or Rtt106, which collaborate with replisome components for deposition. Once deposited, new histones are modified, echoing parental PTMs to maintain the epigenome. Adapted from (69).

1.2.2.2. New histone supply

To maintain nucleosome density after genome duplication, newly synthesised histones are incorporated into sister chromatids. Both the synthesis and the deposition are highly regulated because the lack or excess of histones can lead to genome instability (78).

Delivery of newly synthesized H3-H4

Immediately after synthesis, H3.1 and H4 dimerise and are transported to DNA replication sites by a network of chaperones that deliver them to the chaperone CAF1 (Chromatin assembly factor-1), which will mediate their deposition (Figure 5) (89). PTMs of histones modulate their transfer between chaperones and the replication-coupled nucleosome assembly pathway chosen

(90). Newly synthesised H3.1-H4 interact with HSC70, HSP90 and NASP in the cytoplasm, which promotes their folding and dimerisation. Dimers are then bound by the chaperone Asf1, which works together with many other proteins that modify histones and help in their transport and incorporation. Firstly, Asf1 associates with Importin-4 to facilitate the translocation of H3-H4 dimers into the nucleus. This interaction is stimulated by the acetylation of H4 at K5 and K12 (H4K5ac and H4K12ac) by RBAP46-HAT1, which represents a highly conserved mark really useful to track new histones (91). These acetylation marks are essential for nucleosome assembly and chromatin maturation. Histone H3 is also acetylated, but the sites vary between species. In yeast, acetylation of K56 (H3K56ac) by Rtt109 promotes H3-H4 binding to CAF1 and the Rtt106 chaperone can carry out nucleosome assembly (92). In humans, the acetylation sites are H3K14ac and H3K18ac, but their functions are not clear. Histone H3.1 is also monomethylated on K9 prior to deposition by SETDB1 (H3K9me1), which antagonises the acetylation. This methylation primes H3K9 for trimethylation (H3K9me3) by SUV39H1/2, which is a mark of repressive chromatin (67,93). Other modifications are also essential for histone transport. For example, ubiquitination of histone H3 at K121, 122 and 125 by the $Rtt101^{Mms1}$/ $Cul4A^{DDB1}$ E3 ubiquitin ligase reduces the interaction of H3-H4 dimer with Asf1, which promotes delivery from Asf1 to downstream chaperones (94). The final deposition of the new H3-H4 dimers into newly replicated DNA is accomplished by CAF1, FACT or Rtt106 (Figure 4).

Deposition of newly synthesized H3-H4

CAF1 is a heterotrimeric complex that mediates new histone H3-H4 deposition (Figure 4-Figure 5). It is composed of p150, p60 and p48 subunits (also known as CHAF1A/CHAF1B/RBBP4/RbAp48), where p60 is the subunit binding H3-H4, which is essential for CAF1 chromatin assembly activity. A Cryo-EM structure shows that CAF1 binds to one H3-H4 dimer. When this CAF1-H3-H4 complex binds DNA, it promotes dimerisation

of two complexes forming H3-H4 tetramers (95,96). Although CAF1 can bind DNA itself, nucleosome assembly requires its interaction with PCNA at the replication fork (97). As mentioned, PCNA is essential for the recruitment and organisation of many proteins and also for synchronisation of DNA replication with nucleosome assembly. It has been shown that mutations in CAF1 that abolish both DNA and PCNA binding were synergistic and led to loss of CAF1 role in gene silencing (98). Deletion of the CAF1 subunit that interacts with H3-H4 is not lethal, so other chaperones must be able to perform H3-H4 assembly in its absence. FACT, which also binds new histones, may also work in this pathway as it interacts with CAF1 and Rtt6 (Figure 4) (69).

- On the leading strand, PCNA leads the recruitment of CAF1 and this chaperone together with Polε mediates H3-H4 tetrasome formation (87,96,98). However, the exact mechanism by which nucleosome assembly and DNA synthesis by Polε is coordinated remains unknown.
- On the lagging strand, nucleosome assembly is coordinated with Okazaki fragment maturation. Indeed, nucleosome positioning determines the length of Okazaki fragments. Firstly, nucleosomes promote primer synthesis by Polα on lagging strand (80). Secondly, Okazaki fragment sizes are similar to nucleosome repeats length and CAF1 mutants that delay nucleosome deposition also generate longer Okazaki fragments. Moreover, ligation junctions between Okazaki fragments are located close to nucleosome midpoints (99). In fact, Fen1 and Lig1 can act on DNA assembled into nucleosomes (100,101). Finally, strand displacement synthesis carried out by Polδ/Fen1 cannot progress beyond the nucleosome midpoint, demonstrating that nucleosomes control Okazaki fragment size by restricting Polδ progression (102). Therefore, Polδ synthesises DNA until it reaches a nucleosome assembled on the previous Okazaki fragment, which blocks polymerase progression and leads to its release followed by processing by Fen1, ligation by Lig1 and finally PCNA unloading (67).

Finally, RPA has a key role in replication-coupled H3-H4 assembly. Liu and co-workers revealed that RPA interacts with histone chaperones CAF1, FACT and Rtt106 through H3-H4. RPA binds ssDNA and can act as a platform for histones deposition onto immediately adjacent dsDNA by histone chaperones (82). As RPA is enriched on Okazaki fragments because of the maturation process, it could mediate nucleosome assembly, leading to blockage of Polδ and termination of DNA synthesis.

Replication-coupled histones H3-H4 assembly is also mediated by Rtt106 in yeast, which interacts with DNA, CAF1 and FACT. However, the mechanism of Rtt106 recruitment is not clear. A role of Elg1-RFC complex in the recruitment of Rtt106 to the replication sites has been shown recently (Figure 4). As mentioned, Elg1 mediates PCNA unloading and a lack of Elg1 leads to defects in chromatin formation mainly because of PCNA retention on DNA (103).

Delivery and deposition of newly synthesized H2A-H2B

The supply of newly synthesized H2A-H2B is mediated by the chaperone NAP1 (Figure 5). Soluble H2A-H2B dimers are stabilized by NAP1, which promotes their import into the nucleus by interacting with Importin-9. Once in the nucleus, NAP1 may deliver new H2A-H2B dimers to already formed H3-H4 tetramers to constitute nucleosome. However, FACT could also contribute to this deposition as it interacts with H2A-H2B dimers. The chaperone network that guides newly synthesized H2A-H2B deposition is generally less known (67,89).

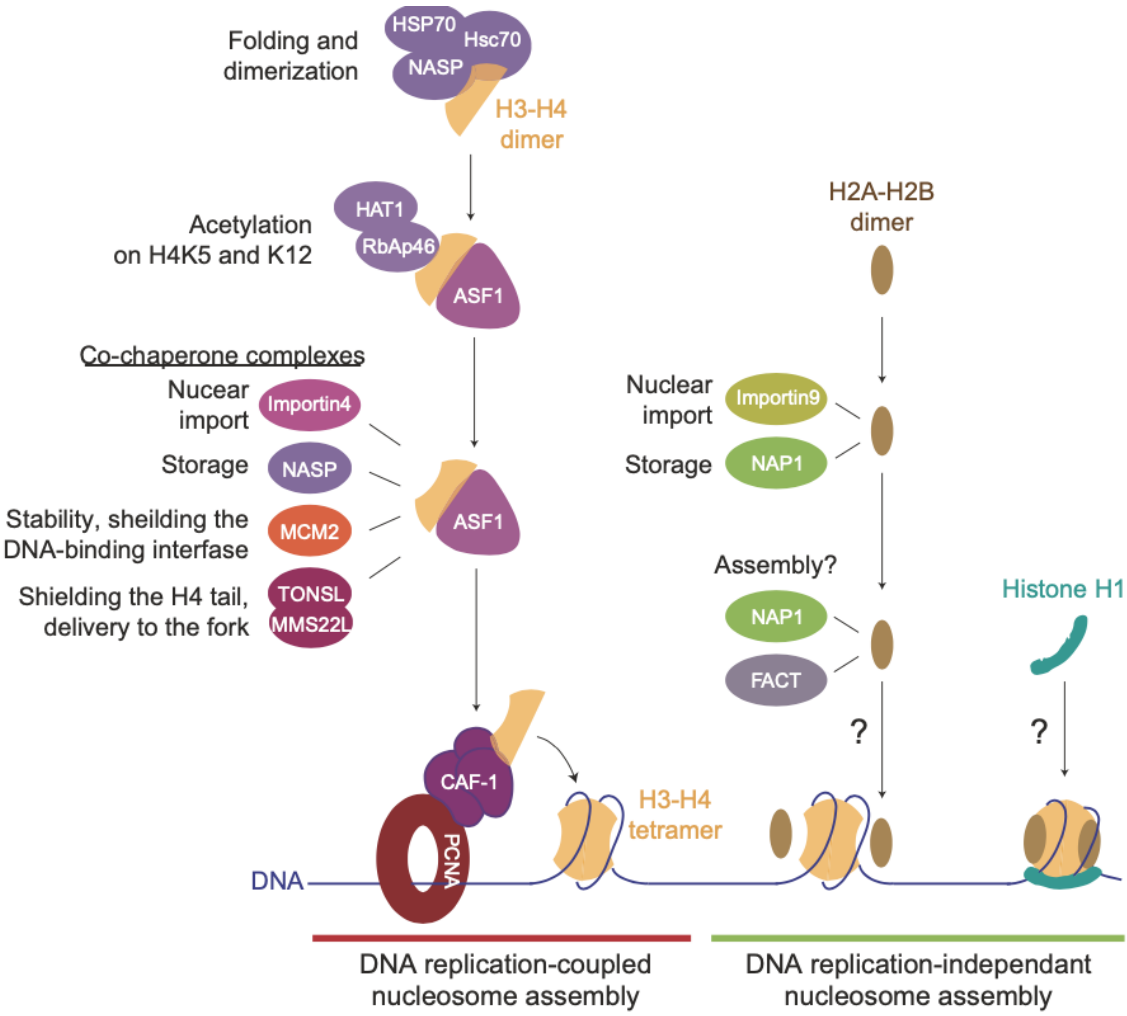


Figure 5. Newly synthesised histone delivery and deposition. After being synthesised, histones H3 and H4 pair up with histone chaperones and are moved to DNA replication sites as dimers. The transfer is mediated by a series of specialised chaperones, interconnected through various interactions commonly regulated by histone modifications. The process concludes with CAF1 assembling the dimers and new DNA into tetrasomes, which become nucleosomes upon the addition of H2A-H2B. (67)

1.2.3. Epigenome maintenance

Epigenetic information controls transcription programs that reflect cell identity. Thus, the epigenome must be preserved throughout cell divisions (71). Re-establishment of the pre-replicative chromatin state after DNA replication involves restoration of nucleosome positioning, histone modifications and DNA methylation on the new daughter strands (67).

1.2.3.1. Nucleosome positioning

Nucleosomes package DNA and locally control gene expression by regulating the access of DNA-binding proteins to DNA. Therefore, restoration of the pre-replicative positions of histones is essential. The speed of nucleosome re-positioning is locus- and factor-specific. Active promoters and enhancers are nucleosome-free regions (NFR), which allows interaction of transcription factors and RNA polymerase. After DNA replication, active regions show reduced accessibility and silencing due to different nucleosome positioning. In *Drosophila*, CAF1 deposits nucleosome indiscriminately throughout the nascent genome, which blocks transcription factor binding sites in active regions. However, restoration of nucleosome organisation and chromatin accessibility is quick - fastest in highly transcribed genes - and seems to require the transcription machinery. For example, the NFRs become accessible in mESCs when RNA polymerase binds (71). However, it has also been shown that intrinsic DNA sequences can guide nucleosome organisation (104). In yeast, poly-dA/dT sequences in promoters destabilise nucleosomes, so NFR restoration is transcription independent (105). Further studies are required to fully understand the role of transcription in epigenome maintenance.

1.2.3.2. Histone PTM maintenance

The inheritance of histone PTMs post replication is a complex process and remains a central question in epigenetics. The current model is that parental histones are recycled to daughter

strands with their modifications and newly synthesised histones echo parental PTM patterns (Figure 4) (71). However, the complete restoration of PTMs is a slow process that continues into the next cell cycle, so chromatin states oscillate during the cell cycle (106,107). It is unclear how these oscillations in histone modifications affect processes such as transcription or DNA repair.

Parental histone modification maintenance

Parental histones are incorporated close to their original positions preserving their methylation and acetylation marks (74,108). It has been proposed that parental H3-H4 are equally distributed between daughter strands (75), with a slight bias for lagging strand in yeast (86) and for leading strand in mammalian cells (77). In addition, as different chaperones and pathways control parental histone recycling in each strand, there is a possible mechanism of asymmetric distribution by the regulation of each pathway factors. Such asymmetric distribution could lead to differentiation during embryonic development.

Modification of new histones to restore the pre-replicative state

New histones create a highly acetylated nascent chromatin which makes DNA more accessible. This chromatin state could be an opportunity for DNA repair and transcription machineries (68). However, a more compact state must be rapidly reached. As parental histones are divided between sister chromatids, PTMs are diluted on the new strands. Thus, new histones must acquire parental modifications once deposited to maintain epigenetic information (106). Restoration of parental PTMs on new histones is a heterogenous process with different kinetics between marks, locus and cell type. Once deposited, new histones need to be deacetylated, which is fast, and methylated following the parental pattern, which is slow and continues throughout the next cell cycle in daughter cells. Additionally, while transcriptionally active

regions have a quicker restoration rate, often completing the restoration of histone marks prior to mitosis, this process is much slower in heterochromatin (71).

Soon after fork passage and nucleosome re-assembly, the first wave of chromatin maturation takes place, which involves DNA methylation, deacetylation of new histones and acquisition of the mono-methylation state. These processes are completed during S phase. PCNA also orchestrates this chromatin maturation during DNA replication (68). In fact, PCNA remains stably bound on replicated DNA for up to 20 minutes to serve as a platform for the recruitment of implicated factors (109). Firstly, nascent chromatin is rapidly deacetylated to achieve a more compact state. It is performed by histone deacetylase 1 (HDAC1), HDAC2 and HDAC3, which interact with PCNA to access the replicated chromatin (110). In the case of histone methylation, different enzymes are recruited depending on the chromatin domain and epigenetic mark. In heterochromatin, SMARCAD1 together with HDAC1, HDAC2, G9A and KAP1 are part of a repressor complex that promotes deacetylation and primes nucleosomes for histone H3K9 mono-methylation, contributing to heterochromatin maintenance (Figure 4) (111,112). Methyltransferase G9A (also known as EHMT1/2) in the repressor complex and SETDB1, recruited with CAF1, are likely responsible for H3K9me1 (68). H3K27me1 is also established in S phase and primes for the other repressive mark H3K27me3 (113). However, heterochromatin marks H3K9me3 and H3K27me3 are not fully restored until the next cell cycle (107,113). The propagation of H3K9me3 and H3K27me3 marks follow a read-write or allosteric self-propagation mechanism, in which methyltransferases are recruited to their own marks (68,71). For H3K9, HP1 protein recognizes parental H3K9me3 and recruits SUV39H1/2 to further methylate new H3K9me1 (114,115). In addition, allosteric activation of PRC2 by H3K27me3 promotes its propagation (116). CAF1 interacts with Polycomb repressive complex 2 (PRC2), responsible for H3K27me3, and has been shown to promote the establishment of H3K27me3 during ESC differentiation, but the precise mechanism is not yet clear (117). In

contrast, the active region mark H3K4me3 is restored before mitosis (108), however, the mechanism of the propagation of this PTM is less well understood.

Histones H2A and H2B are also symmetrically recycled carrying their PTMs. These PTMs are restored in the newly synthesised histones immediately after replication, with a comparable timing to the restoration of transcription (72). The most abundant PTMs on these histones are ubiquitination at H2AK118/119ub1 and H2BK120ub1. These modifications regulate DNA replication and transcription processes. H2AK119ub1 is catalysed by RING1A/B ubiquitin ligase (part of the Polycomb-repressive complex 1) and is associated with a repressive chromatin state. This mark mediates the crosstalk with H3K27me3. In contrast, H2BK120ub1 is characteristic of active chromatin and promotes the H3K4me3 and H3K79me3 marks (61). Post-replication, H2AK119ub1 helps in the accurate restoration of H3K27me3, highlighting the significance of H2A-H2B recycling in epigenome maintenance (72).

1.2.3.3. Restoration of the DNA methylation pattern

During the DNA replication process, in addition to nucleosome re-assembly and the restoration of histone PTMs, DNA methylation marks also need to be copied into the new strands to preserve the entire epigenome. The process of DNA methylation maintenance is also complex and highly regulated, involving many factors and their PTMs, as it needs to be placed in the context of dynamic chromatin replication. Therefore, DNA methylation maintenance occurs during and post-replication. However, it is not completely clear how much time it takes to re-establish this epigenetic mark after fork passage. Different genomic regions have distinct speeds of restoration of the DNA methylation marks. Also, two different pathways seem to regulate the maintenance of this epigenetic mark: one tightly coupled to the replisome on naked DNA and another one, later, after nucleosome re-assembly on chromatinised DNA (118,119). As DNA methylation maintenance is the focus of this thesis, it will be detailed below.

1.3. DNA methylation maintenance

1.3.1. DNA methylation importance

The modification of DNA by the addition of a methyl group to the carbon 5 of cytosines in the context of CpG sites is an epigenetic modification, which is evolutionary conserved, being present from bacteria to mammals. However, some of the common model organisms do not have DNA methylation, such us *Saccharomyces cerevisiae*, *Caenorhabditis elegans* or *Drosophila melanogaster*. In mammals, this epigenetic mark is crucial for embryonic development and cellular physiology (120).

Mice deficient in the enzymes that mediate DNA methylation display pronounced developmental problems that lead to early embryonic lethality (121). This is due to the importance of DNA methylation for development, as it regulates processes such us genomic imprinting and X chromosome inactivation. During the mammalian cell life cycle, the DNA methylome is dynamic and is subjected to two waves of methylation re-programming (Figure 6). Firstly, the methylation marks are erased during early embryogenesis and gametogenesis, to allow the epigenetic plasticity necessary at these crucial developmental stages. The marks are then re-established during the implantation stage and the formation of sex-specific gametes, being tissue-specific to define each cell type. All these changes in the pattern of DNA methylation regulate the expression of different genes at different stages. During embryogenesis, there is a general demethylation post-fertilization that generates a loss of gamete-specific DNA methylation patterns and the expression of pluripotency associated genes, which is followed by a de-novo methylation wave after implantation that leads to the establishment of the embryonic methylation pattern. During gametogenesis, methylation re-programming allows the loss of somatic methylation patterns in primordial germ cells (PGCs)

and the subsequent establishment of the methylation pattern for the expression of germline specific genes (120,122).

The loss of methylation during DNA methylation re-programming primarily results from a deficient DNA methylation maintenance during cell divisions. This occurs due to the silencing of Uhrf1 or exclusion of Dnmt1 from the nuclei. Another mechanism that leads to a rapid loss of methylation is the active removal of the methyl group from a cytosine, known as DNA demethylation. This is performed by the TET enzymes (Ten-Eleven Translocation), which carry out a sequence of modifications of the methylated cytosine that finally results in the replacement with the unmodified form. This final substitution occurs because TET enzymes generate DNA repair intermediates that can be recognize and processed by BER (Base Excision Repair) enzymes, ultimately achieving demethylation (122,123).

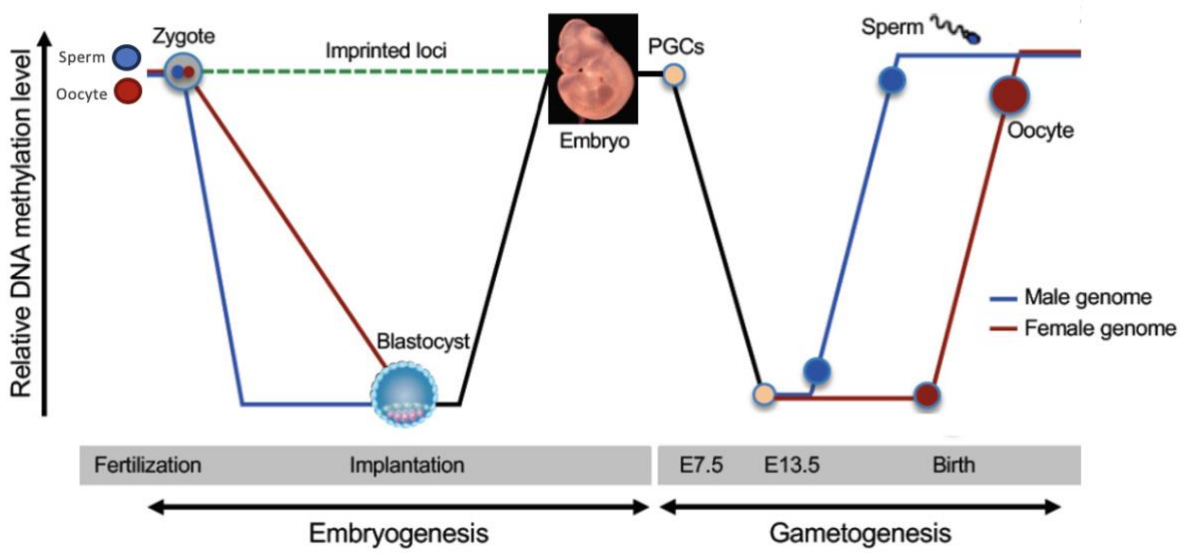


Figure 6. DNA methylation re-programming during mammalian development. Two phases of global DNA demethylation and re-methylation occur during the mammalian cell life cycle, one during early embryogenesis and another one during gametogenesis. After fertilisation, except for imprinted loci, the inherited methylation marks are erased to allow pluripotency. After implantation, de novo methylation forms the initial embryonic methylation pattern. Subsequently, primordial germ cells (PGCs) undergo global demethylation to erase the somatic methylation pattern. Later in development, de novo methylation establishes sex-specific methylation patterns in germ cells, including at imprinted loci. Adapted from (122).

Apart from this, DNA methylation also maintains the centromeric heterochromatin structure, crucial for chromosome distribution, and controls retrotransposons by methylating CpG-rich

promoters for silencing. It also regulates gene expression/transcription, as mentioned above, and splicing. Abnormalities in DNA methylation patterns are often associated with age and diseases such as cancer and neurological disorders. The maintenance of DNA methylation patterns, essential for the integrity of the epigenome, is therefore a key process that needs to be highly regulated to faithfully keep cell identity but also allow flexibility for cellular re-programming during development (119,124).

1.3.2. Mechanism of DNA methylation maintenance

During DNA replication, hemi-methylated DNA is generated with methyl groups present exclusively on the parental strands. Therefore, DNA must be fully methylated before mitosis to preserve cell methylation patterns, in a process known as DNA methylation maintenance. The methylation of the DNA is performed by the DNA methyl transferases (Dnmts). There are three types of Dnmts: Dnmt1, the maintenance methyltransferase, and Dnmt3A and Dnmt3B, the *de novo* methyltransferases (63). Dnmt1 acts to add a methyl group to hemimethylated CpG sites generated after DNA replication. The Dnmt3A and Dnmt3B methyltransferases are able to perform the methylation of unmodified cytosine residues that arise mainly during early development and gametogenesis. Although these enzymes have also been shown to be involved in the DNA methylation maintenance (125), Dnmt1 is the main methyltransferase regulating this process so I will focus on the mechanism of Dnmt1 recruitment to hemi-methylated sites.

The current simplified model is that Dnmt1 is recruited to hemi-methylated DNA by the E3 ubiquitin ligase Uhrf1 (Ubiquitin Like With PHD And Ring Finger Domains 1), which is able to recognize hemi-methylated CpG sites but also other PTMs of neighbouring proteins (such as histone H3, Paf15 and Lig1) for localisation (126). Once Uhrf1 is recruited, different mechanisms have been proposed to explain how Uhrf1 mediates Dnmt1 recruitment. Firstly, a direct interaction between Uhrf1 and Dnmt1. Two domains of Uhrf1 have been shown to bind

Dnmt1 directly and stimulate its methylase activity (127–129). Secondly, indirect recruitment of Dnmt1 through Uhrf1 E3 ubiquitin activity. Uhrf1 di-mono-ubiquitinates histone H3 and PCNA associated factor Paf15, which are both required for Dnmt1 recruitment to chromatin and DNA methylation maintenance (Figure 7) (130).

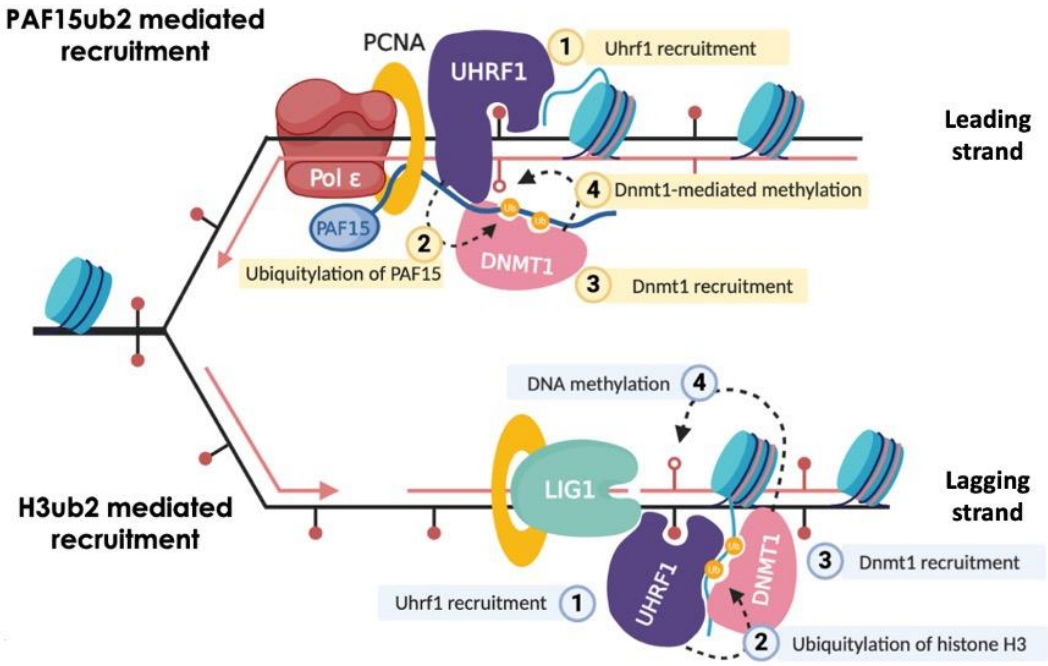


Figure 7. Current DNA methylation model. Uhrf1 is recruited to replication sites and mediates dual mono-ubiquitination of both histone H3 and the PCNA associated factor 15 (Paf15). These ubiquitinations promote Dnmt1 recruitment to chromatin, leading to full methylation of hemi-methylated DNA.

Although the role of Uhrf1 and Dnmt1 in inheritance of DNA methylation is clear, the exact mechanism remains to be clarified. Although it was initially thought to be a simple mechanism, the complexity of the process has been revealed over the years. This complexity is not only due to the fact that Dnmt1 necessitates additional factors such as Uhrf1, which is highly regulated as it will be described later, but DNA methylation maintenance also needs to be coordinated with DNA replication and chromatin assembly processes occurring at the same time.

1.3.3. DNA methylation in the context of chromatin replication

The process of DNA methylation maintenance occurs in the context of chromatinised DNA replication, which makes it more challenging as proteins mediating this process need to co-exist in space and time with DNA replication, nucleosome disassembly and re-assembly machineries and histone remodellers. How DNA methylation is regulated and coordinated in this context is still largely unknown. In recent years, several studies have revealed some insight that gives a better idea of the mechanism of DNA methylation maintenance and how it fits in the context of chromatin replication. However, the sequence in which the different proteins act and the events that occur are not completely clear, leaving many unresolved questions.

It is known that eukaryotic DNA methyltransferases act preferentially on naked DNA substrates, so nucleosomes are significant obstacles to Dnmt1 activity (131). As mentioned, the helicase unwinds the DNA which makes necessary the disassembly of the nucleosomes ahead of the replication fork. This results in the formation of naked DNA immediately after the replisome, potentially providing a favourable opportunity for Dnmt1 to access hemimethylated sites. Soon after fork passage, nucleosomes are re-assembled, but the incorporation of new acetylated histones and the slow restoration of parental histone methylation marks also creates accessible chromatin for DNA methylation maintenance. This hypothesis is supported by the fact that either the removal of CAF1, which mediates the deposition of new histones, or a disruption in the interaction between Mcm2 and H3-H4, which mediates parental histone recycling, accelerate the process of DNA methylation maintenance (118). In addition, the ubiquitination of histone H3 by Uhrf1 could destabilize nucleosomes promoting the recruitment of Dnmt1 by making hemi-methylated sites more accessible (119).

As two different substrates are formed during DNA replication (naked and chromatinised DNA), different mechanisms and factors could regulate Dnmt1 activity in the different contexts.

Supporting this, it has been recently proposed that two DNA methylation pathways could exist (Figure 8):

-Replisome-coupled pathway, acting soon after fork passage and carried out on naked DNA by interactions with the replication machinery. This mechanism would probably be regulated by replisome proteins PCNA, Paf15 and Lig1. Dnmt1 interacts with PCNA, the key factor regulating and coordinating many proteins related with DNA replication, Okazaki fragment maturation, nucleosome assembly and remodelling and DNA repair. This interaction with PCNA was initially thought to recruit Dnmt1 to methylate DNA but it was later shown that this interaction is not essential for DNA methylation maintenance (126,132). Ubiquitinated Paf15, which travels bound to PCNA, is also recognized by Dnmt1 which seems to promote its recruitment and activation (130,133). Finally, Lig1 has been shown to also regulate DNA methylation maintenance by mediating the recruitment of Uhrf1 (134). All of these will be detailed in the next section but this gives an idea of the coordination between DNA replication and DNA methylation machineries.

-Replisome-uncoupled pathway, on chromatinised DNA and mediated by histone PTMs and chromatin remodellers. Dnmt1 can recognise and bind ubiquitinated histone H3, which has also been proposed as a mechanism of Dnmt1 recruitment and DNA methylation maintenance. Uhrf1 also recognises methylated H3K9 and its interaction has been shown to be important for Uhrf1 recruitment and DNA methylation re-establishment (135). This finding localises the DNA methylation process in a later stage of chromatin replication, as restoration of H3K9 methylation is a long process as mentioned before. However, the presence of this epigenetic mark in parental histones could be enough for Dnmt1 recruitment. Other factors such as HDAC or G9a have been shown to interact with Uhrf1/Dnmt1 on chromatin. Indeed, DNA methylation correlates with histone deacetylation and other repressive marks such as H3K9me3 and

H3K27me3 (65,136), which suggest a cooperation between DNA methylation and histone remodeller machineries.

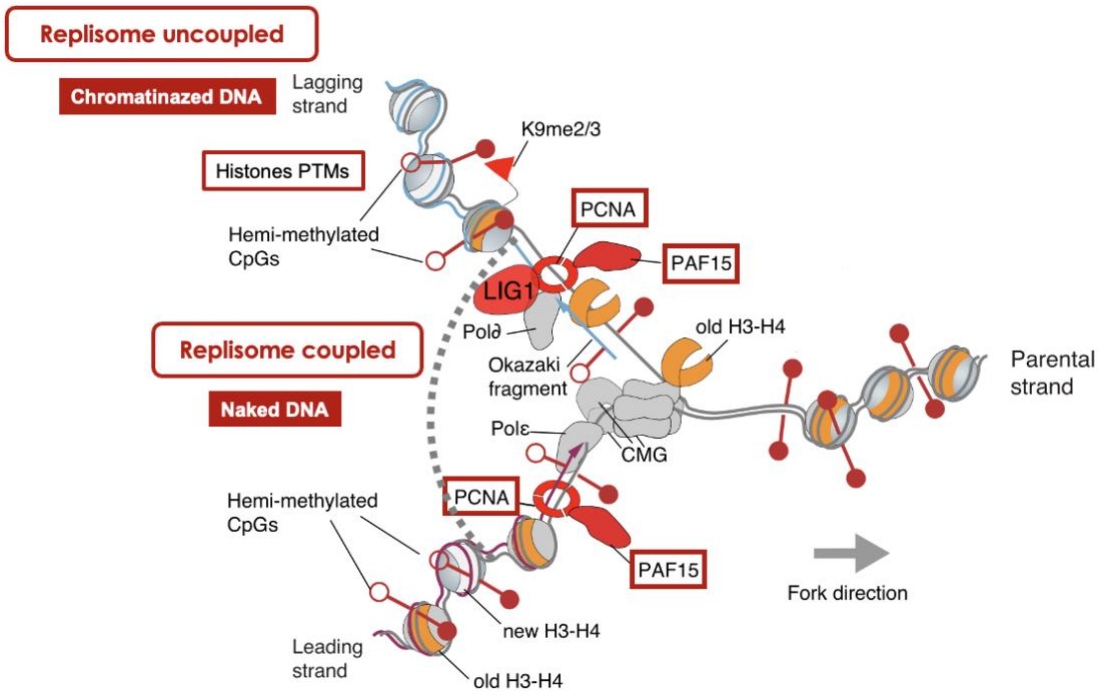


Figure 8. DNA methylation maintenance in the context of chromatin replication. The machinery for DNA methylation maintenance is coordinated with replication, nucleosome assembly and remodelling machineries. It has been proposed that two pathways could govern the maintenance of DNA methylation: the replisome-coupled pathway, which acts shortly after the replication fork on naked DNA through the cooperation with the replisome proteins PCNA, Paf15 and Lig1, and the replisome-uncoupled pathway, which operates later after nucleosome assembly on chromatinised DNA, regulated by the histone post-translational modifications and chromatin remodellers. Adapted from (119).

1.3.4. Kinetics of the restoration of the methylation pattern

The time that it takes to re-establish DNA methylation patterns after DNA replication remains under debate. Some studies revealed that DNA methylation marks were restored within minutes following DNA replication, while others reported that it takes several hours post-replication. Microscopy shows that after S phase, Dnmt1 remains bound to chromatin through G2 and M phases, suggesting that DNA methylation maintenance could continue after DNA replication or that Dnmt1 could have additional roles (137). Also, another study showed that nascent DNA strands are methylated significantly later than replicated (within hours) (138). In contrast, another group compared methylomes of nascent strands with parental strands and showed that

in most cases DNA methylation is maintained within 20 min post-replication (139). However, all these studies relied on biochemical and genetic experiments, and there often exists a discrepancy between genetic data, derived from measuring DNA methylation levels in cells, and biochemical results. This is because measuring the level of DNA methylation offers only endpoint information, not showing the kinetics in which these biochemical mechanisms might act. Ming et al., (2020) used a method capable of analysing the dynamic DNA methylation maintenance process at the single-molecule level with high spatiotemporal resolution, to address the kinetics of DNA methylation maintenance in human cells (118). They showed that more than half of the hemi-methylated CpGs were successfully restored within 4 min of fork passage, but full maintenance of methylation took around 10 hours. They also proposed that methylation maintenance occurs in two distinct phases with different speeds: a fast replication-coupled phase occurring within minutes of fork passage, followed by a later replication-uncoupled phase. The interactions between Uhrf1–Lig1 and PCNA–Dnmt1 facilitate rapid, replication-coupled maintenance, while H3K9me2/3 mark and nucleosomes regulate later maintenance. Importantly, they reported that defects caused in replication-coupled maintenance were compensated later by the other mechanisms, which ensures that this epigenetic mark is preserved. Finally, this study also addressed different kinetics between leading and lagging strands, with lagging strands re-methylated faster. They hypothesised that the assembly of nucleosomes might occur at a faster rate on the leading strand, reducing the accessibility of DNA by shortening the nucleosome-free period and therefore slowing DNA methylation maintenance on this strand (118).

As Uhrf1 is the protein responsible for Dnmt1 recruitment and it is essential for DNA methylation maintenance, its regulation and activity has been the focus of the study of DNA methylation inheritance. Thus, the next section will dissect the structure, regulation and functions of this protein.

1.4. E3 ligase Uhrf1

Uhrf1 is an epigenomic regulator essential for cell proliferation and DNA methylation maintenance. The ability to recognize both hemi-methylated DNA and histone modifications makes Uhrf1 an epigenetic coordinator by mediating epigenetic cross-talk. This explains Uhrf1's roles in DNA methylation inheritance, as well as other processes such as translesion DNA synthesis, damaged DNA repair and regulation of gene expression. All these functions allow Uhrf1 to promote cell cycle progression, cell proliferation and differentiation. As a consequence, Uhrf1 overexpression leads to carcinogenesis and Uhrf1 is considered an oncogene and a biomarker of cancer prognosis and diagnosis (140,141).

1.4.1. Structure and enzymatic activity

Uhrf1, also known as ICBP90 (Inverted CCAAT box-binding protein of 90kDa) in human and Np95 (Nuclear Protein 95) in mouse, is an epigenetic regulator that bridges DNA methylation and histone modifications. It is able to recognise hemi-methylated DNA but also histone H3 marks through distinct domains, which allows Uhrf1 to maintain DNA methylation inheritance through recruitment of Dnmt1 but also to control many other cellular processes. Uhrf1 is composed of five conserved domains: the N-terminal Ubiquitin-Like domain (UBL), Tandem Tudor Domain (TTD), Plant Homeo Domain (PHD), Set and RING Associated domain (SRA) and the Really Interesting New Gene (RING) domain at the C-terminus (Figure 9). All of them cooperatively coordinate Uhrf1 epigenetic function (142).

The only enzymatic activity identified for Uhrf1 is the E3 ubiquitin ligase of the RING domain, which allows Uhrf1 to control target protein levels by ubiquitination-mediated proteasome degradation. This domain also mediates histone H3 lysine 18 and 23 (H3K18/23) and Paf15 lysine 15 and 24 (Paf15K15/24) dual mono-ubiquitination during DNA replication, which

serves as a platform for Dnmt1 recruitment to hemi-methylated sites (130). The rest of the domains show interesting binding and regulatory activities essential for RING activity. The TTD and PHD read out the histone H3 tail (143). The TTD domain is composed of two subdomains TTD_N and TTD_C. The TTD recognises and binds H3K9me2/3 through an aromatic cage in TTD_N and unmodified H3K4 using a groove between both TTD subdomains (144). This binding is impaired by H3K4me3 and H3T6ph, but is not sensitive to H3S10ph (135). The TTD domain of Uhrf1 also binds a methylated H3K9-like mimic within Lig1 (K126), with even more affinity than H3K9me2/3 (134). The PHD recognises the unmodified N-terminal tail of H3 and Paf15, ^{1}ARTK^{4} and ^{2}VRTK^{5}, respectively (130,145). Phosphorylation of a residue in the linker region between the TTD and PHD domains (S298) leads to a conformational change altering the binding affinity of TTD-PHD for H3 (143,146). While Arita *et al*. (2012) first suggested that this modification destabilises TTD-PHD and H3 tail interactions (143), Kori et al. (2020) proposed that it impairs intramolecular interactions within Uhrf1 (see next section below), favouring its binding to H3 (146). The SRA domain mediates the recognition of hemi-methylated DNA and the recruitment of Dnmt1. The crystal structure of this SRA domain of Uhrf1 in complex with hemi-methylated DNA revealed that binding to CpG sites promotes a flip out of the methylated cytosine from the DNA helix to a binding pocket of SRA. Contact between the SRA domain and the non-methylated cytosine on the opposite DNA strand allows discrimination between fully and hemi-methylated DNA (147). The SRA domain also interacts with the RFTS domain of Dnmt1, which could increase Dnmt1's activity and specificity for hemi-methylated DNA (128,148). Cooperative binding of the TTD, PHD and SRA domains is essential for RING-mediated ubiquitination. Many studies have separately reported the requirement of these domains in Uhrf1-mediated DNA methylation (58,60,135). Finally, the UBL domain is structurally similar to ubiquitin and contains two conserved lysines K31 and K50 (similar to ubiquitin K29 and K48) which are subjected to mono- or poly-ubiquitination

(142). It has been shown that the UBL also plays an essential role in Uhrf1-mediated H3 ubiquitination. A hydrophobic patch within the UBL contacts the E2 ligase enzyme UbcH5a, opposite to the active site which is also known to bind ubiquitin. This interaction stabilizes the E2-Uhrf1-ub complex and allows for ubiquitin transfer to H3. The UBL domain has, therefore, a dual role in histone H3 ubiquitination by the recruitment of the E2-ubiquitin conjugate and directing of ubiquitin to the target H3 (149,150). This domain also interacts with Dnmt1 and stimulates its methyl-transferase activity which, together with the H3ub interaction, is required for DNA methylation maintenance (129).

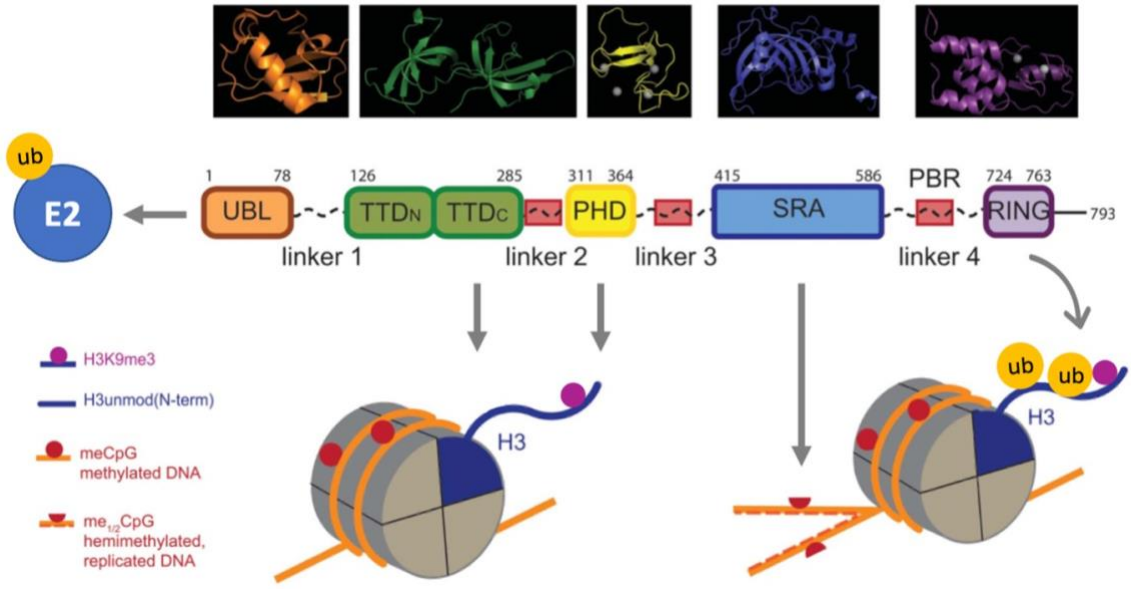


Figure 9. Uhrf1 domain structure and specificity. Uhrf1 is composed of five conserved domains: the N-terminal Ubiquitin-Like domain (UBL), Tandem Tudor Domain (TTD), Plant HomeoDomain (PHD), Set and RING Associated domain (SRA) and Really Interesting New Gene (RING) domain at the C-terminus. The UBL domain interacts with the E2-ubiquitin conjugate facilitating ubiquitin transfer to the substrate. The TTD domain binds to H3K9me3 and Lig1K126me2/3. The PHD recognises H3 and Paf15 at the N-terminal tail. Finally, the SRA domain recognises hemi-methylated DNA and the RING domain has E3 ubiquitin ligase activity. Adapted from (142)

1.4.2. Conformational regulation of Uhrf1

Uhrf1 can adopt multiple conformational states by allosteric regulation (140,142). Intramolecular interactions within Uhrf1 promote a closed state in which the TTD binds to a spacer region between the SRA and RING domains called the polybasic region (PBR), inhibiting the recognition of H3K9me3, while the PHD binds to the SRA, preventing the recognition of H3R2. Hemi-methylated DNA impairs these intramolecular interactions and promotes an open state conformation of Uhrf1 in which the TTD-PHD recognises the H3 tail and the SRA binds to DNA and recruits Dnmt1 for DNA methylation maintenance (Figure 10) (151,152). This conformational switch to an open state is facilitated by the binding of Usp7 and phosphatidylinositol 5-phosphate (PI5P) to the PBR, which disturb the TTD-PBR interaction (153,154). Lastly, it has been shown that methylated Lig1 also binds to the TTD and switches the Uhrf1 structure from a closed to a more open conformation, relieving auto-inhibition (155).

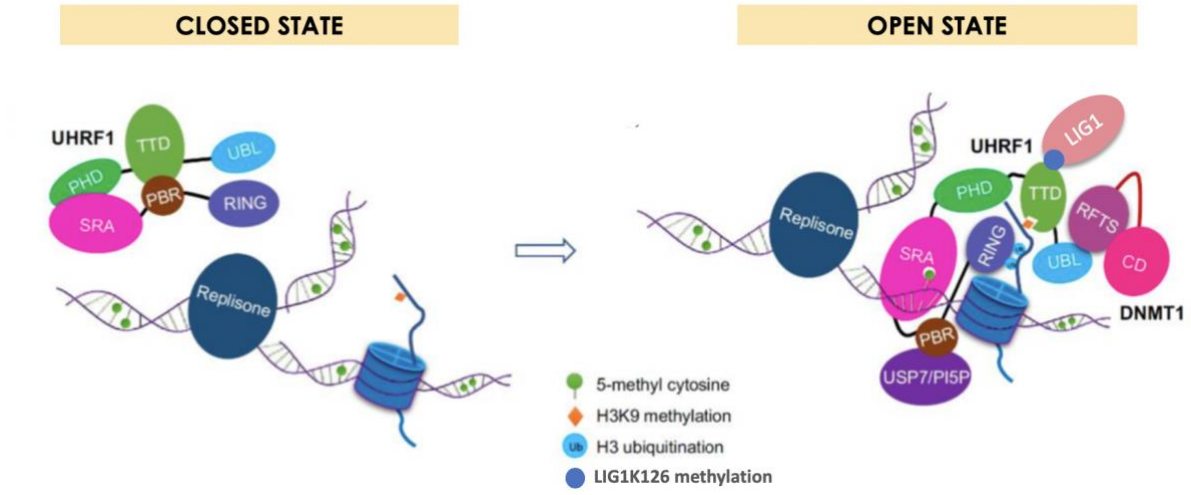


Figure 10. Domain structure, binding properties and allosteric regulation of Uhrf1. Adapted from (151).

Furthermore, Uhrf1 is regulated by post-translational modifications that modify its conformation, stability and activity. For instance, methylation of Uhrf1 at K385 by SET8 promotes its ubiquitination and proteosome-mediated degradation, which is countered by LSD1

de-methylation (156). However, Uhrf1 is mostly modified by phosphorylation, with a great number of residues identified as phosphorylation target sites (Table 1).

Table 1. Identified human Uhrf1 phosphorylation sites and function.

Position	Location	Enzyme	Description	Reference
S108	Linker 1	CK1δ	Increases the interaction with $SCF^{\beta\text{-}TrCP}$.	(157)
S262	TTD	PLK1	Enhances the interaction of Uhrf1 with Usp7 and inhibits proteasome degradation of Uhrf11 in M phase.	(158)
S287	Linker 2	-	During M phase and ESC differentiation.	(159)
S298	Linker 2	PKA PIM1	-Decreases TTD-PHD affinity to H3K9me3. -Enhances binding of LIG1 to Uhrf1, open conformation and Uhrf1 recruitment to chromatin.	(143,146)
S639	Linker 4	CDK1	Impairs the interaction with Usp7 (During M phase), which decreased its stability.	(154)
S651	PBR	-	Impairs the interaction of PBR with TTD, regulating Uhrf1 interaction with H3 and PI5P.	(152,154)
S652	PBR	CDK1-cynclin B	Decreases the interaction with Usp7 in M phase.	(160)
S661	PBR	CDK2-cyclin A2	Required for SET7 methylation that promotes Uhrf1 mediated ub of PCNA required for HR (S phase).	(161,162)
S674	PBR	CDK2-cyclin A	Allows BRCA1 recruitment of Uhrf1 to DSBs in (S phase).	(163) 07/05/2024 14:58:00

1.4.3. Role of Uhrf1 in DNA methylation maintenance

The Uhrf1/Dnmt1 tandem plays a crucial role in DNA methylation inheritance, but the detailed mechanism remains to be elucidated (164). Numerous studies have demonstrated the essential role of Uhrf1 in DNA methylation maintenance (58,60,126,127,135). Knockdown or depletion of Uhrf1 leads to reduced Dnmt1 binding to chromatin and, therefore, global DNA methylation levels. This reduction has been shown to be more pronounced in developmental stages. Moreover, the addition of recombinant Uhrf1 to cells lacking this protein partially rescues normal methylation levels, showing the importance of Uhrf1 in this process.

This key role of Uhrf1 in DNA methylation is due to Uhrf1 mediating recruitment of Dnmt1 to hemi-methylated sites. However, there are different models that explain how Uhrf1 recruits Dnmt1 to chromatin: a direct binding between Uhrf1 and Dnmt1 or through the Uhrf1 dependent ubiquitination of histone H3 or Paf15.

1.4.3.1. Interaction between Dnmt1 and Uhrf1

There are many studies reporting the direct interaction between Uhrf1 and Dnmt1 (126,128,129,165). Specifically, the SRA and UBL domains of Uhrf1 have been shown to bind the isolated RFTS domain of Dnmt1 and increase its activity to methylate hemi-methylated DNA (128,129).

Dnmt1 is composed of a large regulatory N-terminal region and a small catalytic C-terminal region, linked by six Lys/Gly (KG) di-peptide repeats (Figure 11). The N-terminal region is composed of a platform domain, able to interact with numerous proteins such as PCNA, a replication focus targeting sequence (RFTS) domain, which recognises ubiquitinated histone H3 and Paf15, a zinc-finger-like domain (CXXC), two bromo-adjacent homology (BAH) domains and a nuclear localisation signal (136). The platform domain and RFTS domain are mainly responsible for the recruitment of Dnmt1 to DNA replication sites. In addition, the RFTS and CXXC domains are involved in the regulation of the catalytic domain (151). On the one hand, the CXXC domain prevents *de novo* methylation of unmethylated CpG dinucleotides by positioning the CXXC-BAH1 linker region between DNA and the catalytic pocket (166). On the other hand, in the absence of DNA, the RFTS domain of Dnmt1 directly associates with the DNA-binding pocket of the catalytic domain, inhibiting its activity through an auto-inhibitory mechanism (Figure 12) (167). Apart from this allosteric regulation of Dnmt1, its stability and activity are also regulated by post-translational modifications which therefore affect its ability to carry out DNA methylation maintenance (119).

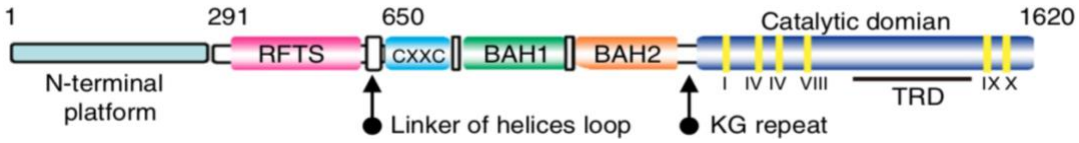


Figure 11. Dnmt1 domain structure. Dnmt1 is composed of five conserved domains: the N-terminal region able to interact with numerous proteins such as PCNA, a replication focus targeting sequence (RFTS) domain which binds the SRA domain of Uhrf1 but also ubiquitinated histone H3 and Paf15, a zinc-finger-like domain (CXXC), two bromo-adjacent homology (BAH) domains and the catalytic domain. Adapted from (167).

1.4.3.2. Uhrf1 mediated histone H3 ubiquitination as a platform for Dnmt1 recruitment

The second model proposes that the recruitment of Dnmt1 to chromatin is through the Uhrf1-mediated histone H3 ubiquitination (Figure 12). Uhrf1 binds hemi-methylated DNA through its SRA domain and to the H3 tail through its TTD-PHD domains and can mediate Dnmt1 recruitment by the ubiquitination of histone H3 through its RING domain (168). This ubiquitination is recognised by Dnmt1, which has been shown to interact with ubiquitinated H3 with high affinity (129,169).

The requirement of Uhrf1-dependent H3 ubiquitination for Dnmt1 recruitment and DNA methylation maintenance was first reported by Nishiyama and co-workers (58). They showed that Uhrf1 depletion impairs Dnmt1 recruitment to chromatin in *X. laevis* egg extract. Also, Dnmt1 depletion or knockdown leads to an accumulation of Uhrf1 and H3 ubiquitination at K23 in *X.laevis* egg extract and HeLa cells. The removal of both Uhrf1 and Dnmt1 resulted in a loss of H3 ubiquitination, which was rescued by the addition of recombinant wildtype Uhrf1, suggesting that Uhrf1 was responsible for H3 ubiquitination. Qin *et al.* (2015) also performed Uhrf1 knockdown in ESCs but this did not completely abolish H3 ubiquitination. The addition of wildtype Uhrf1 could rescue this phenotype back to control ubiquitination levels (60).

Other studies have further shown alternative lysine residues on histone H3, including K14, K18, K23 and K27, that can be ubiquitinated by Uhrf1 (59,60). However, single mono-ubiquitinated H3 is not enough to recruit Dnmt1. Structure-based studies reported that the RFTS domain of Dnmt1 interacts with di-ub-ubiquitinated H3 at K18 and K23 with higher affinity than H3 alone or ubiquitinated once, which could generate a conformational change in Dnmt1 that may facilitate RFTS dissociation from the catalytic domain, leading to the opening of the active site (129,169). The RFTS domain also directly binds H3K9me3 which promotes its interaction with ubiquitinated H3 (170). However, the mechanism by which dual mono-ubiquitinated H3 releases the auto-inhibition state of Dnmt1 cannot be explained by available structures.

Structural analysis of ubiquitinated H3 in complex with full-length Dnmt1 will be needed to demonstrate Dnmt1's conformational change by ubiquitinated H3.

Related to this, it has been also published that Dnmt1 can also bind ubiquitinated histone H2B (171). This study suggests that the Uhrf1/Usp7 complex regulates ubiquitination of both H3 and H2B during S phase, which in turn controls Dnmt1 recruitment and DNA methylation levels. Further studies are required to clarify the mechanism of Dnmt1 recruitment and to find out other factors contributing to this process.

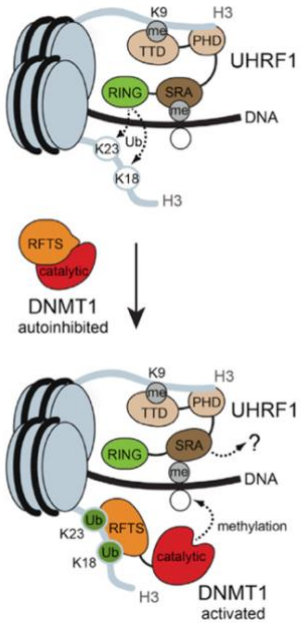


Figure 12. Model of Dnmt1 recruitment through histone ubiquitination. Uhrf1 binds hemi-methylated DNA through its SRA domain and the histone H3 tail through its TTD-PHD domains. The RING domain of Uhrf1 mediates Dnmt1 recruitment by the ubiquitination of lysine residues on histone H3 tail. This ubiquitination is recognised by the RFTS domain of Dnmt1, which could facilitate RFTS's dissociation from the catalytic domain and lead to the opening of the active site, stimulating Dnmt1 activity (168).

1.4.3.3. Uhrf1 mediated Paf15 ubiquitination as a platform for Dnmt1 recruitment

The third model of Dnmt1 recruitment has been published recently. This model involves Uhrf1-mediated di-mono ubiquitination of the PCNA-associated factor Paf15. This protein, also known as p15 or PCLAF, interacts with PCNA during DNA replication, regulating PCNA activity. The crystallography structure of the human PCNA-Paf15 complex showed that three molecules of Paf15 can simultaneously bind PCNA and that the PIP box of Paf15 strongly interacts with the front side of the PCNA. The crystal structures of PCNA with other interactors also show that the PIP-box sequence of these proteins bind to PCNA at the front-face. However, unlike other proteins that interact with PCNA, Paf15 also touches the inner part of the PCNA

ring and goes right through it. The disordered N- and C- terminal domains of Paf15 remain at the back and front faces of PCNA (172). Interestingly it has a histone H3-like N-terminal tail that binds DNA and can also be ubiquitinated in two neighbouring lysines, which can be recognised by Dnmt1. Furthermore, the N-terminal tail of Paf15 has a peptide VRTK similar to ARTK of H3 that is also recognised by the PHD domain of Uhrf1 in a comparable way to how it recognises H3 (130).

For the role of Paf15 in DNA methylation maintenance, firstly a study reported that Uhrf1 is responsible for double mono-ubiquitination of Paf15 and promotes its association with PCNA, which regulates replication block bypass (173). In 2019, another study showed that Paf15 doubly monoubiquitinated at K15 and 24 directly interacts with PCNA and the RFTS domain of Dnmt1, which could lead to the activation of Dnmt1 (133). However, the structure of the Paf15Ub2 in complex with full-length Dnmt1 is not known. Inhibition of Paf15 ubiquitination impairs its DNA binding (130,173), showing that Paf15 ubiquitination is also important for its own chromatin binding. In 2020, another study has proposed Uhrf1-mediated dual mono-ubiquitination of Paf15 as a new mechanism for Dnmt1 recruitment (Figure 13) (130). Indeed, they suggested the existence of two mechanisms for Dnmt1 recruitment: through Paf15 ubiquitination, preferentially during early S phase, and through histone H3 ubiquitination, during late S phase and as a backup mechanism when Paf15-dependent mechanism is compromised (130). Both mechanisms were suggested to be required for high fidelity DNA methylation maintenance. This conclusion agrees with the results obtained in the same year by measuring the kinetics of DNA methylation maintenance mentioned before. Paf15 bound to PCNA would be part of the replisome-coupled maintenance pathway.

Considering that Paf15 interact with PCNA and that PCNA is enriched in the lagging strand (174), this proposed model of Dnmt1 recruitment would mainly explain the maintenance of

DNA methylation on the lagging strand. However, on the leading strand, where a single PCNA is stably associated close to the fork, the availability of Paf15 may be limited. Consequently, the replisome-uncouple pathway could potentially compensate more on the leading strand to overcome the decreased levels of Paf15. How the mechanism of DNA methylation maintenance differs between leading and lagging strands remains uncertain.

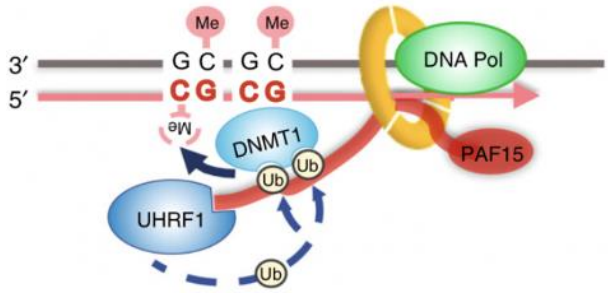


Figure 13. Model of Dnmt1 recruitment through Paf15 ubiquitination. Uhrf1 ubiquitinates Paf15 at K15 and K24 and promote its association with PCNA. This ubiquitination is recognized by RFTS domain of Dnmt1, serving as a platform for Dnmt1 recruitment to hemi-methylated sites (Adapted from Nishiyama et al., 2020).

1.4.3.4. Uhrf1 recruitment to chromatin

Uhrf1 needs to be recruited to hemi-methylated sites to be able to direct Dnmt1. The first model proposes that Uhrf1 is recruited to replicated DNA by its intrinsic ability to recognise hemi-methylated DNA through the SRA domain and the H3 tail through its TTD-PHD domains (126,127,143). Ferry et al. (2017) have proposed an additional model of Uhrf1 recruitment through interaction with Lig1 (134). They demonstrated that G9a and GLP methylate a H3K9-like mimic within Lig1 (K126) to which the TTD domain of Uhrf1 binds more avidly than H3K9me2/3. Mutations that impair Lig1/Uhrf1 interactions prevent Uhrf1 recruitment and caused a loss in DNA methylation. This model would also synchronise Uhrf1 recruitment and DNA methylation with chromatin replication, as Okazaki fragment maturation is coupled with nucleosome assembly. However, as Lig1 is enriched at Okazaki fragments, this model could just explain Uhrf1 recruitment to lagging strands. This model also does not explain why there is no loss of DNA methylation when Lig1 is completely missing. They suggested the possible existence of a backup mechanism of DNA methylation when Lig1 is absent. As mentioned, it has been demonstrated that in the absence of Lig1, Lig3-XRCC1 mediates Okazaki fragment

ligation through PARP1-HPF1-dependent ADP-ribosylation of histone H3 (37). Interestingly, the kinetic study showed that the LIG1-K126A mutant generates a delay in DNA methylation, suggesting that Lig1 would act in the early or replisome-coupled pathway of DNA methylation maintenance, but general DNA methylation levels are compensated later by a replisome-uncoupled pathway (118). Surprisingly, inactivation of the TTD domain of Uhrf1, which would affect early and late DNA methylation maintenance by impairing the interaction of Uhrf1 with H3 and Lig1, just caused a delay in both pathways and must be compensated for by another mechanism.

1.4.3.5. Other factors involved in DNA methylation maintenance

It has been shown that Uhrf1 interacts with other proteins on chromatin such as Usp7. However, the role of this protein is under debate. Usp7 is a pleiotropic deubiquitinating enzyme (DUB) that has been shown to regulate Dnmt1 and Uhrf1 stability by preventing its proteasomal degradation (171,175,176). Moreover, Usp7 has been proposed to be involved in the regulation of DNA methylation, but with discrepancies between its positive and negative effects in this process. The general model is that Usp7 de-ubiquitinates histone H3 and Paf15 and therefore reduces Dnmt1 recruitment to chromatin. The inhibition, depletion or knockout of Usp7 lead to accumulation of Dnmt1 and H3/Paf15 ubiquitination on chromatin in *Xenopus* and mammalian systems (171,177,178). However, the group of Yamaguchi and co-workers showed that depletion of Usp7 decreases DNA methylation in *Xenopus*, suggesting a positive role by releasing Dnmt1 from histone H3 and allowing its further association with DNA (177). Similarly downregulation of Usp7 increases global DNA methylation levels in HeLa, HCT116 and mouse embryos, suggesting that Usp7 prevents excessive DNA methylation by reducing available ubiquitinated H3 (171). Recently, the same group has shown that Usp7 single depletion did not change DNA methylation level while Usp7/ATAD5 double depletion increased DNA methylation levels in *Xenopus* egg extract. This study shows that de-

ubiquitination of Paf15 by Usp7 leads to the removal of Paf15 from chromatin in an ATAD5-dependent manner (178). This suggest that the Usp7/ATAD5 dependent removal of the ubPaf15 signal controls excessive DNA methylation. There is also controversy about when Usp7 interacts with Uhrf1. Zhang *et al.* (2015) showed that Usp7 binds to the PBR region of Uhrf1 and promotes its binding to the H3 tail, suggesting that Usp7 interacts with Uhrf1 before it is recruited to chromatin (153). In contrast, Felle *et al.* (2011) showed that Usp7/Dnmt1 forms a soluble dimeric complex which is recruited to hemi-methylated sites by Uhrf1, forming a trimeric complex on chromatin (175). Further studies are required to elucidate the role of Usp7 and how it is recruited and regulated during this process.

It is likely that all these models are coexisting and coregulated within the cells. In addition to Usp7, the interactions with PCNA, Lig1, Paf15 and H3 also reflect a collaboration between DNA methylation and chromatin replication machineries, which postulates the possibility of a dependency of the DNA methylation machinery on efficient chromatin replication (119). Uhrf1 may interact with additional proteins to ensure that DNA methylation is faithfully propagated, but also to promote other processes during DNA replication such as histone assembly and remodelling. Uhrf1 could also be forming a macro-molecular complex or different sub-complexes with these proteins and other yet unknown proteins recruited on chromatin in S phase to promote DNA methylation, but also to regulate other chromatin maturation processes (136).

These findings show that different mechanisms with different regulations could control DNA methylation maintenance in different circumstances, e.g. in early and late replicated regions, on leading and lagging strands and/or naked and chromatinised DNA. All of them could coexist in different genomic regions, active genes *vs.* repressed genes/ euchromatin *vs.* heterochromatin. It could also be cell-type specific, which would be supported by the differences found between studies carried out in different systems.

1.4.4. Other roles of Uhrf1 in DNA replication: translesion DNA synthesis

During DNA replication, encountered lesions within DNA can block replication machinery progression and lead to genome instability. To avoid this, cells have a DNA damage tolerance strategy: translesion DNA synthesis (TLS) to bypass replication-blocking lesions. It is executed through a switch of regular replicative DNA polymerases for specialized TLS polymerases that can incorporate nucleotides opposite the damage. This process is mediated by ubiquitinated PCNA. As mentioned, di-mono-ubiquitinated Paf15 stably interacts with PCNA during normal DNA replication. When the replisome encounters a blocking lesion, Paf15 is removed from PCNA, probably by ubiquitin-mediated proteasomal degradation, facilitating PCNA interaction with TLS polymerases (179). As Uhrf1 is responsible for the di-mono-ubiquitination of Paf15 promoting its association with PCNA, it thus regulates replication block bypass (173).

1.4.5. Role of Uhrf1 in DNA damage response

In recent years, the involvement of Uhrf1 in the DNA damage response (DDR) and therefore in preserving genome stability has been accentuated and this function has been identified to be as crucial as its role in maintaining the epigenome. Removal of Uhrf1 causes DNA damage in zebrafish and generates chromosomal aberrations and spontaneous sister chromatid exchange in cells. When Uhrf1 is absent or reduced, it compromises the DSBs repair that occur during the S phase. This leads to increased DNA damage signalling (γH2AX) and prolongs the cell cycle, causing an accumulation of cells in the G2/M phases. Therefore, Uhrf1 deficiency makes cells more vulnerable to DNA damage. It was shown in mouse embryonic stem cells that alterations in Uhrf1 enhance their sensitivity to DNA damaging agents: X-rays, UV light, N-methyl-N”- nitro-N-nitrosoguanidine, and hydroxyurea. In these cases, there is a reduction in γH2AX foci making cells more sensitive to DNA damage. This could be explained by a defective DDR (180). All these defects occur because Uhrf1 regulates ICL and DSB repair.

Specifically, Uhrf1 is a sensor for inter-strand crosslinks and serves as a key factor for shifting the DDR towards homologous recombination to resolve double-strand breaks (140,180).

Importantly, the SRA domain of Uhrf1 recognizes and binds inter-strand crosslinks (ICLs) immediately after they appear in the DNA, serving as a platform for FANCD2 binding, which then recruits endonucleases required for ICL repair (181). Uhrf2, which is structurally similar, has been shown to interact with Uhrf1 for the cooperative recruitment of FANCD2 to ICLs (182). Moreover, Uhrf1 directly interacts with and regulates the activity of the ERCC1/XPF and MUS81/EME1 endonucleases involved in ICL repair. The binding between Uhrf1 and the DNA repair enzyme EME1 rescues stalled DNA replication (183). Uhrf1 deficient cells lack accumulation of γH2AX and 53BP1 foci after exposure to mitomycin C which could be a result of nuclease deficiency (184).

Furthermore, Uhrf1 is a key factor for the choice between homologous recombination (HR) and non-homologous end joining (NHEJ) by participating in the interplay between BRCA1 and 53BP1. BRCA1, a promoter of HR, recruits phosphorylated Uhrf1 (Ser674ph) to DSBs in S phase. Uhrf1 in turn carries out polyubiquitination of RIF1 leading to its subsequent dissociation from 53BP1 and DSBs, inhibiting the NHEJ repair pathway and favouring HR initiation (163). In addition, Uhrf1 methylation at K385 by SET7 in response to DNA damage promotes a Uhrf1-PCNA interaction and polyubiquitination of PCNA required for HR induction. Phosphorylation of Uhrf1 at S661 is required for SET7 interaction (162). Another study from the same group found that PARP1 binds methylated Uhrf1 promoting its role in HR (185). In contrast, inhibition of Uhrf1 downregulates Ku70 and Ku80 expression, a protein complex involved in NHEJ repair (186).

Uhrf1 is also additionally involved in single-strand DNA break (SSBs) repair as it interacts with MPG, an enzyme that acts in the DNA base excision repair pathway (187). Thus, Uhrf1 plays a very pleiotropic and crucial role in maintenance of genome stability.

1.4.6. Role of Uhrf1 in gene expression

Initially, Uhrf1 was discovered as a transcription factor involved in the regulation of TopoIIα expression by the binding to a CCAAT box in its promoter (188). Now, it is known that Uhrf1 downregulates expression of many tumour suppressor genes including RB1, p16, p21, BRCA1, PPARG, FOXO4, MEG3, CDH13 and SHP1, SOCS3 and 3OST2, CDX2, RUNX3 and PML. This pro-oncogenic role of Uhrf1 is accomplished by promoting repressive epigenetic marks in the promoters of these genes. Uhrf1 forms a repressive complex with HDAC1, DNMT1, G9A and SUV39H1 that mediate silencing of tumour suppressor genes by inducing hyper-methylation of CpG islands, histone deacetylation and histone methylation through the recruitment of DNMT1, HDAC1 and G9A and SUV39H1 methyltransferases, respectively (140,189). The Uhrf1-mediated recruitment of this repressive complex has been shown to inhibit BRCA1 transcription by inducing DNA methylation and histone modifications (190). The retinoblastoma protein (pRB), encoded by the RB1 gene, is a key tumour suppressor protein that inhibits cell cycle progression. It has been shown that Uhrf1 binds to the methylated RB1 promoter and downregulates its expression, favouring S phase entry (191,192). Uhrf1 also inhibits epigenetically p16, a G1/S cell cycle checkpoint protein that promotes apoptosis and acts upstream of pRB (165). Furthermore, knockdown of Uhrf1 or inhibition of its PHD or SRA domains generates promoter de-methylation and results in a transcriptional reactivation of silenced tumour suppressor genes in cancer cells (193). These studies provide evidence that Uhrf1 acts as an epigenetic coordinator mediating silencing of many genes.

1.4.7. Importance of studying Uhfr1: role as a tumour promoter

As described above, Uhrf1 is involved in many cellular processes that are related to tumour development. Indeed, Uhrf1 is overexpressed in several cancer types, such as lung, breast, gastric, prostate and colorectal. Furthermore, Uhrf1 expression directly correlates with the state or grade of cancer and its upregulation correlates with poorer patient prognosis. Many studies support the potential of Uhrf1 as a powerful diagnostic and prognostic biomarker of cancer. This pro-oncogenic role is due to its role in cell proliferation, migration and invasion (141,189).

As mentioned, cancer cells are characterised by a general DNA hypomethylation that induces genome instability and expression of oncogenes as well as a specific hypermethylation of CpG islands within promoters of tumour suppressor genes that leads to silencing. As a key factor in DNA methylation maintenance by the recruitment of Dnmt1, Uhrf1 deregulation leads to DNA methylation alterations. Generally, Uhrf1 depletion results in global DNA hypomethylation. However, it has been also shown that overexpression of Uhrf1 could cause DNA hypomethylation by reducing Dnmt1 and Dnmt3 levels and their interaction with DNA (189).

1.4.7.1. Uhrf1 promotes cell proliferation

Uhrf1 is mostly expressed in actively proliferating cells, being undetectable in highly differentiated tissues (188). In normal cells, Uhrf1 expression is cell cycle regulated and its levels increase in G1/beginning of S phase, peaking during mid S phase, during replication of heterochromatic regions, and being down-regulated at the end of the M phase (180). However, in cancer cells, Uhrf1 is expressed during the entire cell cycle (141,189). Overexpression of Uhrf1 induces S phase entry and cell proliferation (192). In contrast, depletion of Uhrf1 leads to cell cycle arrest and apoptosis in cancer cells (194).

The induction of cell proliferation is mostly due to its role as a tumour suppressor gene silencer, explained previously. The silencing of tumour suppressor genes, which limit cell growth and proliferation, is a hallmark of cancer (Hanahan and Weinberg, 2011). It has been previously shown that Uhrf1 mediates epigenetic silencing of many tumour suppressor genes and, therefore, the increase of Uhrf1 levels leads to cell proliferation and cancer.

Uhrf1 promotes cell proliferation not only by silencing tumour suppressor genes but also by using its E3 ligase activity. For instance, Uhrf1 induce ubiquitination-mediated degradation of the tumour suppressor protein PML (195). Furthermore, overexpression of Uhrf1 promotes cell proliferation through reduction of protein levels of an inhibitor of DNA replication licensing, Geminin, and activation of PI3K/Akt signalling pathway, which regulates the cell cycle reducing apoptosis (196). Uhrf1 also inhibits p53-mediated growth arrest and apoptosis by inducing degradation-independent ubiquitination of TIP60, supressing its ability to acetylate and activate p53 (197). In addition, Uhrf1 ubiquitinates and down-regulates p53 transactivation activity helping renal carcinoma cells to escape from apoptosis (198). Uhrf1 further favours cell proliferation by helping tumour vascularisation by increasing VEGF expression (165).

1.4.7.2. Other roles of Uhrf1 in tumorigenesis

The role of Uhrf1 in cell mobility, enhancing migration and invasion of cancer cells, also favours tumour spread and metastasis. Uhrf1 promotes migration and invasion of cancer cells by downregulating E-cadherin expression and, therefore, increasing epithelial to mesenchymal transition (EMT) in a Rb1-dependent manner (191). However, the decrease in Uhrf1 levels has also been shown to promote EMT. Hypoxia-induced downregulation of Uhrf1 causes epigenetic changes that lead to upregulation of CXCR4 and subsequent activation of AKT and JNK that increases the expression of IL-6, which activates the JAK/STAT/Snail signalling axis that induces EMT (199). It has been also shown that Uhrf1 promotes angiogenesis, another hallmark

of cancer, by increasing VEGF expression through downregulation of p16, an inhibitor of VEGF expression (165). Finally, Uhrf1 may play an important role in cancer cell resistance to chemo and radiotherapy. Downregulation of Uhrf1 enhances sensitivity to radiotherapy by decreasing the capacity to repair damaged DNA (186).

1.4.8. Regulation of Uhrf1 levels

Considering the role of Uhrf1 in so many important cellular processes, its expression levels are tightly regulated (Figure 14) at the gene level. Transcription factors E2F1, E2F8, SP1 and FOXM1 directly bind to different sites in the UHFR1 promoter and stimulate its expression. CD47 also induces Uhrf1 expression by activating NFκB-mediated signalling (189). Histone H3K9 methyltransferase G9a is recruited to the UHRF1 promoter along with the YY1 factor, repressing Uhrf1 expression by competing with H3 acetylation (200). Uhrf1 is also negatively regulated by the p53 checkpoint proteins at the G1/S transition (201). Induction of p53 in response to many natural anticancer compounds upregulates p21, leading to decreased Uhrf1 expression directly or through inhibition of E2F1 (140).

Secondly, microRNAs (miRs) can also regulate Uhrf1 mRNA stability (202). Finally, Uhrf1 levels can also be controlled by regulating Uhrf1 protein stability. As with many other proteins, Uhrf1 levels depend on ubiquitination and deubiquitination activities that regulate its proteasomal degradation. Uhrf1 can be auto-ubiquitinated by its E3 ligase activity for degradation (189), but the $SCF^{\beta\text{-}TrCP}$ ubiquitin ligase can also ubiquitinate and mediate its degradation. This interaction requires phosphorylation of Uhrf1 at S108 by CK1δ (157). On the other hand, deubiquitinating enzyme Usp7 stabilises Uhrf1 by regulating its proteasomal degradation (153,175). During M phase, the kinase CDK1-cyclin B phosphorylates Uhrf1 at S652, disrupting its interaction with Usp7 and leading to ubiquitination-mediated degradation of Uhrf1 (160). Moreover, Uhrf1 is a Hsp90 client protein, being stabilised by the chaperone

complex. Pharmacological inhibition of Hsp90 causes Uhrf1 ubiquitination and proteasome-dependent degradation independently of SCF$^{\beta\text{-}TrCP}$ or the intrinsic E3 ligase activity of Uhrf1 or previously identified E3 ligases for Hsp90 client proteins (203).

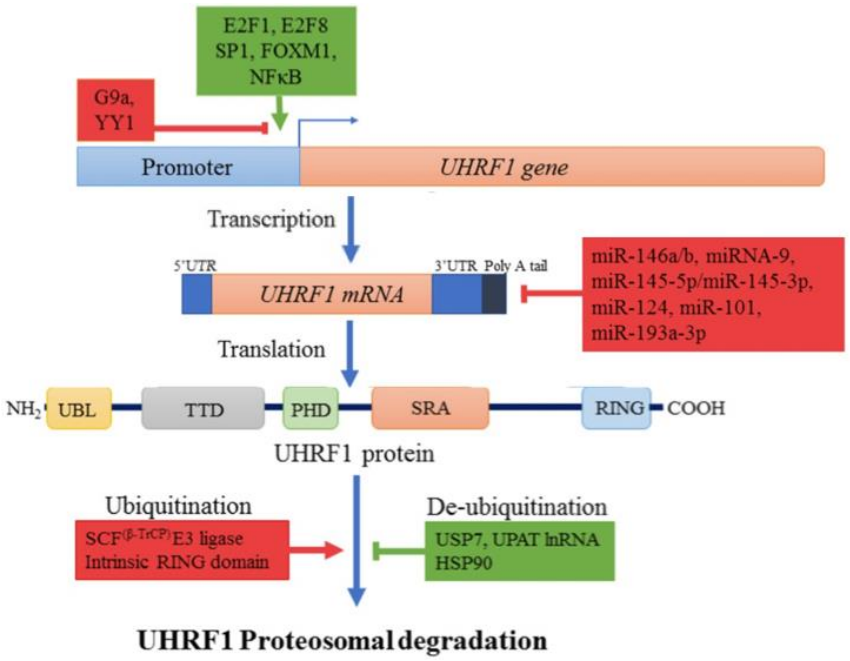


Figure 14. Regulation mechanisms of Uhrf1 levels. Green boxes represent positive regulators that increase Uhrf1 expression or stability. Red boxes represent negative regulators that decrease Uhrf1 expression or mRNA and protein stability. Adapted from (189).

1.5. *Xenopus laevis* egg extract as a model system

The extract obtained from *Xenopus laevis* eggs is a powerful cell-free system to study DNA replication. It is a synchronous system to study the eukaryotic cell cycle and recapitulates *in vitro* many of the fundamental biological processes that occur *in vivo*. In addition, the isolation of the nuclei or chromatin is simpler than in a cell-based model system, which makes it easier to study chromatin bound proteins.

After fertilisation, the egg goes through 12 rounds of cell divisions in the absence of transcription, only using proteins and mRNA that have previously accumulated in the egg. As there is therefore no active transcription in the egg extract model system, this allows us to separate DNA replication and transcription processes, which makes it easier to study the direct role of chromatin bound proteins and their PTMs during DNA replication (204,205).

To obtain the egg extract, unfertilised eggs arrested in metaphase of meiosis II are crushed and subjected to low-speed centrifugation and the cytoplasmic fraction including membranes is collected (low speed supernatant (LSS)) (204,205). When demembranated sperm nuclei are added to the extract, DNA is first decondensed by removing sperm specific proteins (protamines), chromatin is then assembled by formation of nucleosomes and a nucleus is formed (206,207).

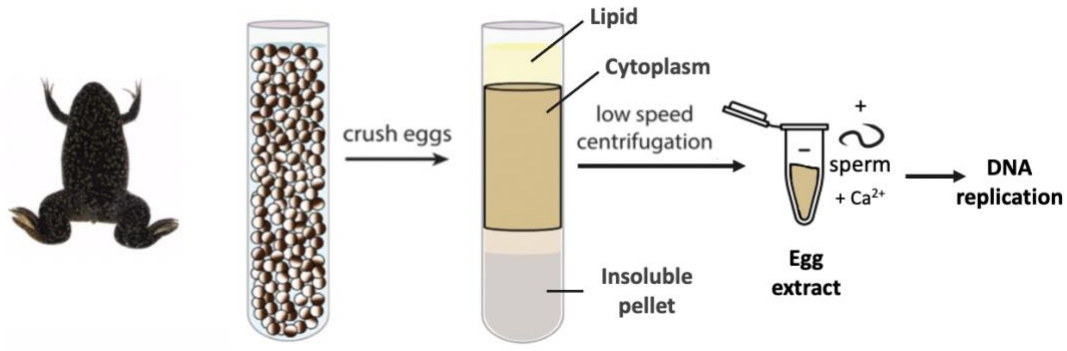


Figure 13. Schematic representation of preparation of *Xenopus laevis* egg extract. Adapted from (204).

1.6. Aims

Previous work in the Gambus lab identified that histone H3 ubiquitinated at lysines 18 and 23 (K18 and K23) was one of the most abundant ubiquitinated proteins during DNA replication in *Xenopus laevis* egg extract. This ubiquitination has been shown by others to be mediated by the E3 ubiquitin ligase Uhrf1 and to be involved in DNA methylation maintenance by the recruitment of the DNA methylase Dnmt1. Although the role of Uhrf1 in DNA methylation maintenance is clear, many questions about the mechanism itself and how it is coordinated with other processes occurring at the same time, such as DNA replication and chromatin re-establishment, remain to be addressed.

Distinct modes of Dnmt1 recruitment have been proposed. Apart from H3, other proteins such as Paf15 and histone H2B are ubiquitinated by Uhrf1 to mediate DNA methylation maintenance. Also, direct interaction with Uhrf1 has been proposed. In addition, different mechanisms for Uhrf1 recruitment to replication sites have been identified. Uhrf1 also interact with many other proteins during DNA replication such as Usp7, Lig1, HDAC1, and probably others still unknown, and that could link DNA methylation with processes taking place at the same time or that could explain other roles of Uhrf1 during DNA replication.

Apart from this, the mechanism of DNA replication and the proteins involved vary between the leading and lagging strands with PCNA/Paf15 and Lig1 enriched at the lagging strand. DNA accessibility for Dnmt1 is different on naked or chromatinised DNA, and histone variants and their PTMs also differ between genomic regions.

Finally, histone H3 ubiquitination is a substantially large modification, considering that the histone H3 is a small protein, so this modification could be regulating other processes during chromatin replication and coordinating them with DNA methylation.

Having all of this in mind, the aim of my project is to understand the roles of Uhrf1 and histone H3 ubiquitination in DNA methylation and chromatin re-establishment during DNA replication. Firstly, I would like to confirm that Uhrf1 mediates histone H3 ubiquitination and Dnmt1 recruitment to chromatin. Secondly, I aim to clarify the mechanism of Dnmt1 recruitment by Uhrf1. Finally, the objective is to find out other roles of Uhrf1 and histone H3 ubiquitination during chromatin replication. To achieve these aims I have used *Xenopus laevis* egg extract as a model system. Immunodepletion of Uhrf1 form the extract combined with the addition of recombinant Uhrf1 or the use of recombinant mutants of histone H3 that cannot be ubiquitinated, allowed the study of the role of these proteins during DNA replication. This is an excellent model system for addressing the mechanism of Uhrf1 regulation during DNA replication because transcription is not present, so indirect effects of disrupting Uhrf1 regulated transcription will not be present. The same is true for exchanging histones during DNA replication - we will not impede transcriptional roles of histones and will just focus on their roles in DNA replication.

2. MATERIALS AND METHODS

2.1. Tables

Table 2. 1. Composition of buffers used in *Xenopus laevis* egg extract protocols.

10X MMR (10x)
1 M NaCl, 20 mM KCl, 10 mM $MgCl_2$, 20 mM $CaCl_2$, 1 mM EDTA, 50 mM HEPES. Adjust pH to 7.8 with NaOH.
UEB
50 mM KCl, 50 mM HEPES, 5 mM $MgCl_2$, 5 mM EGTA. Adjust pH to 7.6 with KOH.
Cysteine solution
2.2% cysteine, 5 mM EGTA. Adjust pH to 7.6 with KOH.
2X ANIB100
100 mM HEPES pH 7.6, 200 mM KAc, 20 mM MgAc, 5 mM Mg-ATP (added from a stock of: 250 mM ATP; 250 mM $MgCl_2$; pH 6.7 with NaOH), 1 mM spermidine, 0.6 mM spermine, 2 µg/ml of each aprotinin, leupeptin and pepstatin, 50 mM β-glycerophosphate, 0.2 mM Na_3VO_4, 0.2 µM microcystin-LR.
1X ANIB
Prepared by mixing 1 volume of 2X ANIB100 with 1 volume of H2O, 0.1% Triton X-100, 0.1 mM PMSF, 10 mM 2-chloroacetamide.
LFB1/50
10% sucrose, 50 mM KCl, 40 mM HEPES pH 8, 20 mM K phosphate pH 8, 2 mM $MgCl_2$, 1 mM EGTA, 2 mM DTT, 1 µg/ml of each: aprotinin, leupeptin and pepstatin. For LFB1/100, 100 mM KCl is used.
PBST
1x PBS, 0.1% Tween 20.
Stop-C
5 mM EGTA, 0.5% SDS, 20 mM Tris-HCl pH7.5.
5% TCA
5% w:v TCA, 0.5% w:v $Na_4P_2O_7$ in 10 l H_2O
10% TCA
10% w:v TCA , 2% w:v $Na_4P_2O_7$ in 10 l H_2O

Table 2. 2. Composition of buffers used for mouse sperm preparation.

PBS based buffers
• PBS containing 0.5% w:v polyvinylpyrrolidone (PVP). • PBS containing 30% glycerol.
SMH buffers
• SMH: 20 mM HEPES-KOH pH 7.5, 250 mM sucrose, 2 mM $MgCl_2$. • SMH containing 3% w:v BSA. • SMH containing 0.4% w:v BSA. • SMH containing 0.4% w:v BSA and 30% glycerol.

Table 2. 3. **Inhibitors used in *Xenopus* egg extract.**

Inhibitor	Concentration of Stock and addition to extract
E1 inhibitor, TAK-243 (mln7243) (S8341, selleckchem)	100 mM dissolved in DMSO (used at 300 µM) Added after sperm DNA addition
p97 inhibitor NMS873 (17674, Cayman Chemical Company)	10 mM dissolved in DMSO (used at 50 µM) Added 15 minutes after sperm DNA addition

Table 2. 4. **Recombinant proteins added to *Xenopus laevis* egg extract.**

Recombinant protein	Addition to extract
GST- *X.laevis* Uhrf1 Purified in this study (Section 2.6.5)	Added at 10 µg/ml after sperm DNA addition
His-SUMO- *X.laevis* Uhrf1 Purified in this study (Section 2.6.5)	Added at 10 µg/ml after sperm DNA addition
Untagged *X.laevis* Uhrf1 Purified in this study (Section 2.6.5)	Added at 10 µg/ml after sperm DNA addition
His-human Uhrf1 Commercial (81015, Active Motif)	Added at 10 µg/ml after sperm DNA addition
His-*X.laevis* histone H3 wild-type Purified from inclusion bodies by a collaborator Andrew Bowman at Warwick University.	Added at 250 µg/ml before sperm DNA addition
His- *X.laevis* H3 mutant (H3K14/K18/K23/K27R) Purified from inclusion bodies by a collaborator Andrew Bowman at Warwick University.	Added at 250 µg/ml before sperm DNA addition
p27 Produced by other members of the lab as previously described (Walter, 2000)	Added at 100 nM after sperm DNA addition
His-human Ubiquitin Commercial (U-530-02M, Boston Biochem)	Added at 500 µg/ml after sperm DNA addition
His-human UbiNOK Commercial (UM-HNOK, Boston Biochem)	Added at 500 µg/ml after sperm DNA addition

Table 2. 5. **List of antibodies used for western blotting.**

Primary antibodies			
Antibody	**Specie**	**Dilution**	**Provider**
Anti-Mcm7	Sheep	1:2000	Previously described (Moreno *et al.*, 2019)
Anti-Cdc45	Sheep	1:500	Previously described (Gambus *et al.*, 2011)
Anti-Psf2	Sheep	1:500	Previously described (Gambus *et al.*, 2011)

Anti -PCNA	Mouse	1:2000	P8825 - Sigma
Anti-Uhrf1	Sheep	1:1000	This study
Anti-Lig1	Rabbit	1:1000	This study
Anti-Dnmt1	Rabbit	1:5000	This study
Anti-H3	Rabbit	1:1000	9715 - Cell Signaling
Anti-CAF-1	Rabbit	1:1000	Kindly provided by Dr. G. Almouzni
Anti-Spt16	Rabbit	1:1000	sc-28734 - Santa Cruz Biotechnology
Anti-Fen1	Rabbit	1:1000	This study
Anti-Paf15	Rabbit	1:500	This study
Anti-RPA	Rabbit	1:500	This study
Anti-His	Mouse	1:1000	H1029 - Sigma
Anti-GST	Rabbit	1:1000	G7781 - Sigma
Anti-ubiquitin	Mouse	1:1000	3936T - Cell Signaling
Secondary antibodies			
Antibody	**Species**	**Dilution**	**Provider**
HRP-sheep-IgG	Donkey	1:10000	A34151ML - Sigma
HRP-rabbit-IgG	Goat	1:25000	A05451ML - Sigma
HRP-mouse-IgG	Goat	1:5000	A52781ML - Sigma

Table 2. 6. List of antibiotics used.

Antibiotic	Concentration of Stock
Ampicillin (Sigma)	100 mg/ml in 50% ethanol
Kanamycin (VWR)	50 mg/ml in distilled water
Chloroamphenicol (Alpha aesar)	30 mg/ml in 100% ethanol
Gentamycin (Sigma)	50 mg/ml in distilled water

Table 2. 7. Antibiotic resistance of plasmids used.

Plasmid	Antibiotic resistance
pGS21-GST-xUhrf1	Ampicillin
pET24-His-SUMO-xUhrf1	Kanamycin
pET24-His-Ulp1	Kanamycin
pGEX-4T-1-GST-xPAF15	Ampicillin
pET22b(+)-His-xLig1	Ampicillin
pET28c(+)-His-xDnmt1	Kanamycin
pET19b-His-xRPA	Ampicillin
pET28b-hFen1-His	Kanamycin

2.2. Working with mouse sperm

2.2.1. Preparation of mouse sperm nuclei

Mouse sperm nuclei were prepared as previously described (206). The sperm was obtained from 9 mouse cauda epididymis freshly isolated from the animals and kept in pre-warmed M2 media (M7167, Sigma). The cauda epididymis were poured in a tissue culture (TC) plate containing fresh M2 media and the sperm was isolated by cutting the duct of the cauda using scissors and then releasing the sperm out by pressing the surface of the cauda with a forceps. The released sperm was incubated 10 min at 37°C in a TC incubator to allow them to disperse in the media. The sperm was then collected in a 12 ml Falcon tube, spun down 5 min at 2,000 g to remove the supernatant and the pellet was washed three times with PBS containing 0.5% polyvinylpyrrolidone (Table 2. 2). The pellet was resuspended in 1 ml of PBS and split into two 1.5 ml Eppendorf tubes.

Heads and tails were then separated by sonication at 4°C (10 cycles of 1-sec ON and 9-sec OFF, at high setting) using an ultrasound generator equipped with a water bath (Bioruptor, Diagenode). Once checked that heads and tails were separated using a phase microscope, both 0.5 ml samples were combined and transferred into a 5 ml Falcon tube containing 4 ml of 30% glycerol-PBS solution, carefully to not disturb the surface of the buffer. Heads were isolated into the glycerol cushion by spinning at 2,000 g for 10 min in a swinging bucket rotor. Detached tails in the top layer were removed and the walls of the tube and the top of the cushion were washed three times with 1 ml of PBS. The cushion was then discarded and the pellet containing the sperm heads was resuspended in 0.5 ml of SMH (Table 2. 2) and split into two 0.5 ml Eppendorf tubes.

For permeabilization of membranes, the samples were incubated with streptolysin-O (S5265-Sigma; final concentration of 40 units/ml) for 15 min on ice. For demembranation, lysolecithin

was used instead (25 µl of 5 mg/ml freshly made stock per cauda). After the incubation, the percentage of permeabilization was checked by spotting a 1 µl sample on a microscope slide and mixing it with 1 µl of Hoechst 33258 dye (5824/50, Tocris Bioscience, 10 µg/ml final concentration) and visualizing at 20x magnification using an EVOS fluorescent microscope. Permeabilized or demembranated sperm were stained blue by the binding of Hoechst with the DNA. After heads were permeabilized, an equal volume of SMH containing 3% BSA (Table 2. 2) was added and the samples were spun down at 3,000 g for 10 min. After the spin, three washes with 0.5 ml of SMH containing 0.4% BSA (Table 2. 2) were carried out and the samples were combined in one single Eppendorf tube. For reduction of protamines, the samples containing the sperm heads were incubated with 2 mM DTT at 37ºC for 15 min. Finally, after three more washes with SMH containing 0.4% BSA, the mouse sperm nuclei sample was obtained by resuspending in 200 µl of SMH containing 30% glycerol and 0.4% BSA. This sample was frozen in liquid nitrogen and stored at -80ºC. The concentration was measured in nuclei/ml by staining sperm DNA with Hoechst 33258 (10 µg/ml final concentration) and counting permeabilized mouse nuclei in a hemocytometer.

2.3. Working with *Xenopus laevis* egg extract

2.3.1. Preparation of metaphase II arrested *Xenopus laevis* egg extract

X. laevis egg extract is obtained from unfertilized female frog oocytes. Metaphase II arrested *Xenopus laevis* egg extract was prepared as previously described (205).

Between 2-7 days before the eggs were needed, a group of around ten frogs received a priming dose of 150 units of follicle-stimulating hormone Folligon (Intervet). At approximately 4 pm on the day before the day of egg collection, these frogs were administered 500 units of chorionic gonadotropin Chorulon (Intervet) and transferred to individual laying tanks containing 2.5 l of 1x MMR solution (Table 2. 1). The frogs were kept in these tanks overnight at ≤ 23°C for egg

laying. The following morning, high-quality eggs, distinguishable by a clear circumferential differentiation between dark animal and light vegetal poles (greatest dark/light contrast), were collected and placed in a 1 l glass beaker. Eggs showing signs of apoptosis, such as being larger and white in appearance or forming strings, were not collected.

Unfertilised good quality eggs were rinsed with 1x MMR (Table 2. 1). Subsequently, the eggs were de-jellied by rinsing in cysteine solution (Table 2. 1) and then washed again with 1xMMR. Finally, a last wash was performed in UEB (Table 2. 1) supplemented with 2 mM DTT (A3668, PanReac AppliChem), removing apoptotic floating eggs using a Pasteur pipette. The eggs were then collected in Ultra Clear 14 x 95 mm centrifuge tubes (344060, Beckman coulter) containing 1 mL of UEB supplemented with 2 mM DTT, protease inhibitors (aprotinin, pepstatin and leupeptin (APL)) and cytochalasin D at a final concentration of 10 mg/ml for both. Eggs were firstly packed by low-speed spin (1,400 g) in a swinging bucket rotor (JS-13.1, Beckman Coulter) for 1 min, removing apoptotic eggs on the surface afterwards, and then crushed by a high-speed spin (23,000g) for 10 min in the same rotor. The brown cytoplasmic layer obtained was collected using a 20-G needle and a 1 ml syringe and supplemented with protease inhibitors, cytochalasin D (final concentration 10 mg/ml for both) and 15% of LFB1/50 (Table 2. 1). Finally, ultracentrifugation at 110,000g in a SW50 swing-out rotor (Beckman Coulter) for 20 min at 4ºC was performed. The yellow lipid layer on the top was removed using a spatula and the cytoplasmic fraction was collected carefully (avoiding disturbing the mitochondrial layer below) using a micropipette. The extract obtained was supplemented with 1% v:v glycerol, frozen in liquid nitrogen in the form of 25-60 µl beads and stored at -80°C.

2.3.2. Use of *Xenopus laevis* egg extract

To use *Xenopus laevis* egg extract for the different experiments, the number of frozen beads corresponding to the required volume of extract were transferred to an Eppendorf tube. After thawing at room temperature, the extract was used immediately after defrosting for the experiments.

2.3.3. Activation of *Xenopus leavis* egg extract

Xenopus laevis egg extract requires activation to perform DNA replication. Normally the eggs are arrested in metaphase II of meiosis and they progress into interphase of the first mitotic cell cycle due to a Ca^{2+} wave generated post-fertilization. By adding 0.3 mM $CaCl_2$ to the extract, we mimic this Ca^{2+} wave in the laboratory, allowing the exit from meiosis and entry into anaphase and the mitotic cycle. In addition, the DNA replication reaction requires a high amount of energy in the form of ATP, achieved in the lab by supplementing the extract with an energy regenerator (ER) solution (25 mM phosphocreatine (13810831, Roche) and 15 μg / ml creatine phosphokinase (10127566001, Roche) at final concentration). Finally, the extract was also supplemented with cycloheximide at 250 μg /ml (CHX, Sigma) to block cyclin synthesis and cell cycle progression. Usually, after the addition of $CaCl_2$, ER and CHX, the extract was incubated for 15 min at room temperature for activation.

2.3.4. Chromatin Isolation

Chromatin was isolated to analyse bound proteins during DNA replication time-courses after different treatments as previously described (205).

Metaphase II arrested egg extract was activated as described above for 15 min. After activation, a 20 μl sample was taken as negative control (-DNA), which was also supplemented with the appropriate treatment when required and treated in the same way to the rest of samples.

Activated extract was then supplemented with demembranated *X. laevis* sperm nuclei (at 7-10 ng/µl) or mouse sperm nuclei (3300 nuclei/µl) and appropriate recombinant proteins (Table 2. 4) or inhibitors (Table 2. 3) and resuspended using pre-cut tips to avoid damaging the DNA. The sample was then aliquoted by transferring 20 µl samples into 1.5 ml Treff tubes (9607811903, TreffLab), one aliquot per time point needed. The aliquots were incubated at 23°C during the duration of the time-course. At each time point the replication reaction was stopped in the appropriate tubes by adding 0.5 ml of cold 1x ANIB (Table 2. 1) and resuspending thoroughly. The samples were then underlaid with 100 µl of 1x ANIB containing 20% sucrose. DNA was isolated in the sucrose cushion by spinning down at 2100 g for 5 min at 4°C in a swinging rotor. The buffer above the sucrose cushion was removed, the walls of the tube and cushion top were washed twice with 100 µl 1x ANIB and most of the cushion was finally discarded. The samples were then spun at maximum speed in a benchtop centrifuge for 2 min at RT. The supernatant was removed and the pellet containing the chromatin was resuspended in 2x NuPAGE LDS loading buffer and boiled for 5 min for immunoblotting analysis.

2.3.5. TCA assay

This assay was carried out to analyse DNA replication kinetics in the extract by measuring the incorporation of radionucleotides into the synthesised DNA at different times. This protocol was previously described (205).

Metaphase II arrested egg extract was activated as above (Section 2.3.3) and the activated extract was supplemented with *Xenopus* or mouse sperm DNA and 16.5 nM α-[P^{32}]-dATP (NEG512H250UC, Perkin Elmer) and mixed thoroughly. When adding recombinant proteins to the extract, the sample was aliquoted in as many 0.5 ml Eppendorf tubes as treatments used and the recombinant proteins were added to the activated extract at the concentration specified

in Table 2. 4 and resuspended. All samples were then split into 3-5 µl aliquots (as many as number of time points needed) and incubated at 23ºC for the duration of the time course. The reaction was stopped at each time point by the addition of 160 µl Stop-C buffer (Table 2. 1) containing freshly added 0.2 mg/ml proteinase K solution (740506, Macherey Nagel; stock: 10 mM Tris-HCl, 20 mg/ml proteinase K, 50% v:v glycerol, pH 7.5) to each sample, resuspension and the incubation at 37ºC for 30 min. Once all samples were incubated for 30 min, DNA was precipitated in all of them by transferring the samples into a 5 ml Falcon tube containing 4 ml of 10% TCA, (Table 2. 1) mixing thoroughly and incubating at 4ºC for at least 30 min.

Samples containing the precipitated DNA were then filtered through 25 mm glass fibre filters (11512083, Fisherbrand) under vacum on a manifold (Millipore). Before filtering, a 40 µl sample was taken from each tube and deposited onto a 25 mm Whatmann paper filter (1001-025, GE healthcare life sciences) to measure the total radiation level. The tubes that were containing the precipitated DNA were re-filled with 10% TCA and this sample also passed through the filter to ensure that there is not DNA remaining in the tubes. Filters were then washed with around 8 ml of 5% TCA (Table 2. 1) solution and rinsed with 70% ethanol by passing the solution through them. The glass fibre and paper filters were finally dried using an infrared lamp and suspended in 0.5 ml of the scintillant Ultima Gold F (6013179, Perkin Elmer) in a scintillation counter tube. The radiation levels were counted in a scintillation counter (Tri-Carb 2900TR). Incorporated α-[P^{32}]-dATP measured on a glass fibre filter was normalized against the total level on the paper filter and ng/ul of synthesized DNA was calculated by multiplying by 0.654 (205). This calculation assumes a dNTP pool in the extract of approximately 50 µM, an average molecular weight of 327 Da for dNMPs and an equal incorporation of all 4 dNMPs into the DNA structure.

2.3.6. Testing nuclear assembly under the microscope

For visualization of nuclei shape under the microscope, Hoechst was used as dye. Metaphase II arrested egg extract was activated as above (Section 2.3.3) and activated extract was then incubated with *Xenopus* or mouse sperm DNA (adding 3300 nuclei/µl for both) at 23°C. At the indicated time points, 1 µl of reaction was spotted onto a microscope slide with 1 µl of Hoechst 33258 (10 µg/ml final concentration) and visualized at 20x or 40x magnification under an EVOS fluorescent microscope (Thermo Fisher Scientific).

For visualization of replicating *Xenopus* or mouse sperm nuclei, the fluorescent dyaminoallyl Cy3-dUTP was used. Activated extract was supplemented with sperm DNA (3300 nuclei/µl of mouse or *Xenopus* sperm) and 10 µM of Cy3-dUTP (Jena Bioscience) and incubated at 23°C. At indicated time points, 1 µl of reaction was spotted onto a microscope slide with 1 µl of Hoechst 33258, 10 µg/ml final concentration, and visualized at 20x or 40x magnification under an EVOS microscope.

Finally, for visualizing the nuclear membrane formation, Dil stain (D282; Thermo Fisher Scientific) was utilized as a dye (Priego *et al*. 2019). *Xenopus* egg extract was activated and incubated with sperm DNA for DNA replication to take place. After 60 min, 1 µl of the sample was spotted onto a microscope slide with 1 µl of a mix Hoechst/Dil stain (1 µg/ml and 10 µg/ml final concentration respectively). The sample was incubated with the dye at room temperature for 30 min and finally visualized at 40x magnification under an EVOS microscope.

2.3.7. Protein release from replicating chromatin

The protocol to release proteins from chromatin was previously described (208). Metaphase II arrested egg extract was activated as above (Section 2.3.3). After activation, sperm DNA (10 ng/ µl) was added, thoroughly mixed and incubated at 23°C for the DNA replication to take place. At the peak of replication (normally 45 min), the replication reaction was stopped by diluting the extract with 10-20 volumes of ice cold 1x ANIB buffer (Table 2. 1), transferring to a 15 ml falcon tube and carefully underlaying with 3 volumes of the original extract of 1x ANIB containing 40% sucrose using a Pasteur pipette. Chromatin was then isolated in the sucrose cushion by spinning the sample at 2,500 g in a swinging bucket rotor for 5 minutes at 4°C. The spin was repeated until a chromatin pellet was clearly observed at the bottom of the tube. The buffer above the sucrose cushion was discarded and the top of the cushion was washed three times with 1 ml of 1x ANIB. After the washes, the sucrose cushion was removed from above the pellet. The pellet was then transferred using a 200 µl pipette tip to a 1.5 ml Eppendorf tube and resuspended in one-third volume of 1x ANIB containing 40% sucrose and supplemented with 100x HALT protease inhibitor cocktail (PI87786, Thermo Fisher Scientific). A chromatin sample was taken and resuspended with 4x NuPAGE LDS loading buffer for immunoblotting analysis. Another sample was taken as "-DNAase sample" before the benzonase treatment and processed alongside other samples after sonication. Benzonase nuclease was added to 2 units/µl final concentration and incubated for 20 min at room temperature, with intermittent mixing. Samples were then sonicated in a sonicator with a water bath (Bioruptor, Diagenode) for 2 minutes at 4ºC with 15 sec ON/OFF cycles, medium setting. The sample was spun at maximum speed for 5 min at 4°C and the supernatant taken as the solubilized chromatin. Input or soluble sample was prepared by mixing the supernatant with 4x NuPAGE LDS loading buffer. Insoluble samples were obtained by resuspending the pellets in 1x NuPAGE LDS loading buffer. Finally, all samples were analysed by immunoblotting.

For testing salt concentrations higher than 100 mM, the chromatin sample was split into 7 aliquots after digestion with benzonase and sonication. The potassium acetate concentration in each aliquot was adjusted to the desired concentration (150-400 mM) by using 1x ANIB and 2M KAc. The samples were then incubated for 5 min at room temperature before the final spin. Samples extracted before the benzonase treatment (-DNAase) were also spun. Insoluble samples were obtained by resuspending the pellets in 1x NuPAGE LDS loading buffer.

2.3.8. Small-scale immunoprecipitation (IP) from extract (Uhrf1, Dnmt1, Lig1, Fen1, Paf15 and RPA)

Metaphase II arrested egg extract was activated as above (Section 2.3.3). The activated extract was diluted in 4 volumes of LFB1/50 (Table 2. 1) and spun down at maximum speed for 15 min at 4ºC in a benchtop centrifuge. A sample from the supernatant (input) was taken and resuspended in 2x NuPAGE LDS loading buffer for immunoblotting analysis. The input was then incubated with IgG from rabbit or sheep serum (I5006 or I5131, Sigma) or purified antibodies against the protein of interest (anti-Uhrf1, anti-Lig1, anti-Fen1, anti-Paf15 or anti-RPA, described in Section 2.6. 6) on ice for 1 hour - 100 µl of input extract per 1 µg of purified antibody. When using sera for the IP, pre-immune serum or serum against the protein of interest were used instead (anti-Uhrf1, anti-Dnmt1, anti-Lig1, anti-Fen1, anti-Paf15 or anti-RPA). In this case 5 µl of serum was used per 100 µl of diluted input extract.

During the incubation, Dynabeads Protein A or G (10002D or10004D, Invitrogen), for antibodies raised in rabbit or sheep respectively, were prepared by taking 15 µl of beads per sample and washing once with 1 ml of PBS and twice with 1 ml of LFB1/50 (Table 2. 1). For the washes, tubes containing beads were resuspended in the buffer, subjected to a quick spin and then placed on a magnetic rack (DynaMag™-2 Magnet, 12321D, Thermo Fisher Scientific)

to remove all buffer once the beads settle on the wall. After the incubation with the antibodies, the samples were incubated with the corresponding beads for 1 h rotating at 4ºC.

Proteins bound to beads were isolated by placing in the magnetic rack and removing unbound material (depleted). A depleted sample was taken and resuspended in 2x NuPAGE LDS loading buffer for immunoblotting analysis. The beads were then washed with 1 ml of LFB1/50 thrice and the buffer was completely removed afterwards using the magnetic rack. Immunoprecipitated proteins were eluted from the beads by boiling each sample in 30 µl of 2x NuPAGE LDS loading buffer for 5 minutes, followed by separation from the beads by placing the tubes in a magnetic rack. IP samples were run in an SDS-PAGE gel, together with Input and depleted samples for visualization by immunoblotting using the antibody against the protein being IP (anti-Uhrf1, anti-Dnmt1, anti-Lig1, anti-Fen1, anti-Paf15 or anti-RPA).

2.3.9. Pull-down of GST-Uhrf1 from *Xenopus* egg extract

Xenopus laevis egg extract was activated as described above (Section 2.3.3). The activated extract was then supplemented with *Xenopus* sperm DNA, mixed and aliquoted into 4 samples of 50 µl each. Each aliquot was then supplemented with either or both affinity purified GST-xUhrf1 and His-SUMO-xUhrf1 (Table 2. 4, Section 2.6.5). A control adding the same volume of LFB1/100 (Table 2. 1) was also performed. All samples were incubated at 23ºC for 45 min.

After incubation, the samples were diluted in 4 volumes of LFB1/100 and spun down at maximum speed during 15 min at 4ºC in a benchtop centrifuge. A sample from the supernatant (input) was taken and resuspended in 2x NuPAGE LDS loading buffer. Input samples were then incubated with Glutathione Sepharose 4B beads (GE Healthcare) 1 hour at 4ºC, previously prepared by washing in LFB1/100 buffer trice and removing buffer completely by spinning at 920 g for 3 min at 4°C – 25 µl of beads were used per sample.

After the incubation, samples were spun at 920 g for 3 min at 4°C. A sample from the supernatant containing the unbound proteins (depleted) was taken and resuspended in 2x NuPAGE LDS loading buffer. The remaining depleted sample was discarded. The beads were then washed with LFB1/100 thrice, by gently resuspending in the buffer and spinning at 920 g for 3 min at 4°C. The buffer was completely removed afterwards. Immunoprecipitated proteins were eluted from beads by boiling each sample in 40 µl of 2x NuPAGE LDS loading buffer for 5 minutes. Beads were then separated from IP proteins by spinning at 920 g for 3 min at 4°C. Supernatant containing IP samples were run in an SDS-PAGE gel, together with Input and depleted samples for visualization by immunoblotting using anti-Uhrf1 antibodies.

2.3.10. Coupling antibodies to beads

Coupling antibodies from sera to Protein A beads for immunodepletion

To perform immunodepletion of Uhrf1 and Lig1 using sera, antibodies from rabbit sera were coupled to Protein A beads overnight directly prior the experiment.

500 µl of Affi-Prep Protein A Resin (1560006, Biorad) were transferred into a 12 ml Falcon tube and washed once with 5 ml of 100 mM HEPES pH 7.6, by resuspending, spinning at 200 g for 1 min and removing the buffer completely using gel loading tips. The prepared beads were then mixed with 500 µl of rabbit pre-serum or serum against the protein of interest (anti-Uhrf1 or anti-Lig1) and 50 µl of 1 M HEPES pH 7.6 and transferred to a 1.5 ml Eppendorf tube. To couple the antibodies from the sera to the beads, the samples were incubated at 4°C overnight with rotation.

The next day, the samples were spun at 1000 rpm for 1 min to remove unbound proteins and the beads were transferred to a 5 ml Falcon tube. The beads were then washed with 2.5 ml of HEPES pH 7.6 trice by gently mixing, spinning at 1000 g for 1 min and removing the buffer

afterwards. Another wash with 1 ml of 100 mM HEPES pH 7.6 supplemented with 1 µl of PMSF protease inhibitor was performed, mixing at room temperature for 15 min. Finally, another wash with 2.5 ml of 100 mM HEPES pH 7.6, followed by two washes with 2.5 ml of LFB1/50 (Table 2. 1) were carried out. Beads were kept on ice in LFB1/50 for the subsequent use in the immunodepletion protocol.

Coupling purified antibodies to Protein A or G Dynabeads for immunodepletion

To carry out immunodepletion using purified antibodies, the antibodies were coupled to Protein A or Protein G Dynabeads overnight immediately prior to the experiment.

Dynabeads Protein A (for antibodies raised in rabbit) or Protein G (for antibodies raised in sheep) (10002D or 10004D, Life Technologies) were washed once with 1 ml of 100 mM HEPES pH 7.6, by resuspending in the buffer, placing in a magnetic rack and removing the buffer. The beads were subsequently mixed with commercial unspecific IgG from rabbit or sheep serum (I5006 or I5131, Sigma) or the corresponding affinity purified antibody. For small scale immunodepletion, 300 ul of Dynabeads were couple to 180 µg of antibody. For large scale immunodepletion, 900 µl of Dynabeads were coupled to 540 µg of antibody. The volume of the mixture in both samples was topped up to 180 µl, for small scale, or 540 µl, for large scale, with 100 mM HEPES pH 7.6. To couple the antibody to Dynabeads, the samples were incubated at 4^{o}C overnight with rotation.

The next day, the samples were placed on the magnetic rack to remove unbound proteins. Beads were then washed with 2 ml of HEPES pH 7.6 trice by gently mixing. Another wash with 1.5 ml of 100 mM HEPES pH 7.6 supplemented with 1 µl of PMSF protease inhibitor was performed mixing at room temperature for 15 min. Finally, another wash with 2 ml of 100 mM HEPES pH 7.6, followed by two washes with LFB1/50 (Table 2. 1) was carried out. The beads were kept on ice in LFB1/50 for the subsequent use in the immunodepletion protocol.

Coupling antibodies to Protein A or G Dynabeads using BS3 crosslinker for IP

To carry out immunoprecipitations (IP) from chromatin, antibodies were couple to Protein A or Protein G Dynabeads overnight prior the experiment.

50 µl Dynabeads Protein A (for antibodies raised in rabbit) or Protein G (for antibodies raised in sheep) (10002D or 10004D, Life Technologies) per sample were washed once with 1 ml of PBS, by resuspending in the buffer, placing in a magnetic rack and removing the buffer. The beads were subsequently mixed with 10 µg of commercial IgG from rabbit or sheep serum (I5006 or I5131, Sigma) or the corresponding affinity purified antibody. The volume of the mixture was topped up to 150 µl with PBST in both samples. To couple the antibody to Dynabeads, the samples were incubated at 4°C overnight rotating.

The next day, before performing the IP, the antibodies were covalently bound to the Dynabeads by using BS3 crosslinker (S5799, Sigma). Specifically, the tubes were place on a magnetic rack, the supernatant removed, and the beads washed with 1 ml of PBST by gently resuspension. The samples were then incubated with 250 µl of 5 mM BS3 in conjugation buffer (20 mM sodium phosphate pH 7-9, 150 mM NaCl) for 30 min rotating at room temperature. After the incubation, 50 µl of quenching buffer (1M Tris-HCl pH 7.5) was added and another incubation of 15 min mixing at room temperature was performed. Finally, the samples were washed with 1 ml of PBST thrice and stored in 100 µl of PBST (using 0.02% sodium azide for long storage) at 4°C until the IP protocol was performed.

Coupling antibodies to Epoxy Dynabeads M-270 for large-scale IP of Uhrf1

Two days prior to the large scale Uhrf1 IP, Epoxy Dynabeads M-270 (14301, Thermo Fisher Scientific) were covalently coupled to either IgG from sheep serum or affinity purified sheep Uhrf1 antibodies following Invitrogen's protocol.

2 ml of Dimethylformamide (DMF) was added to the Dynabeads M-270 epoxy vial to get a final concentration of $2x10^9$ beads/ml and resuspended by vortexing. 450 µl of the beads solution was then transferred to a 1.5 ml tube, placed in a magnetic rack and the DMF solvent removed. The beads were then mixed with 1 ml of 0.1 M sodium phosphate pH 7.4 using a vortex and incubated for 10 minutes mixing at room temperature. Fresh buffer was then added and another 10 minutes incubation was performed. The buffer was then removed and the beads mixed with 300 µl of 3 M ammonium sulphate in phosphate buffer pH 7.4 and with 300 µg of either IgG from sheep sera or affinity purified anti-Uhrf1 antibody. The mixture volume was topped up to 900 µl with sodium phosphate buffer pH 7.4. The beads-antibody mixture was incubated for two days at 4°C with rotation.

Two days later, the beads were washed four times with 1 ml of PBS. Another wash with PBS supplemented with 0.5% Triton X-100 was then performed for 10 minutes at room temperature with rotation. Finally, the beads were washed another three more times with 1 ml of PBS, mixing at room temperature for 5 minutes. Beads coupled to antibodies were finally resuspended in 900 µl of PBS (using 0.02% of sodium azide for long storage) and stored at 4°C until the IP protocol was performed.

2.3.11. Small-scale Immunoprecipitation (IP) from chromatin (Uhrf1 and RPA)

To perform IPs of Uhrf1 and RPA from chromatin, chromatin was first isolated and chromatin bound proteins were release as described in Section 2.3.7. For small-scale IP, 100 µl of egg extract per sample was initially activated and incubated with 10 ng/ µl of sperm DNA as previously described.

The supernatant (input) containing the soluble chromatin was incubated with 100 µl of Dynabeads, previously coupled covalently to either anti-IgG, anti-Uhrf1 or anti-RPA antibodies, as described in Section 2.3.10, rotating for 2 hours at 4ºC. After the incubation, samples were place in a magnetic rack and a sample of the unbound proteins (depleted) was taken and resuspended in 2x NuPAGE LDS loading buffer for immunoblotting analysis. The rest of the depleted sample was discarded. Beads were then washed 5 times, mixing 5 minutes at 4ºC with 1 ml of 1x ANIB (Table 2. 1) (washes 1, 2, 4 and 5) or 1x ANIB supplemented with 0.1% Triton X-100 (wash 3). The magnetic rack was used in the washes to separate the beads from the buffer. Finally, immunoprecipitated proteins were eluted from beads by boiling each sample in 40 µl of 2x NuPAGE LDS loading buffer for 5 minutes, followed by separation from the beads by placing in a magnetic rack. IP samples were run in an SDS-PAGE gel, together with Input and depleted samples, for visualization by immunoblotting using the antibody against the protein being IP (anti-Uhrf1 or anti-RPA) and the antibodies to test co-IP'd proteins.

When using the DTSSP (3,3'-dithiobis(sulfosuccinimidyl propionate)) crosslinker to stabilize the protein interactions (to capture them when immunoprecipitating Uhrf1), chromatin was isolated as described in section 2.3.7 and then incubated with either 1 mM of freshly prepared DTSSP crosslinker in 1x ANIB or the same volume of 1x ANIB buffer. The samples were then incubated 30 min at RT with rotation. To quench the crosslinker, 20 mM of Tris HCl pH 7.5 was added and another 15 min incubation was performed mixing at RT. After crosslinking, proteins were released from chromatin by benzonase treatment and sonication as described in section 2.3.7. Finally, Uhrf1 immunoprecipitation was carried out as before.

2.3.12. Large-scale IP of Uhrf1 for mass spectrometry analysis

Large-scale IP of Uhrf1 from chromatin was performed similar to the small-scale IP but adding more material of egg extract and scaling up the rest of the volumes of the protocol. In addition, the salt concentration was increased to 200 mM after benzonase treatment.

Specifically, 3.8 ml of *Xenopus* egg extract was activated and incubated with 10 ng/µl of sperm DNA at 23ºC for 50 min as previously described. Chromatin was then transferred to a 50 ml Falcon tube containing 1x ANIB buffer (Table 2. 1), isolated in a sucrose cushion and proteins were released from chromatin as described in Section 2.3.7.

After benzonase treatment and sonication, 50 µl of 2M Kac was added to the sample to raise the salt concentration to 200 mM. This was incubated for 5 min at room temperature before spinning at maximum speed for 10 min at 4ºC in a tabletop centrifuge. After the spin, soluble chromatin protein complexes were incubated with 450 µl of Dynabeads coupled to antibodies, as explained in section 2.3.10, mixing at 4°C for 2 hours. After the incubation, the beads were washed 5 times with rotation for 5 min at 4°C: twice with 1x ANIB, once with LFB1/50 (Table 2. 1) supplemented with 0.1% Triton X-100, and again twice with 1x ANIB. Immunoprecipitated proteins were eluted from the beads by boiling each sample in 50 µl of 2x NuPAGE LDS loading buffer for 5 min. IP samples were run in an SDS-PAGE gel, then Coomassie stained and prepare for MS as described in Section 2.7.4. MS analysis was carried out as explained in (45) with the collaboration of Dr Richard Jones from MS Bioworks LLC.

2.3.13. Immunodepletion of Uhrf1, Lig1 and Paf15

Immunodepletion of *Xenopus laevis* egg extract was carried out after preparing beads and activating the extract as described in sections 2.3.10 and 2.3.3 respectively. For Uhrf1 and Paf15 depletions, Dynabeads coupled to purified antibodies were used. For depletion of Uhrf1 and Lig1 using rabbit sera, Affi-prep Protein A beads coupled to the specific antibodies from the sera were used.

Immunodepletion of Uhrf1 and Paf15 using purified antibodies

Depletion of activated extract required three rounds of 45 min incubations rotating at 4ºC with Dynabeads previously coupled to IgG or affinity purified antibody (Section 2.3.10) for IgG and Uhrf1-depleted, respectively, at 50% beads/extract ratio. Beads kept on ice were aliquoted into three tubes, one for each round of incubation, and buffer was completely removed using the magnetic rack. For small scale immunodepletion, 100 µl of beads solution coupled with 60 µg of antibody were used per round for 200 µl of extract. For large scale immunodepletion 300 µl of beads solution coupled with 180 µg of antibody were used per round for 600 µl of extract. Depleted extract was isolated from beads by placing the sample in a magnetic rack to remove the beads from the extract, the immunodepleted extract was then frozen in liquid nitrogen and kept at -80 ºC.

Immunodepletion of Uhrf1 and Lig1 using rabbit sera

For Uhrf1 and Lig1 Uhrf1 depletions from activated extract using rabbit sera, two rounds of 40 min incubations with beads were required. Therefore, Affi-prep Protein A Support (156-0006, Bio-rad) previously coupled to antibodies from rabbit pre-sera or sera against the protein of interest (Uhrf1 or Lig1) were divided in two tubes. The tubes were spun at 200 g for 1 min and the buffer was completely removed using gel loading tips to avoid unnecessary extract dilution.

The amount of beads was measured in each tube (it is easy to lose some beads during the procedure) and the volume of activated extract required was estimated (200 µl of extract was depleted per 120 µl of beads). After activating the extract as described in Section 2.3.3, the extract was incubated with the prepared beads for 40 min rotating at 4ºC. After the incubation, the depleted extract was filtered using a filter cloth to separate it from the beads and it was incubated with the other set of beads. Finally, the depleted extract was filtered, frozen in liquid nitrogen and kept at -80 ºC.

2.4. *In vitro* Assays

2.4.1. *In vitro* Ubiquitination Assay

In vitro ubiquitination assays were performed on ice in 20 µl reactions containing 200 nM E1 UBA1 (E-305-025, Boston Biochem), 1 µM E2 UbcH5a/UBE2D1 (E2-616-100, Boston Biochem), 0.75 µM Uhrf1 (xUhrf1 affinity purified in this study, containing or not Ulp1 protease (Section 2.6.5), or commercial His-hUhrf1 (Table 2. 4, 30 µM His_6-Ubiquitin (U-530-02M), Boston Biochem) and 12.5 µM xPaf15 (purified in this study, Table 2. 4) in the ubiquitination reaction buffer (50 mM HEPES pH 8.0, 150 mM NaCl, 5 mM $MgCl_2$, 0.1% Triton X-100, 2 mM DTT and 250mM MgATP). Control reactions with no E1, E2, Uhrf1 or Paf15 were also set up in parallel, adding correspondingly buffer or water instead. The mixtures were incubated at 37°C for 1 h and 30°C for another 1 h shaking to allow the ubiquitination reaction to take place. After the incubation, the reactions were stopped by adding 4x NuPAGE LDS loading buffer and boiling at 95°C for 5 min. The samples were finally run in a SDS-PAGE gel, analysed by western blotting using anti-xUhrf1, anti-xPaf15 and anti-ubiquitin antibodies (Table 2. 5).

2.5. Working with DNA

2.5.1. Polymerase chain reaction (PCR) of xUhrf1 to prepare it for cloning

The plasmid containing GST-tagged *Xenopus laevis* Uhrf1 (pGS21-GST-xUhrf1) was subjected to PCR to add a BsaI restriction site and the Gly-Gly motif (Ulp1 cleavage site) to the Uhrf1 N-terminal and a SalI restriction site to the Uhrf1 C-terminal. Therefore, the following primers were designed:

Primer BsaI Forward: GTGGGTCTCAGGTGGTATGtggatacaggtgc

Primer SalI Reverse: GTGGTCGACTCAccggccgctctcata

To modify the xUhrf1 gene to be subsequently cloned, a 25 µl PCR reaction was prepared on ice adding 1X Q5 Reaction Buffer (B9027S, New England BioLabs), 10 mM dNTPs, 10 µM Fordward Primer, 10 µM Reverse Primer, 1 ng/µl of plasmid (pGS21-GST-xUhrf1), 0.02 U/µl of Q5 High-Fidelity DNA Polymerase (M0491, New England BioLabs) in nuclease-free water. The reaction was mixed and transferred to a thermocycler for the PCR reaction to take place. An initial denaturation step of 30 sec at 98 ºC was performed, followed by 25 cycles of: 10 sec at 98 ºC, 30 sec at 52.2 ºC and 72 sec at 72 ºC. An extension step at 72 ºC for 2 min was finally carried out. The amplified Uhrf1 DNA was visualized by running in an agarose gel as described in section 2.5.4. Finally, the PCR product was isolated from the rest of the components of the PCR reaction using a QIAquick PCR Purification kit (28104, Qiagen), following the manufacturer's protocol.

2.5.2. Cloning of Uhrf1

A plasmid to express His-SUMO tagged mouse Uhrf1 (pET24-His-SUMO-mUhrf1) was kindly provided by Dr Benjamin Foster and Dr Till Bartke. This plasmid was designed to cut the His-SUMO tag by the Ulp1 protease immediately before the first methionine of the Uhrf1 protein.

Therefore, to express His-SUMO tagged *Xenopus laevis* Uhrf1 to then cut off the tag, the PCR amplified xUhrf1 gene was cloned into the pCA528-His-SUMO plasmid.

The *Xenopus laevis* Uhrf1 PCR product and pCA528-His-SUMO-mUhrf1 were digested using BsaI and SalI (R3733 and R0138, New England BioLabs) restriction enzymes. Digestion of 2 µg of plasmid or all purified PCR product from Section 2.5.1 were performed in 50 µl reactions containing 1 µl of each restriction enzyme, 5 µl of CutSmart buffer and nuclease-free water for 2h at 37ºC. After the digestion, insert and vector were isolated by running the samples on a 0.8% agarose gel (Section 2.5.4), cutting insert and vector bands and purifying them using a QIAquick Gel Extraction kit (28704, Qiagen) following the manufacturer's instructions. The ligation of the insert with the vector was performed adding 1 µl of vector, 7 µl of xUhrf1 sample, 1 µl of T4 DNA ligase and 1 µl of 10xT4 buffer (M0202, New England BioLabs) and incubating the mixture on ice overnight. A control reaction with no insert added was also performed in parallel. 1 µl of each ligation reaction was transformed into 10 µl NEB-10 β (C3019, New England BioLabs) following the protocol in Section 2.6.1. The efficiency of the cloning was tested by growing some colonies, purifying plasmid (described in Section 2.6.2) and digesting the plasmids using the same strategy of the previous digestion but in 10 µl reaction. Finally, the plasmid containing the expected vector and insert sizes were sent for sequencing to analyse that Uhrf1 was cloned in the His-SUMO vector with no mutations.

2.5.3. Cloning of Dnmt1

A cell-free expression plasmid for *Xenopus laevis* Dnmt1 was kindly provided by Howard Lindsay. The Dnmt1 gene was cloned from the provided pEPEX plasmid into pET28c using NdeI and SalI (R0111 and R0138, New England BioLabs) restriction enzymes. Digestions of 2 µg of each plasmid were performed in 50 µl reactions containing 1 µl of each restriction enzyme, 5 µl of CutSmart buffer and nuclease-free water for 2h at 37ºC. After the digestion,

insert and vector were purified by running the samples on a 0.8% agarose gel, cutting insert and vector bands and purifying them using a QIAquick Gel Extraction kit (28704, Qiagen) following the manufacturer's instructions. The ligation of the insert with the vector was performed by adding 1 µl of pET28c sample, 7 µl of xDnmt1 sample, 1 µl of T4 DNA ligase and 1 µl of 10xT4 buffer (M0202, New England BioLabs) and incubating the mixture overnight at 16°C. A control reaction with no insert added was also performed in parallel. 2 µl of each ligation reaction was transformed into 30 µl XL10 gold cells (200315, Agilent) following the protocol in Section 2.6.1. The efficiency of the cloning was tested by growing some colonies, purifying plasmid (described in Section 2.6.2) and digesting the plasmids using the same strategy of the previous digestion but in 10 µl reactions. Finally, the plasmid containing the expected vector and insert sizes were sent for sequencing to analyse that Dnmt1 was cloned in pET28c with no mutations.

2.5.4. Agarose gel electrophoresis

To visualize DNA in an 0.8% agarose gel, 0.8 g of agarose were melted in 1x TBE buffer (Invitrogen). When it was cooled down to ~55°C, 10 µl of SYBR Safe DNA gel stain (Thermo Scientific) was added and the agarose gel was poured into an electrophoresis gel tank tray containing a well comb. When the agarose gel was solidified, the comb was removed and the DNA samples were mixed with 6x purple gel loading dye (New England BioLabs) and loaded into the gel wells, as well as a 1 kb plus DNA ladder (Thermo Fisher Scientific). Electrophoresis was carried out at 100 V for 1 h and the gel was finally visualised using a UV transilluminator.

2.6. Working with bacteria

2.6.1. Transformation

For protein expression and purification, 10 µl of Rosetta (DE3) pLysS (709564, Millipore) or Arctic Express (DE3) (230192, Agilent) competent cells were defrosted on ice, transformed with 100 ng of plasmid DNA and incubated on ice for 30 min. Heat shock was performed in a water bath set at 42ºC for 30 sec and the samples were then placed on ice for 2 min. After this incubation, 250 µl of SOC media (B9020S, New England BioLabs) (pre-warmed at 37ºC) was added and bacterial samples were incubated in a shaking incubator at 37ºC for 1 hour. Finally, the bacteria were spread on LB agar plates containing appropriate antibiotics (1:1000 from stock (Table 2. 6)) and left growing overnight in an incubator at 37ºC.

2.6.2. Plasmid purification

To obtain high amounts of plasmids and purify them, bacterial colonies obtained after transformation were inoculated in 50 ml Falcon tubes containing 5 ml LB broth supplemented with appropriate antibiotics and incubated overnight in a shaking incubator at 37°C. The next day, bacteria were isolated by spinning at 6800 g for 3 min at room temperature and removing the supernatant. Bacteria were then lysed and plasmids purified using a QIAprep Spin Miniprep kit (27104, Qiagen) following the manufacturer's instructions. Finally, the concentration of the plasmid was checked using a nanophotometer.

2.6.3. Testing expression of recombinant proteins

Before the purification of the different recombinant proteins, the protein expression was tested in both *E. coli* strains (Rosetta and Artic). After the transformation (Section 2.6.1), 2 colonies from each bacterial strain were inoculated in 5 ml LB broth containing appropriate antibiotics and grown at 37°C overnight shaking. Fresh cultures were grown by diluting 1:100 in 15 ml of

either LB broth or auto induce media (AIM) supplemented with appropriate antibiotics and incubating at 37°C shaking until the Optical Density (OD_{600}) value reached 0.4-0.6. Once reached, 1 mM IPTG was added to cultures in LB to induce expression. Samples were induced for 2 h at 37°C or overnight at 18°C shaking. Uninduced and induced samples were collected, spun down at maximum speed for 5 min in a benchtop centrifuge and supernatants were discarded. The pellet was resuspended in 2x NuPAGE LDS loading buffer, boiled at 95°C for 5 min and analysed on a SDS-PAGE gel by Coomassie staining or western blotting using appropriate antibodies. The remaining induce sample was pelleted in a 2 ml Eppendorf tube and frozen at -80°C for the solubility test.

2.6.4. Testing solubility

For those samples showing protein expression in the expression test, the solubility of the protein was tested in appropriate lysis buffers (see purification section for details of the buffer used). Frozen pellets from the previous section were resuspended in the lysis buffer (200 µl per 2 ml of culture) supplemented with Benzonase (25 U/ml), 10 mg/ml APL protease inhibitors and 1 mg/ml of lysozyme and incubated for 20 min rotating at room temperature. Samples were then divided into two, one being subjected to sonication (3 times, 10 sec ON and 10 sec OFF). Both samples were spun down at maximum speed for 5 min in a benchtop centrifuge. Soluble and insoluble fractions were obtained from the supernatant and pellet resuspended in 200 µl of lysis buffer, respectively. A sample from each was mixed with 2x NuPAGE LDS loading buffer and boiled at 95°C for 5 min. They were then analysed on SDS-PAGE gel by Coomassie staining and immunoblotting using the appropriate antibody (usually anti-HIS or anti-GST).

2.6.5. Protein expression and purification

Purification of GST-xUhrf1

The plasmid containing GST-tagged *X. laevis* Uhrf1 (pGS21-GST-xUhrf1) created by another member of the lab was transformed into 10 µl of Rosetta cells as described above. Two colonies were grown in 10 ml of LB broth with appropriate antibiotics (Table 2. 7) at 37°C overnight shaking. The culture was then diluted 1:100 in 2 l of LB broth containing antibiotics (2x 1l LB in 2.5 l Erlenmeyer baffled flask) and incubated at 37°C shaking until the OD_{600} value reached 0.4-0.6. When the OD was reached, cultures were induced by adding 1 mM IPTG and incubated at 20°C overnight shaking. Uninduced and induced samples were collected, spun down and the pellet was resuspended in 2x NuPAGE LDS loading buffer as for expression test. Cultures were spun down at 6,000 g for 10 minutes at 4°C and the pellets were kept at -80°C.

For lysis, the bacterial pellet was thawed, resuspended in 30 ml of lysis buffer (10 mM Tris-HCl pH 8.0, 300 mM NaCl, 10% glycerol, 0.1% NP40, 5 mM β-mercaptoethanol, 2 mM $MgCl_2$, 1 mM PMSF) supplemented with APL protease inhibitors (Aprotinin, Pepstatin and Leupeptin; 10 mg/ml) and lysozyme (1 mg/ml), and sonicated. The lysate was then mixed with 25 U/ml of benzonase and incubated for 20 min at RT. The homogenate was spun down at 16,000 g for 30 min at 4°C and a supernatant (input) sample was mixed with 2x NuPAGE LDS loading buffer for further analysis. The rest of the input was mixed with 4 ml of pre-washed Glutathione Sepharose 4B beads (GE Healthcare) and rotated for 2 h at 4°C. The beads were then spun down at 200 g for 3 min at 4°C, the supernatant was mixed with 2x NuPAGE LDS loading buffer for depleted sample, and the beads were washed once with 30 ml of lysis buffer. Then, two more washes were carried out using 30 ml of wash buffer (lysis buffer without detergent and protease inhibitors) and the sample was transferred to a Poly-Prep Chromatography Column (7311550, Biorad). Finally, the beads were incubated twice with 1 ml of lysis buffer

supplemented with 25 mM glutathione for the elution of the protein. A sample from each elution was mixed with 2x NuPAGE LDS loading buffer and all the samples of the purificiation process were run in a SDS PAGE gel for visualization by Coomassie staining and immunoblotting.

Purified protein was dialyzed into LFB1/100 overnight at 4°C using Pur-A-Lyzer TM dialysis tube (Sigma Aldrich). The concentration of the sample was then measured by Bradford assay using BSA standards (Section 2.7.5). Finally, aliquots were prepared and kept at -80 °C.

Purification of GST-xPAF15

The plasmid containing GST-tagged *X. laevis* PAF15 was purchased from Biomatik corporation (pGEX-4T-1-GST-xPAF15). After testing induction and solubility, the protein was purified using Glutathione Sepharose 4B beads (GE Healthcare). The purification was performed as described for GST-Uhrf1 but using thrombin (27-0846-01, Cytiva) for elution. Two incubations with 50 U of thrombin in 1 ml of cleavage buffer were performed for 2 h at RT and 16 h at 4ºC for elutions 1 and 2 respectively. A third elution was obtained by washing the beads with 1 ml of cleavage buffer. Buffers used for the purification were lysis buffer (20 mM HEPES-KOH pH 7.6, 0.5 M NaCl, 0.5 mM EDTA, 10% glycerol, 1 mM DTT, 0.5% NP40), wash buffer 1 (20 mM HEPES-KOH, pH 7.5, 150 mM NaCl, 1% TritionX-100, 1 mM DTT), wash buffer 2 (20 mM HEPES-KOH, pH 7.5, 150 mM NaCl), wash buffer 3 and cleavage buffer (PBS).

For *in vitro* ubiquitination assays, the purified protein was dialysed into LFB1/100 overnight at 4°C. The concentration of the sample was then measured by Bradford assay using BSA standards (Section 2.7.5). Finally, aliquots were prepared and kept at -80 °C until use.

Purification of His-Ulp1

The plasmid containing His-tagged Ulp1 protease (pET24-His-Ulp1), kindly provided by Dr Benjamin Foster and Dr Till Bartke, was transformed into 10 µl of Rosetta cells as described

above. Two colonies were grown in 10 ml of LB broth with appropriate antibiotics (Table 2. 7) at 37°C overnight shaking. The culture was then diluted 1:100 in 2 l of LB broth containing antibiotics (2x 1 l LB in 2.5 l Erlenmeyer baffled flask) and incubated at 37°C shaking until the OD_{600} value reached 0.4-0.6. When the OD was reached, cultures were induced by adding 1 mM IPTG and incubated it at 20°C overnight shaking. Uninduced and induced samples were collected, spun down and the pellet was resuspended in 2x NuPAGE LDS loading buffer as for expression tests. The cultures were spun down at 6,000 g for 10 minutes at 4ºC and pellets were kept at -80ºC.

For lysis, the bacterial pellet was thawed, resuspended in 30 ml of lysis buffer (50 mM Tris pH 7.5, 300 mM NaCl, 20 mM Imidizole) supplemented with 25 mM DTT, 1 mM PMSF, APL protease inhibitors (10 mg/ml) and lysozyme (1 mg/ml), and sonicated (five times, 30 sec ON and 10 sec OFF, medium amplitude). The lysate was then mixed with 25 U/ml of benzonase and incubated for 20 min at RT. The homogenate was spun down at 16,000 g for 30 min at 4°C and a supernatant (input) sample was mixed with 2x NuPAGE LDS loading buffer for further analysis. The rest of the input was mixed with pre-washed Nickel NTA Resin (88222, Thermo Scientific) and incubated for 2 h at 4°C. The beads were then spun at 200 g for 3 min at 4°C, a sample from the supernatant was mixed with 2x NuPAGE LDS loading buffer for a “depleted” sample and the beads were washed twice with 30 ml of lysis buffer. Then, a final wash was carried out using 15 ml of lysis buffer and the sample was transferred to a Poly-Prep Chromatography Column (7311550, Biorad). For the elution of the protein, the beads were incubated with 1 ml of elution buffer (50 mM Tris pH 7.5, 300 mM NaCl, 250 mM Imidazole, 0.5 mM DTT) supplemented with protease inhibitors (1 mM PMSF and 10 mg/ml APL protease inhibitors). A total of 5 elutions were obtained using 250 mM Imidazole. Another 5 samples were eluted using 400 mM Imidazole. A sample from each elution was mixed with 2x NuPAGE

LDS loading buffer and all the samples of the purification process were run in a SDS PAGE gel for visualization by Coomassie staining and immunoblotting.

Purified protein was dialyzed into 50 mM Tris pH 7.5, 300 mM NaCl, 1 mM DTT buffer overnight at 4°C using Pur-A-Lyzer TM dialysis tube (Sigma Aldrich). The next day, the sample was supplemented with an equal volume of glycerol and the concentration was measured by Bradford assay using BSA standards (Section 2.7.5). Finally, 50 µl aliquots were prepared and kept at -80°C until use.

Purification of His-SUMO-xUhrf1

The plasmid containing His-SUMO tagged *X. laevis* Uhrf1 was (pET24-His-SUMO-xUhrf1) was generated as described in Section 2.5.2. The protein was purified in a similar way to the His-tagged Ulp1 protein but just using one concentration of Imidazole in the elution buffer (300 mM). The lysis buffer used was 20 mM HEPES-KOH pH 7.5, 300 mM NaCl, 10% glycerol, 20 mM imidazole. The elution buffer was lysis buffer but with 300 mM Imidazole instead. All buffers were supplemented with 1 mM PMSF and 10 mg/ml APL protease inhibitors.

The purified protein was dialysed into LFB1/100 overnight at 4°C. The concentration of the sample was then measured by Bradford assay using BSA standards (Section 2.7.5). Finally, aliquots were prepared and kept at -80°C until use.

Purification of untagged xUhrf1

Untagged *X. laevis* Uhrf1 was obtained after incubating His-SUMO-xUhrf1 protein with purified Ulp1 protease, both purified in the previous sections. 1 ml of fresh His-SUMO-xUhrf1 purified protein was dialysed into LFB1/100 overnight at 4°C with rotation, incubating with 50 µl of purified Ulp1 added for the cleavage of the tag. The sample was then subjected to size exclusion chromatography using an AKTA system (25 ml column), for the separation of Uhrf1

from Ulp1 protease. LFB1/100 was used to equilibrate the column. After the collection of the elutions, the samples were run on an SDS-PAGE gel and visualized by Coomassie staining. Samples containing untagged Uhrf1 were chosen, and their concentration were estimated by comparison with BSA standards by SDS-PAGE and Coomassie staining. Finally, samples containing untagged Uhrf1 were aliquoted and kept at -80°C until use.

Purification of His-xLig1

The plasmid containing His-tagged *X. laevis* Lig1 was purchase from Biomatik corporation (pET22b(+)-His-xLig1). The plasmid was transformed and protein expressed in bacteria as above. His-tagged Lig1 was purified as described for His-Ulp1 but with some differences. 6 l of bacterial culture were grown in AIM media. For the lysis, the pellet was resuspended in 100 ml of lysis buffer (50 mM NaH_2PO_4 pH8, 300 mM NaCl, 10% glycerol, 5 mM β-Mercaptoethanol,) supplemented with 1 mM of PMSF, APL protease inhibitors (10 mg/ml and lysozyme (1 mg/ml). The purified protein was dialysed against 50 mM NaH_2PO_4, 300 mM NaCl buffer and sent for anti-Lig1 antibody production to Eurogentec company.

Purification of His-xDnmt1

The plasmid containing His-tagged *X. laevis* Dnmt1 (pET28c(+)-His-xDnmt1) was obtained in this study (Section 2.5.3). After testing induction and solubility as previously described (Section 2.6.3 and 2.6.4), protein was purified as described for His-Ulp1. Binding to the Nickel NTA Resin was performed for 3 h at 4°C and the lysis buffer used was 20 mM HEPES, pH 7.5, 250 mM NaCl, 10% sucrose, 3 mM $MgCl_2$, 0.1% NP40. The purified protein was sent for anti-Dnmt1 antibody production to Eurogentec company.

Purification of His-xRPA

The plasmid expressing simultaneously the three subunits of *X. laevis* RPA (RPA1 containing the His-tag) (pET19b-His-xRPA) was kindly provided by Dr. Hidenori Nakaoka. After testing induction and solubility as previously described (Section 2.6.3 and 2.6.4), protein was purified in a similar way to His-Ulp1 but from 4 l of bacterial culture. The lysis buffer used was 50 mM NaH_2PO_4 pH 8.0, 500 mM NaCl, 20 mM imidazole, 0.2% NP40. The elution buffer was 50 mM HEPES-NaOH, pH 6.8, 300 mM sucrose, 500 mM NaCl, 3 mM $MgCl_2$, and 0.2% Triton X-100 containing 250 mM Imidazole or 500 mM Imidazole and the wash buffer was the elution buffer but with 20 mM Imidazole. The purified protein was sent for anti-RPA antibody production to Eurogentec company.

Purification of His-Fen1

The plasmid containing human Fen1 (pET28b-hFen1-His) was kindly provided by Jane Grasby. After testing induction and solubility as previously described (Section 2.6.3 and 2.6.4), protein was purified as described for His-Ulp1. The lysis buffer used was 20 mM HEPES pH 7.5, 10 mM Imidazole, 250 mM KCl. The elution buffer was 20 mM HEPES pH 7.5, 250 mM KCl, containing 250 mM Imidazole or 500 mM Imidazole and the wash buffer was the elution buffer but with 20 mM Imidazole. The purified protein was sent for anti-Fen1 antibody production to Eurogentec company.

2.6. 6. Antibody purification

Using the purified proteins described above, the following antibodies were affinity purified by coupling the recombinant proteins to columns and passing the sera against the protein of interest through the columns. Using this method sheep anti-xUhrf1 (3.1 mg/ml), rabbit anti-xLig1 (1.8

mg/ml), rabbit anti-xPaf15 (0.79 mg/ml), rabbit anti-xRPA (2.5 mg/ml) and rabbit anti-hFen1 (1.13 mg/ml) were purified.

Before coupling to the column, the proteins were dialyzed into the coupling buffer (100 mM $NaHCO_3$ pH 8.3 and 0.5 M NaCl) overnight at 4°C using Pur-A-Lyzer TM dialysis tubes (Sigma Aldrich). After the dialysis, the protein was collected and the concentration was measured by Bradford assay (Section 2.7.5). The HiTrapTM NHS-activated HP column (GE Healthcare) was firstly washed with 6 ml of 1 mM HCl and then incubated with 1-3 mg of dialysed protein at room temperature for 30 min, avoiding creating any air bubbles. The antigen solution was then removed and the column incubated with 10 ml of blocking buffer (500 mM Ethanolamine pH 8.3 and 500 mM NaCl) for 30 min to block unreacted NHS groups. The column was then washed 4 times with 10 ml of 10 mM Tris-HCl pH 8 (wash 1 and 3), 0.1 M Glycine pH 2.0 (wash 2) and 0.1 M trimethylamine pH 11.5 (wash 4). All the washes were repeated once more and finally a wash with 30 ml of PBS was performed using a peristaltic pump at 3 ml/min flow rate at 4°C. After the washes, the column was ready for the use.

The serum against the protein of interest was thawed on ice and mixed with an equal volume of PBS for sheep anti-Uhrf1 serum. For rabbit sera, 20 ml of serum was mixed with 10 ml of PBS. The solution was then filtered using a 0.2 mm Stericup filter (Millipore) and recirculated through the column for at least 3 hours. The column was then washed with 30 ml of washing buffer (PBS, 0.5 M NaCl, 0.1% Triton X 100) and then with 30 ml of PBS. After the washes, the antibodies were eluted from the column with 0.1 M Glycine pH 2.0 collecting 1 ml fractions in 1.5 ml Eppendorf tubes containing 100 µl of 2 M Tris-HCl pH 8.5 to neutralise the pH. The column was finally washed with 30 ml of 10 mM PBS and stored at 4°C for further use.

2.7. General procedures

2.7.1. SDS-PAGE (Sodium Dodecyl Sulphate Poly Acrylamide Gel Electrophoresis)

Protein samples were analysed on precast gradient 4-12% NuPAGE Bis-Tris gels (InvitrogenTM) or 8-10% SDS PAGE gels prepared in the lab. Samples were denatured by mixing with 2x NuPAGE loading buffer and boiling at 95°C for 5 min. The gel tank was filled with 1x MOPS SDS (NuPAGE®) running buffer for precast gels and run at 160 V for 70 min. Home-made gels were run using 1x Tris-glycine buffer and at 100 V for 1 h. To compare protein sizes, 3 µl of Page Ruler TM plus Prestained protein ladder (Thermo scientific) was used.

2.7.2. Coomassie staining

After running the gel, proteins were visualised by staining the gel with Coomassie stain (Brilliant Blue R- 250) mixing for at least 30 min. After staining, an incubation with de-staining solution (H_2O, methanol and acetic acid in the ratio 5:4:1) was performed until proteins were visible.

For the visualization of histones as a loading control of chromatin isolation and for the gels to send for mass spectrometry, Simply Blue TM Safe Stain (Thermo Scientific) was used instead of Coomassie. These gels were washed 3 times for 5 min in water and then incubated with the stain for 1 hour or overnight mixing. Water was used for de-staining until the bands were visible.

2.7.3. Western blotting or immunoblotting

Proteins run on SDS-PAGE gels were also analysed by immunoblotting. The proteins were transferred onto Immobilon-P PVDF membranes (Merck) by electroblotting at 100 V for 90 min. Membranes were then blocked with 20-50 ml of 5% Milk (Marvel) in PBST (Table 2. 1)

and incubated overnight at 4°C with the primary antibodies (Table 2. 5) diluted in 3% BSA or 5% Milk in PBST + 0.02% sodium azide to cover the surface of the membrane piece. The unbound antibodies were removed by washing the membranes in 20-50 ml of PBST three times for 10 min. Membranes were then incubated with the specific HRP labelled secondary antibodies (Table 2. 5) diluted in 5% Milk in PBST for 1-2 h at RT and washed again as before. Finally, membranes were incubated for 5 min with enough volume of chemiluminescent HRP substrate Western Bright ECL spray (Advansta) to cover the surface of the membrane piece and exposed to X-ray film (Scientific Laboratory Supplies) in the darkness.

2.7.4. Preparation of gels for mass spectrometry (MS)

Large-scale immunoprecipitated Uhrf1 from chromatin detailed in section 2.3.12 and samples of the peak of replication from IgG and Uhrf1 depleted extracts were resolved in SDS-PAGE gels. Specifically, 10 well NuPAGE 4-12% Midi Bis-Tris gels (NP0335BOX, Invitrogen) were run in NuPAGE MOPS SDS buffer at 160 volts for a duration of 10 minutes. After the electrophoresis, protein bands were visualized using SimplyBlue SafeStain (LC6060, Invitrogen), followed by division of each lane into 10 separate bands using a clean scalpel. These gel bands were transferred into different wells within a 96 well reaction plate (40.010, Intavis), containing water below, using a clean forceps to maintain samples hydratated. The 96 well plate was securely covered using an Axygen sealing mat (AM96PCRRD, Scientific Laboratory Supplies). Subsequently, the protein samples were sent for MS analysis to Dr. Richard Jones from MS Bioworks LLC.

2.7.5. Bradford Assay

To prepare the standards, a 1 mg/ml stock solution of Bovine Serum Albumin (BSA) was prepared in water. Serial dilutions using the BSA stock were prepared in 100 µl volumes to get a range of concentrations (0.02 µg/µl -14 µg/µ). For the analysis of protein samples, 1-5 µl of

the sample was combined with 99-95 µl of water. Several repeats were performed to account for pipetting errors. Each standard solution and protein sample were then mixed with 1 ml of PierceTM Coomassie Plus (Bradford) Assay Reagent in a Fisher Brand polystyrene cuvette.

After the sample preparation, the absorbance of the standards and the sample solutions was measured at 595 nm using a spectrometer (Biowave). This absorbance data was used to construct a standard curve by plotting the known concentrations of the BSA standards against their respective absorbance values. To determine the concentrations of the protein samples, their absorbance values were plotted against the standard curve. The concentration of the protein samples were determined based on their corresponding absorbance values and the mean was used as the final concentration value.

2.8. Computational analysis

2.8.1. Quantifications using ImageJ

Pixel densities for bands in the Western blot and the scanned Coomassie-stained histones were quantified using Image J software as described in (16). The values obtained for each band of Coomassie-stained histones were normalized against the band in the no DNA sample for experiments adding recombinant histone H3. For the other experiments, the values from each western blot band were normalized to the corresponding loading controls (bands of Coomassie-stained histones from the same sample). Analyses of control and treated samples were performed in parallel, and the fold difference between these samples was calculated. Data from replicate experiments were presented in a graph showing the fold change, along with the mean value and the standard error of the mean (SEM).

2.8.2. Alpha Fold Modelling

Models in AlphaFold (AF) were carried out using the AF- multimer software as described in (16). AF was conducted on BlueBEAR, the University of Birmingham's high-performance computing (HPC) cluster. For predicting the structures of *Xenopus laevis* Uhrf1 protein, the standalone version of AlphaFold (2.1.1-foss-2021a-CUDA-11.3.1) was employed. The selected AlphaFold models were chosen based on the production of five conformations, each ranked according to their per-residue confidence scores (pLDDT). The molecular graphics and analyses were carried out using UCSF ChimeraX.

3. RESULTS

3.1. Histone H3 is di-mono-ubiquitinated during DNA replication

3.1.1. Introduction

Histones proteins maintain and form the core of chromatin structure and at the same time are highly modified with different post-translational modifications (PTMs) to regulate the accessibility of the DNA to the different cell factors. During DNA replication histone modifications orchestrate chromatin changes that allow the replisome proteins to access the DNA (68). Specifically, ubiquitination is one of the common post-translational modifications of histones. Furthermore, histones are among the most mono-ubiquitinated proteins. This is well known for histones H2A and H2B, whose ubiquitinations are key PTMs regulating DDR. But also during unperturbed DNA replication di-mono-ubiquitination of H2A at lysines K13/K15 is required for efficient fork progression (209). However, it has been found that histones undergo many other less common ubiquitination that are essential for regulating crucial chromatin processes.

On the other hand, the role of ubiquitination in DNA replication has been emphasized in the last years by the number of replication-related proteins that are regulated by this modification. Proteomic studies revealed that numerous replisome components undergo ubiquitination in unperturbed human cells (210). This modification promotes the recruitment and/or removal of replisome components from chromatin, regulates the interaction between them and also, if the replisome encounters an obstacule or damage, ubiquitination makes the replisome stop and allows DDR (211). For instance, previous research in the lab showed that poly-ubiquitination of Mcm7 promotes replisome unloading from chromatin during DNA replication termination (43). Another example is the mono-ubiquitination of PCNA at lysine K164, which alters the affinity of PCNA for different DNA polymerases (39). While we are

starting to have a better understanding of the role of ubiquitination in DNA replication, there are still many identified ubiquitinated sites on replisome proteins whose function and regulation remain not well understood.

In the lab, we are interested in how ubiquitination regulates DNA replication processes. For this reason, a previous member of the lab performed a large scale His-ubiquitin pulldown from DNA during replication termination in *Xenopus laevis* egg extract treated with NMS873, which inhibits p97 activity accumulating replisomes, and potentially other ubiquitinated proteins, on chromatin. These samples were sent for Mass spectrometry analysis (MS) to identify ubiquitinated proteins on chromatin during DNA replication. This allows us to then follow up the role of this modification and subsequently investigate the underlying biochemical processes that regulate them. Preliminary results from this experiment showed that histone H3 was one of the most ubiquitinated proteins on replicating chromatin (Table 3.1). When organizing proteins detected by MS based on the number of identified peptides with most mapped ubiquitination sites, histone H3 was first in the list (Table 3.2). Looking at which lysine residues were ubiquitinated, most peptides were ubiquitinated on lysine K23 and K18 (30 and 22 peptides respectively), with a great number (17 peptides) simultaneously ubiquitinated in K18 and K23 residues (Figure A.1 in Appendix).

Qin et al. and Nishiyama et al. later showed that histone H3 ubiquitination at lysines K18 and K23 serves as a platform for Dnmt1 recruitment to hemi-methylated sites for maintaining DNA methylation (58,60). Other residues of histone H3 have been shown to be ubiquitinated in the last few years. In yeast, lysine K14 ubiquitination stimulates the methyltransferase responsible for depositing the H3K9me2/3 repressive mark (212). In human cells, ubiquitination of K23/36/37 promotes acetylation of H3K9 and H3K14 for transcriptional activation (213). Finally, K121/122/125 are ubiquitinated in free histone H3 to regulate its

transfer between chaperones during histone assembly (94). However, considering the small size of the histone H3 protein (15 kDa), the attachment of two ubiquitin proteins (8.5 kDa each) simultaneously at K18 and K23 is a considerably large modification potentially regulating various processes during DNA replication and synchronizing them with DNA methylation. The potential importance of these modifications is also supported by the fact that histone H3 is the most abundant ubiquitinated protein on replicating chromatin in *Xenopus* extract. For this reason, the aim of this chapter of the thesis was to further investigate the mechanism by which H3 ubiquitination regulates Dnmt1 recruitment during chromatin replication as well as find out other possible roles of histone H3 ubiquitination during DNA replication.

Table 3.1. Number of peptides found of histone H3 in a His-ubiquitin pull-down from chromatin in an extract treated with NMS-873 for replisome factor accumulation. TSC (Total Spectral Counts) refers to the total number of mass spectra identified for a protein, interpreted as peptide counts per protein. This serves as an indicator of protein abundance, allowing to detect patterns within the sample. Note that these measurements are not quantitative due to their reliance on spectral counts. To confirm findings, these data is validated using western blotting for precise quantification.

Protein (kDa)	Ub TSC (coverage)	His_6-Ub TSC (coverage)
RPA1 (67)	73 (49%)	536 (77%)
MCM7 (82)	54 (44%)	360 (68%)
ATR (301)	92 (22%)	337 (45%)
HSC70 (71)	26 (31%)	180 (53%)
RAD50 (154)	18 (12%)	174 (50%)
TOPBP1 (169)	6 (4.3%)	160 (36%)
SMARCA5 (116)	0	135 (42%)
H3.2 (15)	15 (31%)	134 (60%)
MMCM6 (93)	105 (45%)	128 (45%)
FANCM (244)	70 (17%)	119 (23%)

Table 3.2. Number of peptides modified by ubiquitination in histone H3. For identifying ubiquitinated proteins and residues through mass spectrometry, peptides with GG remnant were selected. TSC: Total Spectral Counts.

Protein (kDa)	Ub TSC (coverage)	His_6-Ub TSC (coverage)
H3.2 (15)	0	54 (40%)
RPA1 (67)	0	39 (22%)
H3.3 (15)	0	21 (39%)
XRCC5 (82)	0	17 (16%)
H2B 1.1 (14)	0	6 (20%)
H4 (11)	0	6 (22%)
RPA3 (13)	0	5 (16%)
H2A (15)	0	4 (9.4%)
PAF15 (13)	0	4 (20%)
TOPBP1 (169)	0	3 (2%)

3.1.2. Results

3.1.2.1. Histone H3 ubiquitination characterization

Considering that the model of histone H3 ubiquitination promoting Dnmt1 recruitment was not proposed when this project started, we were interested in understanding the role of this modification during DNA replication. Therefore, I firstly wanted to detect ubiquitinated histone H3 bound to replicating chromatin using western blotting. To this aim, I incubated *Xenopus laevis* egg extract with demembranated sperm nuclei, allowing the DNA replication reaction to occur, and then I isolated chromatin at different times. Subsequently, proteins bound to the chromatin were analysed through immunoblotting to monitor the DNA replication progression. Figure 3. 1 A shows that the binding of replisome components peaked after 45 minutes of sperm addition. This corresponds to the moment in which more replications forks were active and most of the DNA was replicated, as shown in the graph that measures the incorporation of radioactive dATP into nascent DNA (Figure 3. 1 B). The histone H3 antibody showed that unmodified histone H3 was continuously interacting with chromatin throughout the entire time course, as part of the chromatin structure, increasing its binding from 45 minutes due to the doubling of the DNA amount (Figure 3. 1A). This antibody also detected two upper bands corresponding to ubiquitinated forms of histone H3, as confirmed by a previous student in the lab using a ubiquitin antibody (data not shown). Importantly, while the ubiquitinated histone H3 followed the same binding pattern as the replisome, it exhibited prolonged DNA binding.

In addition, I could show that this modification was specific to S phase, as it was impaired when the extract was incubated with the CDK inhibitor p27 (Figure 3. 1 C). Finally, to determine whether the two bands detected by the H3 antibody were di-mono-ubiquitinated or poly-ubiquitinated forms, the extract was supplemented with sperm DNA and either His-ubiquitin or a His-ubiquitin mutant with all lysines mutated (UbiNOK) that cannot be ubiquitinated. This experiment was performed by Suzanne Herron and showed that the mono-ubiquitinated histone

H3 band did not change after the addition of UbiNOK while three bands corresponding to histone H3 ubiquitinated with either two unmodified ubiquitin, a combination of unmodified/His ubiquitin or two His-ubiquitin could be more clearly seen. As His-UbiNOK cannot for chains, the presence of two His-Ubi modification indicates that histone H3 is subjected to di-mono-ubiquitination.

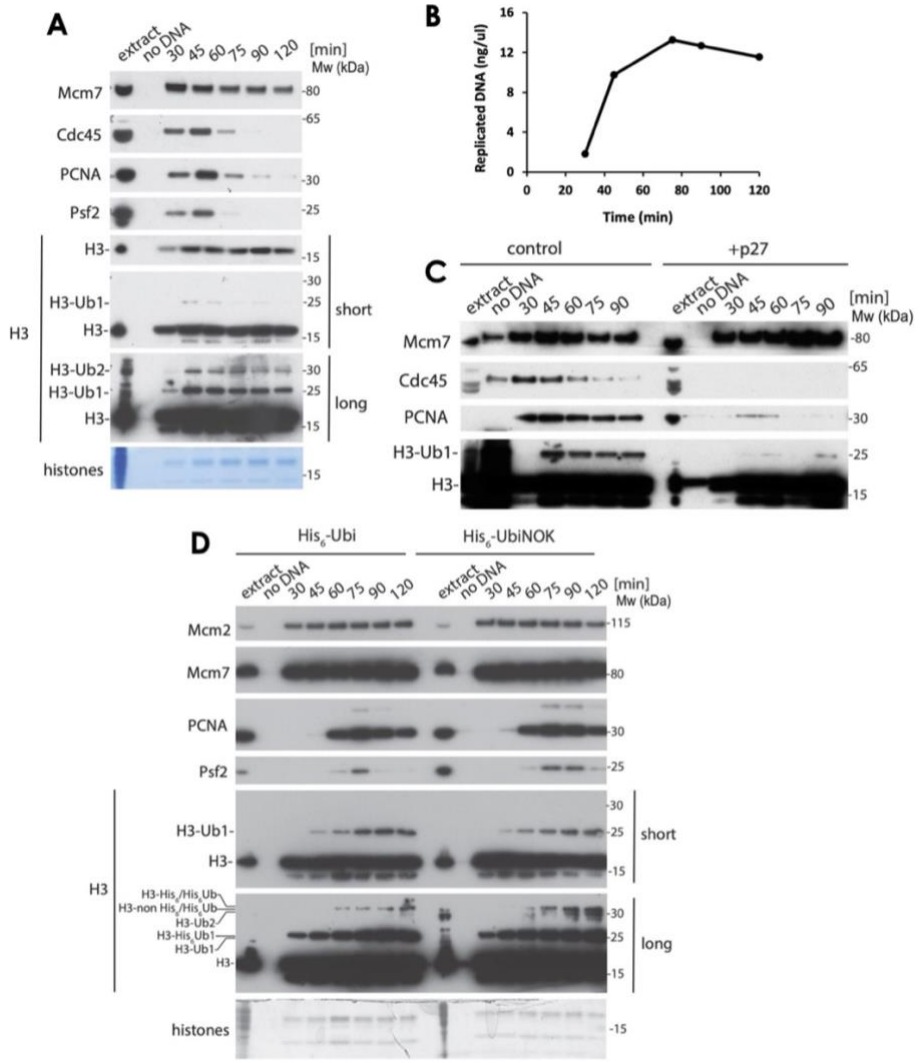


Figure 3. 1. Histone H3 is di-mono-ubiquitinated on chromatin in a DNA replication dependent manner. A) Ubiquitination of histone H3 is confirmed by immunoblotting. *Xenopus* extract was incubated with demembranated sperm nuclei and chromatin was isolated at indicated times. Proteins bound to chromatin were analysed by immunoblotting using indicated antibodies. In each condition, a sample with no DNA was also performed as a chromatin specificity control, while an extract sample was used as a western blotting positive control. Histones were stained using colloidal Coomassie as a loading control. This is a representative experiment of more than ten performed. **B)** DNA replication kinetics. Extract was incubated with sperm nuclei and α-[P32] dATP. DNA replication reaction was stopped at indicated time points and synthesised DNA was measured by quantifying α-[P32] dATP incorporation. **C)** Histone H3 ubiquitination is replication dependent. Sperm DNA was replicated in an extract supplemented with sperm DNA and either buffer or the CDK inhibitor p27, isolated at indicated times and chromatin bound proteins were analysed by immunoblotting using indicated antibodies. This experiment was carried out twice. **D)** Histone H3 is di-mono-ubiquitinated. Extract was supplemented with either recombinant His-ubiquitin or a His-ubiquitin mutant with all lysins mutated (UbiNOK). Proteins bound to chromatin were analysed by western blotting. This is a representative experiment of two performed.

3.1.2.2. Recombinant histone H3 recapitulates endogenous histone H3 ubiquitination

After confirming by immunoblotting that histone H3 was ubiquitinated on chromatin during DNA replication, the next aim was to create histone H3 mutants with the mapped ubiquitinated residues mutated to be able to identify the role of this modification. To achieve that, I first analysed and optimized the addition of wild type recombinant histone H3 to the extract before working with the mutants. Recombinant *Xenopus laevis* His-tagged histone H3 was purified from inclusion bodies by a collaborator Andrew Bowman at the University of Warwick, and its concentration was measured by comparison to a BSA standard on a gel (Figure 3. 2 A). The extract was then supplemented with sperm DNA, radioactive nucleotide and either recombinant histone H3 or the solution in which H3 was dissolved in (water) as control to analyse the levels of DNA synthesis. As shown in Figure 3. 2 B, the addition of recombinant H3 did not affect DNA replication efficiency. This was also confirmed by western blotting (Figure 3. 2 C), as the binding of the replisome factors was not altered by the addition of recombinant histone H3. The appearance of two bands in Coomassie stained histones suggest that recombinant histone H3 was incorporated into chromatin, corresponding to the top band. In a replicate experiment blotting with anti-His antibody (Figure 3. 2 D), it can be clearly seen that the recombinant histone H3 was successfully incorporated into chromatin and was subjected to di-mono-ubiquitination.

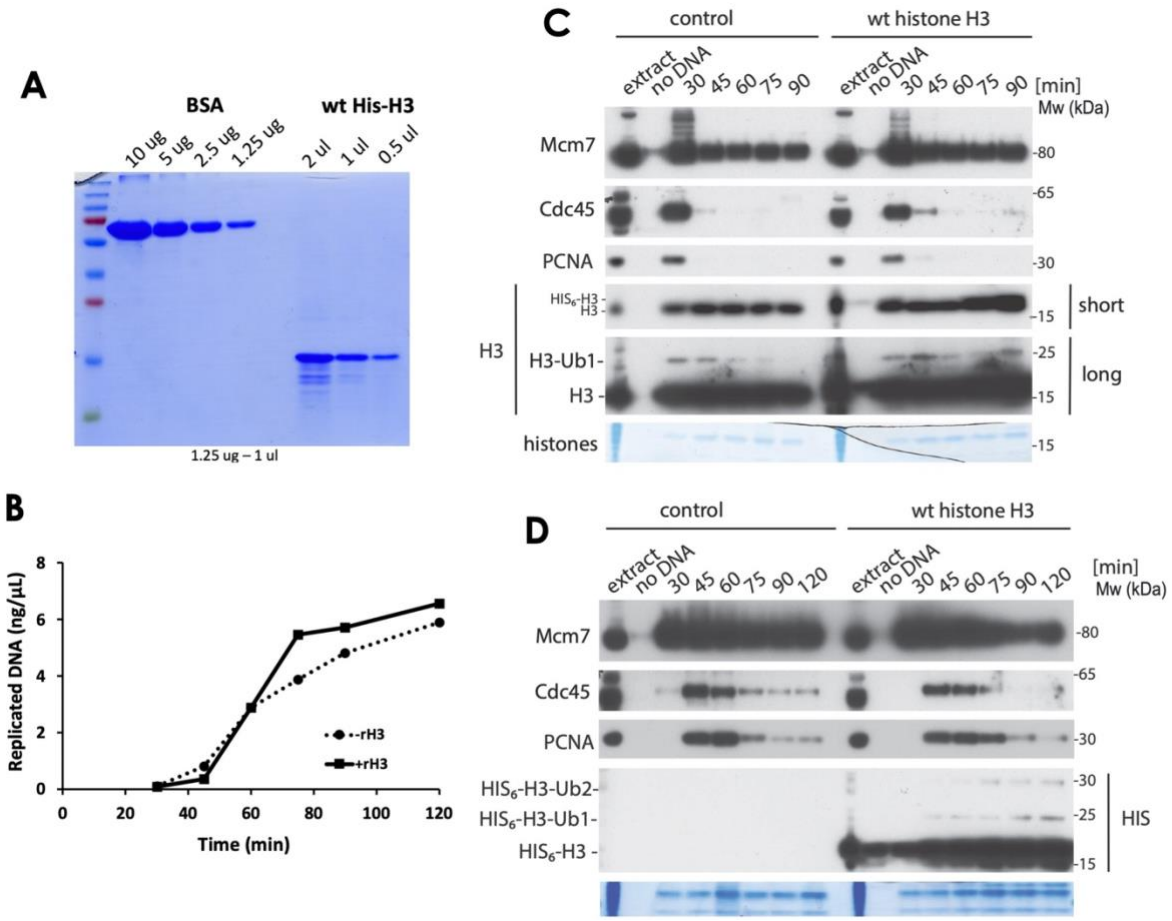


Figure 3. 2. Recombinant histone H3 is ubiquitinated on replicating chromatin. A) Purified recombinant *X.laevis* His-tagged histone H3. Recombinant wild type histone H3 was expressed in *E.coli* and purified from inclusion bodies by a collaborator. The purified protein was subjected to SDS-PAGE alongside BSA standards, and its concentration was estimated using Coomassie staining (indicated under the gel). **B)** The addition of recombinant histone H3 does not affect DNA synthesis kinetics. The extract was supplemented with sperm DNA, α-[P32] dATP and either water or recombinant histone H3. Newly synthesised DNA was measured at indicated time points by quantifying the incorporation of α-[P32] dATP into DNA. This experiment was performed twice. **C** and **D)** Recombinant histone H3 is incorporated and ubiquitinated on replicating chromatin. Sperm nuclei were added to the extract and optionally water or recombinant histone H3. Chromatin was isolated at indicated times and bound proteins were detected by immunoblotting using indicated antibodies. Both endogenous and recombinant histone H3 were detected using anti-H3 antibody (C) while only recombinant histone H3 was detected by anti-His antibody (D). These are two independent experiments from five repeats.

3.1.2.3. The impairment of histone H3 ubiquitination by using histone H3 mutant does not affect Dnmt1 recruitment

After optimizing the addition of recombinant histone H3 to *Xenopus laevis* egg extract, the next step was to create mutants that cannot be ubiquitinated to see the effect on DNA replication. As mass spectrometry analysis identified a significant number of peptides with lysines K18 and K23 residues ubiquitinated on histone H3, I designed single and double mutants of these residues (H3K18R, H3K23R, H3K18/K23R). Recombinant proteins were purified from inclusion bodies by a collaborator and the concentrations were measure as for wild type histone H3 (Figure 3. 3 A). The extract was supplemented with sperm DNA and either the mutants or wild type protein for the subsequent analysis of DNA replication. As the addition of histone H3K18R and H3K23R single mutants did not cause any defect in the DNA replication process (data not shown), only experiments using the double mutant are shown. DNA synthesis was not affected by the addition of the histone H3K18/K23R mutant (Figure 3. 3 B). Importantly, mutations in both known ubiquitinated sites did not impair histone H3 ubiquitination since the double mutant exhibited similar modification levels on replicating chromatin as the wild type (Figure 3. 3 C).

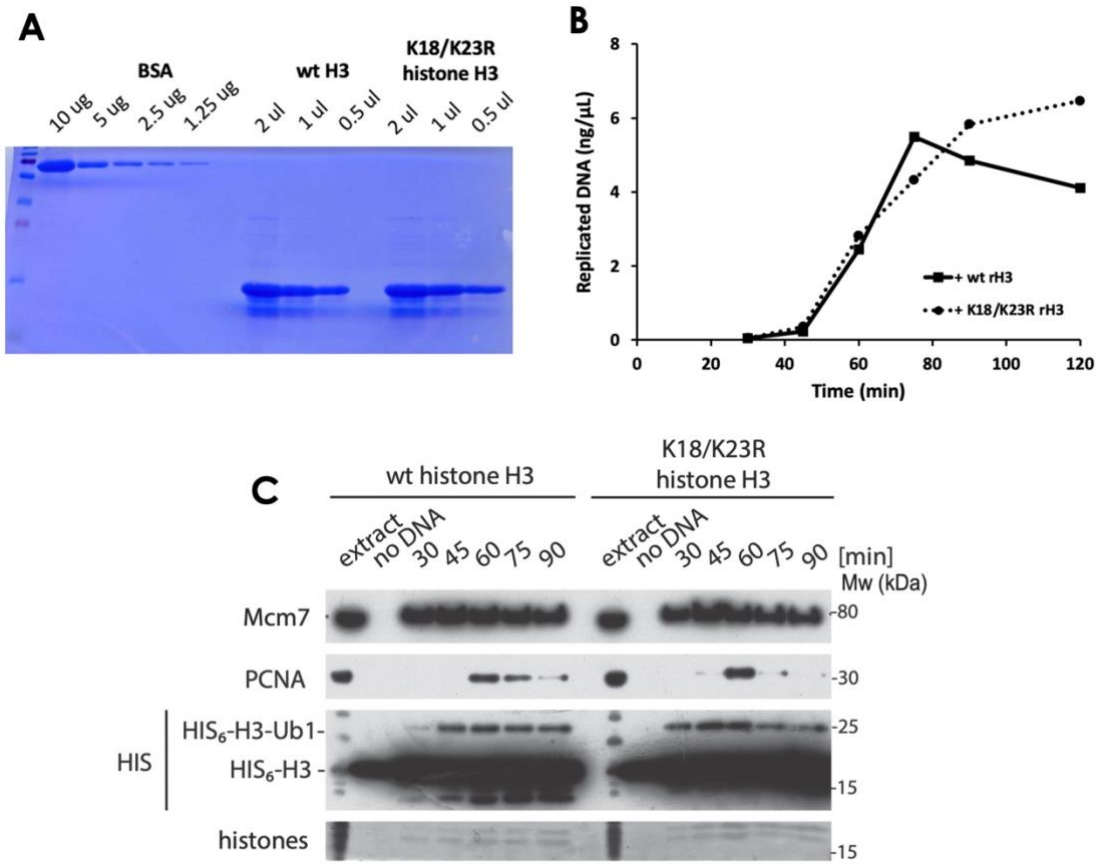


Figure 3. 3. Histone H3K18/K23R mutant can still be ubiquitinated on chromatin. A) Purified recombinant *X.laevis* His-tagged histone H3 wild type and K18/K23R mutant. Recombinant histone H3 mutant was purified from inclusion bodies and the concentration was estimated by comparison with BSA standards using SDS-PAGE and coomassie staining. **B)** Histone H3 mutant does not affect DNA synthesis. DNA replication levels were measured at indicated times in extract supplemented with sperm DNA, α-[P32] dATP and either wt or K18/K23R mutant histone H3 by quantifying the incorporation of radionucleotides. This experiment was carried out once. **C)** Histone H3K18/K23R mutant is ubiquitinated on replicating chromatin. Extract was incubated with sperm nuclei either wt or mutant K18/K23R histone H3. At specified times, chromatin was isolated and associated proteins were identified via western blotting with the indicated antibodies. This is a representative experiment of two performed.

Given that histone the H3K18/K23R mutant could still undergo ubiquitination on chromatin, triple and quadruple mutants were produced modifying the two neighbouring lysines (H3K14/K18/K23R, H3K18/K23/K27R, H3K14/K18/K23/K27R). This was because commonly ubiquitination can modify neighbouring lysines when the optimal ones are not available. Furthermore, lysines K14 and K27 were also found ubiquitinated in MS from our lab and from another study (59). The purified quadruple mutant is shown in Figure 3. 4 A (triple mutants not shown). The mutants or wild type protein were added to the extract before sperm DNA to ensure the incorporation of the recombinant proteins during chromatin assembly and prevent precipitation. Then proteins associated with chromatin during replication were analysed by immunoblotting. Triple mutants did not show any defect in histone H3 ubiquitination (data not shown). Interestingly, the quadruple mutant impaired ubiquitination (Figure 3. 4 C), suggesting that when K18 and K23 are not available, K14 and K27 may act as alternative ubiquitination sites. However, inhibiting histone H3 ubiquitination neither affected the binding pattern of replisome factors nor levels of synthesised DNA (Figure 3. 4 B, experiment performed by Dr Rebecca Jones). Surprisingly, the recruitment of Dnmt1 to chromatin was also not impaired by the lack of this modification. These results could be explained by the residual endogenous wild type H3 on chromatin, which can still be ubiquitinated and may promote Dnmt1 binding. Furthermore, alternative pathways of Dnmt1 recruitment could also be the cause of this finding.

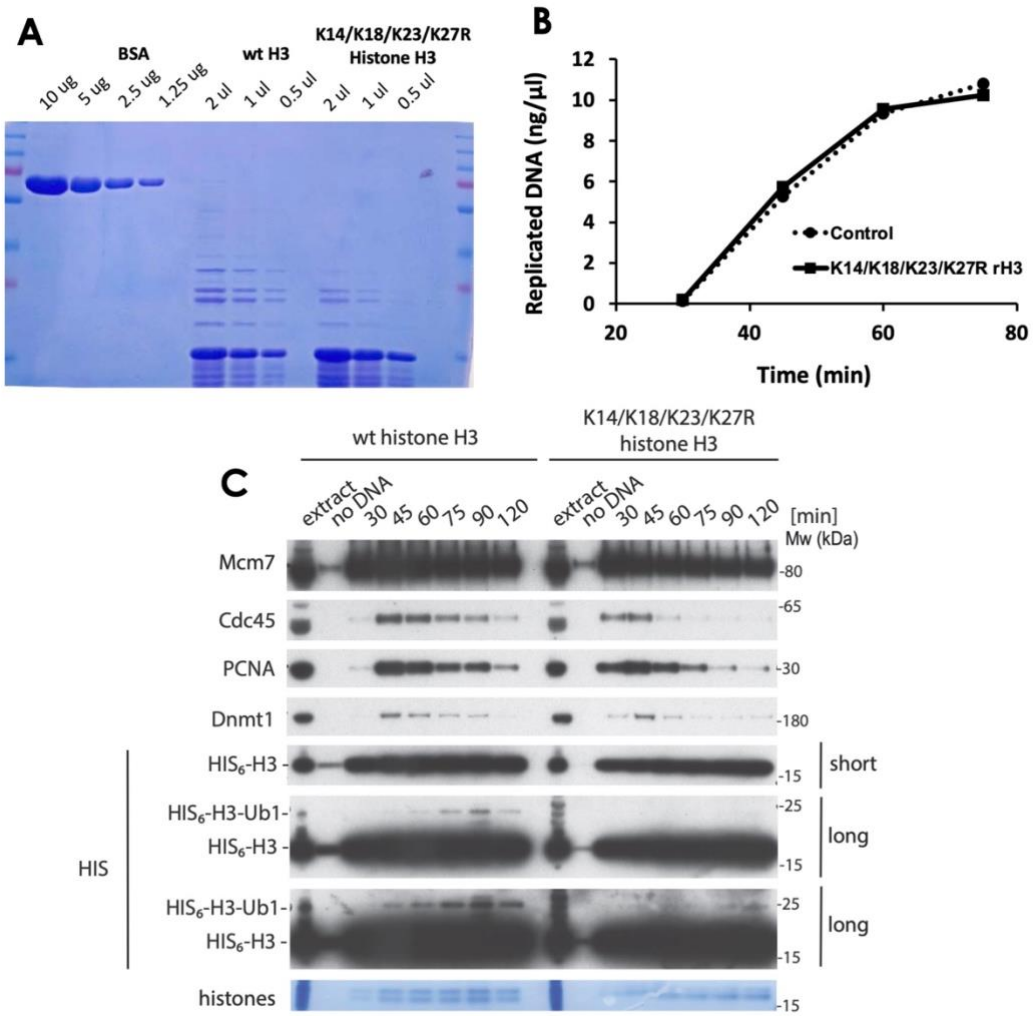


Figure 3. 4. Histone H3 quadruple mutant impairs ubiquitination. A) Purified recombinant *X.laevis* His-tagged histone H3 wild type and K14/K18/K23/K27R mutant. Histone H3 quadruple mutant was purified from inclusion bodies and run in SDS-PAGE with BSA standards for measuring the concentration by Coomassie staining. **B and C)** Histone H3 quadruple K14/K18/K23/K27R mutant cannot be ubiquitinated on chromatin. DNA replication was performed in extract supplemented with sperm DNA and either wt or K14/K18/K23/K27R mutant histone H3. To quantifying the synthesised DNA levels, α-[P32] dATP was also added to measure its incorporation (B). This experiment was performed once. **C)** At specified times, chromatin was isolated and indicated proteins were identified via western blotting as in previous figures. This is a representative experiment of two performed.

3.1.2.4. Using mouse sperm to incorporate rH3 wild type and mutants more efficiently

Interestingly, a study was published a study showing that *Xenopus* sperm DNA still retains significant amounts of histones H3 and H4, making it impossible to fully replace them with the recombinant proteins (206). To overcome this limitation, the authors developed a protocol to isolate mouse sperm nuclei to use in *Xenopus laevis* egg extract since mouse spermatozoa contains only about 1% of the histone H3 found in somatic cells (214) (Figure 3. 5 A, B). Knowing this, we hypothesised that the recruitment of Dnmt1 could be due to the ubiquitination of the already assembled histones H3. Therefore, we decided to use mouse sperm nuclei in my experiments to be able to incorporate a higher percentage of the recombinant histones and then be able to see the effect of the impairment of H3 ubiquitination. Following the published protocol, permeabilized mouse sperm nuclei were successfully isolated from mouse testis. This was confirmed through microscopy visualization, using transmitted light or Hoechst staining (Figure 3. 5 C).

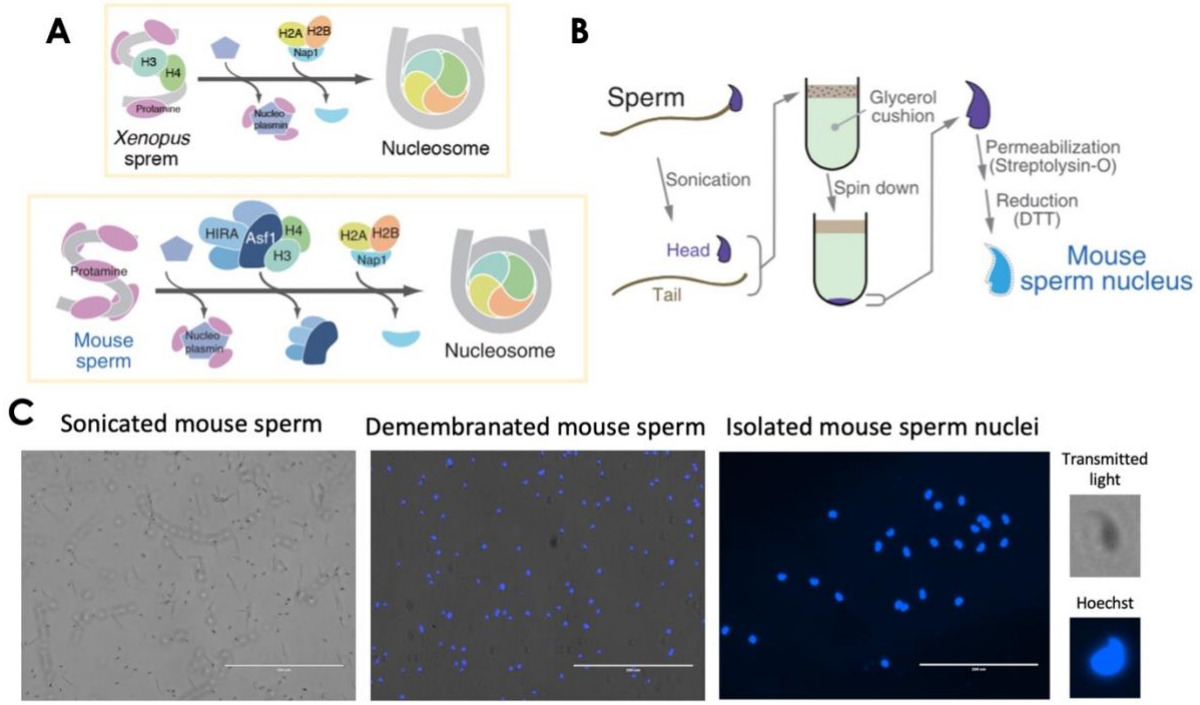


Figure 3. 5. Mouse sperm nuclei isolation. A) Scheme of protamine and histone composition of Xenopus sperm and mouse sperm. **B)** Schematic representation of the method followed for mouse sperm nuclei isolation (Adapted from (205)). **C)** Images taken during the process of purification of mouse sperm nuclei. Scale bar, 200 µm.

Next, to test whether mouse sperm nuclei could be efficiently replicated in *Xenopus* egg extract, I incubated isolated mouse sperm DNA with the extract. The progression of the DNA replication reaction was firstly monitored using the microscope, by staining the DNA with Hoechst. After adding mouse sperm to the extract, the nuclei gradually lost their teardrop-like shape and adquired a more rounded and large form, similar to what is seen with *Xenopus* sperm but slower (Figure 3. 6 A). I also confirmed by using Dil dye, which specifically stain lipophilic membranes, that the nuclear membrane was formed around mouse nuclei as occurs with *Xenopus* nuclei (Figure 3. 6 B). Afterwards, DNA synthesis was measured by quantifying radionucleotide incorporation (Figure 3. 6 C). This experiment showed that mouse sperm was undergoing replication in the extract, but the replication process took longer to reach the plateau phase and showed lower efficiency compared to the natural substrate. This led me to investigate whether the reduced levels of synthesized DNA were a result of inefficient replication within each nucleus or because fewer nuclei were accessible and replicated.

To gain deeper insights into the replication dynamics using mouse sperm, the extract was incubated with Cy3-dUTP (allowing to monitor nascent DNA synthesis under the microscope) and either mouse or *Xenopus* sperm (Figure 3. 6 D). While all *Xenopus* sperm nuclei were replicated within 45 minutes, mouse nuclei were not all fully replicated even after 180 minutes. Although a faint red signal was visible in all mouse nuclei, only about half of them showed a strong signal. However, the replication seemed to be efficient in those nuclei that were actively replicating, as the stain intensity was comparable to the one observed in *Xenopus*. For that reason, chromatin isolation was finally performed at different times in the extract supplemented with mouse sperm to analyse DNA associated proteins (Figure 3. 6 E). As expected, replisome factors were binding to mouse DNA at later time points compared with *Xenopus* DNA. Interestingly, histone H3 was also ubiquitinated on mouse chromatin confirming that this

strategy can be used to study recombinant histones incorporation since it recapitulates *Xenopus* DNA replication.

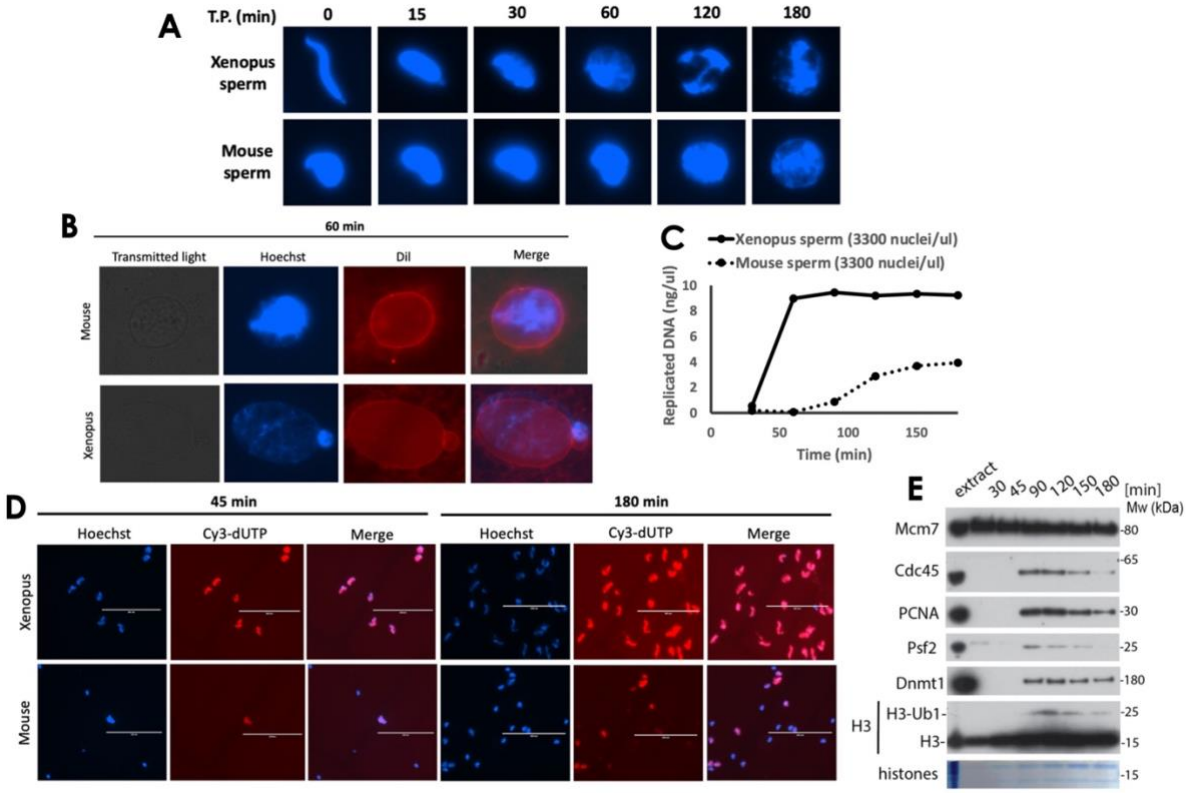


Figure 3. 6. Histone H3 is ubiquitinated on mouse chromatin replicated in *Xenopus* extract. A and B) Round mouse nuclei are formed in the extract. Extract was supplemented with either *Xenopus* or mouse sperm and the DNA replication reaction was visualized at indicated times using Hoechst **A)** and Dil **B). C)** Mouse sperm DNA is replicated in the extract. Extract was incubated with optionally *Xenopus* or mouse sperm and α-[P32] dATP. The reaction was stopped at indicated times and DNA synthesis was then measured by α-[P32] dATP incorporation. **D)** Some mouse sperm nuclei have problems to replicate. Extract supplemented with Cy3-dUTP and either *Xenopus* or mouse sperm was incubated at 23ºC for the indicated length of time. Nuclei replication was monitored under the microscope using Hoechst stain for DNA and Cy3-dUTP for nascent DNA synthesis. Scale bar, 200 μm. **E)** Histone H3 is ubiquitinated on mouse chromatin. Mouse sperm was incubated in the extract, chromatin was isolated at indicated times and associated proteins were detected by immunoblotting.

To optimize the use of mouse sperm in *Xenopus* egg extract and achieve more similar DNA replication kinetics, I produced another batch of mouse sperm nuclei using lysolecithin for demembranation instead of streptolysin-O for permeabilization. Notably, lysolecithin is commonly used in the lab for the preparation of *Xenopus* sperm nuclei. We hypothesised that this alternative demembranation approach could increase the accessibility to the sperm DNA within the nuclei, accelerating the DNA replication process and perhaps allowing replication of those problematic nuclei. To compare the mouse sperm batches for DNA replication analysis, I first carried out a radionucleotide incorporation assay using both batches. As shown in Figure 3.7 A the levels of synthesized DNA were higher in demembranated nuclei. Quantifying the number of replicating nuclei using Cy3-dUTP dye, both batches had a similar percentage of replicated nuclei after 210 minutes (Figure 3.7 B). However, the batch of demembranated nuclei exhibited a faster and more efficient replication process, with replicated nuclei being visible at earlier time points, and the majority displaying a robust, round shape and intense red staining at 210 minutes (Figure 3.7 C). Finally, both batches were compared by analysing the binding of the replisome proteins at different times during DNA replication (Figure 3.7 D). The recruitment of the different proteins was similar between samples, with all being recruited from 90 min. However, in line with previous results, demembranated nuclei showed slightly faster proteins disassembly. Altogether these findings suggest that demembranated mouse sperm nuclei replicate DNA more efficiently and display the completed replication reaction in a shorter period of time.

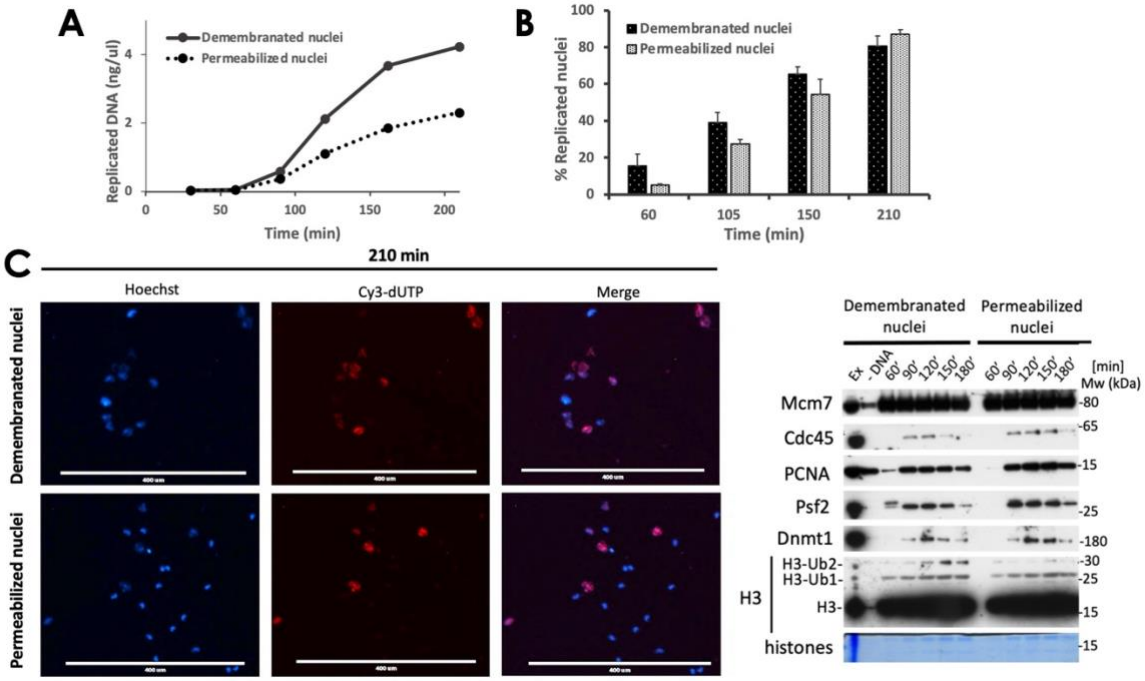


Figure 3.7. Demembranated mouse sperm nuclei replicates faster than permeabilized DNA. A) Levels of synthesised DNA are higher in demembranated nuclei. Interphase *Xenopus laevis* egg extract was incubated with α-[P32] dATP and either demembranated or permeabilized mouse sperm nuclei during indicated times. DNA was precipitated and replicated DNA was measured by α-[P32] dATP incorporation. **B)** Quantification of replicated nuclei at different times in the two different mouse nuclei batches. Extract was supplemented with Cy3-dUTP and either one of both batches of mouse sperm. Nuclei replication was monitored under the microscope using Hoechst stain. The number of replicated nuclei (red nuclei) was counted per 100 nuclei in each time point. The mean of three independent experiments with SEM is shown. **C)** Demembranated nuclei are generally bigger, rounder and more intense than permeabilized nuclei. The same procedure as for **B)** was carried out to visualised nuclei. Scale bars, 400 μm. **D)** Chromatin bound proteins are disassembled earlier in demembranated nuclei. Each batch of mouse sperm nuclei was incubated with the extract, chromatin was isolated at different times after DNA addition and bound proteins were detected by western blotting.

After optimizing the replication of mouse sperm DNA in *Xenopus* egg extract, the next step was to test whether the incorporation of the recombinant histone H3 into chromatin could be indeed improved. To achieve this, the extract was supplemented with wild type His-tagged histone H3 prior to the addition of demembranated mouse sperm nuclei, to allow the DNA to form nucleosomes using the recombinant proteins. Successfully, recombinant histone H3 was being incorporated and ubiquitinated on mouse chromatin (Figure 3. 8 A).

Next, I wanted to analyse whether the quantity of recombinant histones bound to chromatin was higher in comparison to using *Xenopus* sperm DNA. For this, I quantified the bands of recombinant histone H3 and endogenous histones bound to replicating chromatin seen by Coomassie staining (upper and lower band respectively). As seen in Figure 3. 2 C and D for *Xenopus* sperm, the addition of recombinant histone H3 created a double band, corresponding the extra top band to the recombinant His-H3. Also, in the histones of Figure 3. 8 A there is a band in the no DNA sample corresponding to some recombinant protein precipitating in the extract. All this evidence indicate that the upper band in the Coomassie staining is recombinant H3. The quantification was performed at various time points across three different experiments for both mouse and *Xenopus* nuclei using ImageJ. Subsequently, the ratios between recombinant and endogenous H3 were calculated. Mean ratios were determined for the early time point (before the peak of replication), all time points and the final time point during the replication reaction and represented with SEM bars in a graph (Figure 3. 8 B). As hypothesised, the incorporation of recombinant histones relative to endogenous was improved in mouse compared to *Xenopus*, with higher recombinant/endogenous ratios in all the conditions. In *Xenopus* DNA, fewer recombinant histones were initially bound since it already contains histones. Then with replication doubling the DNA, more recombinant histones were incorporated reaching a ratio of approximatly 1 in the later times of replication. However, although the mouse system was better to get more recombinant protein on chromatin to study

the ubiquitination of histone H3, the addition of both mouse sperm nuclei and the recombinant histone H3 had a considerable negative impact on the *Xenopus* egg extract replication dynamics. This can be seen by the slowdown in DNA replication indicated by the delayed replication factor binding. This could be expected given that the introduction of either recombinant histone H3 or mouse sperm DNA individually already caused delays in the DNA replication reaction. However, when both conditions were combined, the replication reaction was strongly affected.

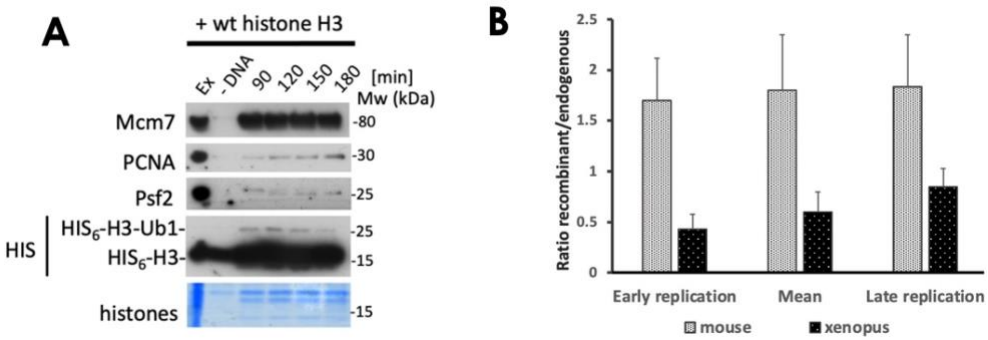


Figure 3. 8. Mouse sperm nuclei incorporate recombinant histone H3 more efficiently. A) Recombinant histone H3 is ubiquitinated on mouse chromatin. Interphase *Xenopus* extract was supplemented with wild-type His-tagged histone H3 and demembranated mouse sperm nuclei. The replication reaction was stopped at the indicated times and chromatin associated proteins were analysed by western blotting using specified antibodies. **B)** Mouse sperm DNA shows higher recombinant histone H3 incorporation than *Xenopus* sperm DNA. Experiments were performed as in A) using mouse or *Xenopus* nuclei. Quantification of the bands corresponding to recombinant histone H3 and endogenous histones bound to replicating chromatin was performed in ImageJ across different times. The ratios between recombinant and endogenous histone H3 were calculated for each time point. Mean ratios of n=3 experiments were graphically represented with SEM bars.

As a final attempt, I tried to immunodeplete histone H3 from *Xenopus* egg extract to overcome the limitation of the binding of endogenous histone H3 when using *Xenopus* sperm DNA. For this purpose, purified His-tagged histone H3 was sent to the company Eurogentec for making antibodies. The sera from two different rabbits before and after antigen injection were obtained and their specificity for recognizing histone H3 was tested by immunoblotting. Unfortunately, as shown in Figure 3. 9 neither of the antibodies could recognize endogenous histone H3 in either extract or on chromatin. This result excluded the possibility of immunodepleting histone H3 from the extract, forcing us to explore new strategies for studying histone H3 ubiquitination. This will be developed in the next chapter.

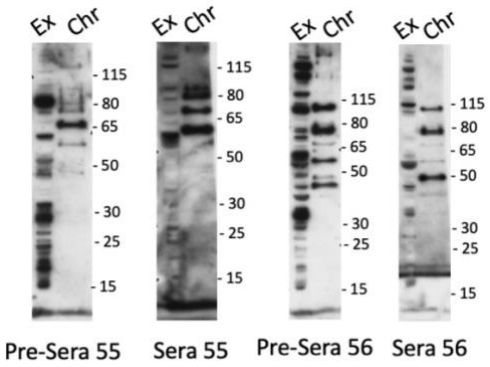


Figure 3. 9. Histone H3 sera do not recognize endogenous histone H3. Samples from extract and chromatin isolated at peak of replication where run in a SDS-PAGE gel. Western blotting using pre-immune sera and sera after immunization with recombinant histone H3 from two rabbits was performed.

3.1.3. Discussion

This chapter has confirmed that histone H3 is di-mono-ubiquitinated on chromatin at lysines K18 and K23 during DNA replication. Using *Xenopus laevis* egg extract as a model system, preliminary MS data identified histone H3 ubiquitinated at K18 and K23 as one of the most ubiquitinated proteins on chromatin during DNA replication. These ubiquitinations of histone H3 have been reported by other groups to promote Dnmt1 recruitment and DNA methylation maintenance (58,60). In this part of the thesis, several findings were achieved. Firstly, I have confirmed that histone H3 is ubiquitinated on these residues during DNA replication. Additionally, I also showed that when K18 and K23 are not available, histone H3 can still be ubiquitinated on neighbouring lysines K14 and K27. However, the partial inhibition of histone H3 ubiquitination using a quadruple mutant (H3K13/18/23/27R) is not enough to impair Dnmt1 recruitment. Finally, I have established a protocol to replicate mouse sperm DNA in S phase *Xenopus* egg extract to better study recombinant histones on chromatin. This system recapitulates the DNA replication process and importantly histone H3 ubiquitination similarly as occurs with *Xenopus* DNA.

The results in this chapter demonstrate that histone H3 is di-mono-ubiquitinated in a DNA replication dependent manner since histone H3 ubiquitination bands disappeared when DNA replication was blocked by the addition of p27. In addition, the experiment using the ubiquitin mutant UbiNOK that cannot be ubiquitinated clarifies that two single ubiquitin moeties are added to different lysines of histone H3. These findings were also shown by the Nakanishi group in similar experiments using p27 in an extract depleted for Dnmt1 and UbiNOK in extracts treated with ubiquitin vinyl sulfone (UbVS) to inhibit deubiquitination (58,169). Although in Figure 3. 1 A the ubiquitination levels correlated with the binding of replisome factors, indicating again the replication link of the modification, it stayed on chromatin for longer even in the later time points. The same group has recently suggested that histone H3

ubiquitination would mediate Dnmt1 recruitment in late S phase (130). They showed that this modification is increased in later time points during DNA replication. However, ubiquitinated histone H3 is also detected in my experiments from the beginning of S phase, even before the strong binding of the replisome factors. This suggests that this modification could regulate additional processes occurring earlier and later during DNA replication, such as nucleosome assembly and remodelling, and coordinating them with DNA methylation maintenance.

The addition of recombinant histone H3 to the extract recapitulates endogenous histone H3 incorporation and ubiquitination, which allows to study this modification using mutants. While the mutation of the known ubiquitination sites H3K18/23R did not impair histone H3 modification, the quadruple mutant H3K14/18/23/27R did. These findings suggest that histone H3 ubiquitination could "jump" to adjacent lysines when the preferred ones are not available. However, the ubiquitination of lysine K14 and K27 were also identified to be less abundant in our MS analysis and in another study (59), meaning that these sites are also ubiquitinated in normal conditions. It is interesting since the ubiquitination of H3K14 has been shown to promote H3K9 methylation for heterochromatin formation (212). On the other hand, H3K27 is itself a well characterised site that is tri-methylated acting as a repressive mark (65). Therefore, the ubiquitination of this residue could also promote the methylation or compete with this modification. Thus, these findings could reveal a link between DNA methylation and histone remodelling machineries a well as a crosstalk between epigenetic marks.

Surprisingly, this study reveals that a partial inhibition of histone H3 ubiquitination by using histone H3 mutant does not have any impact on the recruitment of Dnmt1. Previous studies showed that the impairment of histone H3 ubiquitination by the removal of Uhrf1 ubiquitin ligase suppressed Dnmt1 binding (58). However, the use of H3 mutant did not have this effect. One explanation is the presence of endogenous histone H3 on chromatin. Despite the excess of

recombinant histone H3 that was added to the extract and that it was assembled on chromatin, endogenous histone H3 was still recognized bound to chromatin and ubiquitinated by the H3 antibody. It could then be possible that a mixture of mutant and endogenous H3 was forming the nucleosomes, so even a small proportion of ubiquitinated endogenous H3 was sufficient to promote Dnmt1 recruitment and other possible functions associated with histone H3 ubiquitination. Another explanation could be the existence of alternative pathways for recruiting Dnmt1. Currently the model suggests the existence of distinct modes of recruitment regulated by different factors. Paf15 di-mono-ubiquitination at K15 and K24 has recently been proposed as another mechanism of Dnmt1 recruitment acting preferentially during early replication (130). In addition, the ubiquitinated histone H2B has also been shown to be recognized by Dnmt1 for DNA methylation maintenance (171). Interestingly, in all the proposed models, ubiquitination mediates the recruitment of Dnmt1 and these ubiquitinations are carried out by the same E3 ubiquitin ligase, Uhrf1. Therefore, the recruitment through Paf15 or H2B ubiquitination could explain the binding of Dnmt1 in the absence of histone H3 ubiquitination.

To overcome the limitation of endogenous histone H3, I showed that mouse sperm DNA increases the incorporation of recombinant histones. After finding out that *Xenopus* sperm DNA retains a great amount of histone H3 (206), we hypothesised that most of the endogenous histones detected on chromatin were originally bound to DNA when forming the sperm. So, I standardised a protocol to replicate mouse sperm nuclei in *Xenopus* extract to study the ubiquitination of recombinant H3, since mouse sperm DNA rarely retains histones (214). Interestingly, mouse nuclei recapitulated all the DNA replication events: the decondensation of sperm nuclei, the formation of a rounded membranated nucleus, the synthesis of DNA and the assembly and disassembly of the replisome factors. These findings align with the results obtained in mitotic extracts by the group that stablished the protocol for mouse sperm nuclei

isolation (206). Histone H3 was also ubiquitinated on mouse chromatin replicated in *Xenopus* extract. However, it took more time to accomplish all these processes compared to *Xenopus* nuclei possibly because it is not the natural substrate. Successfully, the recombinant wild-type H3 was incorporated into the chromatin more efficiently than in *Xenopus* DNA as predicted.

Despite the successful findings, the extreme delay in DNA replication, showed by the prolonged PCNA chromatin binding, suggests problems with DNA replication when using mouse nuclei. The addition of mouse DNA and recombinant histone H3 simultaneously was affecting DNA replication to levels that make it difficult to the study the ubiquitination of histone H3. In the future, radionucleotide incorporation assay to test DNA synthesis kinetics could be additionally performed to prove this defect. Apart from this, optimizing the addition of recombinant histone H3 into the extract was a challenging task in every experiment. To compete with the large quantity of endogenous histones already present in the extract, a high concentration of recombinant histones needed to be added. This led to precipitation as evidenced in the no DNA samples. For this reason, it was always difficult to determine the right quantity of histones added to avoid precipitation but at the same time give a high incorporation ratio. This could be improved in the future by adding recombinant H3 in complex with histone H4, since histone H3 is mainly found in the extract as heterodimers with histone H4. The addition of H3 as monomer could potentially result in less efficient incorporation of recombinant histones compared to the preferred endogenous ones.

Considering all these facts described above, we decided to stop using mouse sperm and look for another strategy to solve the problem of the incorporation of endogenous histone H3. However, in the future the optimized protocol to replicate mouse sperm in *Xenopus* extract could be useful to study other processes during DNA replication such us histone assembly. This process remains not well understood, and since it occurs early in replication when mouse DNA

showed increased histone incorporation compared to Xenopus DNA, it would be a better system to label histones and track their recruitment to chromatin.

As a new strategy, immunodepletion of H3 was considered the best option found to avoid the binding of endogenous protein, despite the high concentration of histones in the extract and the challenges associated with achieving significant depletion. This method would also solve the problem of precipitation, since without the need to compete with endogenous histones less recombinant protein could be added to the extract. Unfortunately, sera raised against recombinant H3 did not recognize the endogenous protein for immunodepletion. The failure in generating and effectively using histone specific antibodies could be due to several reasons. Firstly, the fact that histones are highly conserved proteins, being less likely to be perceived as foreign antigens by the animal. Additionally, the great amount of PTMs present in these small proteins along with the numerous reader and writer factors that bind to these sites, could diminish epitope recognition. The requirement for generating specific antibodies for the proteins of interest, which are required for techniques like immunoblotting, immunoprecipitation or immunodepletion, is a limitation of the *Xenopus* egg extract system. Generally, commercially available antibodies are designed for human proteins and often do not recognize *Xenopus* variants. Additionally, they are not affordable considering the quantities needed for immunodepleting a protein from the entire extract. All these factors led us to find a new method to study H3 ubiquitination in *Xenopus* extract, which will be discussed in the next chapter.

Altogether, the data presented in this chapter confirmed that histone H3 is di-mono-ubiquitinated at lysines K14/18/23/27 on chromatin during DNA replication. Furthermore, I have established a procedure for replicating mouse sperm DNA using *Xenopus* egg extract, which could be useful for future research.

3.2. Uhrf1 as the E3 ubiquitin ligase responsible of histone H3 ubiquitination

3.2.1. Introduction

The difficulties with effectively using histone H3 mutants in *Xenopus laevis* egg extract to study the role of H3 di-mono-ubiquitination during DNA replication raised the need of finding a new strategy to study this modification. Considering that all the proposed models of Dnmt1 recruitment were regulated by ubiquitination and that Uhrf1 was proposed to be the E3 ligase responsible for all these modifications, we decided to study the effect of histone H3 ubiquitination and Dnmt1 recruitment through Uhrf1.

The essential role of Uhrf1 in the maintenance of DNA methylation is now well established (58,60,126,127,135). Uhrf1 can recognize and bind hemi-methylated DNA (147). In addition, the lack of Uhrf1 has been shown to impair Dnmt1 binding to chromatin and DNA methylation (58,60). However, the mechanism and the context in which this epigenetic mark is maintained during DNA replication remains unclear. Dnmt1 interacts with di-mono-ubiquitinated histone H3 at K18 and K23, which has been proposed to stimulate its activity (129,169). Furthermore, Nishiyama and co-workers have shown that when Dnmt1 is not present, histone H3 ubiquitination is increased, but when both Dnmt1 and Uhrf1 are missing, this modification is not detected (58). As the addition of Uhrf1 rescued this defect in H3 ubiquitination, it was proposed that Uhrf1 promotes Dnmt1 recruitment through ubiquitination of histone H3.

The aim of this chapter of the thesis was to confirm that Uhrf1 mediates histone H3 ubiquitination and Dnmt1 recruitment. Additionally, I wanted to understand how DNA methylation maintenance is coordinated with DNA replication and chromatin assembly. Finally, I was interested in finding out other roles of Uhrf1 and Uhrf1-mediated H3 ubiquitination.

3.2.2. Results

3.2.2.1. Uhrf1 immunodepletion inhibits histone H3 ubiquitination and Dnmt1 recruitment

Given that Uhrf1 is the E3 ligase proposed to mediate histone H3 ubiquitination as well as Dnmt1 recruitment, I decided to carry out immunodepletion of Uhrf1 from *Xenopus laevis* egg extract to confirm that both processes depend on Uhrf1 and to find out other possible consequences of the lack of Uhrf1 and histone H3 ubiquitination. To this aim, specific antibodies against *Xenopus* Uhrf1 were needed.

Sera against Uhrf1 were already raised in the lab so I needed to purify specific antibodies from whole sera using an antigen column. To get the antigens needed for purifying antibodies, I firstly expressed full-length His-tagged *Xenopus* Uhrf1 in *E.coli* and purified it using Nickel columns. Samples taken during the expression and purification process were run in an SDS-PAGE gel and visualized by Coomassie staining (Figure 3. 10) to follow the course of the purification. Uhrf1 protein was successfully purified, although the protein seems to be degraded/truncated (bands below 80 kD visible on Coomassie gel). As the aim was to purify antibodies, elution 3 was dyalized into coupling buffer and the concentration was measured by gel comparison with BSA standards (not shown).

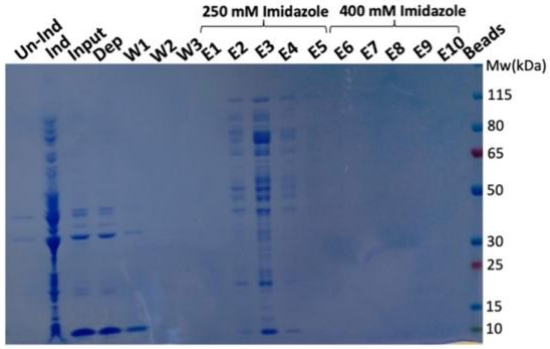


Figure 3. 10. Purification of recombinant *Xenopus laevis* His-tagged Uhrf1. Expression of His-xUhrf1 was induced in *E.coli* (Ind) and purified as specified in the methods section using Nickel affinity purification. Supernatant from bacterial lysate containing soluble proteins (Input), un-bound proteins (Dep), samples from beads washes (W1-3) and elutions using two concentrations of Imidazole (E1-E10) are shown. A sample from the beads was also taken to check non-eluted protein (Beads). Samples from the purification process were run in a SDS-PAGE gel and visualized by Coomassie staining

The next step was to use purified Uhrf1 to create an antigen column for antibody purification from whole sera. Consequently, purified Uhrf1 was incubated with an HiTrap NHS-activated column for the binding. The specificity of sheep and rabbit sera against Uhrf1 from different animals already raised in the lab was tested by immunoprecipitation (IP) from whole egg extract (Figure 3. 11 A, experiment performed by Dr Rebecca Jones). Since sheep and rabbit 69 sera showed greater efficiency in immunoprecipitating Uhrf1, I affinity purified anti-Uhrf1 antibodies by running sheep serum through the Uhrf1 antigen column. Five rounds of purification were carried out and the most concentrated sample of the first three rounds were tested for specificity by IP comparing with whole sera (Figure 3. 11 B). Purified antibodies could IP Uhrf1 from the extract with similar efficiency to serum but showed cleaner signal in western blotting (not shown).

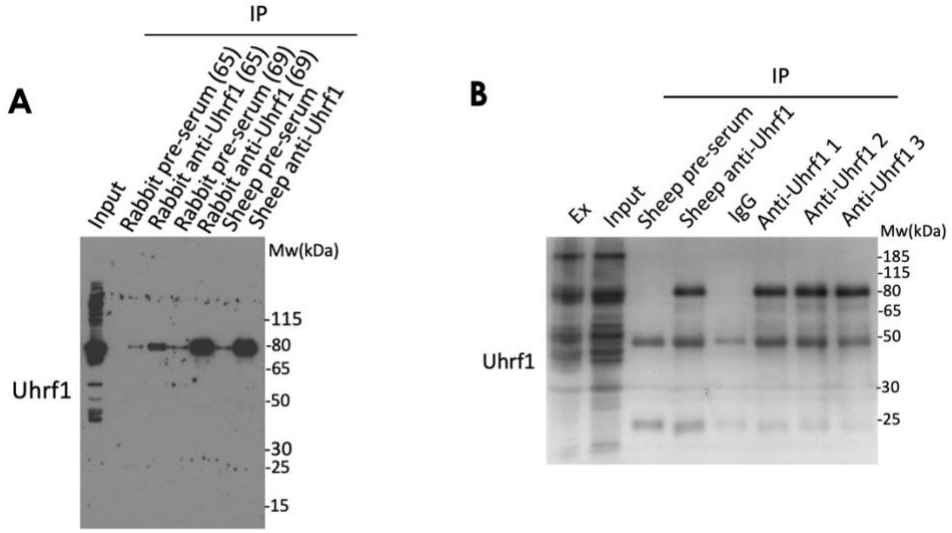


Figure 3. 11. Purification of *Xenopus laevis* anti-Uhrf1 antibodies from whole sera. A) Testing rabbit and sheep anti-Uhrf1 sera by immunoprecipitation. Sera against *Xenopus laevis* Uhrf1 were previously raised in two different rabbits (65 and 69) and in a sheep. Immunoprecipitation (IP) from whole egg extract was performed to test the specificity of the sera in recognizing Uhrf1. Pre-sera were used as a negative control. Input and IPs samples were visualized by western blotting using anti-Uhrf1 sheep serum. **B)** Testing affinity purified anti-xUhrf1 sheep antibodies. Anti-Uhrf1 antibodies were purified from whole sheep serum in different rounds of purification. The specificity against Uhrf1 of the three most concentrated antibody preparations was tested by immunoprecipitation comparing with whole sera. Pre-serum and non-specific sheep IgG antibodies were used as a negative control. Input and IPs samples were visualized by western blotting using anti-Uhrf1 sheep serum.

Once the antibodies were purified, I wanted to detect Uhrf1 chromatin binding during DNA replication by wester blotting. To this aim, *Xenopus laevis* egg extract was incubated with sperm DNA and the replication reaction was followed by analysing chromatin bound proteins at different times by immunoblotting. As shown in Figure 3. 12, purified antibodies were recognizing Uhrf1 associated to chromatin at the peak of replication. Since Uhrf1 follows a similar pattern than the rest of the replisome proteins, this result suggests that Uhrf1 is part of the replication machinery.

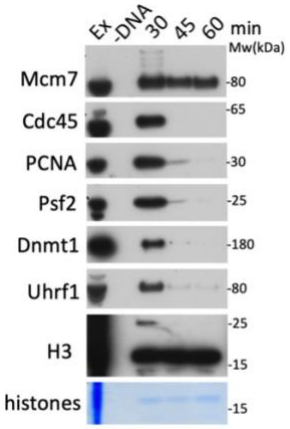


Figure 3. 12. Uhrf1 is part of the replisome. The extract was incubated with sperm DNA for DNA replication to take place. Chromatin was isolated at different times of the replication reaction and bound proteins were analysed by immunoblotting using indicated antibodies. Affinity purified anti-Uhrf1 sheep antibodies from Figure 3. 11 B were used. A sample without DNA was also performed and used as a chromatin specificity control, while extract sample was used as a positive control for immunoblotting. Histones were stained with colloidal Coomassie as loading control. This is a representative experiment of more than ten repeats.

The next step was to use purified anti-xUhrf1 antibodies to perform immunodepletion of endogenous protein from the extract. Thus, the extract was incubated with either non-specific IgG (as a control) or purified anti-Uhrf1 antibodies coupled to Protein G beads. The efficiency of the depletion was analysed by detecting levels of Uhrf1 in whole extract by western blotting (Figure 3. 13 A). Successfully, more than 98% of Uhrf1 was depleted from the extract. Immunodepletion worked efficiently also using anti-Uhrf1 rabbit serum 69 (Figure 3. 13 D), in which the extract was incubated with Protein A beads coupled to rabbit antibodies from serum 69 against Uhrf1 (Uhrf1 depleted) or pre-serum 69 (IgG depleted). Then, I confirmed that both, sheep and rabbit, IgG and Uhrf1 depleted extracts were active and could synthesise DNA after the depletion process by measuring the incorporation of α-[P32] dATP into nascent DNA (Figure 3. 13 B and E). These experiments show that the absence of Uhrf1 does not affect the ability of the extract to synthesise DNA, as the levels of replicated DNA were similar to those in IgG depleted extract in both sheep and rabbit depletions. After depleting Uhrf1 and confirming that the extract was active, I wanted to check whether Uhrf1 removal from the extract indeed inhibit histone H3 ubiquitination and Dnmt1 recruitment as shown in the literature. Consequently, the DNA replication reaction was set up in these depleted extracts by incubating them with sperm DNA. Chromatin was isolated at different times during replication and associated proteins were identified by immunoblotting. The depletion of Uhrf1 from the extract using either sheep or rabbit antibodies clearly impaired histone H3 ubiquitination and Dnmt1 recruitment (Figure 3. 13 C and F). These results suggest that Uhrf1 is responsible for these phenotypes. Importantly, at least 98% of Uhrf1 needed to be immunodepleted from the extract to be able to efficiently impair Uhrf1 binding to chromatin and see these defects on H3 ubiquitination and Dnmt1 recruitment. Immunodepleting 95% of Uhrf1 (Figure 3. 13 G) did not cause any defect in Uhrf1 recruitment to chromatin (Figure 3. 13 H), showing that just a small amount of the protein in the extract is enough for DNA replication.

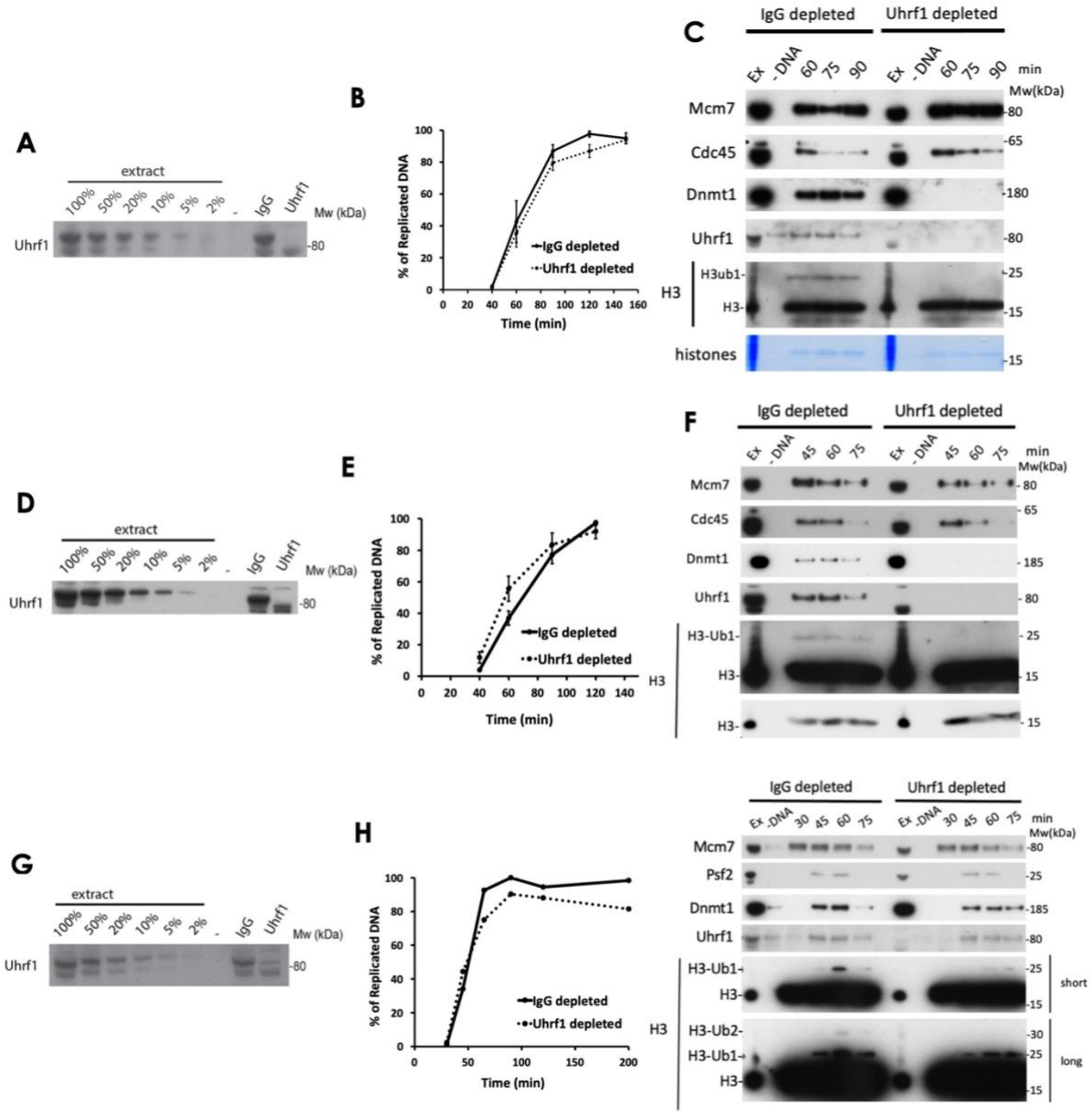


Figure 3. 13. The immunodepletion of Uhrf1 from the extract impaired histone H3 ubiquitination and Dnmt1 recruitment to chromatin. A, D and G) *Xenopus* egg extract was incubated with Uhrf1 sheep (A and G) or rabbit (D) antibodies coupled to beads to immunodeplete endogenous Uhrf1. The levels of Uhrf1 in whole extract were detected by western blotting to analyse the efficiency of the depletion. Purified anti-Uhrf1 sheep antibodies were used for immunoblotting. These are representative experiments of n=6 for A), n=4 for D) and n=3 G) performed. **B, E and H)** IgG- and Uhrf1- depleted extracts were incubated with sperm nuclei and α-[P32] dATP. The DNA replication reaction was stopped at indicated time points and synthesised DNA was measured by α- [P32] dATP incorporation. Means with SEM of n=6 (B and E) were plotted for each depletion. For (H) just one repeat was performed. **C, F and I)** Sperm DNA was replicated in IgG- and Uhrf1-depleted extracts and chromatin isolated at indicated times. Proteins associated to chromatin were analysed by immunoblotting using indicated antibodies. These are representative experiments of n=6 for C), n=4 for F) and n=2 for H) performed in exactly the same way using different extracts.

3.2.2.2. The removal of Uhrf1 also impaired Lig1, Fen1 and CAF1 recruitment

After confirming that Uhrf1 removal impaired histone H3 ubiquitination and Dnmt1 recruitment, we were interested in finding out other possible roles of Uhrf1 and histone H3 ubiquitination during DNA replication. To this aim, we decided to perform a mass spectrometry analysis (MS) of chromatin bound proteins (Chromass) in the middle of S phase in the presence or absence of Uhrf1. Samples from chromatin isolated in the middle of S phase from IgG and Uhrf1 sheep depleted extracts were run for about 2 cm in an SDS-PAGE gel, stained with Colloidal Coomassie, and whole lanes were cut into 10 slices and sent for MS. Proteins identified by MS were organized in different tables depending on their roles (Appendix). Only the proteins showing a fold change over 2 or under 0.5 in Uhrf1 depleted compared with IgG depleted extracts were included in the tables. The most interesting findings obtained were summarised in Table 3. 3. As expected, Dnmt1 and Usp7 binding to chromatin was decreased after Uhrf1 depletion since they recognize the histone H3 ubiquitination mark. Interestingly, the recruitment of other proteins related to Okazaki fragment maturation and nucleosome assembly was also affected by Uhrf1 removal. The proteins Lig1 and Fen1 were undetectable when Uhrf1 was missing, while Dna2 was increased. The binding of the histone chaperone CAF1 was also impaired after Uhrf1 depletion. This would create a problem with new histone deposition, which is supported by the decrease of histones on chromatin when Uhrf1 is missing. Nucleosome assembly has been shown to control Okazaki fragment synthesis and both processes are tightly coordinated so it is interesting that the removal of Uhrf1 affected both processes. Although this mass spectrometry (MS) analysis provides semiquantitative data using Total Spectral Counts (TSC), it gives valuable preliminary insights. Therefore, the next step is to further investigate these findings using other methods like western blotting for validation and quantification.

Table 3. 3. Chromatin bound proteins from IgG and Uhrf1 immunodepleted extracts in the middle of S phase identified by mass spectrometry. TSC: Total Spectral Counts. This refers to the total number of mass spectra identified for a protein, which serves as an indicator of the protein abundance.

	Chromatin isolated from immunodepleted extract in mid S phase		
Protein (kDa)	IgG depleted	Uhrf1 depleted	Fold Change
	TSC (coverage)		
Uhrf1 (87)	35 (16%)	0	-
Dnmt1 (168)	68 (21%)	0	-
Usp7 (129)	11 (8%)	2 (2%)	0.2
Chaf1 (101)	11 (7%)	0	-
H3.2 (15)	117 (74%)	52 (60%)	0.4
Lig1 (120)	23 (14%)	0	-
Fen1 (43)	9 (17%)	0	-
Dna2 (120)	3 (2%)	11 (10%)	3.7

To further study the role of Uhrf1 in the recruitment of Lig1, Fen1 and CAF1, specific antibodies against *Xenopus* proteins were needed. For CAF1, rabbit serum against CAF1 was kindly provided by Dr. G. Almouzni. For the other proteins, similarly as for Uhrf1 antibodies, recombinant proteins were firstly purified in bacteria to raise antibodies against them and to create an antigen column for antibody purification from the whole sera. The plasmids to express Dnmt1 and Fen1 were kindly provided by Howard Lindsay and Jane Grasby, respectively. Full-length His-tagged *Xenopus* Lig1, Dnmt1 and human Fen1 proteins were expressed in *E.coli* and purified using Nickel beads. Samples taken during the expression and purification processes were run in SDS-PAGE gels and visualized by Coomassie staining (Figure 3. 14 A, C and E) or western blotting (Figure 3. 14 B, D and F). All the proteins were successfully purified between the first elutions, although with some degradation product in Lig1 and Dnmt1, most probable because of their greater size. The most concentrated elution of each protein was dialyzed in non-harmful buffer for the animals and sent for antibody generation by Eurogentec company.

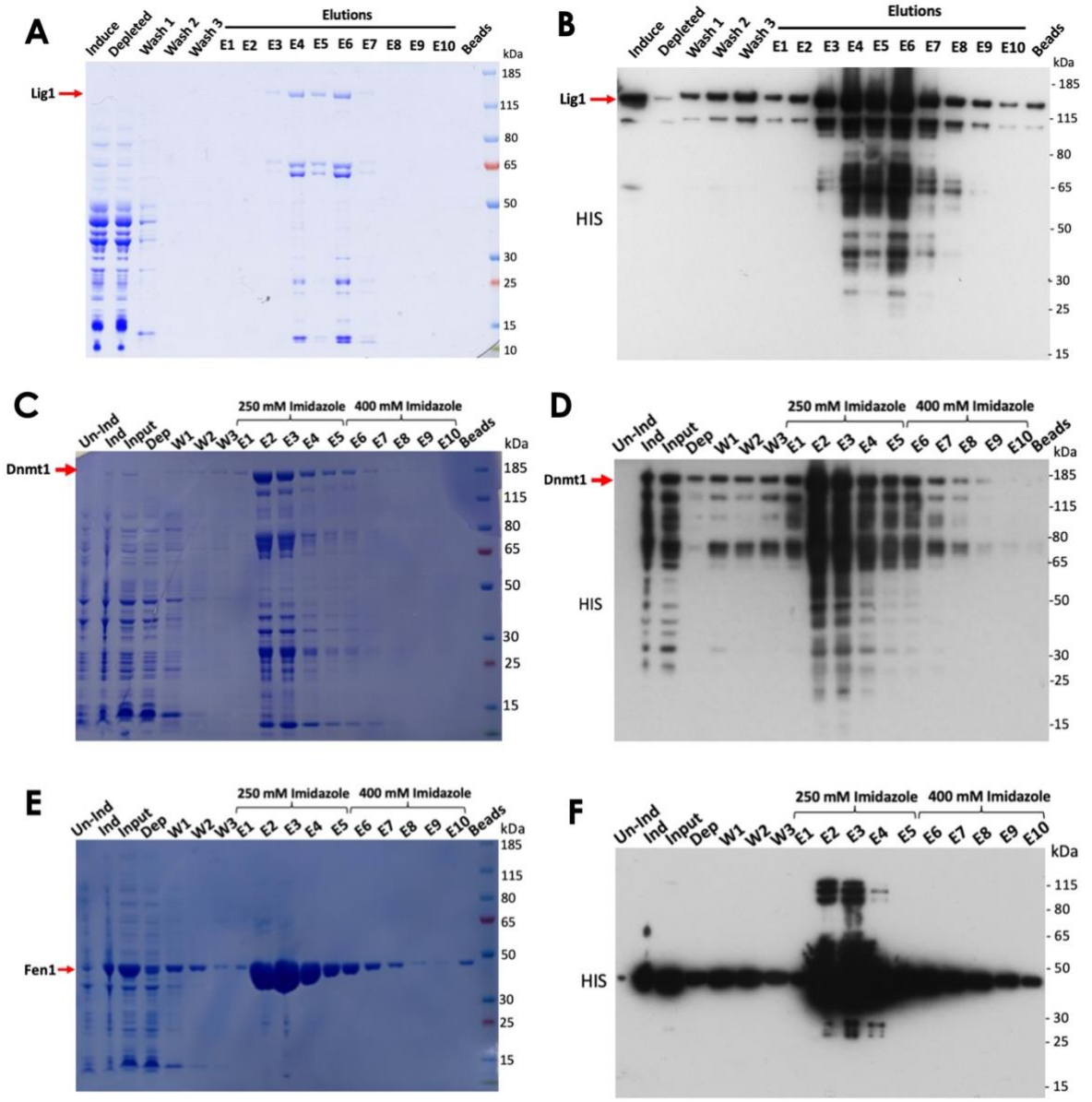


Figure 3. 14. Purification of His-tagged *Xenopus* Lig1, *Xenopus* Dnmt1 and human Fen1. His-tagged *Xenopus* Lig1 **(A)**, Dnmt1 **(C)** and human Fen1 **(E)** were expressed in *E.*coli and purified using Nickel affinity purification. Induced samples were taken before bacteria lysis. The soluble bacterial lysates (input), unbound proteins (flowthrough, depleted), samples of beads washes and of elutions from beads using two concentrations of Imidazole are presented. Samples from the purification process were run in a SDS-PAGE gel and visualized by Coomassie staining **(A, C and E)** or immunoblotting **(B, D and F)** using anti-HIS antibody.

Two different rabbit sera against each protein were obtained. Their specificity was tested by western blotting of whole extract (Figure 3. 15 A, D and F) or by IP (Figure 3. 15 B, E and G) comparing with pre-immune serum as a negative control. Both sera against Lig1 and Dnmt1 recognized and even IP the proteins from extract equally well, while for Fen1 neither serum was able to IP the protein from whole extract. Afterwards, as for Uhrf1 antibodies, purified Lig1 and Fen1 proteins were coupled to HiTrap NHS-activated columns for antibody purifications from whole serum. Most concentrated antibody elution of each protein was tested for specificity by IP from extract (Figure 3. 15 C and H). Both affinity purified antibodies against Lig1 and Fen1 could IP these proteins, therefore these antibodies were used from now on for western blotting in the rest of the analyses. For Dnmt1, whole serum was used for immunoblotting as it already showed great affinity.

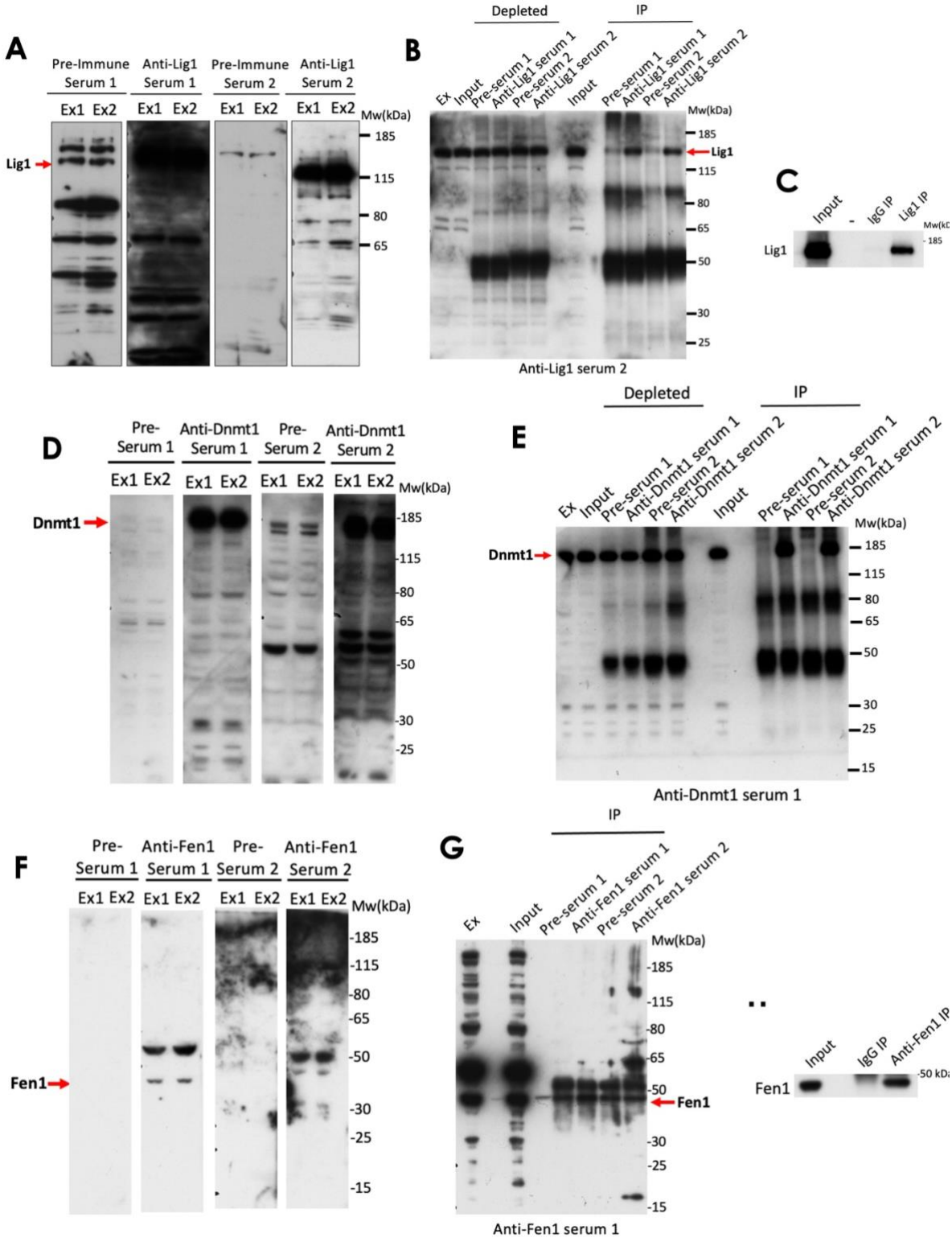


Figure 3. 15. Purification of anti-Lig1, anti-Dnmt1 and anti-Fen1 antibodies. Sera against *Xenopus laevis* Lig1, Dnmt1 an human Fen1 were raised in two different rabbits. Immunoblotting of whole extract **(A, D and F)** or immunoprecipitation (IP) **(B, E and G)** was performed to test the specificity in recognizing these proteins. Input and IPs samples were visualized by western blotting using serum 1 or 2. Pre-serum was used as a negative control in both experiments. **C and H)** Purified His-tagged xLig1 and hFen1 (Figure 3. 14) were bound to HiTrapTM NHS-activated column and rabbit sera were subsequently re-circulated through the column for the isolation of anti-xLig1 and anti-hFen1 antibodies from whole sera. The specificity of the most concentrated antibody elution was tested by immunoprecipitation (B and G). Purified antibodies were used for visualizing by immunoblotting.

Once specific antibodies were generated, I wanted to confirm by western blotting that Lig1, Fen1 and CAF1 are not recruited to chromatin when Uhrf1 is depleted. Thus, chromatin was isolated at different times from both IgG and Uhrf1 sheep depleted extract and associated proteins were analysed by immunoblotting (Figure 3. 16 A). As observed in the MS data, the removal of Uhrf1 not only impaired histone H3 ubiquitination and Dntm1 recruitment but also Lig1, Fen1 and CAF1 association to chromatin. The fold change of chromatin bound proteins at the peak of replication in IgG and Uhrf1 depleted extract were quantified in n = 3 experiments using ImageJ. The levels were normalised to the levels in IgG depleted extract. Fold change means with SEM were plotted (Figure 3. 16 B). These results confirm that H3 ubiquitination and the recruitment of Dnmt1, Lig1, Fen1 and CAF1 are significantly reduced when Uhrf1 is depleted. Although PCNA was showing decreased signal after Uhrf1 removal by western blotting, quantification show that Cdc45 was also reduced to similar levels suggesting that Uhrf1 depletion is causing some replication defects. The levels of the Spt16 subunit of the histone chaperone complex FACT were also reduced after Uhrf1 depletion, being between PCNA and CAF1 levels. However, opposed to the MS data, quantifications showed that histone H3 levels were similar in both conditions even when chaperones were diminished. Finally, to test whether these proteins were reduced because they were co-depleted with Uhrf1, I carried out immunoblotting of whole IgG and Uhrf1 depleted extracts using antibodies against these proteins. As shown in Figure 3. 16 C, all the proteins were present in Uhrf1 depleted extract confirming that Uhrf1 removal is affecting their association with chromatin. Altogether, these findings suggest other potential roles of Uhrf1 and histone H3 ubiquitination in regulating Okazaki fragment maturation and nucleosome assembly during DNA replication and a possible mechanism of coordination between DNA methylation and chromatin replication.

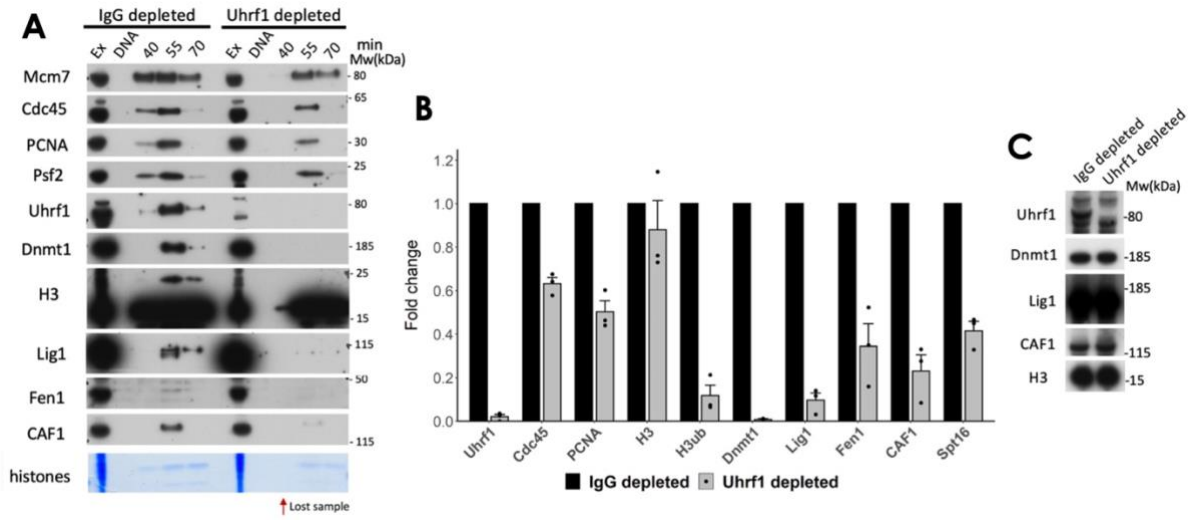


Figure 3. 16. Uhrf1 removal not only impaired histone H3ubiquitination and Dnmt1 recruitment but also Lig1, Fen1 and CAF1 binding to chromatin. A) Replication reaction was set up in IgG and Uhrf1-sheep depleted extracts by supplementation with sperm DNA. Chromatin was isolated at specified times and associated proteins were analysed by western blotting using indicated antibodies. **B)** Quantification of fold change of specified chromatin bound proteins at the peak of replication in IgG and Uhrf1 depleted extracts in n = 3 experiments (different extracts used). Fold change levels were normalised to the levels in IgG-depleted extract. Mean with SEM are plotted. **C)** Indicated proteins were detected in whole IgG and Uhrf1 depleted extracts by immunoblotting.

3.2.2.3. Uhrf1 mediates histone H3 ubiquitination and Dnmt1 and Lig1 recruitment

In order to confirm that Uhrf1 was directly regulating the recruitment of these proteins and it was not other potential protein co-immunodepleted with Uhrf1, I needed to purify recombinant Uhrf1 to add back to the extract to rescue these phenotypes. To this aim, *Xenopus laevis* His-tagged Uhrf1 and GST-tagged Uhrf1 were firstly purified in *E.coli* and dialyzed into LFB1/100 (data not shown). Then, the DNA replication reaction was set up in IgG and Uhrf1 depleted extracts supplemented or not with the recombinant Uhrf1. However, the addition of either His-xUhrf1 or GST-xUhrf1 to the extract could not rescue any of the phenotypes associated with Uhrf1 (Figure 3. 17 A). Although GST-Uhrf1 showed better solubility than His-Uhrf1 during the purification, it was still mostly insoluble. In addition, both proteins were degraded/truncated during the process of purification, which together suggest that the proteins were not stable after expression. *In vitro* ubiquitination assays were also performed to test recombinant GST or His-xUhrf1 activity towards recombinant histone H3 by incubating them with ubiquitin, E1 enzyme mUBA1 and E2 enzyme UbcH5, as they showed the strongest stimulation of the activity of Uhrf1 in other studies (130,150). As shown in Figure 3. 17 B these proteins were not increasing the ubiquitination of histone H3 compared to the control, indicating that they were inactive after the purification. To solve this issue, I also attempted the rescue experiment using a commercial His-tagged human Uhrf1 recombinant protein, as human Uhrf1 was purified successfully by many labs from *E.coli*. Despite commercial hUhrf1 showing more activity *in vitro* when incubating it with recombinant H3 (Figure 3. 17 B), the addition of hUhrf1 to the extract could not rescue the phenotypes either. These results collectively show that purified His- or GST-tagged *Xenopus* Uhrf1 proteins are inactive after purification, and commercial human Uhrf1 while being active in ubiquitination assays is not able to act in *Xenopus* egg extract.

Interestingly, the addition of His-xUhrf1 or GST-xUhrf1 to the IgG-extract was stimulating histone H3 ubiquitination and the recruitment of Dnmt1 and Lig1 even though they were inactive (Figure 3. 17 A). Furthermore, the addition of GST-tagged protein to Uhrf1 depleted extract with some remaining endogenous Uhrf1 was stimulating Uhrf1 binding and rescuing phenotypes (data not shown). These findings led us to hypothesize that Uhrf1 could work as a dimer, so the inactive form of Uhrf1 was helping to recruit endogenous Uhrf1 to chromatin.

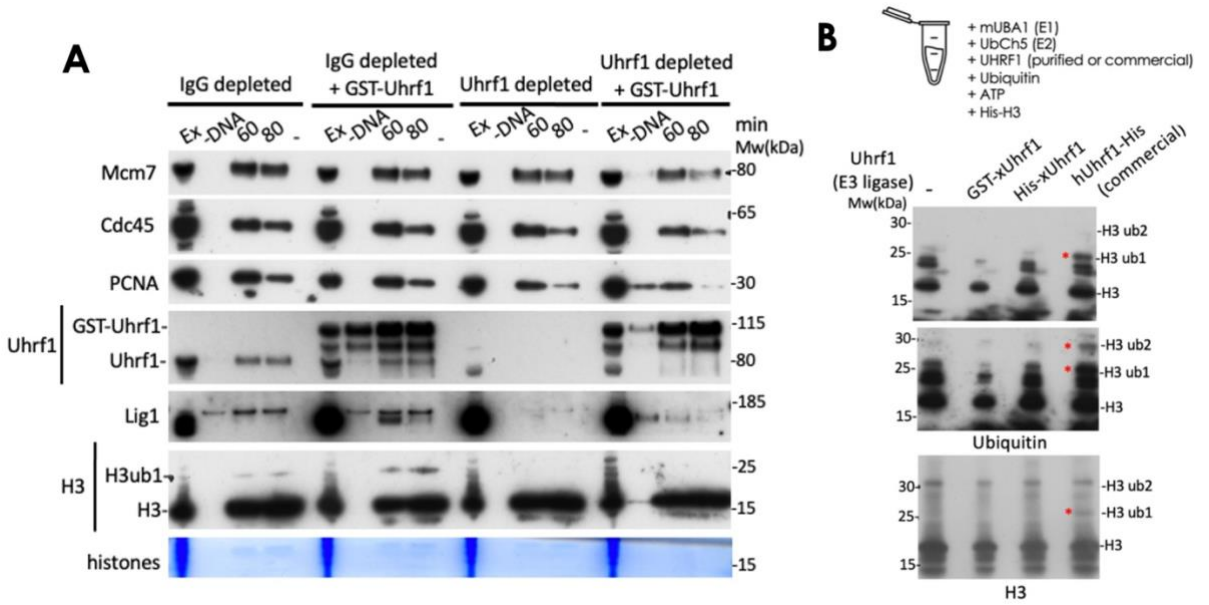


Figure 3. 17. Purified GST-xUhrf1 is not fully active but stimulates H3 ubiquitination and Lig1 recruitment. **A)** A DNA Replication reaction was set up in IgG and Uhrf1 depleted extracts with optional addition of recombinant GST-tagged xUhrf1. DNA replication was stopped at indicated times, chromatin was isolated and associated proteins were identified by immunoblotting with indicated antibodies as described in the previous figures. The experiment showed here is a representative of three repeats. **B)** *In vitro* ubiquitination assay using His-H3 purified in the previous chapter as a substrate and either GST-xUhrf1, His-xUhrf1 or commercial His-hUhrf1 as E3 ubiquitin ligase. Anti-ubiquitin or anti-H3 antibodies were used to identified ubiquitination by western blotting. This experiment was repeated twice.

To test this hypothesis, size-exclusion chromatography was firstly performed by Dr Paolo Passaretti to check whether Uhrf1 was eluted in larger size fractions from the extract indicating the presence of some type of interaction (Figure 3. 18 A). This experiment showed that Uhrf1 was eluted in a wide peak, suggesting that it could be forming a dimer or even larger complexes with other proteins. Interestingly, Dnmt1 was also forming larger complexes, being co-eluted in some of the fractions with Uhrf1. Next, to explore whether Uhrf1 could be forming a dimer, we used AlphaFold to predict the structure of a Uhrf1 dimer (Figure 3. 18 B). However, the program was unable to generate reliable predictions for a Uhrf1 dimer structure based on available structures, as indicated by low confidence of prediction. This result from AlphaFold did not allow me to draw conclusions from the predicted model, bringing the need to validate the dimerization experimentally, using the co-immunoprecipitation technique. Therefore, the extract was incubated with sperm DNA and either or both recombinant GST-xUhrf1 or His-SUMO-xUhrf1. GST beads were used to perform pull-downs from extracts to check interactions with His-SUMO-Uhrf1 and with endogenous Uhrf1 (Figure 3. 18 C). This experiment showed that recombinant proteins were not interacting with each other or with endogenous Uhrf1 in the extract. Altogether these results suggest that while Uhrf1 may form large complexes in the extract, it is unlikely to exist naturally as a dimer when in recombinant form. However, it could potentially dimerize upon binding to chromatin.

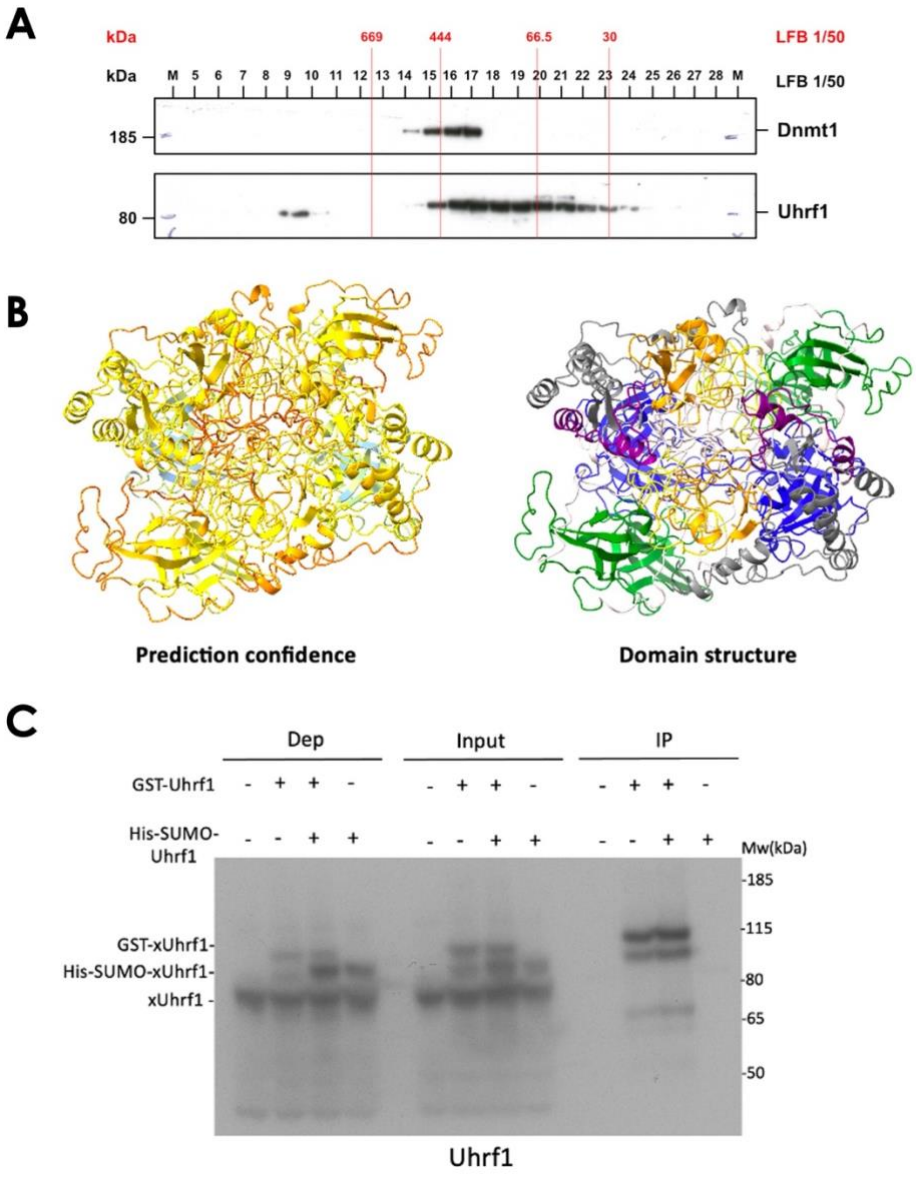


Figure 3. 18. Uhrf1 could be forming large complexes in the extract. A) Size exclusion chromatography was performed by Dr Paolo Passaretti from a sample of the whole egg extract. The different fractions collected were analysed by immunoblotting using indicated antibodies. **B)** AlphaFold prediction of a Uhrf1 dimer 3D structure from monomer sequences. High confidence prediction in blue, low confidence prediction in yellow/orange (left figure); UBL domain in orange, TTD in green, PHD in yellow, SRA in blue and RING purple (right figure). **C)** Pulldown of GST-xUhrf1 from extract incubated with sperm DNA and either or both GST-xUhrf1 and His-SUMO-xUhrf1. Glutathione beads were used to pull-down GST-Uhrf1. This experiment was performed once.

To better understand possible differences in the conformation between endogenous Uhrf1 and GST-tagged xUhrf1 that could explain the lack of activity, Dr Paolo Passaretti used AlphaFold to predict the structure of both *Xenopus* Uhrf1 versions. This time the program predicted very reliable structures for both proteins (Figure 3. 19 A), as indicated by the high proportion of blue coloured regions in both proteins corresponding to the main domains of Uhrf1. The parts of the protein not well predicted by AlphaFold (orange or yellow) correspond to the linker regions (Figure 3. 19 B). Looking at the predicted domain organization within GST-tagged Uhrf1 compared to untagged protein (Figure 3. 19 C), it is evident that the GST tag pushes the UBL domain closer to RING domain making the structure of the protein much more closed. It could render the protein inactive due to a lack of accessibility of the UBL and RING domains to the substrate, even when the SRA or TTD domains can still bind to substrates and recruit Uhrf1 to chromatin. Similar results were obtained for the His-SUMO-xUhrf1 recombinant protein (data not shown) suggesting that even a smaller tag could impair the conformation and activity of Uhrf1. This finding led us to find new strategies for the purification.

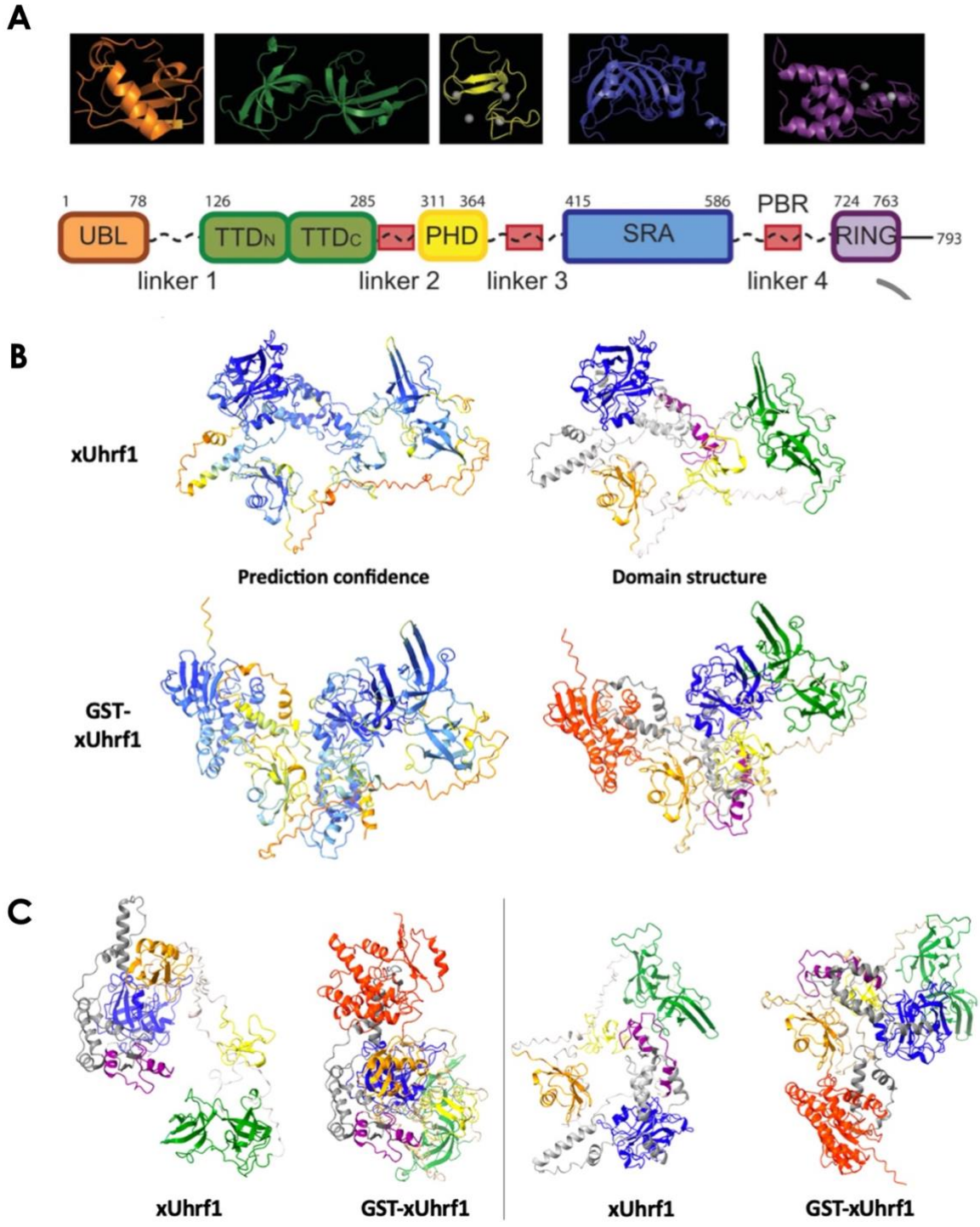


Figure 3. 19. The recombinant GST-xUhrf1 3D structure is much more closed. A) Uhrf1 domain structure adapted from (142). **B)** AlphaFold prediction of *Xenopus* Uhrf1 and recombinant GST-Uhrf1 3D structure. The structure is coloured based on confidence of the prediction (left), with high confidence prediction in blue and low confidence prediction in yellow/orange, and on the disposition of domains (right), with the different domains coloured as indicated in B). GST tag is represented in red. **C)** Comparison between Uhrf1 and GST-xUhrf1 3D conformation from two different orientations. Domains are represented coloured as in A).

Given that the phenotypes could not be rescued even with xUhrf1 tagged with the small 6xHis tag and considering Dr Benjamin Foster's finding that the N-terminal UBL domain of Uhrf1 is crucial for its E3 ubiquitin ligase activity, I followed a new purification strategy to get untagged Uhrf1. This approach, suggested by Dr Ben Foster and Dr Till Bartke, aimed to purify His-SUMO-Uhrf1 and then cleave off the tag just before the first methionine of the protein sequence using Ulp1 protease (Figure 3. 20 A). This strategy would keep the N-terminal part of Uhrf1 unaltered due to its importance for Uhrf1 function. I carried out expression and purification of both His-Ulp1 and His-SUMO-xUhrf1 from *E.coli* (Figure 3. 20 B and C respectively). Both proteins were successfully purified between elution 1-4. The first elution of Uhrf1 was dialyzed overnight in LFB1/100 incubating with Ulp1 for the removal of the His-SUMO tag. Untagged protein was obtained as shown in a Coomassie stained gel comparing it to a BSA standard (Figure 3. 20 D). Initially, I carried out size exclusion chromatography afterwards to separate Uhrf1 form Ulp1, but this step was making the purification protocol longer, affecting the activity of Uhrf1. To avoid that, the Uhrf1 elution containing Ulp1 was directly used for the experiments. Finally, to test the activity of the newly purified untagged xUhrf1 an *in vitro* ubiquitination assay was performed by incubating the protein with recombinant xPaf15 as substrate (Figure 3. 20 E). Purified untagged xUhrf1 containing Ulp1 not only showed increased Paf15 ubiquitination compared to the xUhrf1 preparation isolated from Ulp1 (xUhrf1), as previously mentioned, but also it exhibited more activity than His-tagged hUhrf1.

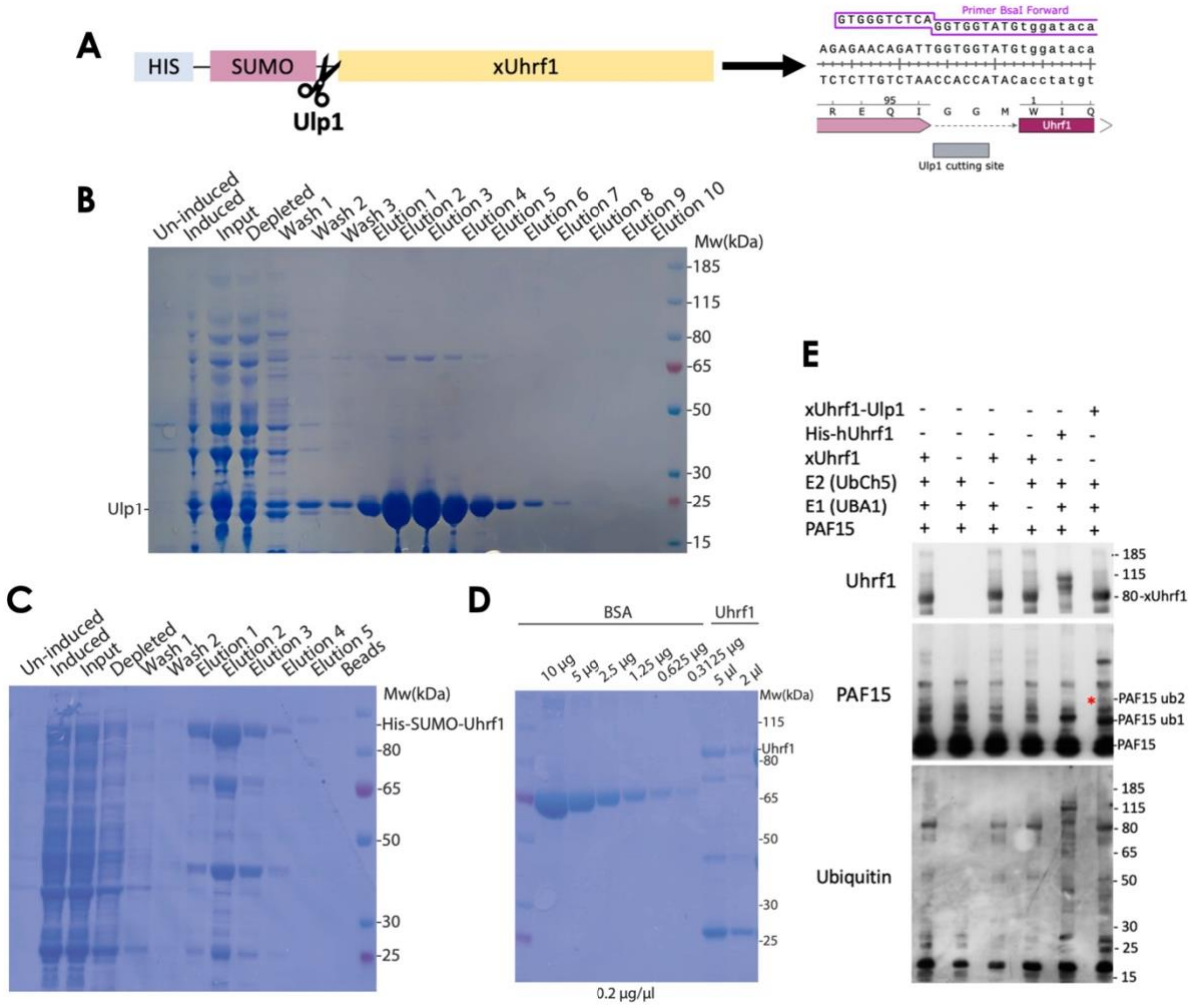


Figure 3. 20. Purification of untagged xUhrf1. A) Schematic representation of the Uhrf1 purification and cloning strategy. **B)** Purification of His-tagged Ulp1 catalytic domain. Ulp1 was expressed in *E.coli* (Induced) and after lysis, soluble proteins (Input) were used for nickel affinity purification. The protein was eluted using Imidazole. Samples taken during the purification were analysed by SDS-PAGE and Coomassie staining. **C)** Purification of His-SUMO-tagged xUhrf1. Expression and purification were performed as for Ulp1 (B). **D)** Uhrf1 tag removal. Untagged Uhrf1 was obtained by incubating it with Ulp1 for tag removal during dialysis into LFB1/100. The concentration was estimated by comparison with BSA standards and Coomassie staining. **E)** *In vitro* ubiquitination assay using recombinant *Xenopus* PAF15 as a substrate and either His-tagged hUhrf1 or untagged xUhrf1 alone or mixed with Ulp1. This experiment was performed once.

Once I confirmed that recombinant untagged Uhrf1 was active *in vitro*, the next step was to test its activity in the extract. To this end, IgG and Uhrf1 depleted extracts were incubated with either buffer or untagged Uhrf1. After checking that the extracts could synthesise DNA after the addition of recombinant Uhrf1 by measuring the incorporation of radionucleotides (Figure 3. 21 A), chromatin associated proteins were analysed by immunoblotting. As shown in Figure 3. 21 B, the addition of Uhrf1 to the depleted extract not only rescued the ubiquitination of histone H3 and Paf15 but also the recruitment of Dnmt1, Lig1 and CAF1. Fold change of chromatin bound proteins at the peak of replication in the four conditions were quantified in n = 2 experiments using ImageJ. The levels were normalised to the levels in the IgG depleted extract. Fold change mean with SEM were plotted (Figure 3. 21 C). This graph clearly showed that Uhrf1 was stimulating H3 ubiquitination and Dnmt1 and Lig1 recruitment when added to IgG depleted extract. In addition, Uhrf1 was rescuing these phenotypes to similar levels as in the control when added to the Uhrf1 depleted extract. For Fen1 and CAF1 more repeats need to be done to confirm the dependency on Uhrf1. These findings collectively confirm that Uhrf1 mediates histone H3 and Paf15 ubiquitination and regulates the recruitment of Dnmt1 and Lig1.

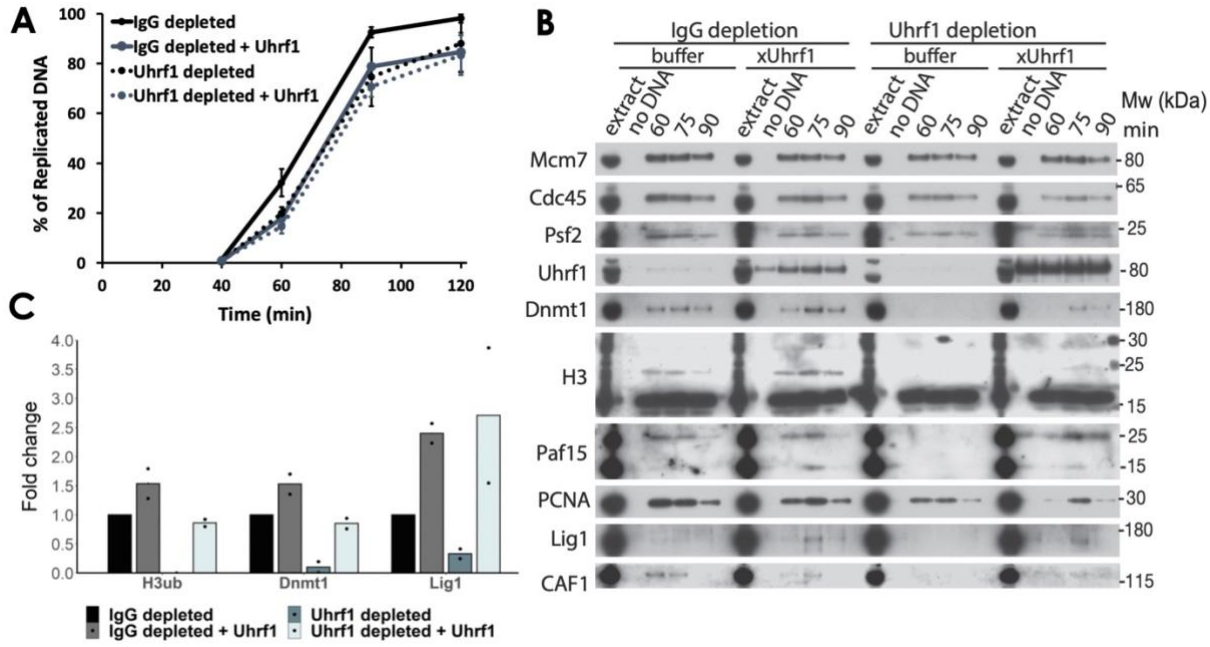


Figure 3. 21. Untagged Uhrf1 rescues histone H3 ubiquitination and the recruitment of Dnmt1 and Lig1. (A, B and C) Replication reactions were set up in IgG and Uhrf1 depleted extracts with optionally recombinant untagged Uhrf1. **A)** The level of nascent DNA synthesis was followed by measuring the incorporation of radionucleotides into newly synthesised DNA. Mean of n = 3 experiments (using different extracts) is presented with SEM. **B)** Chromatin was isolated at indicated times and analysed by immunoblotting with indicated antibodies as described in other figures, representative of two experiments. **C)** Quantification of fold change of chromatin bound ubiquitinated H3, Dnmt1 and Lig1 was performed at the peak of replication in IgG and Uhrf1 depleted extracts with optional addition of untagged Uhrf1 in n = 2 experiments (using extracts from different depletions). The levels were normalised to the levels in IgG depleted extract. Mean is shown.

3.2.2.4. Lig1 removal does not impair Uhrf1 recruitment

Finally, considering that Lig1 was proposed by other groups to interact with Uhrf1 to mediate its recruitment, I wanted to test whether there is a co-dependency in Uhrf1 and Lig1 recruitments. Therefore, anti-xLig1 rabbit serum (Figure 3. 15 B) was used to immunodeplete Lig1 from *Xenopus* egg extract since purified anti-xLig1 antibodies (Figure 3. 15 C) were less efficient in immunodepleting the protein. More than 98% of Lig1 was successfully depleted from the extract using rabbit serum (Figure 3. 22 A). Next, I performed nucleotide incorporation assay to test the ability of IgG and Lig1 depleted extracts to synthesise DNA (Figure 3. 22 B). The removal of Lig1 did not affect the levels of replicated DNA when comparing to IgG control. Finally, proteins associated with replicating chromatin at different times were analysed in IgG

and Lig1 depleted extracts using immunoblotting (Figure 3. 22 C). Surprisingly, Lig1 depletion did not affect Uhrf1 recruitment. Interestingly, the absence of Lig1 not only stimulated PCNA and Fen1 binding to chromatin, as expected due to their dependence on Lig1 activity for unloading, but it also increased histone H3 and Paf15 ubiquitination along with the recruitment of Dnmt1 and CAF1. These findings suggest that Lig1 is not essential for Uhrf1 chromatin binding while Uhrf1 is required for recruiting Lig1. Furthermore, Uhrf1 seems to act earlier in the pathway, since the lack of Lig1 in Uhrf1 depleted extract is not causing an increase in the recruitment of these factors but the opposite.

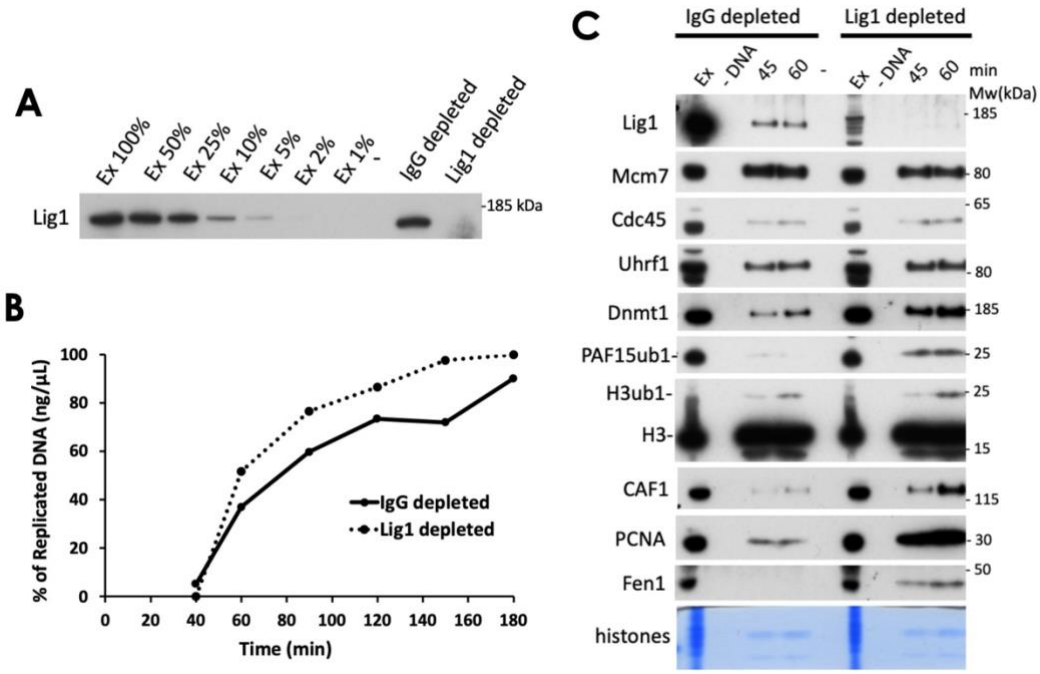


Figure 3. 22. Lig1 removal does not impair Uhrf1 recruitment. A) Lig1 immunodepletion from the extract. The extract was immunodepleted using pre-serum and serum raised against Lig1 (Figure 3. 15 B). The efficiency of the depletion was analysed by detecting the levels of Lig1 in the whole extract by western blotting. **B)** IgG and Lig1 depleted extracts were incubated with sperm nuclei and α-[P32] dATP. DNA replication reaction was stopped at indicated time points and synthesised DNA was measured by α-[P32] dATP incorporation. This experiment was performed twice. **C)** Sperm DNA was replicated in IgG and Lig1 depleted extracts and isolated at the indicated times. Chromatin bound proteins were analysed by immunoblotting as described in previous figures. This is a representative of two experiments performed.

3.2.3. Discussion

This chapter of the thesis focuses on the role of the Uhrf1 ubiquitin ligase in chromatin re-establishment during DNA replication. The work from the previous chapter showed that histone H3 was dual mono-ubiquitinated at K18 and K23 on replicating chromatin in *Xenopus* egg extract. This ubiquitination has been reported to be executed by Uhrf1 and promote DNA methylation maintenance by recruiting Dnmt1 to hemi-methylated sites (58). However, the specific mechanism to deposit this epigenetic mark is still not fully understood because of the complexity and highly regulated nature of this process. This is due to the context in which DNA methylation maintenance occurs: on a chromatinised DNA and co-existing with DNA replication and nucleosome assembly and remodelling. The findings presented in this chapter confirm that Uhrf1 mediates ubiquitination of histone H3 and Paf15 and the recruitment of Dnmt1. Furthermore, we have identified other proteins whose chromatin association is regulated by Uhrf1, such as Lig1, Fen1 and CAF1, linking Uhrf1 and the DNA methylation process with Okazaki fragment maturation and nucleosome assembly. These new insights provide a broader perspective of the multifaceted role of Uhrf1 through the replication process and could give a better understanding of how DNA methylation is regulated in different contexts and how it is coordinated with other processes occurring at the same time during DNA replication.

Firstly, I showed that Uhrf1 removal impaired histone H3 and Paf15 ubiquitination and the chromatin binding of Dnmt1. These phenotypes were rescued by the addition of recombinant Uhrf1 confirming that these processes are mediated by Uhrf1. These results support the findings from Nishiyama and co-workers using similar approaches also in *Xenopus laevis* egg extract (130). However, different models have been proposed to explain the mechanism of Dnmt1 recruitment through Uhrf1: a direct interaction between both proteins (127–129) and indirectly

through histone H3 and Paf15 ubiquitination (60,130). Therefore, the mechanism of this process will be explored in the next chapter.

Interestingly, the fact that Uhrf1 recruitment and activity is only affected after 98% depletion, shows that an excess of Uhrf1 is normally present in the extract. Generally, *Xenopus* egg extract contains abundant reserves of all the proteins to undergo many rounds of cell division without transcription (205). Another possible explanation is that Uhrf1 might have a particularly high affinity for binding partners on chromatin, so a small quantity could be enough to effectively bind and act on chromatin. Finally, the excess of Uhrf1 in the extract could also suggest additional roles of this protein, which is probable considering Uhrf1's role in other processes such as DDR or protein expression (140,180,189). The greater efficiency of Uhrf1 and its multifunctionality are supported by the fact that Uhrf1 is highly regulated and that various back-up pathways mediate its recruitment and activity. Given that Uhrf1 is highly expressed in actively proliferating tissues and that it is essential for embryonic development (180), embryonic systems may have evolved mechanisms to ensure Uhrf1 function even under significant protein depletion to maintain fundamental processes like DNA replication.

Importantly, this chapter shows that the depletion of Uhrf1 also affected Lig1 recruitment to chromatin, which was rescued by the addition of the recombinant Uhrf1. These findings suggest that Uhrf1 mediates Lig1 recruitment. This is interesting since previous research demonstrated that Lig1 recruits Uhrf1 to chromatin through an H3K9-like mimic methylated by G9a and GLP, which is recognized by the TTD of Uhrf1 (134). In contrast, my results show that Uhrf1 is still recruited to chromatin in the absence of Lig1. This is supported by the finding of the same group that cells lacking Lig1 exhibit unaltered DNA methylation level, while Lig1 mutants with impaired Uhrf1 binding showed reduced DNA methylation. These lines of evidence support the existence of backup pathways regulating Uhrf1 recruitment, such us the

reported interactions with hemi-methylated DNA, histone H3 and Paf15 (126,127,130,143), and suggest a co-dependency in both protein recruitments. In addition, the recruitment of Fen1 was also impaired by the removal of Uhrf1, while Dna2 was increased in mass spectrometry data. This would be expected since Dna2 processes longer flaps that would be created in the absence of Fen1 (215,216). It is then possible that reduced Lig1 levels on chromatin are due to impaired Okazaki fragments flap processing and lack of Lig1 substrate. Altogether, these findings suggest that Uhrf1 also regulates Okazaki fragment maturation and coordinate it with DNA methylation maintenance.

Related to Uhrf1's involvement in Okazaki fragment maturation is the fact that Uhrf1 removal also affected CAF1 binding to chromatin. The FACT subunit protein Spt16 was also reduced after Uhrf1 depletion although to lower levels. The lack of these histone chaperones would affect histone deposition (69), which is reflected in the reduced histone content on chromatin in mass spectrometry results. However, quantification of the fold change of western blot signals after Uhrf1 depletion did not show differences in histone H3 levels. This could be explained by the fact that normalization was performed using histones, which were generally decreased in Uhrf1 depletion as well. This finding is particularly interesting since nucleosome assembly is tightly coordinated with Okazaki fragment maturation, indeed nucleosome assembly determines the length of the Okazaki fragments (99). It has been proposed that the newly deposited nucleosomes inhibit the progression of the polymerase, promoting Okazaki fragment maturation (102). This means that CAF1 would act prior to Fen1 and Lig1, possibly generating the defect in these proteins. In summary, the involvement of Uhrf1 in the recruitment of Lig1, Fen1 and CAF1 supports the idea of Uhrf1 regulating both processes and coupling them with DNA methylation maintenance.

Unfortunately, the problems purifying active recombinant Uhrf1 affected the progress of this chapter and limited the exploration of the mechanism of recruitment of these proteins using Uhrf1 activity mutants. The extensively regulation of Uhrf1, where each domain is essential for its role in DNA methylation maintenance, makes Uhrf1 very sensitive to changes in its sequence. This probably explains the inactivity of tagged-Uhrf1, especially after tagging the N-terminal UBL domain, which has been shown to be crucial for Uhrf1 activity (149,150). This is supported by the activity of untagged Uhrf1 both *in vitro* and in rescuing the phenotypes. The use of AlphaFold for predicting Uhrf1 structure is a powerful tool since the structural analysis of the full-length protein by current experimental approaches is challenging due to its size and conformational flexibility. Currently, the only available structures are of the isolated domains in different contexts. The predictions from the programme suggest that adding tags like GST or His-SUMO could lead to a more closed Uhrf1 conformation, potentially interfering with substrate or binding partner recognition. It has been shown that Uhrf1 undergoes a conformational switch from a closed to an open state upon binding to DNA, histone H3 and Paf15 as well as Usp7 and Lig1, relieving the auto-inhibition caused by intramolecular interactions (151–155). Phosphorylation in the linker region (S298) within Uhrf1 also impairs intramolecular interactions promoting a conformational change that increase Uhrf1 binding to H3 (146). As tagged-Uhrf1 was being recruited to chromatin, it could be then possible that the addition of the tag is affecting the release of some of these intramolecular interactions affecting the RING domain. Although the overall prediction of Uhrf1 structure was reliable, the flexible linker regions known for their intramolecular interactions, crucial for Uhrf1 general conformation (142,151), were not accurately predicted. This along with the fact that Uhrf1 adopts multiple conformations upon binding to DNA or binding partners, makes the prediction of the real structure virtually impossible. In the future, it would be interesting to investigate conformational variations in Uhrf1 wt and mutants by adding binding partners and subsequently

validating these experimentally. Altogether, however, these findings suggest that the addition of an N-terminal tag to Uhrf1 affects its activity because it promotes a conformational change in the protein to a closed state and obstacles to UBL activity.

In this chapter I also explored the possibility that Uhrf1 could act as a dimer because the addition of inactive recombinant Uhrf1 to the extract with some remaining endogenous Uhrf1 stimulated the binding and activity of Uhrf1. However, the inability of AlphaFold to predict a reliable structure of Uhrf1 as a dimer and the failure in pulling down endogenous Uhrf1 with GST-Uhrf1 suggest that Uhrf1 does not form a stable dimer in the whole egg extract. It could be possible that recombinant Uhrf1 purified from bacteria lack some PTMs essential for the conformation of Uhrf1. For example, phosphorylation has been shown to highly regulate Uhrf1 conformation and activity, promoting an open state in S phase (Table 1). Therefore, recombinant Uhrf1 could be in a close state in the extract affecting its interaction with endogenous Uhrf1. Considering that AlphaFold predicts static structures and that Uhrf1 is a very dynamic and flexible protein, the protein could undergo conformational changes upon interaction with DNA or binding partners on chromatin not considered by AlphaFold, giving lower confidence scores in the dimer structure. It could then be possible that the dimerization occurs on chromatin, after recombinant Uhrf1 changes the conformation to a more open state (151–155), which might then facilitate the recruitment of endogenous protein by bound recombinant Uhrf1. This is also supported by the finding that the Uhrf1 PHD domain forms a dimer in the crystal structure analysis of the PHD in complex with unmodified H3 (217). Furthermore, the fact that Uhrf1 undergoes many intramolecular interactions between domains, that could equally occur intermolecularly, also support this hypothesis. Finally, the fact that long arrays of nucleosomes enhanced the activity of Uhrf1 *in vitro* (150) suggest that either the presence of more linker DNA and neighbouring nucleosomes stimulate Uhrf1 activity by reliving auto-inhibition or that the proximity of adjacent Uhrf1 molecules favour its activity through intermolecular

interactions, or possibly a combination of both factors. Immunoprecipitation analysis of Uhrf1 from chromatin will allow to prove dimerization on DNA. To sum up, my results suggest that Uhrf1 may not form stable dimers in the extract but could potentially dimerize upon binding to chromatin.

Considering that the binding to PCNA is crucial for Lig1, Fen1 and CAF1 recruitment (33), Uhrf1 could mediate their binding to chromatin by regulating PCNA. We initially hypothesised that Uhrf1 could regulate the recruitment of these proteins by ubiquitinating PCNA. The ubiquitination of PCNA promotes efficient Okazaki fragment maturation and CAF1 mediated-nucleosome assembly during normal S phase (40). Furthermore, the lack of Lig1 leads to PCNA mono-ubiquitination (218). Although, my results generally show less ubiquitinated PCNA after Uhrf1 removal, it was not rescued by the addition of Uhrf1. Since PCNA levels were also decreased after Uhrf1 depletion, this could explain the reduction in ubiquitination. This decrease in PCNA could also be due to DNA replication delays, since Cdc45 was also decreased. Given that the lower levels of Cdc45 on chromatin were not reflected in the total levels of synthesised DNA, this could mean that a smaller number of origins were firing and therefore fewer CMG complexes were formed. Altogether, PCNA ubiquitination seems unlikely as a mechanism through which Uhrf1 would regulate Lig1, Fen1 and CAF1 chromatin recruitment.

Consequently, considering that Paf15 probably travels bound to PCNA and is a substrate of Uhrf1, I hypothesise that Uhrf1 could regulate the recruitment of these proteins through ubiquitinating Paf15. This modification could mediate the switch in the recruitment of proteins by PCNA, since PCNA coordinates OFM sequentially binding Pol δ, Fen1, Dna2, Lig1 and CAF1 (33). This is supported by the fact that Uhrf1 depletion impaired ubiquitination and recruitment of Paf15, which was rescued by adding Uhrf1. This showed that Paf15

ubiquitination is essential for its chromatin association, as shown by another study (130). Therefore, the lack of Paf15 could affect the ability of PCNA to recruit Lig1, Fen1 and CAF1, if they need Paf15 to be coordinated. This hypothesis would explain also why Lig1 depletion increased PCNA, Fen1, CAF1 and Dnmt1 binding while the decrease in Lig1 in Uhrf1 depleted extract did not stimulate their recruitment. They were reduced because they would depend on Paf15 ubiquitination. This hypothesis is presented in a model in Figure 3. 23, representing that Uhrf1 and Paf15 ubiquitination apart from maintaining DNA methylation through Dnmt1 recruitment, may also regulate nucleosome assembly and Okazaki fragment maturation by recruiting Lig1, Fen1 and CAF1. This hypothesis will be explored in the next chapter.

In summary, this chapter demonstrates that Uhrf1 mediates the ubiquitination of histone H3 and Paf15 and the recruitment of Dnmt1 and Lig1. These findings suggest an additional role of Uhrf1 in Okazaki fragment maturation, which provide a deeper understanding of the coordination between DNA replication and chromatin re-establishment.

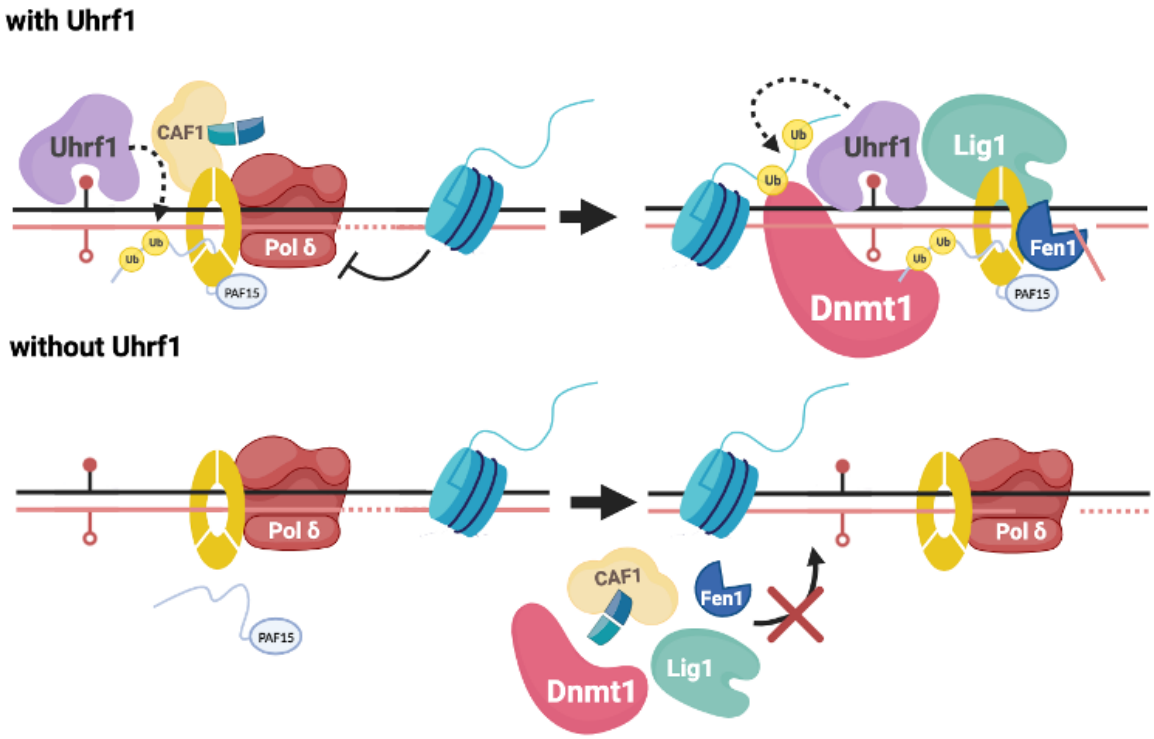


Figure 3. 23. Model of Uhrf1's role during DNA replication. During normal DNA replication, PCNA acts a platform for the recruitment of many proteins. This protein travels through the DNA associated with ubiquitinated Paf15. Specifically, PCNA coordinates Okazaki fragment maturation by the sequential and coordinated binding of Pol δ, Fen1, Dna2, Lig1 and CAF1. Uhrf1 is recruited to chromatin by interacting with DNA, histone H3, Paf15 and Lig1. Once on chromatin, Uhrf1 mediates dual mono-ubiquitination of histone H3 and Paf15 which promote the recruitment of Dnmt1 to fully methylate DNA. Apart from this, Uhrf1 maintains Paf15 ubiquitination which maintain its stable binding to PCNA. This could potentially regulate PCNA activity in protein switching, being essential for the recruitment of Lig1, Fen1 and CAF1. In the absence of Uhrf1, Paf15 is not ubiquitinated, which affect its stability and PCNA association. Furthermore, Lig1, Fen1 and CAF1 are no longer recruited when Uhrf1 is missing. The lack of Paf15 recruitment could lead to problems in the recruitment of Lig1, Fen1 and CAF1 by PCNA, since they would need Paf15 ubiquitination to be coordinated.

3. 3. Deciphering the mechanism of Dnmt1, Lig1, Fen1 and CAF1 recruitment through Uhrf1

3. 3. 1. Introduction

In the previous chapters, I showed that histone H3 was ubiquitinated on chromatin during DNA replication and that Uhrf1 mediates this modification as well as Dnmt1 recruitment. However, my results suggest that Uhrf1 has other important roles during DNA replication and histone assembly, by regulating the binding of Lig1, Fen1 and CAF1 to chromatin. Therefore, this chapter will focus on understanding the mechanism by which Uhrf1 regulates and coordinates the recruitment of all these proteins.

Different mechanisms have been proposed to explain the mechanism by which Uhrf1 recruits Dnmt1 to hemi-methylated sites. Firstly, a direct interaction between Uhrf1 and Dnmt1. Two domains of Uhrf1 (SRA and UBL) have been shown to directly bind the RFTS domain of Dnmt1 and stimulate its methylase activity (128,129). Secondly, an indirect recruitment of Dnmt1 through Uhrf1 E3 ubiquitin activity. It has been proposed that the dual mono-ubiquitination of histone H3, histone H2B and Paf15 by Uhrf1 are required for Dnmt1 chromatin binding and DNA methylation maintenance (60,130,171). Therefore, the mechanism of Dnmt1 recruitment through Uhrf1 still needs to be clarified.

On the other hand, there is not much information in the literature about additional roles of Uhrf1 during unperturbed DNA replication. Therefore, I wanted to further investigate how Uhrf1 regulates the chromatin association of Lig1, Fen1 and CAF1 to determine its role in Okazaki fragment maturation and nucleosome assembly. Given that all these proteins are recruited through PCNA (33) and that Uhrf1 mediates dual mono-ubiquitination of the PCNA associated factor Paf15 (173), I firstly hypothesised that Uhrf1 mediates their recruitment though Paf15

ubiquitination. This modification could regulate and coordinate the sequential recruitment of these proteins by PCNA, since PTMs have been shown to regulate Fen1 binding and dissociation as well as PCNA function (38,39). In addition, Uhrf1 has been shown to directly interact with Lig1 to be recruited to chromatin (134), which could at the same time regulate Lig1 binding to chromatin.

The aim of this chapter of the thesis is to clarify the mechanism by which Uhrf1 bridges histone H3 and Paf15 ubiquitination and Dnmt1, Lig1, Fen1 and CAF1 recruitment, whether it is doing it by acting as a scaffold protein or through ubiquitinating H3 and Paf15. This would give a better understanding of how DNA methylation is coordinated with Okazaki fragment maturation and nucleosome assembly.

3. 3. 2. Results

3. 3. 2. 1. Investigating which phenotypes are regulated by Uhrf1-mediated Paf15 ubiquitination

It has been proposed that Uhrf1 recruits Dnmt1 by preferentially ubiquitinating Paf15 (130). Considering that Paf15 stably binds to PCNA on chromatin and that PCNA mediates the recruitment of Lig1, Fen1 and CAF1, I firstly wanted to investigate whether Uhrf1 stimulates the recruitment of these proteins though Paf15 ubiquitination. To this aim, I decided to immunodeplete Paf15 from *Xenopus laevis* egg extract to find out the effect of the absence of Paf15 on the recruitment of the proteins.

As previously described for other proteins, to raise specific antibodies against Paf15 for immunodepletion, recombinant protein was firstly needed as an antigen. Full-length GST-tagged *Xenopus* Paf15 was expressed in *E.coli* and affinity purified using Glutathione beads. Thrombin protease was used to elute untagged Paf15 from the beads. Samples taken during the expression and purification processes were run in SDS-PAGE gels and visualized by Coomassie staining (Figure 3. 24 A) and western blotting (Figure 3. 24 B). These results show that untagged Paf15 was successfully purified. The three elutions containing Paf15 were combined and sent for antibodies generation by Eurogentec company.

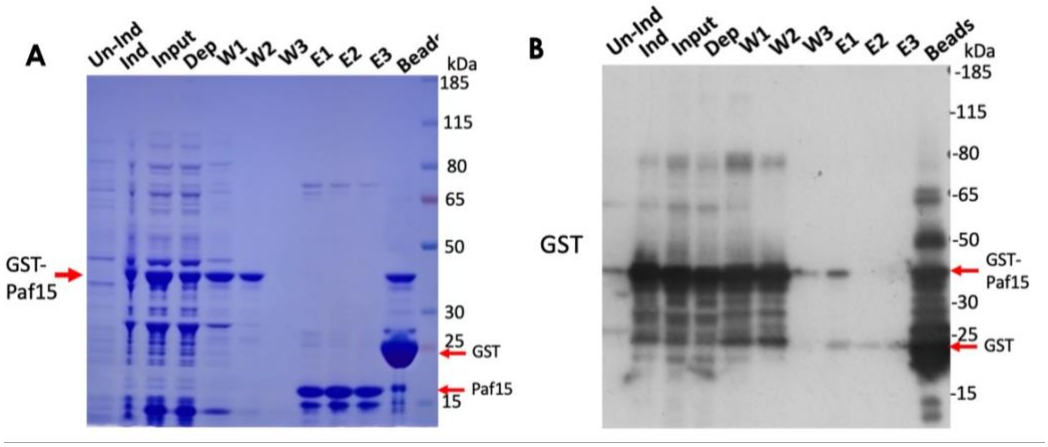


Figure 3. 24. Purification of recombinant *Xenopus laevis* GST-tagged Paf15. Expression of GST-xPaf15 was induced in *E.coli* (induced) and purified as specified in the methods section using Glutathione affinity purification. The induced sample was taken before bacteria lysis. The soluble bacterial lysates (input), unbound proteins (flowthrough, depleted), samples of beads washes, elutions off the beads using thrombin protease and a sample from the beads to check non-eluted protein (beads) are presented. The samples from the purification process were run on an SDS-PAGE gel and visualized by Coomassie staining and immunoblotting using anti-GST antibody.

Two sera from different rabbits against *Xenopus* Paf15 were obtained and their specificity in recognizing Paf15 was tested by immunoblotting of whole extract (Figure 3. 25 A) or by IP (Figure 3. 25 B) compared to pre-immune serum (negative control). Serum 2 was more efficient at recognizing and immunoprecipitating Paf15 from the extract, although the signal was very faint. Next, aPaf15 antigen column was created using purified Paf15 and serum 2 was run through the column for the isolation of anti-Paf15 specific antibodies. The specificity of the most concentrated antibody elution was tested by IP from extract (Figure 3. 25 C). This time, the purified antibodies were able to recognize and IP Paf15 from chromatin very efficiently.

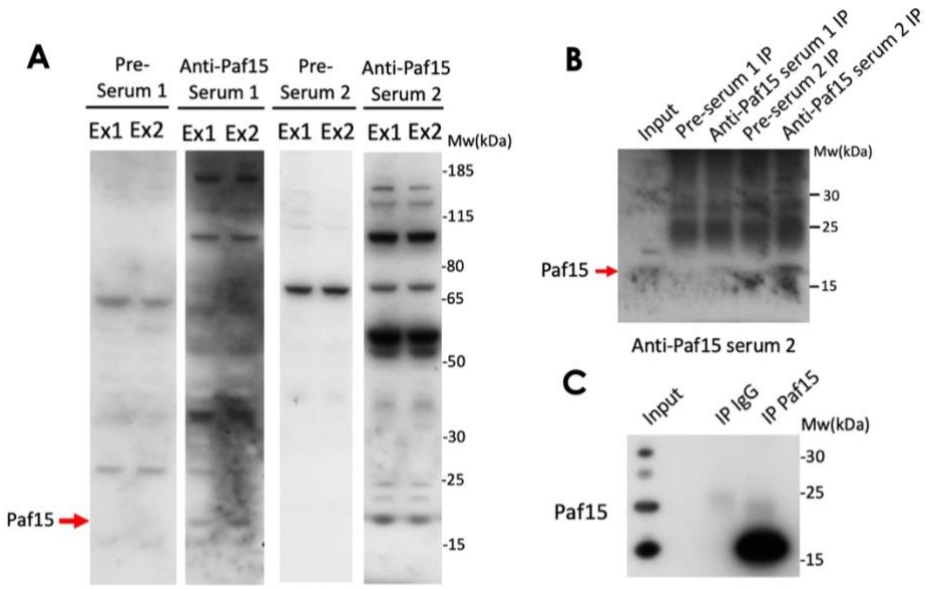


Figure 3. 25. Purification of anti-xPaf15 antibodies. The specificity of two rabbit sera against *Xenopus* Paf15 were tested by immunoblotting of whole extract **(A)** or by immunoprecipitation (IP) from the extract **(B)**. Samples were visualized by western blotting using serum 1 or 2. Pre-serum was used as a negative control in both experiments. **C)** Anti-xPaf15 antibodies isolated from whole sera using purified xPaf15 coupled to a HiTrapTM NHS-activated column were tested by immunoprecipitation of Paf15 from the whole egg extract. These purified antibodies were used for the detection by immunoblotting.

Next, I wanted to characterise Paf15 chromatin binding during DNA replication using purified anti-Paf15 antibodies. Towards this aim, the extract was supplemented with sperm DNA, chromatin was isolated at different times during DNA replication and chromatin associated proteins were analysed by immunoblotting. As shown in Figure 3. 26, Paf15 was detected on chromatin peaking at 30 minutes – the same time as the other replisome proteins. Furthermore, two upper bands were also detected at the same time point with the same size than the described mono and di-mono-ubiquitinated forms of Paf15. Therefore, this result indicates that Paf15 is part of the replication machinery, binding chromatin in an unmodified and ubiquitinated form.

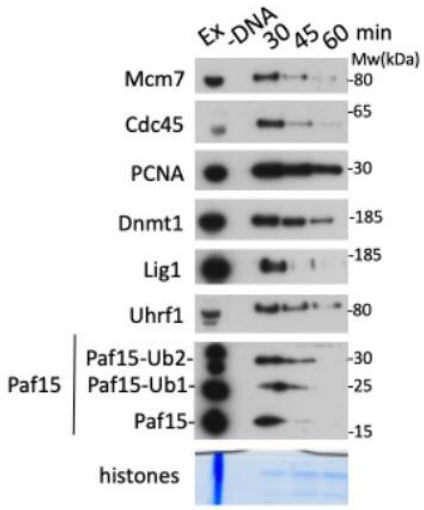


Figure 3. 26. Paf15 is part of the replication machinery in an unmodified and ubiquitinated form. *Xenopus laevis* egg extract was incubated with sperm DNA and the DNA replication reaction was followed by analysing isolated chromatin proteins by immunoblotting using indicated antibodies. Paf15 was detected using purified anti-Paf15 rabbit antibodies from Figure 3. 25 C. A chromatin specificity control was performed by using a sample without DNA, while an extract sample was used as a positive control for immunoblotting. Histones were stained with colloidal Coomassie as loading control. This is a representative experiment of two.

To confirm that Uhrf1 mediates this Paf15 ubiquitination during DNA replication as proposed in the literature, I used purified antibodies to detect Paf15 in replicating chromatin from Uhrf1 depleted extract (Figure 3. 27 A). This experiment showed that the removal of Uhrf1 not only impaired Paf15 ubiquitination but also its association to chromatin. The addition of recombinant Uhrf1 to the depleted extract rescued both Paf15 recruitment and its ubiquitination (Figure 3. 21 B, Figure 3. 27 B). I also quantified the signal of ubiquitinated Paf15 on chromatin at the peak of replication in the four conditions (IgG and Uhrf1 depleted extract with or without adding rUhrf1) in two different experiment using ImageJ (Figure 3. 27 C). The levels were normalised to the levels in the IgG depleted extract. This figure showed that the addition of recombinant Uhrf1 to the Uhrf1-depleted extract strongly stimulated the ubiquitination of Paf15. Altogether, these results confirm that Uhrf1 mediates Paf15 ubiquitination and suggest that this modification could also regulate Paf15 association to chromatin.

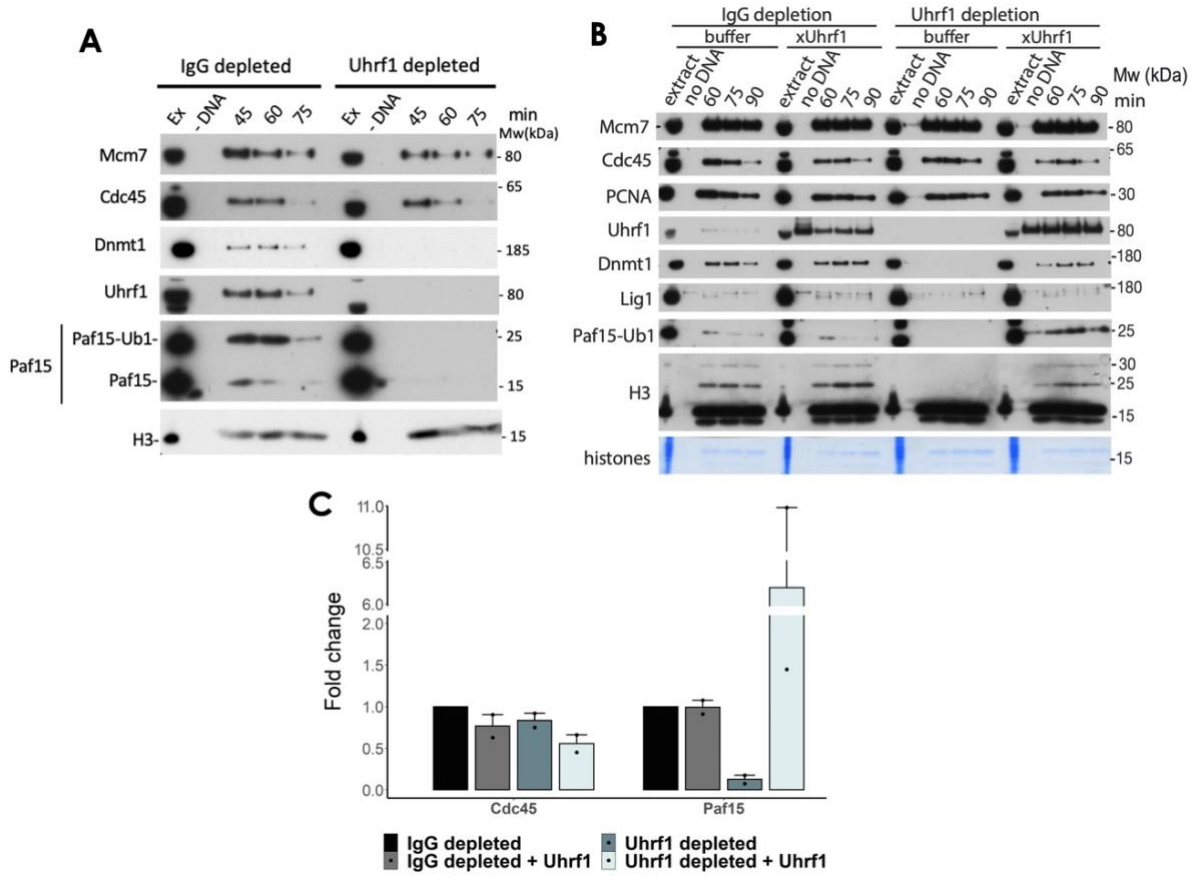


Figure 3. 27. Uhrf1 mediates Paf15 ubiquitination. A) Replication reactions were set up in IgG and Uhrf1-sheep antibody depleted extracts by incubating with sperm DNA. Chromatin bound proteins were analysed at specified times by western blotting using indicated antibodies. This experiment is a representation of four repeats. **B and C)** Depleted extracts (IgG and Uhrf1) were supplemented with sperm DNA and either buffer or recombinant untagged Uhrf1. Chromatin was isolated at indicated times and bound proteins were analysed by immunoblotting. This is a representative experiment of two performed. **C)** Quantification of fold change of chromatin bound ubiquitinated Paf15 was performed at the peak of replication in the four conditions in n = 2 (using extracts from different depletions). The levels were normalised to the level in the IgG depleted extract. Mean with SEM are shown.

Once anti-Paf15 rabbit antibodies were purified and Paf15 chromatin binding characterised, I wanted to investigate whether Paf15 was mediating Dnmt1, Lig1, Fen1 and CAF1 recruitment. Therefore, immunodepletion of endogenous Paf15 was carried out in a similar way than for Uhrf1 and Lig1. As shown in Figure 3. 28 A more than 98% of Paf15 was efficiently depleted from the extract. The depletion of Paf15 did not affect the ability of the extract to synthesise DNA (Figure 3. 28 B). Finally, proteins associated with chromatin at different times during replication in both IgG and Paf15 depleted extracts were analysed by western blotting (Figure 3. 28 C). This experiment showed that the removal of Paf15 did not impair the recruitment of

Dnmt1, Lig1 and CAF1, conversely it enhanced Dnmt1 and Lig1 association with chromatin. Histone H3 ubiquitination and Uhrf1 were also increased after the depletion, suggesting that in the absence of Paf15 the chromatin association of these proteins could be regulated by Uhrf1-mediated H3 ubiquitination. Thus, these results indicate that either Paf15 is not contributing to Uhrf1-mediated Dnmt1, Lig1 or CAF1 recruitments or that back-up pathways exist to ensure the completion of this process, such as the ubiquitination of histone H3.

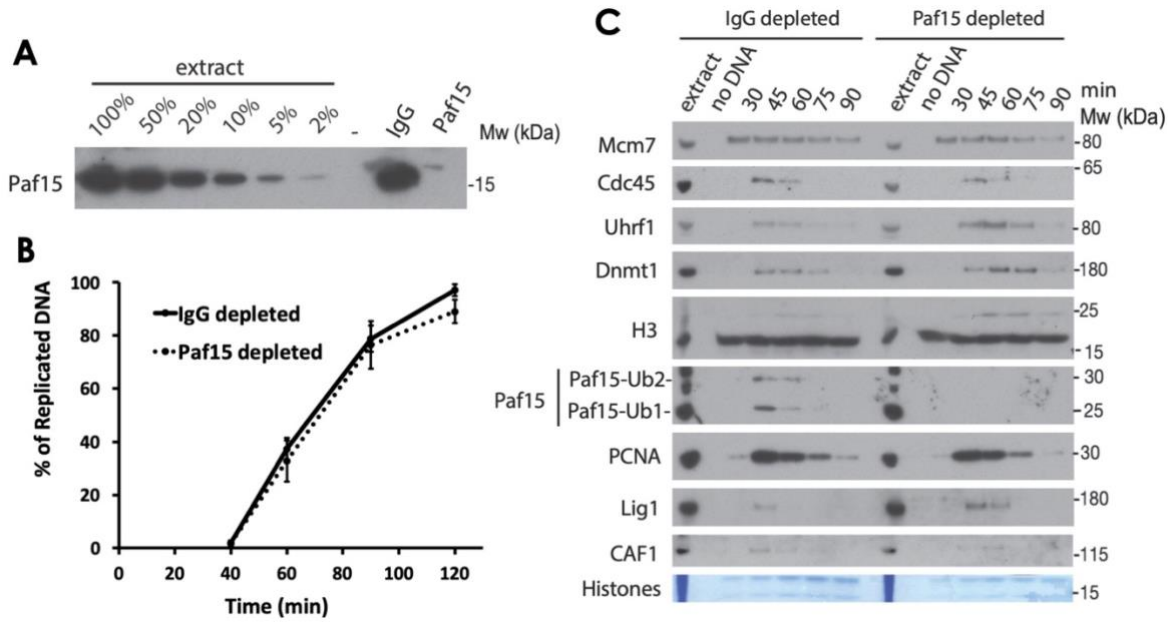


Figure 3. 28. The depletion of Paf15 does not impair Dnmt1, Lig1 and CAF1 recruitment to chromatin. A) Immunodepletion of Paf15 was carried out in *Xenopus* extract using purified anti-Paf15 antibodies (Figure 3. 25 C). Western blotting was used to analyse the efficiency of the depletion by detecting the levels of Paf15 in whole extract. **B)** Depleted extracts (IgG and Paf15) were incubated with sperm nuclei and α-[P32] dATP and the synthesised DNA was measured by α-[P32] dATP incorporation into DNA at the indicated times. This experiment was performed four times. **C)** Sperm DNA was replicated in IgG and Paf15 depleted extracts and chromatin was isolated at the indicated times. Proteins associated with chromatin were analysed by immunoblotting as described in previous figures. This is a representative of two experiments performed.

3. 3. 2. 2. Uhrf1 as a scaffold protein

Given that the recruitment of Dnmt1, Lig1 and CAF1 was not impaired by the depletion of Paf15 and the finding that Uhrf1 interacts with Lig1 and Dnmt1, I next wanted to test whether Uhrf1 was regulating their recruitment by direct interaction, acting as a scaffold protein. To this aim, I performed a large-scale immunoprecipitation of Uhrf1 from chromatin during the peak of replication and subjected the samples to mass spectrometry analysis. This approach would also reveal other possible factors associated and working with Uhrf1 on chromatin. Proteins identified with more than 10 peptides (or TSC) and with a fold change over 2 or under 0.5 in the Uhrf1 IP compared to the non-specific IgG IP were selected and presented in the Appendix. The most interesting findings obtained were summarised in Table 3. 4. Notably, between the most significantly enriched proteins in the Uhrf1 IP were RPA1, the Mcm2-7 complex, Spt16 (FACT complex), and Lig1. This is interesting, as Spt16 was also reduced on chromatin after Uhrf1 depletion (Figure 3. 16 B). Surprisingly, Dnmt1 was not detected interacting with Uhrf1 on chromatin. These findings support the model of Dnmt1 recruitment through ubiquitination and suggest that Lig1 could be recruited through direct interaction with Uhrf1. In addition, RPA, Mcm2-7 and FACT have been identified as potential novel interacting partners of Uhrf1. Although these MS data are not quantitative due to the use of TSC and only one repeat has been performed, it gives valuable preliminary insights. The next step is to validate these findings using western blotting.

Table 3. 4. Replisome proteins identified by mass spectrometry of Uhrf1 immunoprecipitation from chromatin in the middle of S phase. TSC: Total Spectral Counts. This refers to the total number of mass spectra identified for a protein, which serves as an indicator of the protein abundance.

	IP from chromatin in mid S phase		
Protein (kDa)	IgG	Uhrf1	Fold Change
	TSC (coverage)		
Uhrf1 (87)	29 (19%)	789 (69%)	27.2
Rpa1 (67)	24 (24%)	377 (65%)	15.7
Mcm3 (90)	14 (12%)	316 (56%)	22.6
Spt16 (118)	5 (4.7%)	124 (37%)	24.8
Ssrp1 (79)	0	45 (20%)	-
Lig1 (120)	0	143 (36%)	-
Dna2 (120)	0	12 (9%)	-
Dnmt1 (168)	-	-	-

Furthermore, MS analysis also revealed some interesting modifications of Uhrf1 on chromatin. Endogenous *Xenopus* Uhrf1 was mainly modified by phosphorylation, with high number of peptides phosphorylated at Serine S290 and S631 (34 peptides each), and one peptide phosphorylated at the S641 residue. Serine S290 could correspond to the known phosphorylated site S298 in mouse and human, since this residue is not conserved in *Xenopus* and it would be the nearest serine residue (Figure 3. 29 A). This residue has been shown to promote a conformational change in Uhrf1, but the consequences are still unclear (143,146). However, the recognition motif of PKA (R-R-x-S/T), the kinase that mediates phosphorylation of S298 in human cells, is not conserved in *Xenopus*. Considering that the S290 residue is follow by a proline residue and S/T-P is a very evolutionary conserved motif for many kinases (219), other kinases could mediate this phosphorylation in *Xenopus*. PIM1 has also been shown to phosphorylate S298, however there is not a well-defined recognition motif for this kinase. Interestingly, two neighbouring residues (N287 and Q292) were found deaminated surrounding S290, which could modulate the phosphorylation effect in Uhrf1 (Figure 3. 29 B). These sites are also not conserved in mouse and human. Finally, I found two residues phosphorylated in the PBR region (mainly S631 but also S641) flanking the Usp7 binding site, also characterised in human Uhrf1 (Figure 3. 29 C). These phosphorylations have been shown to disturb the interaction with Usp7 in M phase (153). Altogether, these results confirm that Uhrf1 is highly regulated through phosphorylation also when associated to chromatin.

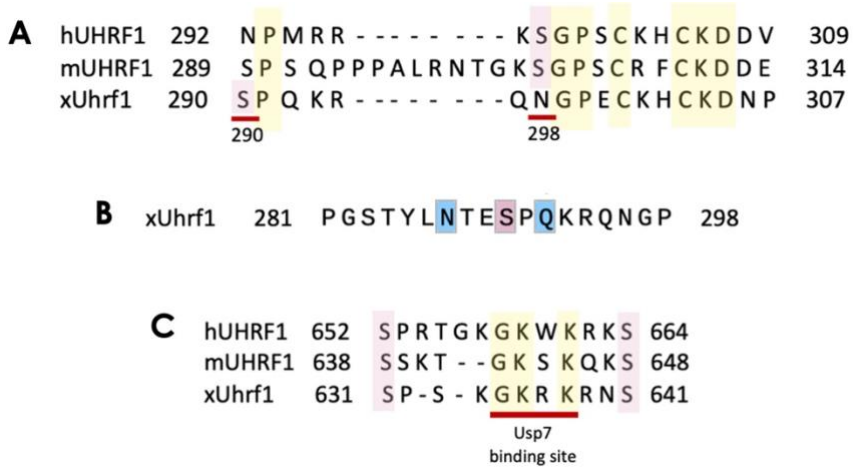


Figure 3. 29. Modifications of xUhrf1 identified by MS. Summary of modifications found in the IP-MS performed in Table 3. 4. Alignment of human, mouse and *Xenopus laevis* Uhrf1 sequences **(A and C)**. Identical residues are highlighted in yellow, phosphorylated sites in pink and deaminated in blue.

To verify and further analyse some of the interesting proteins identified by MS interacting or possibly being regulated by Uhrf1, specific antibodies were needed. As for the previous proteins, purification of recombinant proteins was first carried out to raise antibodies against them. The plasmids to express *Xenopus* RPA and the human Ssrp1 subunit of the FACT complex were kindly provided by Dr Hidenori Nakaoka and Professor Vincenzo Costanzo respectively. Full-length GST-Flag-tagged hSsrp1 was purified in *E.coli*, sent to Eurogentec company for raising antibodies and the obtained sera were tested for specificity against Ssrp1. Unfortunately, none of the sera were recognizing Ssrp1 neither in the extract nor on chromatin (data not shown). Full-length His-tagged xRPA1, RPA2 and RPA3 were simultaneously expressed in *E.coli* and purified in *E.coli* using Nickel beads. Samples from the expression and purification processes were run in SDS-PAGE gels and visualized by Coomassie staining (Figure 3. 30 A) and western blotting using an anti-His antibody (Figure 3. 30 B). Considering the immunoblotting results, the RPA1 subunit was mainly purified, although faint bands corresponding to RPA2 and RPA3 could also be detected. Elution 2 was dialyzed into a compatible buffer and sent for antibody generation by Eurogentec company.

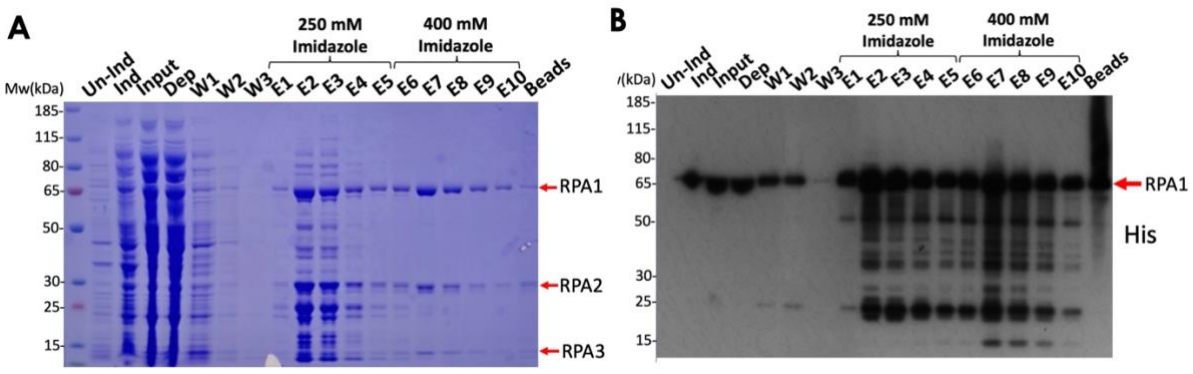


Figure 3. 30. Purification of RPA. His-tagged *Xenopus* RPA1, RPA2 and RPA3 were simultaneously expressed and purified using Nickel affinity beads. Presented in this figure are: the induced sample taken before lysis of the bacteria, the soluble bacterial lysate (input), unbound proteins (flowthrough, depleted), samples of bead washes and of elutions from the beads using two concentrations of Imidazole. All these samples from the purification process were run in a SDS-PAGE gel and visualized by Coomassie staining **(A)** or immunoblotting **(B)** using anti-HIS antibody.

Similar to previous proteins, two rabbit sera against RPA were obtained and tested for specificity by immunoblotting (Figure 3. 31 A) or by IP from extract (Figure 3. 31 B) using pre-sera as negative controls. Both anti-RPA sera were recognizing and immunoprecipitating RPA from the extract. However, these sera were unable to detect RPA3. Anti-RPA antibodies were then purified from whole serum 1 using purified RPA coupled to a HiTrap NHS-activated column. Purified anti-RPA antibodies were efficiently immunoprecipitating RPA from the extract (not shown) and from chromatin (Figure 3. 31 C). Since sera against Ssrp1 were not detecting Ssrp1 effectively, I used commercial antibodies against the other subunit of the FACT complex, Spt16, from now on to detect this chaperone by western blotting.

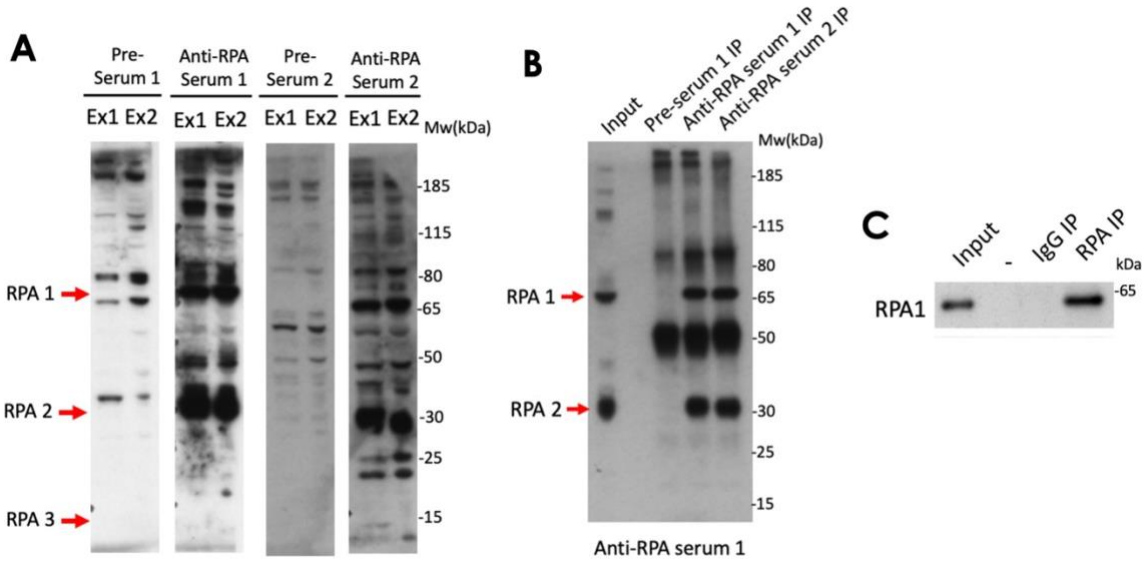


Figure 3. 31. Purification of anti-RPA antibodies. Two rabbit sera raised against *Xenopus* RPA were tested by western blotting of whole extract **(A)** or by immunoprecipitation (IP) from the extract **(B)**. Samples from the IP were visualized by immunoblotting using serum 1 or 2. Pre-serum was used as a negative control in both experiments. **C)** Antibodies against RPA were isolated from whole sera and their specificity were tested by immunoprecipitating RPA from chromatin. These purified anti-RPA antibodies were used for the visualization by immunoblotting.

Once antibodies against interesting proteins were obtained, I wanted to confirm Uhrf1 interactors on chromatin identified by mass spectrometry using western blotting. Therefore, immunoprecipitation of Uhrf1 from chromatin in the middle of S phase was performed and associated proteins were analysed by immunoblotting using specific antibodies. As shown in Figure 3. 32 A, I could co-immunoprecipitate Mcm7, Cdc45 and Spt16, confirming that the CMG helicase and FACT complex are novel interactors of Uhrf1. The interaction with RPA was also confirmed by co-immunoprecipitating Uhrf1 with RPA from chromatin using purified anti-RPA antibodies (Figure 3. 32 B). However, the interaction with Lig1 or Dnmt1 were not detected by immunoblotting (Figure 3. 32 A). Since Lig1 was detected to bind Uhrf1 by MS, I also tried to IP Lig1 from chromatin to detect whether I could co-IP Uhrf1. Unfortunately, Lig1 antibodies were not efficient enough to IP Lig1 (data not shown). In summary, these results confirmed Uhrf1 interactions with RPA, the FACT complex and the helicase, while Uhrf1-Lig1 binding was not detected by immunoblotting.

To optimize the immunoprecipitation of Uhrf1 in complex with interactors, the effect of the salt concentration on the solubility of indicated chromatin bound proteins was tested by immunoblotting after chromatin isolation and digestion (Figure 3. 32 C). As shown in Figure 3. 32 D, most proteins were more soluble at higher salt concentrations, since the high salt disassembles the large complexes that these proteins are forming. In contrast Uhrf1 was soluble even in –DNase sample condition where DNA was not digested, suggesting that Uhrf1 is likely to interact with chromatin in a very dynamic and transient way.

Finally, to stabilize the protein interactions and to be able to capture them when immunoprecipitating Uhrf1, the isolated chromatin was incubated with the crosslinker DTSSP (3,3'- dithiobis(sulfosuccinimidyl propionate)). As shown in Figure 3. 32 E, the treatment with the crosslinker did not improve the results. This could be explained by the fact that the crosslinker was added after the chromatin was isolated, when Uhrf1 could already be dissociated from chromatin as Uhrf1 does not need the benzonase treatment to be released. Altogether, the facility of Uhrf1 to be solubilized from chromatin and the difficulties to co-immunoprecipitate significant amounts of interacting proteins to be detected by western blotting, suggest that Uhrf1 is not tightly associated with either these interactors or with chromatin and is likely to regulate the recruitment of Dnmt1 and Lig1 indirectly. Therefore, the hypothesis of Uhrf1 acting as a scaffold protein becomes less likely.

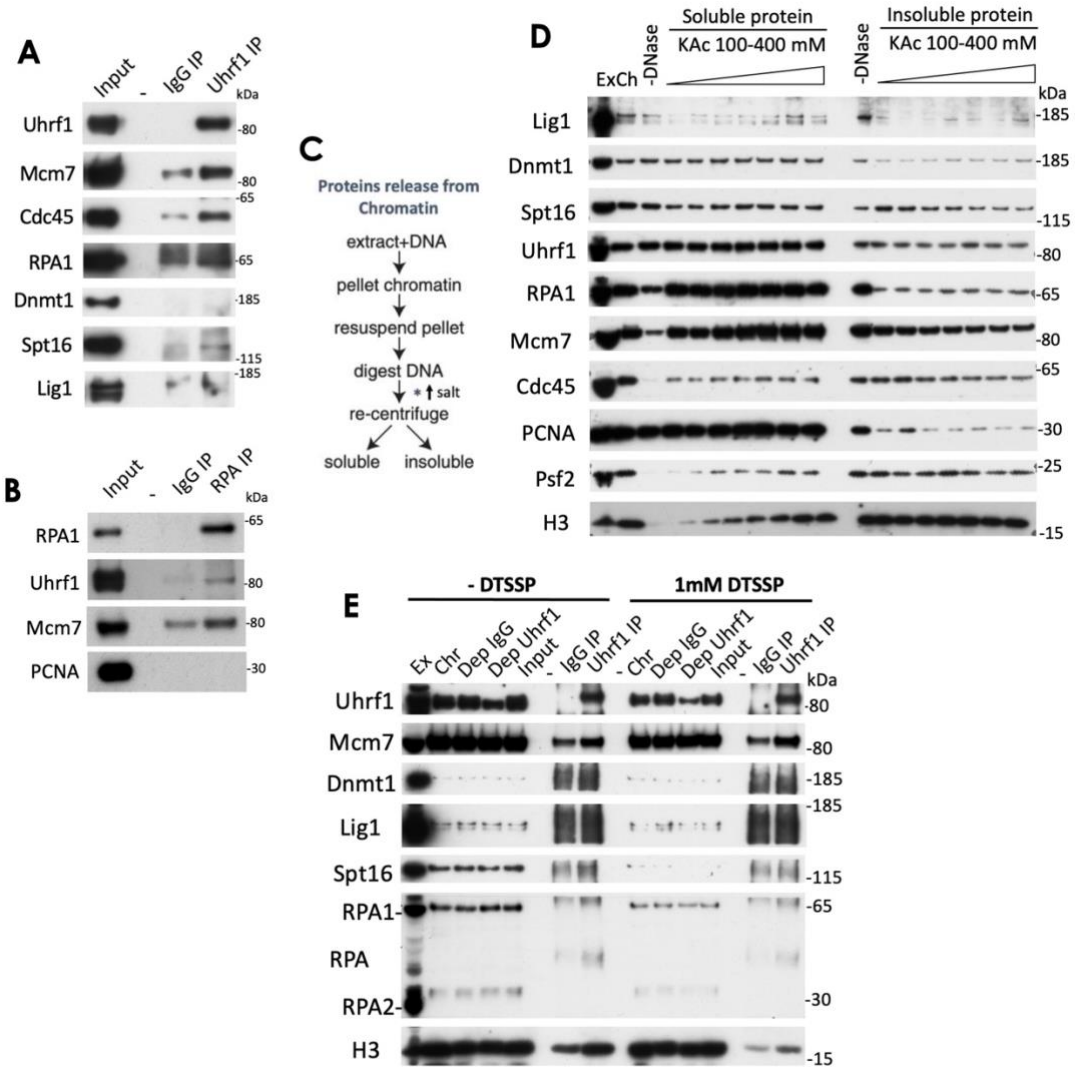


Figure 3. 32. Uhrf1 interacts with RPA, the helicase and the FACT complex in a dynamic manner. A and B) *Xenopus* egg extract was incubated with sperm DNA, chromatin was isolated at the peak of replication using a buffer with 100 mM potassium acetate and protein complexes were released by benzonase treatment and subsequent sonication. Purified Uhrf1 antibodies were used to immunoprecipitate Uhrf1 (**A)**, purified RPA antibodies to immunoprecipitate RPA **(B)** and nonspecific sheep and rabbit IgG antibodies were used respectively as a negative control. Samples were then analysed by immunoblotting using indicated antibodies. The experiment was performed twice in **(A)** and once in **(B)**. **C)** Scheme of the procedure to release proteins from chromatin using different salt concentrations. **D)** After isolating chromatin at 100 mM potassium acetate, a fraction was taken before digestion with benzonase (-DNase). After benzonase treatment, the salt concentrations were adjusted to 100, 150, 200, 250, 300, 350, 400 mM of potassium acetate. All the samples were then separated into soluble and insoluble fractions by centrifugation. Indicated proteins were detected by immunoblotting using indicated antibodies. This experiment was carried out once. **E)** Replicating chromatin isolated in mid S phase was resuspended at 100 mM salt and incubated with DTSSP (3,3'-dithiobis(sulfosuccinimidyl propionate)) crosslinker before release by benzonase treatment and sonication. Then Uhrf1 immunoprecipitation was performed as in (A). This is a representative experiment of three performed.

3. 3. 2. 3. Analysing which phenotypes are regulated by ubiquitination

Since Uhrf1 does not seem to act as a scaffold protein recruiting Dnmt1, Lig1, Fen1 and CAF1 by stable interactions, the indirect regulation through its E3 ubiquitin ligase activity should mediate these protein recruitments. Given that the absence of Paf15 and Uhrf1-mediated Paf15 ubiquitination did not impair the recruitment of these proteins, I hypothesised that Uhrf1 may use H3 and Paf15 ubiquitination, and possibly the ubiquitination of other unknown factors, as back up pathways to control the recruitment of these proteins. The failure to efficiently inhibit H3 ubiquitination (chapter 1) and the absence of an Uhrf1 RING mutant to test the requirement of its ubiquitin activity due to the difficulties in purifying active recombinant Uhrf1 (chapter 2), led us to use a general inhibition of ubiquitination in the extract to test the dependency of these protein recruitments on ubiquitination.

Therefore, the TAK-243 (mln7243) inhibitor which targets the first enzyme of the ubiquitin cascade (E1 ubiquitin activating enzyme) was chosen, since it was previously used in NPE (Nucleoplasmic Extract), the nuclear fraction of the *Xenopus* egg extract (Figure 3. 33 A, (49)). The use of the E1 inhibitor (E1i) in the extract was firstly optimized by incubating the extract with sperm DNA and different concentrations of the inhibitor (Figure 3. 33 B). After performing this experiment, 300 μM concentration was chosen to ensure a complete inhibition of ubiquitination without affecting the DNA replication reaction. The extract was then incubated with sperm DNA and either DMSO or E1i and chromatin bound proteins were analysed at different times by immunoblotting. As shown in Figure 3. 33 C, the addition of the E1 inhibitor to the extract inhibited histone H3 ubiquitination at the beginning of replication, although this inhibition seemed to be relieved with time. The effective activity of the inhibitor could also be seen by the impairment of the Mcm7 poly-ubiquitination at 30 min and the accumulation of the replicative helicase (Mcm7, Cdc45 and Psf2) on chromatin, as expected since poly-

ubiquitination drives the helicase disassembly. Successfully, the inhibition of ubiquitination impaired Dnmt1 and CAF1 recruitment to chromatin, confirming that ubiquitination regulates their recruitment. In contrast, Lig1 and Fen as well as Uhrf1 and PCNA were accumulated on chromatin when ubiquitination was inhibited, being gradually disassembled when inhibition was gone and the ubiquitination of histone H3 was detected. Altogether, these findings suggest that ubiquitination mediates Dnmt1 and CAF1 recruitment and regulate Lig1 and Fen1 association to chromatin.

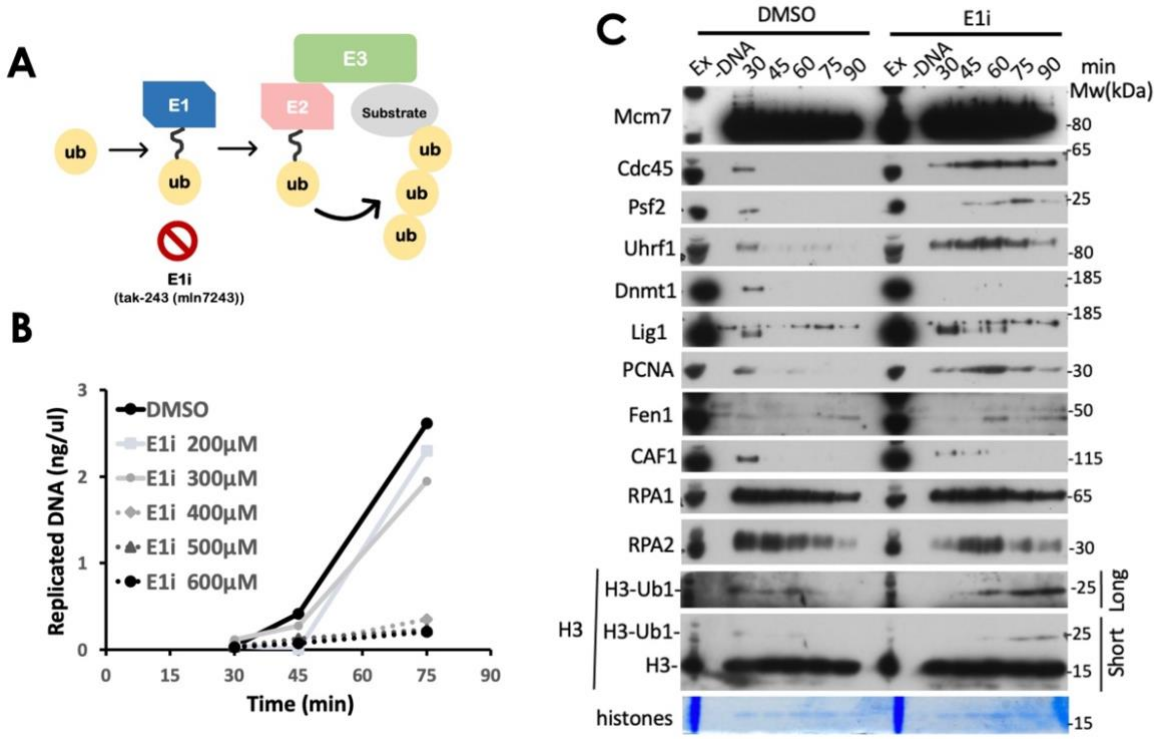


Figure 3. 33. Ubiquitination regulates chromatin association of Dnmt1 and CAF1. A) Schematic representation of ubiquitination cascade and the target of TAK-243 (mln7243) inhibitor. **B)** Sperm DNA was added to *Xenopus* egg extract and optionally DMSO or different concentrations of E1i TAK-243 (mln7243). DNA replication was stopped at indicated times and synthesised DNA was measured by quantifying radioactive nucleotide. This experiment was performed once. **C)** The extract was incubated with sperm DNA and either DMSO or E1i at 300µM, chromatin was isolated at different times and bound proteins were analysed by western blot using indicated antibodies. This experiment is a representative of two performed.

Since the inhibition of ubiquitination also affected the disassembly of the helicase accumulating Mcm7 and Cdc45 on chromatin, I next wanted to investigate whether the accumulation of Uhrf1 and the other proteins was due to a general accumulation of the replisome or because of the block of mono-ubiquitination. To this aim, a chain-terminating mutant of ubiquitin with all

lysines mutated (UbiNOK) was used to specifically inhibit poly-ubiquitination and compare phenotypes with general ubiquitination inhibition. Thus, the extract was supplemented with either buffer, the E1 inhibitor or ubiquitin chain terminating mutant UbiNOK (Figure 3. 34 A). As shown in Figure 3. 34 B, the addition of the E1i slightly affected synthesised DNA levels, probably due to the number of proteins regulated by ubiquitination during DNA replication.

I then analysed chromatin bound proteins by immunoblotting in the three conditions (Figure 3. 34 C and D). Furthermore, quantifications of the fold change of these proteins on chromatin at 30 min, 45 min and 90 min in the three conditions (DMSO, E1i and UbiNOK) were also performed in two different experiments (experiment in Figure 3. 34 C and another not shown) using ImageJ. The levels were normalised to levels in DMSO at 30 min (Figure 3. 34 E and F). These figures showed that the addition of UbiNOK stimulated histone H3 and PCNA mono-ubiquitination confirming that the strategy worked. This can also be seen by the enhanced Paf15 mono-ubiquitination in Figure 3. 34 D. While Cdc45 was accumulated on chromatin in E1i, Dnmt1 and CAF1 were strongly decreased (Figure 3. 34 C, D and E). Importantly, enabling mono-ubiquitination using UbiNOK allowed Dnmt1 and CAF1 recruitment confirming that mono-ubiquitination regulate their recruitment. On the other hand, the inhibition of H3 ubiquitination by E1i at the early time points was accompanied by a significant accumulation of Uhrf1 and Lig1 on chromatin (Figure 3. 34 C, D and F). The addition of the UbiNOK mutant strongly stimulated histone H3 mono-ubiquitination and promoted a faster disassembly of Uhrf1 and Lig1. By 90 min, Lig1 was disassemble from chromatin, which coincided with a restoration of H3 ubiquitination to control levels. In summary, these results support the model of Dnmt1 and CAF1 recruitment through ubiquitination, probably mediated by Uhrf1, and suggest that Lig1 binding to chromatin does not require ubiquitination, but its disassembly could be regulated by this modification.

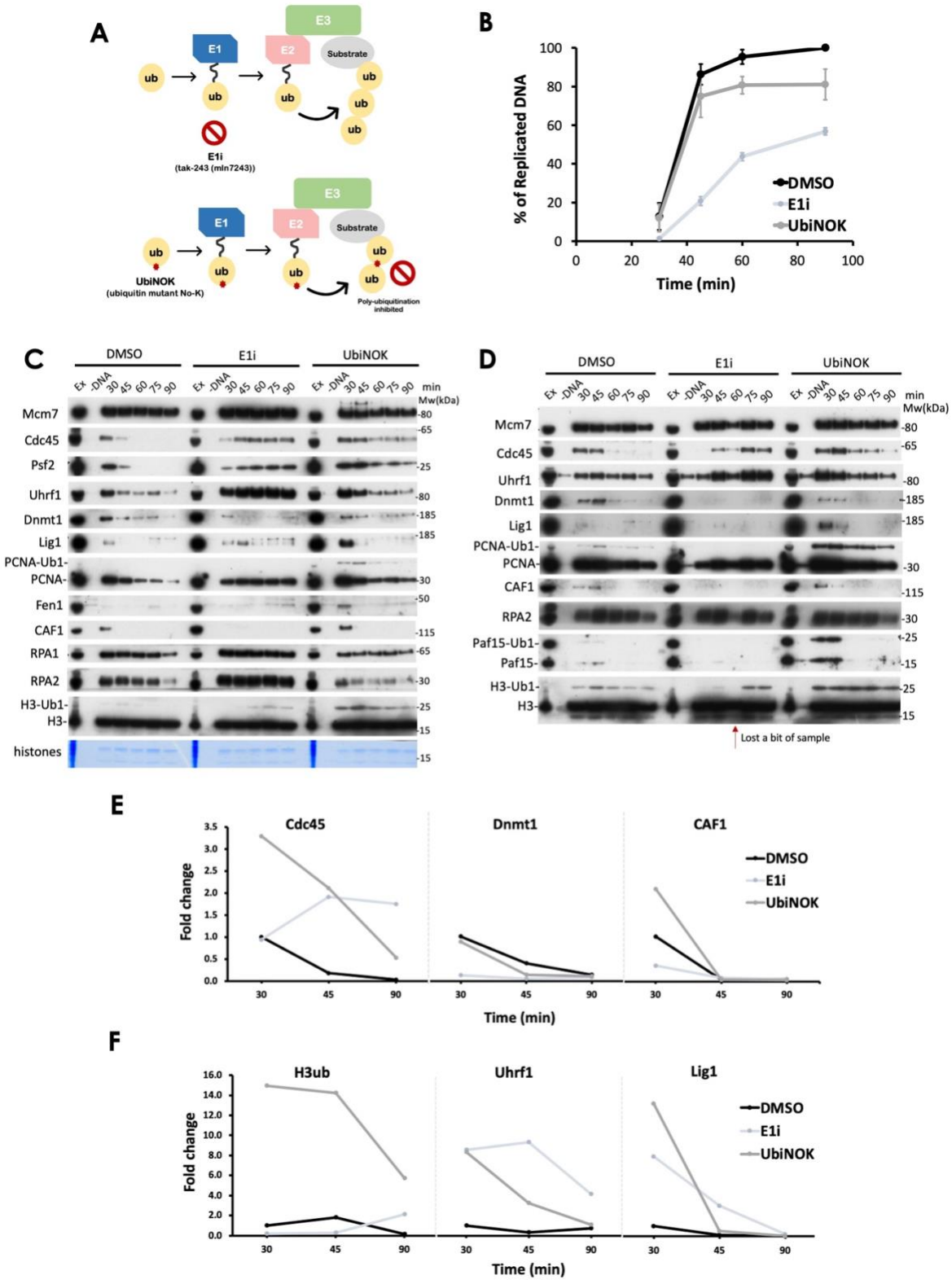


Figure 3. 34. Mono-ubiquitination mediates Dnmt1 and CAF1 recruitment and regulates Lig1 disassembly. **A)** Scheme of the ubiquitination cascade and the treatments applied in B-F. **B-F)** Sperm DNA was added to *Xenopus* egg extract and either DMSO, E1i TAK-243 (mln7243) or the ubiquitin mutant UbiNOK. The DNA replication reaction was stopped at the indicated times. **B)** Synthesised DNA was measured by quantifying α-[P32] dATP incorporation. **C-F)** Chromatin bound proteins were analysed by western blot using indicated antibodies. These are two representative experiments of three. **E-F)** Quantification of fold change of chromatin bound proteins was performed at the peak of replication in the three conditions in n = 2. The levels were normalised to level in DMSO 30 min condition. Mean is shown.

3. 3. 3. Discussion

This chapter of the thesis has brought new insights into the mechanism by which Uhrf1 regulates chromatin re-establishment during DNA replication. In the previous chapter, I showed that Uhrf1 mediates histone H3 and Paf15 ubiquitination as well as Dnmt1 recruitment. In addition, I also found out that Uhrf1 could have additional roles during DNA replication by the regulation of Lig1, Fen1 and CAF1 recruitment. However, different mechanisms could mediate these protein recruitments based on current knowledge: a direct interaction, Uhrf1 has been shown to interact with Dnmt1 and Lig1, or an indirect regulation through ubiquitination of H3 and Paf15. The results presented on this chapter suggest that ubiquitination regulates the association of Dnmt1 and CAF1 to chromatin, while it seems to promote the disassembly of Lig1. The interaction of Lig1 with Uhrf1 on chromatin suggests a possible mechanism of recruitment through direct interaction. Furthermore, I have identified RPA, the FACT complex and the CMG helicase as novel interactors of Uhrf1. These new findings provide a wider picture of how Uhrf1 could coordinate DNA methylation with DNA replication and nucleosome assembly.

Initially, I hypothesised that Uhrf1 could mediate the recruitment of Dnmt1, Lig1, Fen1 and CAF1 through Paf15 ubiquitination, since Paf15 stably interacts with PCNA which is essential for the binding of these proteins to chromatin (33). However, my results showed that depleting Paf15 did not impair these proteins' recruitment but on the contrary, Dnmt1 and Lig1 were increased on chromatin after Paf15 depletion. This was unexpected because Paf15 ubiquitination was proposed as a mechanism for Dnmt1 recruitment (130,133). Furthermore, Lig1 depletion showed in the previous chapter enhanced PCNA and Paf15 ubiquitination on chromatin, as well as Fen1, CAF1 and Dnmt1, while the lack of Lig1 in Uhrf1 depleted extract reduced their recruitment, suggesting that they could depend on Uhrf1-mediated Paf15

ubiquitination. Therefore, these findings indicate that either Paf15 ubiquitination is not the mechanism used by Uhrf1 to mediate Dnmt1, Lig1 or CAF1 recruitments or that back-up pathways ensure the completion of this process.

Given that Uhrf1 was also increased after the removal of Paf15 and was proposed to act in a macromolecular complex interacting with many proteins (140,189), I firstly investigated whether Uhrf1 could act as a scaffold protein mediating the recruitment of Dnmt1, Lig1 and CAF1 by direct interaction. This would explain the stimulation of these proteins on chromatin after Paf15 depletion. However, from my experiments neither MS nor western blotting analysis showed Uhrf1 interacting with Dnmt1 or CAF1 at the peak of replication. This was unexpected since many studies have reported the direct interaction between Uhrf1 and Dnmt1 (126,128,129,165). A possible explanation is the fact that these studies were performed *in vitro* with purified fragments of the proteins (128,129) or the interaction was detected by co-IP analysis in mammalian cells either in complex with PCNA (which tightly bind Paf15) (127) or in asynchronous cultures (126). Considering that Uhrf1 has been proposed to form a repressive complex with Dnmt1 and other histone remodellers for the regulation of gene expression (220), the interaction detected by these studies could be showing Uhrf1's capacity to bind Dnmt1 for transcription regulation and not for the recruitment of Dnmt1 during normal DNA replication-coupled DNA methylation maintenance. In this study, the use of *Xenopus* egg extract focuses on the DNA replication process excluding Uhrf1's roles in gene expression, which could explain why the interaction with Dnmt1 is not captured. Thus, these findings suggest that Uhrf1 does not interact with Dnmt1 and CAF1 on chromatin at the peak of replication and their recruitments may be regulated through Uhrf1 ubiquitin ligase activity.

In the case of Lig1, the interaction with Uhrf1 was detected in the MS analysis. Although this interaction could not be confirmed by immunoblotting, other studies have shown that the TTD

of Uhrf1 binds to the methylated K126 residue of Lig1 (134,155). One possible reason to explain the inability to detect this interaction by immunoblotting could be the low efficiency of the purified anti-Lig1 antibodies used, as evidenced by their weak detection of Lig1 on replicating chromatin. This hypothesis is further supported by the failure of these antibodies to IP Lig1 from chromatin. Given that MS is a more sensitive technique, it could also be possible that only a small amount of Lig1 protein interacts with Uhrf1 on chromatin. Moreover, considering that the Lig1-Uhrf1 interaction promotes an open conformation of Uhrf1 and that this interaction does not require hemi-methylated DNA (134), there is a possibility that Uhrf1 and Lig1 mainly interact prior to chromatin binding, which may activate Uhrf1.

Importantly, in this chapter RPA, the FACT complex and the CMG helicase have been identified as novel interactors of Uhrf1. Both MS and immunoblotting analysis showed Uhrf1 interacting on chromatin with RPA1, Spt16 (FACT complex) and the helicase proteins Mcm7 and Cdc45 during the peak of DNA replication. This is interesting since all these proteins have been proposed to act as histone chaperones mediating replication-coupled nucleosome assembly.

Firstly, RPA was the top interactor of Uhrf1 on chromatin. This protein apart from binding single-strand DNA during DNA replication, has been linked to both Okazaki fragment maturation and nucleosome assembly, stabilizing longer 5'-flaps displaced by Pol δ and directly binding histones and histone chaperones to promote nucleosome assembly (34,82). Therefore, the interaction with Uhrf1 could reveal the ubiquitination of RPA by Uhrf1 to regulate these processes. RPA is known to be ubiquitinated by the E3 ligases RFWD3 and PRP19 for the progression of stalled forks and repair of DNA damage sites (221,222). On the other hand, RPA has been shown to promote mono-ubiquitination of PCNA and H2B, a substrate of Uhrf1, by interacting and promoting the recruitment of the E3 ubiquitin ligases Rad18 and Bre1, respectively, to regulate DNA damage signalling and repair (223,224). Therefore, RPA could

also recruit Uhrf1 for the ubiquitination of Paf15 and H3 or other potential substrates, which would indirectly regulate and coordinate DNA replication, Okazaki fragment maturation and nucleosome assembly. However, more experiments need to be done to clarify the role of the RPA-Uhrf1 interaction during DNA replication.

Secondly, my findings reinforce the role of Uhrf1 in nucleosome dynamics by also regulating the FACT complex, which is involved in the assembly and disassembly of both parental and new H3-H4 tetramers and H2A-H2B dimers (69). This is evidenced by the interaction between Uhrf1 and the FACT complex subunits on chromatin and further supported by the decrease in Spt16 and histones content on chromatin after Uhrf1 depletion. Interestingly, MS data not shown in this report detected Uhrf1 interacting on chromatin with ubiquitinated Spt16 and revealed that Ssrp1 ubiquitination on replicating chromatin was lost after Uhrf1 depletion. Although there is not much known about FACT complex regulation through ubiquitination, it was shown that Spt16 is ubiquitinated by the cullin-E3 ligase Rtt101 to promote FACT binding to replication origins and the CMG helicase in *Saccharomyces cerevisiae* (225). Thus, Uhrf1 could potentially ubiquitinate this histone chaperone to promote its recruitment and regulate histone assembly and/or disassembly.

Finally, the interaction of Uhrf1 with the helicase is another novel finding that couples DNA methylation with DNA replication. Apart from its role in unwinding DNA, the subunit Mcm2 also act as a chaperone regulating parental histone recycling to the lagging strand (75,76). Therefore, this interaction could again be showing the regulation of nucleosome dynamics by Uhrf1 during DNA replication. Supporting this, FACT interacts with both RPA and Mcm2 (79,82) and FACT-mediated nucleosome recycling is essential for replisome progression (80). Thus, Uhrf1 could also be helping in the histone recycling between Mcm2 and the FACT chaperone that allows the replisome to progress.

Taken together, the Uhrf1 interaction with RPA, the FACT complex and the helicase again suggests a new role of Uhrf1 in regulating nucleosome dynamics during DNA replication. Considering that these proteins have important roles during DNA replication and that Uhrf1 also mediates replication block bypass by promoting TLS and is involved in other DNA damage repair pathways, these interactions with Uhrf1 could also be revealing novel functions of Uhrf1 in dealing with replication stress and potentially in resolving stalled replication forks. Further experiments to follow up these interesting findings will help to understand the role of these interactions during DNA replication.

Although some interactions with Uhrf1 have been identified, the hypothesis of Uhrf1 acting as a scaffold protein seems unlikely. The facility with which Uhrf1 can be released from chromatin, combined with the difficulties in co-immunoprecipitating detectable quantities of interactors, suggest that Uhrf1 may not be tightly bound to neither its interactors nor to chromatin and this association may be brief and dynamic.

This led us to hypothesise that Uhrf1 may recruit Dnmt1, Lig1 and CAF1 indirectly through ubiquitination using alternative pathways to ensure the completion of chromatin re-establishment. The increase of Dnmt1 and Lig1 after Paf15 depletion together with the increase in Uhrf1 and H3 ubiquitination suggest that Uhrf1-mediated H3 ubiquitination could act as a backup mechanism for these protein recruitments and compensate the lack of Paf15. This increase in H3 ubiquitination and Dnmt1 recruitment after Paf15 removal is supported by the results obtained by Nishiyama and co-workers in a similar experiment depleting Paf15 also in *Xenopus* egg extract (130). They also showed that Dnmt1 co-immunoprecipitated significant amounts of ubiquitinated H3 and Paf15, while the levels of Uhrf1 were very low. Since the interaction with ubiquitinated H3 was enhanced after Paf15 depletion, they proposed that Paf15 acts as preferred mechanism for Dnmt1 recruitment in early S phase and when Paf15 is absent,

H3 ubiquitination acts as a back-up pathway to compensate for Paf15 defect. As this cooperative mechanism between H3 and Paf15 seems to regulate Dnmt1 recruitment, the same could be applied for Lig1 and CAF1. Furthermore, other, yet unknown, substrates could also be regulated by Uhrf1 to faithfully complete the task. Therefore, the inhibition of H3, Paf15 and other possible pathways are required to test this hypothesis. Lacking Uhrf1 RING mutant to test the role of its ubiquitin ligase activity in the recruitment of these proteins, E1 inhibitor and ubiquitin mutant UbiNOK were used to inhibit general ubiquitination and mono-ubiquitination respectively.

Using this strategy, I have confirmed in this chapter that mono-ubiquitination regulates Dnmt1 and CAF1 recruitment. My experiments showed that the inhibition of ubiquitination impaired Dnmt1 and CAF1 recruitment. Since these proteins were bound to chromatin when allowing mono-ubiquitination by the addition of UbiNOK, I conclude that mono-ubiquitination should be the mechanism used, probably by Uhrf1, to recruit these proteins. Considering that I am generally inhibiting ubiquitination which could generate many other problems during DNA replication, as evidenced by the decreased levels of DNA replication, further experiments need to be performed using Uhrf1 catalytic mutant. This would also confirm that Uhrf1 is the E3 ubiquitin ligase responsible of this ubiquitination.

Furthermore, this chapter has shown that Lig1 recruitment is not regulated by ubiquitination and of may be the interaction with Uhrf1 that regulates its recruitment. The inhibition of ubiquitination did not affect Lig1 recruitment, showing that the binding of this protein to chromatin is independent of this modification. However, the lack of ubiquitination prolonged Lig1 association to chromatin. Since both experiments impairing Paf15 recruitment and ubiquitination showed that Lig1 disassembly coincided with the ubiquitination of H3, I hypothesise that ubiquitination may promote Lig1 dissociation from chromatin. As PCNA

needs to orderly bind Fen1, Lig1, CAF1 and Dnmt1, it is expected that ubiquitination regulates PCNA interactions with some of these proteins while promoting the dissociation of others. The fact that Fen1 dissociation from PCNA, that allows Lig1 to bind, is regulated by sequential PTMs supports this finding. In the future, the use of the Uhrf1 RING mutant but also a mutant of the TTD that affects binding to H3, Lig1 and Paf15 would be interesting to find out how the sequential recruitment of these proteins is regulated and coordinated by Uhrf1.

Finally, I have found out that Uhrf1 is highly phosphorylated on chromatin during DNA replication in *Xenopus* extract. The IP of Uhrf1 from chromatin revealed that Uhrf1 is phosphorylated at S290 in the linker region between TTD and PHD domains. This phosphorylation could correspond to the known S298 phosphorylation in humans. Investigating the role of this modification in Uhrf1 further would be interesting, given the contradictions in the literature about the effect of this modification on the Uhrf1 binding affinity to H3 (143,146). This has been proposed to promote a change in the Uhrf1 conformation that favours the association with the interactors Lig1 and H3 on chromatin (146), but also to destabilize the Uhrf1 interaction with H3 (143). Apart from this site, I have also found two other sites phosphorylated in the PBR region (mainly S631 but also S641) surrounding the Usp7 binding site, also characterised in human Uhrf1 to disturb the interaction with Usp7 in M phase (153). Given that the PBR region is crucial for the regulation of the open and close conformation of Uhrf1 through intra and inter-molecular interactions, further studying these modifications using Uhrf1 mutants will give a better understanding of how Uhrf1 is regulated and coordinates its function in DNA methylation maintenance, DNA replication and nucleosome assembly.

In summary, this chapter has provided new insights that suggest a model in which Uhrf1 would mediate Dnmt1 and CAF1 binding to chromatin through ubiquitination of H3 and Paf15, while a direct interaction with Lig1 would mediate its recruitment.

7. DISCUSSION

This thesis has brought new insights into the process of chromatin re-establishment during DNA replication. The aim of this project was to better understand the roles of Uhrf1 and histone H3 ubiquitination in DNA methylation maintenance within the context of replication of chromatinized DNA. Uhrf1 is an essential protein in maintaining DNA methylation by facilitating the recruitment of Dnmt1. Although in the recent years we have gained a greater knowledge about the regulation of these proteins and how they could be coordinated with DNA replication, nucleosome assembly and remodeller functions, the sequential order of events and the order in which all the proteins involved act, remain unclear. In this thesis, I have confirmed the role of Uhrf1 in mediating the di-mono-ubiquitination of histone H3 and Paf15 and in recruiting Dnmt1 through ubiquitination. Importantly, I have also shown additional functions of this protein during DNA replication. Uhrf1 recruits Lig1 to replicating chromatin and its absence also impairs the binding of Fen1 and CAF1. Furthermore, novel interactions of Uhrf1 with RPA, the FACT complex and the helicase on replicating chromatin have been identified. All these findings strongly suggest that Uhrf1 plays a central and multifaceted role in chromatin-re-establishment, coordinating DNA methylation with DNA replication and nucleosome dynamics and remodelling.

Firstly, the data presented in this thesis confirmed that Uhrf1 mediates di-mono-ubiquitination of histone H3 at lysines K14/18/23/27 on chromatin during DNA replication. Both the removal of Uhrf1 and the use of a H3 K14/18/23/27R mutant inhibited H3 ubiquitination, confirming that H3 is ubiquitinated on these lysins by Uhrf1. Apart from histone H3, I have also confirmed that Uhrf1 ubiquitinates Paf15 and promotes its stable association to chromatin during DNA replication, since the depletion of Uhrf1 impaired Paf15 ubiquitination and recruitment to chromatin. Considering that Paf15 association with chromatin was also affected using E1i, and

these phenotypes were revealed by both the addition of Uhrf1 or the use of UbiNOK, I conclude that Uhrf1 promote Paf15 association with PCNA by ubiquitinating Paf15. This hypothesis is supported by the studies of Karg *et al*. 2017 and Nishiyama *et al.* 2020 showing that the use of a Paf15 double mutant or Uhrf1 depletion respectively impaired Paf15 recruitment. In summary, both findings support the proposed model of Uhrf1 modifying both H3 and Paf15 as alternative mechanisms to regulate replisome coupled or uncoupled DNA methylation maintenance (119).

Additionally, this thesis has revealed that both Uhrf1 and mono-ubiquitination are essential for Dnmt1 and CAF1 recruitment. Although I could not confirm that the mono-ubiquitination regulating the association of these proteins to chromatin is carried out by Uhrf1 due to the lack of its catalytic mutant, my experiments collectively showed that either the removal of Uhrf1 or the inhibition of ubiquitination impaired Dnmt1 and CAF1 recruitment. Since these proteins were recruited when adding either recombinant Uhrf1 or UbiNOK, I conclude that both Uhrf1 and ubiquitination mediate the binding of Dnmt1 and CAF1 to chromatin. Many previous studies have shown the important role of Uhrf1 in recruiting Dnmt1. Furthermore, Uhrf1-mediated H3, H2B and Paf15 ubiquitination has been proposed previously as a mechanism for bringing Dnmt1 to hemi-methylated DNA. However, the specific details of this mechanism are still ambiguous because of the complexity and high regulation of this process. My results strongly support the model of Dnmt1 recruitment through Uhrf1-mediated H3 and Paf15 ubiquitination. In contrast, the crucial role of Uhrf1 in regulating the association CAF1 to chromatin is a novel finding, not described in the literature yet. The decrease in the recruitment of the chaperones CAF1 and Spt16 after Uhrf1 immunodepletion, together with the reduced histone content on chromatin, indicate that Uhrf1 also plays a role in nucleosome assembly during DNA replication. Altogether, these findings suggest that Uhrf1 recruits Dnmt1 and

CAF1 through its E3 ubiquitin ligase activity, probably by mono-ubiquitinating H3 and Paf15, or even other substrates still to be identified.

Furthermore, I have shown evidence, which indicates that Uhrf1 also mediates the recruitment of Lig1 to chromatin. Uhrf1 removal impaired Lig1 recruitment, which was rescued by the addition of Uhrf1. Given that ubiquitination was not the mechanism to recruit Lig1 and that these proteins interacted on chromatin, my findings suggest that Uhrf1 interacts with Lig1 to promote its association to replicating chromatin. This is further supported by the fact that the addition of recombinant Uhrf1 to the extract was highly stimulating Lig1 recruitment, even when the inactive form of Uhrf1 was used. Considering that Ferry *et al*. 2017 demonstrated that a Lig1 mutant that cannot bind Uhrf1 impaired Uhrf1 association to chromatin, it is possible that there may be a co-dependency in the recruitment of both proteins. We can speculate that the Uhrf1-Lig1 interaction mainly occurs prior to their recruitment to chromatin to promote an open conformation and activation of Uhrf1. The fact that their interaction does not require DNA (134) and that Lig1 binding switches Uhrf1 conformation to an open state relieving auto-inhibition (155) support this hypothesis. However, the depletion of Lig1 from the extract did not impair Uhrf1 recruitment, suggesting that back-up pathways may exist to ensure that Uhrf1 is recruited to undertake its function. The interaction with Usp7 and phosphatidylinositol 5-phosphate (PI5P) as well as the binding to hemi-methylated DNA, H3 and Paf15 are other mechanism proposed to promote an open conformation or recruit Uhrf1 respectively, which may compensate for the lack of Lig1. Altogether, these findings suggest that the Uhrf1 interaction with Lig1 promotes Uhrf1 activation which leads to the recruitment of both proteins to chromatin.

Interestingly, my experiments showed that the disassembly of Lig1 may be regulated through ubiquitination. The depletion of Paf15 as well as the inhibition of ubiquitination prolonged Lig1

association to chromatin. In both cases, when ubiquitination bands appear in H3, Lig1 dissociated from chromatin, while Dnmt1 recruitment was stimulated. Considering that Uhrf1-mediated ubiquitination of both H3 or Paf15 act as parallel pathways to regulate Dnmt1 recruitment, these mechanisms could also promote Lig1 disassembly from chromatin. On the one hand, histone H3 ubiquitination could slightly alter DNA-nucleosome interaction or destabilize nucleosomes facilitating Lig1 access to DNA, to ligate it and dissociate faster (Figure 4. 1 A). This is supported by the fact that histone ubiquitination by Cul4A/DDB1 in response to DNA damage reduced their interaction with DNA promoting the recruitment of repair proteins (226). Although Fen1 and Lig1 can act on DNA assembled into nucleosomes, naked DNA would simplify the process since free DNA showed ten times faster kinetic of ligation than nucleosomal DNA (100,101). Interestingly, the same study suggested that Lig1 activity is affected by the disposition of the histone tails within the nucleosomes, because Lig1 exhibited increased activity on nucleosomes composed of histones with tails removed (100). Thus ubiquitination of the H3 tail could somehow regulate Lig1 access to DNA. On the other hand, since Lig1 accumulates on chromatin after Paf15 depletion and *vice versa*, both proteins could compete for PCNA binding (Figure 4. 1 B). Another explanation of this result could be that Paf15 needs Lig1 recruitment to PCNA to be completely disassembled, which could be regulated by Paf15 de-ubiquitination (Figure 4. 1 C). Interestingly, PCNA does not dissociate after Lig1 fulfils ligation of Okazaki fragments (36,37) and both PCNA and Paf15 are unloaded by ATAD5, which requires Paf15 de-ubiquitination by Usp7 (178) (Figure 4. 1 C). Therefore, Paf15 ubiquitination could regulate the termination of Okazaki fragment maturation.

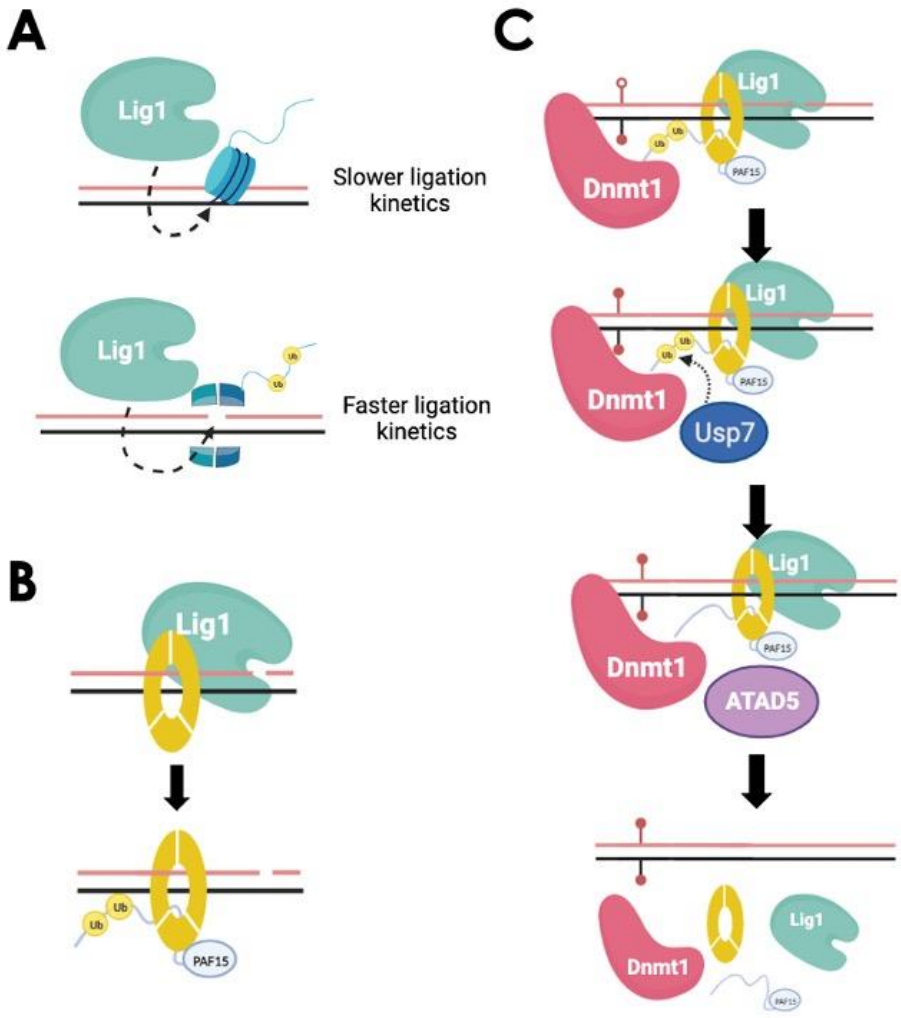


Figure 4. 1. Possible mechanisms of ubiquitination mediated Lig1 action and disassembly.

Taking all this knowledge together, I hypothesised that Uhrf1 mediates the di-mono-ubiquitination of H3 and Paf15, and probably other factors like H2B, which promote the disassembly of Lig1 and the recruitment of CAF1 and Dnmt1 (Figure 4. 2). Considering that PCNA mediates the sequential recruitment of Dnmt1, CAF1, Fen1 and Lig1 by interacting with all of them, it is expected that Uhrf1-mediated ubiquitination regulates the recruitment of some of them while promoting the unloading of others. Thus, Uhrf1 would act as a central protein regulating and coordinating the orderly and serial recruitment of all these proteins to ensure a synchronized completion of DNA replication, nucleosome assembly and the restoration of the epigenetics marks.

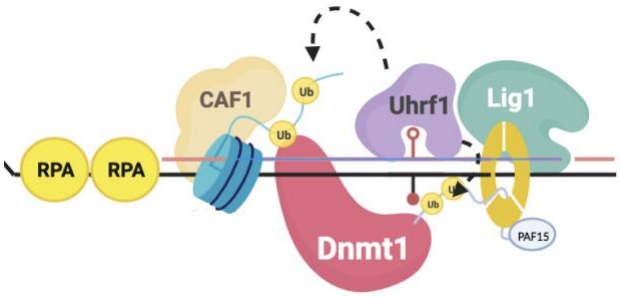


Figure 4. 2. Simplified model of Uhr1-mediated Dnmt1, CAF1 and Lig1 recruitments. Uhrf1 is recruited to replication sites together with Lig1 and mediates Paf15 and H3 di-mono-ubiquitination that allow the recruitment of CAF1 and Dnmt1. These ubiquitinations somehow stimulate Lig1 function and disassembly. This is a simplified model showing both pathways, Paf15 ubiquitination and H3 ubiquitination-mediated recruitments, in the same diagram. However, Dnmt1 recognizes both ubiquitinated substrates with its RFTS domain and both pathways have been proposed to mediate DNA methylation maintenance in early and late replication, respectively.

How Uhrf1 could coordinate DNA methylation, nucleosome assembly and remodelling?

In this thesis, I have shown evidence that strongly suggest a key role of Uhrf1 in nucleosome dynamics, additionally to the regulation of DNA methylation maintenance. Apart from recruiting CAF1, MS analysis showed that Uhrf1 interacts on chromatin with RPA, the FACT complex and the MCM helicase. Since these proteins are involved in the nucleosome disassembly ahead of the replication fork, parental histone transfer, new histone transport and/or their deposition behind the fork, these findings indicate that Uhrf1 may facilitate DNA replication-coupled nucleosome assembly (Figure 4. 3). This finding fits well with the regulation of Lig1 by Uhrf1 since nucleosome assembly is tightly coordinated with Okazaki fragment maturation. Indeed it has been proposed that nucleosomes determine the length of the Okazaki fragments by blocking the progression of Polδ and promoting Okazaki fragment maturation by Fen1 and Lig1 (102). Considering that CAF1 mutants generate longer Okazaki fragments by delaying nucleosome deposition (99), CAF1 should act prior to Lig1 depositing the histones to form the nucleosomes that would lead to Okazaki fragment maturation. Altogether, these findings would further couple DNA methylation maintenance with DNA replication, giving a novel link with Okazaki fragment maturation and nucleosome assembly.

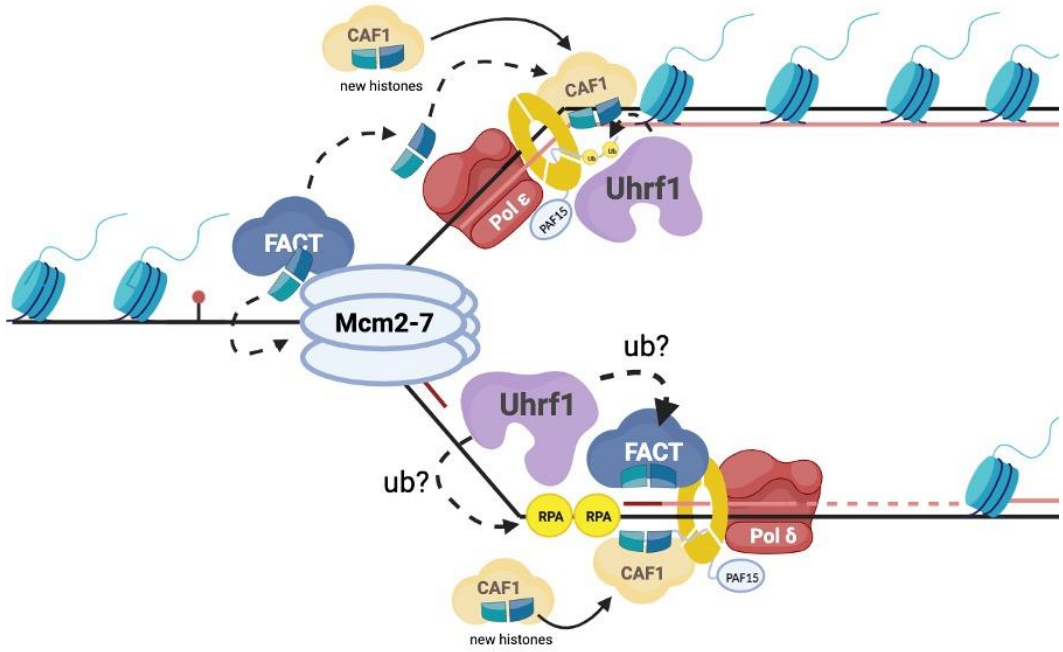


Figure 4. 3. Schema of the possible Uhrf1 role in nucleosome dynamic and assembly during DNA replication. Uhrf1 interacts on chromatin with RPA, the helicase (Mcm2-7) and Spt16 (FACT complex). Furthermore, the lack of Uhrf1 impair CAF1 and FACT recruitment, suggesting that Uhrf1 promote their recruitment. Uhrf1-mediated ubiquitination of H3, PAF15, or other possible factors may recruit CAF1 and coordinate histone deposition by CAF1 and FACT.

Given that DNA methylation maintenance co-exists with DNA replication, nucleosome assembly and remodelling, it is unsurprising that Uhrf1 also has the chance to regulate proteins involved in these processes. Other factors like the histone deacetylase HDAC or the histone methylase G9a have been shown to interact with Uhrf1/Dnmt1 on chromatin. Furthermore, it has been shown that Uhrf1 forms a repressive complex with HDAC1, DNMT1, G9A and SUV39H1 that mediates silencing of tumour suppressor genes (140,189). Supporting this, my MS data showed that HDAC1 and HDAC2 were reduced on replicating chromatin after Uhrf1 depletion (Appendix). This multifaceted role of Uhrf1 would be expected since Uhrf1 is an epigenetic coordinator able to read both hemi-methylated DNA and histones marks promoting epigenetic crosstalk. Indeed, DNA methylation correlates with histone deacetylation and other repressive marks such as H3K9me3 and H3K27me3 (65,136), which again suggest a cooperation between DNA methylation and histone remodeller machineries.

PCNA is a key factor regulating and coordinating many proteins related to DNA replication, Okazaki fragment maturation, nucleosome assembly and remodelling and DNA repair. Since Uhrf1 can ubiquitinate Paf15, it is a window of opportunity to regulate and coordinate all these processes. In addition to this, histone modifications have been shown to regulate the transfer between chaperones and the recruitment of histone remodellers. For example, acetylation of newly synthesised H3 at K56 by Rtt109 promotes H3-H4 binding to CAF1 and nucleosome assembly (92). Therefore, Uhrf1-mediated histone H3 ubiquitination could also regulate at some point the coordinated deposition of new and parental H3-H4 tetramers and H2A-H2B dimers from CAF1 and FACT to chromatin. Supporting this, it has been shown that H2B ubiquitination reduces the binding affinity of FACT to H2A-H2B dimers and enhances their deposition onto DNA during transcription (227). Apart from this, the finding that H3 can be ubiquitinated at H3K14, H3K18, H3K23 and H3K27 is interesting since some of these sites have been shown to be acetylated or methylated during DNA replication. In yeast, H3K9 and H3K27 are acetylated, while H3K14 and H3K18 are acetylated in some mammals (226). On the other hand, H3K27 is a well characterised site that is tri-methylated acting as a repressive mark (65). Therefore, there may be a competition between these histone modifications that regulate different steps during nucleosome assembly and remodelling. Additionally, H3 ubiquitination could promote the modification of other residues within H3. For example, while the acetylation of H3K14 and H3K18 has been proposed to prevent H3K9me1 (68), the ubiquitination of H3K14 has been shown to promote H3K9 methylation for heterochromatin formation (210). Therefore, H3 ubiquitination could also be involved in the epigenetic crosstalk that mediates the restoration of histone PTMs. Related to this, it is remarkable that CAF1 has been shown to bind the methylases involved in the methylation of H3K9 and H3K27 (68,117), such as G9A, SETDB1, HP1, to facilitate heterochromatin formation, linking this chaperone to both H3 marks. Altogether, these findings suggest that Uhrf1-mediated H3 ubiquitination could

also promote histones deposition from the chaperones and lead to the subsequent restoration of epigenetic marks.

In conclusion, the results obtained in this thesis and the current published knowledge make me speculate about how Uhrf1 could coordinate all these processes during DNA replication (Figure 4. 4). Uhrf1 could regulate the assembly of nucleosomes by coordinating parental and new histone deposition through FACT/helicase and CAF1 respectively. The top interactor of Uhrf1, RPA would be binding the ssDNA formed and would act as a platform for the deposition of histones by the chaperones, since it interacts with both CAF1 and FACT. PCNA/Paf15 would also mediate histone deposition since this process requires also CAF1 interaction with PCNA. Uhrf1 could regulate this histone transfer and deposition by ubiquitinating H3, H2B, Paf15 or other still unknown substrates. These Uhrf1-dependent ubiquitinations could also recruit Dnmt1. Dnmt1 binds di-mono-ubiquitinated H3 and Paf15 which allow DNA methylation maintenance. Nucleosomes assembled after the replication fork would act as a barrier for Polδ, promoting its unloading from PCNA and the actions of Fen1 and Lig1. Once DNA is fully methylated by Dnmt1 and ligated by Lig1, the ubiquitination signal is removed by Usp7, which promotes PCNA/Paf15/Lig1 unloading (Figure 4. 1 C). It has been proposed that Usp7 de-ubiquitinates Paf15 and unmodified Paf15 is unloaded by ATAD5. This disassembly would occur after Okazaki fragment maturation and DNA methylation, since depletion of Lig1 or Dnmt1 accumulates ubiquitinated Paf15 on chromatin.

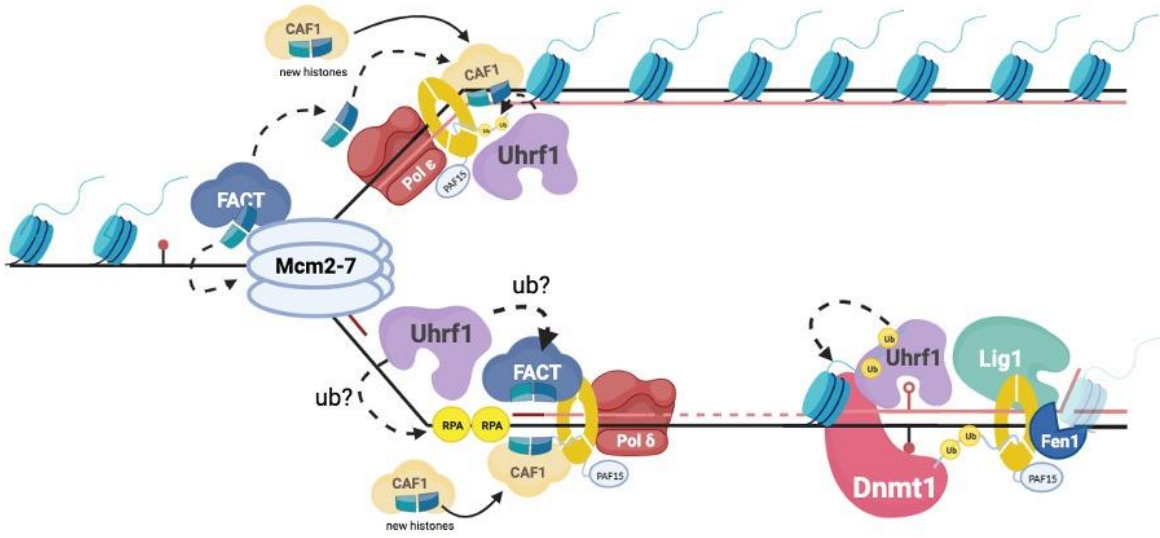


Figure 4. 4. Final model of Uhrf1-mediated chromatin re-establishment during DNA replication.

This proposed model is only one possible solution for the puzzle formed by all the pieces of knowledge currently available. However, many other models based on these and future findings could explain Uhrf1's role in chromatin re-establishment. Moreover, this model and findings would explain only the replication-coupled DNA methylation maintenance focused on the lagging strand, leaving many unresolved questions in the process of chromatin re-establishment in later stages of DNA replication and on the leading strand. On the other hand, these different roles of Uhrf1 identified in this study could be regulating DNA methylation maintenance in different scenarios: in early and late replicated regions, on leading and lagging strands and/or naked and chromatinised DNA. All of them could differentially act or coexist in different genomic regions, euchromatin vs. heterochromatin. Finally, chromatin re-establishment could vary highly between cell-types, which would be supported by the differences found between studies carried out in different systems. Therefore, placing all these findings in space and time and further studying them in different genomic regions and systems would clarify how DNA replication is coordinated with the maintenance of DNA and histone epigenetic marks in the different cases and how Uhrf1 and histone H3 ubiquitination contribute to this.

Conclusion

DNA methylation maintenance is a highly regulated process involving many factors and PTMs, since it must be coordinated with the processes occurring simultaneously during DNA replication. This thesis has revealed that Uhrf1 has a key role in chromatin re-establishment, synchronizing the maintenance of DNA methylation with Okazaki fragment maturation and nucleosome assembly. Apart from recruiting Dnmt1 to hemi-methylated sites, Uhrf1 also regulates the assembly of histone chaperones CAF1 and the FACT complex. This action facilitates the deposition of histones, which is crucial for chromatin formation. Additionally, this study showed that Uhrf1 is essential for the recruitment of Fen1 and Lig1, key proteins in the maturation of the Okazaki fragments, highlighting the multifaceted function of Uhrf1. Placing these findings in a spatiotemporal context is a challenging task, which is required to clarify the intricate process of chromatin re-establishment during DNA replication.

Relevance of this research

The findings of Uhrf1's roles during DNA replication in DNA methylation maintenance and chromatin re-establishment have biological and medical implications. Given Uhrf1 overexpression in many cancers, coupled with the fact that alterations in DNA methylation and histone modification patterns as well as the DSBs created by un-ligated Okazaki fragments are hallmarks of cancer, these new findings are valuable for cancer research. Understanding how Uhrf1 coordinates DNA methylation and chromatin re-establishment in normal and altered conditions could reveal new targets for cancer therapy. Additionally, due to the importance of both epigenetics marks during development and aging, increasing our knowledge of Uhrf1’s function during chromatin replication is important for understanding epigenetic de-regulation in developmental and inherited diseases as well as aging and age-related diseases, opening the way for new treatments. Overall, these findings are important for increasing our knowledge of fundamental cellular processes, which could lead to potential therapeutic applications.

Questions to address and future work

This study has uncovered novel insights into the process of chromatin re-establishment during DNA replication, raising many questions about the different steps involved in this complex process:

1. How does Uhrf1 coordinate DNA methylation with DNA replication and nucleosome assembly? Although these findings give valuable information linking Uhrf1 with all the main processes co-existing with the maintenance of DNA methylation, how Uhrf1 sequentially regulates these processes remains unclear.

2. How does Uhrf1 differentially regulate chromatin re-establishment in the different strands (leading *vs.* lagging strand), chromatin regions (naked or early replicated regions *vs.* chromatinized or post-replication regions) and in the different parts of the genome (euchromatin *vs.* heterochromatin)?

3. Could Uhrf1 act as a dimer promoting its multifaceted role?

4. How does the binding to RPA, FACT complex, helicase or Lig1 regulate Uhrf1 conformation and activity?

5. Are there other factors modified by Uhrf1 apart from histone H3, H2B and Paf15 during DNA replication?

In the future, the use of the Uhrf1 catalytic mutant will firstly confirm that Uhrf1 is the E3 ligase mediating the ubiquitination that recruits Dnmt1 and CAF1. This will also elucidate other potential substrates of Uhrf1, like RPA or the FACT complex. In addition, the use of other mutants of Uhrf1, modifying key residues within the domains of the protein, will give a better understanding of the importance of each domain in Uhrf1 activation, its interaction with these

different proteins and its various roles during DNA replication. Apart from this, setting up an experiment to check the generation of un-ligated Okazaki fragments will confirm the effect of Uhrf1 depletion in Okazaki fragment maturation. Finally, using mutants of the proteins regulated by Uhrf1 will help to clarify the sequence in which these processes occur during DNA replication. On the one hand, a Lig1 mutant that cannot bind Uhrf1 will help to understand the co-dependency between these proteins' recruitment to chromatin. On the other hand, the catalytic mutant will show the importance of completion of OFM for the termination of Paf15/H3 ubiquitination signalling and the disassembly of PCNA, Paf15, Lig1 as well as Dnmt1, CAF1 and Uhrf1, ending the DNA methylation and nucleosome assembly processes. Finally, the use of a Paf15 mutant that cannot be ubiquitinated will contribute to discern which phenotypes are regulated through Uhrf1-mediated Paf15 ubiquitination, since Paf15 depletion leads to the activation of back-up pathways, such as H3 ubiquitination, to ensure the completion of the process. These experiments will give valuable information to construct a more reliable model of chromatin re-establishment.

In addition, the measurement of the DNA methylation levels in the different conditions, especially when using histone H3 mutant or depleting Paf15, will clarify the importance of these mechanism for the maintenance of this epigenetic mark, since Dnmt1 could be recruited in these cases but not active.

Importantly, considering that *Xenopus laevis* egg extract is a great system for biochemical manipulations in an almost "in vivo" setting and that the system is already optimized, its exploitation is crucial to address some of these questions that could not be answered by other mechanisms. Therefore, the combination of the different drugs/depletions in the extract could help to clarify the order in which these different events that are occurring take place. For instance, an experiment combining Paf15 depletion with the addition of histone H3 mutant

could be done to confirm whether Dnmt1 recruitment rely only in these mechanisms or there are other alternative ways of recruitment. Another possible experiment could be treating the extract with E1 inhibitor together with either or both Fen1 and Lig1 inhibitors. This experiment could help to understand if the ubiquitinationof histone H3 and Paf15 are important for Dnmt1 and CAF1 recruitment before or after OFM.

Lastly, it would be significant to investigate whether these findings are conserved in human cells. Taking advantage of the auxin induced degron (AID) system to rapidly degrade Uhrf1 within cells will allow to observe the importance of various roles of Uhrf1 immediately after degradation and in different stages of the cell cycle. Investigating the function of Uhrf1 within S phase using the AID system will allow to study chromatin re-establishment process more easily in the different strands (leading *vs.* lagging strand), chromatin regions (naked or early replicated regions *vs.* chromatinised or post-replication regions) and in the different parts of the genome (euchromatin *vs.* heterochromatin). To be able to do this, the combination of next generation sequencing and IP experiments will be required, such as Repli-seq, OK seq, micrococcal nuclease (MNase) strand-specific sequencing (MNase-ssSeq), ChIP-ssSeq and eSPAN (enrichment and sequencing of protein associated nascent strand DNA). For example, MNase-ssSeq or OK seq could be used in chromatin replicated in the presence or absence of Uhrf1 to see defect in nucleosome assembly and OFM respectively. Additionally, to investigate whether histone H3 and Paf15 ubiquitination could differentially regulate the recruitment of Dnmt1 to the leading and lagging strand respectively, strand-specific sequencing of DNA replicated in cells lacking Paf15 and isolated from a chromatin IP (ChIP) of Dnmt1(eSPAN) could answer this question. In addition, the use of this system, which replicates the post-translational modifications that occur in human proteins, will help to understand better Uhrf1 conformation regulation and functions. Finally, research in AID cells will provide a more relevant model for human biology and diseases compared to *Xenopus*.

5. LIST OF ABBREVIATIONS

ANIB – Acetate nuclear isolation buffer

ATAD5 – ATPase Family AAA Domain Containing 5

ATP – Adenosine triphosphate

ATR – Ataxia-Telangiectasia and Rad3 protein

bp – base pair

BRCA1 – Breast and ovarian cancer susceptibility protein 1

BSA – Bovine Serum Albumins

CAF1 – Chromatin assembly factor 1Cdc6 – Cell division cycle protein 6

Cdc – Cell division cycle protein

CDK – Cyclin dependent kinase

Cdt1 – Chromatin licensing and DNA replication factor 1

Chromass – Chromatin mass spectrometry

CMG – Cdc45/Mcm2-7/GINS complex

Ctf4 – Chromosome transmission fidelity 4

DDK – Dbf4 dependent kinase

DDR – DNA damage response

DMF – Dimethylformamide

DNA – Deoxyribonucleic acid

DNMT – DNA (cytosine 5) methyl transferase

dNTP - Deoxyribonucleotide

DSB – Double strand break

dsDNA – Double stranded DNA

DUB – Deubiquitylating enzyme

E1i – E1 inhibitor

ER – Energy regenerator

FACT – Facilitates chromatin transcription complex

Faf1 – FAS associated factor 1

FANC – Fanconi anemia complementation group protein

FEN1 – Flap endonuclease 1

GINS – Go, Ichi, Nii, and San

H – Histone

IgG – Immunoglobulin G

IP – Immunoprecipitation

IPTG – Isopropyl-β-D-1-thiogalactopyranoside

K – Lysine

LB – Luria broth

LIG1- DNA ligase 1

LIG3- DNA ligase 3

LRR1 – Leucine rich repeat protein 1

MCM – Mcm2-7 complex

MS – Mass spectrometry

MTBP – MDM2 binding protein

OD – Optical density

OFM – Okazaki fragment maturation

ORC – Origin recognition complex

PAGE – Polyacrylamide gel electrophoresis

PARP – Poly ADP ribose polymerase

PBS – Phosphate buffered saline

PCNA – Proliferating cell nuclear antigen

PIP box – PCNA interacting protein box

PMSF – Phenylmethylsulfonyl fluoride

Pol – Polymerase

Pre-RC – Pre-replication complex

PTM – Post translational modification

PVDF – Polyvinylidene

RFC – Replication factor C

RING – Really interesting new gene

RNA – Ribonucleic acid

RPA – Replication protein A

SDS – Dodecyl sulfate sodium

SEM – Standard error of the mean

SMARCA – SWI/SNF-related matrix-associated actin-dependent regulator of chromatin subfamily A

Smc – Structural Maintenance of Chromosomes Protein

SOC – Super optimal broth with catabolite repression

SPRTN – SprT-Like N-Terminal Domain

SPT16 – Suppressor of Ty 16 protein

SRA – SET and Ring finger associated domain

SSB – Single strand break

ssDNA – Single stranded DNA

SSRP1 – Structure-Specific Recognition Protein 1

SUMO – Small ubiquitin like modifier

TCA – Trichloroacetic acid

TopBP1 – DNA topoisomerase 2 binding protein 1

TRAIP – TRAF interacting protein

UBE2M – Ubiquitin Conjugating Enzyme E2 M

Ubi – Ubiquitin

UbiNOK – Ubiquitin no lysine

UBL – Ubiquitin-like domain

UBX – Ubiquitin regulatory X domain

Uhrf1 – Ubiquitin like with PHD and RING finger domain containing protein 1

UIM – Ubiquitin interacting motifs

USP7 – Ubiquitin specific protease 7

UV – Ultra violet

wt – wild type

6. REFERENCES

1. WATSON JD, CRICK FHC. Molecular Structure of Nucleic Acids: A Structure for Deoxyribose Nucleic Acid. Nature. 1953;171(4356):737–8.

2. Meselson M, Stahl FW. The Replication of DNA in Escherichia coli. Proc Natl Acad Sci U S A. 1958;44(7):671–82.

3. Machida YJ, Hamlin JL, Dutta A. Right place, right time, and only once: replication initiation in metazoans. Cell. 2005 Oct 7;123(1):13–24.

4. Vijg J, Suh Y. Genome Instability and Aging. Annu Rev Physiol. 2013 Feb 10;75(1):645–68.

5. Gaillard H, García-Muse T, Aguilera A. Replication stress and cancer. Nat Rev Cancer. 2015 May 1;15(5):276–89.

6. Cortez D. Replication-Coupled DNA Repair. Mol Cell. 2019 Jun;74(5):866–76.

7. Ekundayo B, Bleichert F. Origins of DNA replication. PLOS Genet. 2019 Sep 12;15(9):e1008320.

8. Leonard AC, Mechali M. DNA Replication Origins. Cold Spring Harb Perspect Biol. 2013 Oct 1;5(10):a010116–a010116.

9. Petryk N, Kahli M, d'Aubenton-Carafa Y, Jaszczyszyn Y, Shen Y, Silvain M, et al. Replication landscape of the human genome. Nat Commun. 2016 Jan 11;7(1):10208.

10. Blow JJ, Dutta A. Preventing re-replication of chromosomal DNA. Nat Rev Mol Cell Biol. 2005 Jun;6(6):476–86.

11. Moreno SP, Gambus A. Mechanisms of eukaryotic replisome disassembly. Biochem Soc Trans. 2020 Jun 30;48(3):823–36.

12. Parker MW, Botchan MR, Berger JM. Mechanisms and regulation of DNA replication initiation in eukaryotes. Crit Rev Biochem Mol Biol. 2017 Mar 4;52(2):107–44.

13. Kang S, Kang MS, Ryu E, Myung K. Eukaryotic DNA replication: Orchestrated action of multi-subunit protein complexes. Mutat Res Mol Mech Mutagen. 2018 May;809:58–69.

14. Moreno S, Gambus A. Regulation of Unperturbed DNA Replication by Ubiquitylation. Genes. 2015 Jun 25;6(3):451–68.

15. Tanaka S, Umemori T, Hirai K, Muramatsu S, Kamimura Y, Araki H. CDK-dependent phosphorylation of Sld2 and Sld3 initiates DNA replication in budding yeast. Nature. 2007 Jan 18;445(7125):328–32.

16. Kingsley G, Skagia A, Passaretti P, Fernandez-Cuesta C, Reynolds-Winczura A, Koscielniak K, et al. DONSON facilitates Cdc45 and GINS chromatin association and is essential for DNA replication initiation. Nucleic Acids Res. 2023 Aug 28;gkad694.

17. Lim Y, Tamayo-Orrego L, Schmid E, Tarnauskaite Z, Kochenova OV, Gruar R, et al. In silico protein interaction screening uncovers DONSON's role in replication initiation. Science. 2023 Aug 17;eadi3448.

18. Evrin C, Alvarez V, Ainsworth J, Fujisawa R, Alabert C, Labib KP. DONSON is required for CMG helicase assembly in the mammalian cell cycle. EMBO Rep. 2023;

19. Xia Y, Sonneville R, Jenkyn-Bedford M, Ji L, Alabert C, Hong Y, et al. DNSN-1 recruits GINS for CMG helicase assembly during DNA replication initiation in *Caenorhabditis elegans*. Science. 2023 Sep 22;381(6664):eadi4932.

20. Lõoke M, Maloney MF, Bell SP. Mcm10 regulates DNA replication elongation by stimulating the CMG replicative helicase. Genes Dev. 2017 Feb 1;31(3):291–305.

21. Burgers PMJ, Kunkel TA. Eukaryotic DNA Replication Fork. Annu Rev Biochem. 2017 Jun 20;86(1):417–38.

22. Wold MS. REPLICATION PROTEIN A: A Heterotrimeric, Single-Stranded DNA-Binding Protein Required for Eukaryotic DNA Metabolism. Annu Rev Biochem. 1997 Jun 1;66(1):61–92.

23. Gambus A, Jones RC, Sanchez-Diaz A, Kanemaki M, Van Deursen F, Edmondson RD, et al. GINS maintains association of Cdc45 with MCM in replisome progression complexes at eukaryotic DNA replication forks. Nat Cell Biol. 2006 Apr 1;8(4):358–66.

24. Gambus A, van Deursen F, Polychronopoulos D, Foltman M, Jones RC, Edmondson RD, et al. A key role for Ctf4 in coupling the MCM2-7 helicase to DNA polymerase α within the eukaryotic replisome. EMBO J. 2009 Oct 7;28(19):2992–3004.

25. Stodola JL, Burgers PM. Mechanism of Lagging-Strand DNA Replication in Eukaryotes. In: Masai H, Foiani M, editors. DNA Replication [Internet]. Singapore: Springer Singapore; 2017 [cited 2023 Sep 18]. p. 117–33. (Advances in Experimental Medicine and Biology; vol. 1042). Available from: http://link.springer.com/10.1007/978-981-10-6955-0_6

26. Georgescu RE, Schauer GD, Yao NY, Langston LD, Yurieva O, Zhang D, et al. Reconstitution of a eukaryotic replisome reveals suppression mechanisms that define leading/lagging strand operation. eLife. 2015 Apr 14;4:e04988.

27. Yeeles JTP, Janska A, Early A, Diffley JFX. How the Eukaryotic Replisome Achieves Rapid and Efficient DNA Replication. Mol Cell. 2017 Jan 5;65(1):105–16.

28. Miyabe I, Kunkel TA, Carr AM. The Major Roles of DNA Polymerases Epsilon and Delta at the Eukaryotic Replication Fork Are Evolutionarily Conserved. PLOS Genet. 2011 Dec 1;7(12):e1002407.

29. Boehm EM, Gildenberg MS, Washington MT. Chapter Seven - The Many Roles of PCNA in Eukaryotic DNA Replication. In: Kaguni LS, Oliveira MT, editors. The Enzymes [Internet]. Academic Press; 2016. p. 231–54. Available from: https://www.sciencedirect.com/science/article/pii/S1874604716300051

30. Sengupta S, van Deursen F, de Piccoli G, Labib K. Dpb2 Integrates the Leading-Strand DNA Polymerase into the Eukaryotic Replisome. Curr Biol. 2013 Apr 8;23(7):543–52.

31. Zheng L, Shen B. Okazaki fragment maturation: nucleases take centre stage. J Mol Cell Biol. 2011 Feb 1;3(1):23–30.

32. Balakrishnan L, Bambara RA. Eukaryotic Lagging Strand DNA Replication Employs a Multi-pathway Mechanism That Protects Genome Integrity. J Biol Chem. 2011 Mar;286(9):6865–70.

33. Sun H, Ma L, Tsai YF, Abeywardana T, Shen B, Zheng L. Okazaki fragment maturation: DNA flap dynamics for cell proliferation and survival. Trends Cell Biol. 2023 Mar;33(3):221–34.

34. Balakrishnan L, Bambara RA. Okazaki Fragment Metabolism. Cold Spring Harb Perspect Biol. 2013 Feb 1;5(2):a010173–a010173.

35. Ryu E, Ha NY, Jung W, Yoo J, Myung K, Kang S. Distinct Motifs in ATAD5 C-Terminal Domain Modulate PCNA Unloading Process. Cells. 2022 Jun 3;11(11):1832.

36. Kubota T, Katou Y, Nakato R, Shirahige K, Donaldson AD. Replication-Coupled PCNA Unloading by the Elg1 Complex Occurs Genome-wide and Requires Okazaki Fragment Ligation. Cell Rep. 2015 Aug;12(5):774–87.

37. Kumamoto S, Nishiyama A, Chiba Y, Miyashita R, Konishi C, Azuma Y, et al. HPF1-dependent PARP activation promotes LIG3-XRCC1-mediated backup pathway of Okazaki fragment ligation. 2021;

38. Guo Z, Kanjanapangka J, Liu N, Liu S, Liu C, Wu Z, et al. Sequential Posttranslational Modifications Program FEN1 Degradation during Cell-Cycle Progression. Mol Cell. 2012 Aug 10;47(3):444–56.

39. González-Magaña A, Blanco FJ. Human PCNA Structure, Function and Interactions. Biomolecules. 2020 Apr 8;10(4):570.

40. Thakar T, Leung W, Nicolae CM, Clements KE, Shen B, Bielinsky AK, et al. Ubiquitinated-PCNA protects replication forks from DNA2-mediated degradation by regulating Okazaki fragment maturation and chromatin assembly. Nat Commun. 2020 May 1;11(1):2147.

41. Pommier Y, Sun Y, Huang S yin N, Nitiss JL. Roles of eukaryotic topoisomerases in transcription, replication and genomic stability. Nat Rev Mol Cell Biol. 2016 Nov;17(11):703–21.

42. Dewar JM, Walter JC. Mechanisms of DNA replication termination. Nat Rev Mol Cell Biol. 2017 Aug;18(8):507–16.

43. Priego Moreno S, Bailey R, Campion N, Herron S, Gambus A. Polyubiquitylation drives replisome disassembly at the termination of DNA replication. Science. 2014 Oct 24;346(6208):477–81.

44. Maric M, Maculins T, De Piccoli G, Labib K. Cdc48 and a ubiquitin ligase drive disassembly of the CMG helicase at the end of DNA replication. Science. 2014 Oct 24;346(6208):1253596.

45. Sonneville R, Moreno SP, Knebel A, Johnson C, Hastie CJ, Gartner A, et al. CUL-2LRR-1 and UBXN-3 drive replisome disassembly during DNA replication termination and mitosis. Nat Cell Biol. 2017 May;19(5):468–79.

46. Villa F, Fujisawa R, Ainsworth J, Nishimura K, Lie-A-Ling M, Lacaud G, et al. CUL2LRR1, TRAIP and p97 control CMG helicase disassembly in the mammalian cell cycle. EMBO Rep. 2021 Mar 3;22(3):e52164.

47. Tarcan Z, Poovathumkadavil D, Skagia A, Gambus A. The p97 segregase cofactor Ubxn7 facilitates replisome disassembly during S-phase. J Biol Chem. 2022 Aug;298(8):102234.

48. Fujisawa R, Polo Rivera C, Labib KPM. Multiple UBX proteins reduce the ubiquitin threshold of the mammalian p97-UFD1-NPL4 unfoldase. eLife. 2022 Aug 3;11.

49. Kochenova OV, Mukkavalli S, Raman M, Walter JC. Cooperative assembly of p97 complexes involved in replication termination. Nat Commun. 2022 Nov 3;13(1):6591.

50. Fan Y, Köberlin MS, Ratnayeke N, Liu C, Deshpande M, Gerhardt J, et al. LRR1-mediated replisome disassembly promotes DNA replication by recycling replisome components. J Cell Biol. 2021 Aug 2;220(8):e202009147.

51. Rebecca M. Jones, Joaquin Herrero Ruiz, Shaun Scaramuzza, Sarmi Nath, Marta Henklewska, Toyoaki Natsume, et al. Characterising replisome disassembly in human cells. bioRxiv. 2022 Jan 1;2022.07.12.499744.

52. Deng L, Wu RA, Sonneville R, Kochenova OV, Labib K, Pellman D, et al. Mitotic CDK Promotes Replisome Disassembly, Fork Breakage, and Complex DNA Rearrangements. Mol Cell. 2019 Mar 7;73(5):915-929.e6.

53. Jenkyn-Bedford M, Jones ML, Baris Y, Labib KPM, Cannone G, Yeeles JTP, et al. A conserved mechanism for regulating replisome disassembly in eukaryotes. Nature. 2021 Dec 1;600(7890):743–7.

54. Bailey R, Priego Moreno S, Gambus A. Termination of DNA replication forks: “Breaking up is hard to do”. Nucleus. 2015 May 4;6(3):187–96.

55. van Emmerik CL, van Ingen H. Unspinning chromatin: Revealing the dynamic nucleosome landscape by NMR. Prog Nucl Magn Reson Spectrosc. 2019 Feb;110:1–19.

56. Bannister AJ, Kouzarides T. Regulation of chromatin by histone modifications. Cell Res. 2011 Mar;21(3):381–95.

57. Tessarz P, Kouzarides T. Histone core modifications regulating nucleosome structure and dynamics. Nat Rev Mol Cell Biol. 2014 Nov 1;15(11):703–8.

58. Nishiyama A, Yamaguchi L, Sharif J, Johmura Y, Kawamura T, Nakanishi K, et al. Uhrf1-dependent H3K23 ubiquitylation couples maintenance DNA methylation and replication. Nature. 2013 Oct;502(7470):249–53.

59. Harrison JS, Cornett EM, Goldfarb D, DaRosa PA, Li ZM, Yan F, et al. Hemi-methylated DNA regulates DNA methylation inheritance through allosteric activation of H3 ubiquitylation by UHRF1. Workman JL, editor. eLife. 2016 Sep 6;5:e17101.

60. Qin W, Wolf P, Liu N, Link S, Smets M, Mastra FL, et al. DNA methylation requires a DNMT1 ubiquitin interacting motif (UIM) and histone ubiquitination. Cell Res. 2015 Aug;25(8):911–29.

61. Mattiroli F, Penengo L. Histone Ubiquitination: An Integrative Signaling Platform in Genome Stability. Trends Genet. 2021 Jun;37(6):566–81.

62. Kliza K, Husnjak K. Resolving the Complexity of Ubiquitin Networks. Front Mol Biosci [Internet]. 2020;7. Available from: https://www.frontiersin.org/articles/10.3389/fmolb.2020.00021

63. Quina AS, Buschbeck M, Di Croce L. Chromatin structure and epigenetics. Biochem Pharmacol. 2006 Nov;72(11):1563–9.

64. Tost J. DNA methylation: an introduction to the biology and the disease-associated changes of a promising biomarker. Methods Mol Biol Clifton NJ. 2009;507:3–20.

65. Flavahan WA, Gaskell E, Bernstein BE. Epigenetic plasticity and the hallmarks of cancer. Science. 2017 Jul 21;357(6348):eaal2380.

66. Tiffon C. The Impact of Nutrition and Environmental Epigenetics on Human Health and Disease. Int J Mol Sci. 2018 Nov 1;19(11):3425.

67. Alabert C, Jasencakova Z, Groth A. Chromatin Replication and Histone Dynamics. In: Masai H, Foiani M, editors. DNA Replication [Internet]. Singapore: Springer Singapore; 2017 [cited 2023 Sep 29]. p. 311–33. (Advances in Experimental Medicine and Biology; vol. 1042). Available from: http://link.springer.com/10.1007/978-981-10-6955-0_15

68. Alabert C, Groth A. Chromatin replication and epigenome maintenance. Nat Rev Mol Cell Biol. 2012 Mar;13(3):153–67.

69. Zhang W, Feng J, Li Q. The replisome guides nucleosome assembly during DNA replication. Cell Biosci. 2020 Dec;10(1):37.

70. Xu M, Long C, Chen X, Huang C, Chen S, Zhu B. Partitioning of Histone H3-H4 Tetramers During DNA Replication–Dependent Chromatin Assembly. Science. 2010 Apr 2;328(5974):94–8.

71. Stewart-Morgan KR, Petryk N, Groth A. Chromatin replication and epigenetic cell memory. Nat Cell Biol. 2020 Apr;22(4):361–71.

72. Flury V, Reverón-Gómez N, Alcaraz N, Stewart-Morgan KR, Wenger A, Klose RJ, et al. Recycling of modified H2A-H2B provides short-term memory of chromatin states. Cell. 2023 Mar 2;186(5):1050-1065.e19.

73. Gruszka DT, Xie S, Kimura H, Yardimci H. Single-molecule imaging reveals control of parental histone recycling by free histones during DNA replication. Sci Adv. 2020 Sep;6(38).

74. Radman-Livaja M, Verzijlbergen KF, Weiner A, van Welsem T, Friedman N, Rando OJ, et al. Patterns and mechanisms of ancestral histone protein inheritance in budding yeast. PLoS Biol. 2011 Jun;9(6):e1001075.

75. Wen Q, Zhou J, Tian C, Li X, Song G, Gao Y, et al. Symmetric inheritance of parental histones contributes to safeguarding the fate of mouse embryonic stem cells during differentiation. Nat Genet. 2023 Sep;55(9):1555–66.

76. Gan H, Serra-Cardona A, Hua X, Zhou H, Labib K, Yu C, et al. The Mcm2-Ctf4-Polα Axis Facilitates Parental Histone H3-H4 Transfer to Lagging Strands. Mol Cell. 2018 Oct;72(1):140-151.e3.

77. Petryk N, Dalby M, Wenger A, Stromme CB, Strandsby A, Andersson R, et al. MCM2 promotes symmetric inheritance of modified histones during DNA replication. Science. 2018 Sep 28;361(6409):1389–92.

78. Groth A, Corpet A, Cook AJL, Roche D, Bartek J, Lukas J, et al. Regulation of Replication Fork Progression Through Histone Supply and Demand. Science. 2007 Dec 21;318(5858):1928–31.

79. Foltman M, Evrin C, De Piccoli G, Jones RC, Edmondson RD, Katou Y, et al. Eukaryotic Replisome Components Cooperate to Process Histones During Chromosome Replication. Cell Rep. 2013 Mar;3(3):892–904.

80. Kurat CF, Yeeles JTP, Patel H, Early A, Diffley JFX. Chromatin Controls DNA Replication Origin Selection, Lagging-Strand Synthesis, and Replication Fork Rates. Mol Cell. 2017 Jan;65(1):117–30.

81. Liu Y, Zhou K, Zhang N, Wei H, Tan YZ, Zhang Z, et al. FACT caught in the act of manipulating the nucleosome. Nature. 2020 Jan;577(7790):426–31.

82. Liu S, Xu Z, Leng H, Zheng P, Yang J, Chen K, et al. RPA binds histone H3-H4 and functions in DNA replication–coupled nucleosome assembly. Science. 2017 Jan 27;355(6323):415–20.

83. Evrin C, Maman JD, Diamante A, Pellegrini L, Labib K. Histone H2A-H2B binding by Pol α in the eukaryotic replisome contributes to the maintenance of repressive chromatin. EMBO J. 2018 Oct 1;37(19).

84. Donham DC 2nd, Scorgie JK, Churchill MEA. The activity of the histone chaperone yeast Asf1 in the assembly and disassembly of histone H3/H4-DNA complexes. Nucleic Acids Res. 2011 Jul;39(13):5449–58.

85. Franco AA, Lam WM, Burgers PM, Kaufman PD. Histone deposition protein Asf1 maintains DNA replisome integrity and interacts with replication factor C. Genes Dev. 2005 Jun 1;19(11):1365–75.

86. Yu C, Gan H, Serra-Cardona A, Zhang L, Gan S, Sharma S, et al. A mechanism for preventing asymmetric histone segregation onto replicating DNA strands. Science. 2018 Sep 28;361(6409):1386–9.

87. Bellelli R, Belan O, Pye VE, Clement C, Maslen SL, Skehel JM, et al. POLE3-POLE4 Is a Histone H3-H4 Chaperone that Maintains Chromatin Integrity during DNA Replication. Mol Cell. 2018 Oct;72(1):112-126.e5.

88. Kimura H, Cook PR. Kinetics of core histones in living human cells: little exchange of H3 and H4 and some rapid exchange of H2B. J Cell Biol. 2001 Jun 25;153(7):1341–53.

89. Hammond CM, Strømme CB, Huang H, Patel DJ, Groth A. Histone chaperone networks shaping chromatin function. Nat Rev Mol Cell Biol. 2017 Mar;18(3):141–58.

90. Young TJ, Cui Y, Pfeffer C, Hobbs E, Liu W, Irudayaraj J, et al. CAF-1 and Rtt101p function within the replication-coupled chromatin assembly network to promote H4 K16ac, preventing ectopic silencing. PLoS Genet. 2020 Dec;16(12):e1009226.

91. Alvarez F, Muñoz F, Schilcher P, Imhof A, Almouzni G, Loyola A. Sequential establishment of marks on soluble histones H3 and H4. J Biol Chem. 2011 May 20;286(20):17714–21.

92. Li Q, Zhou H, Wurtele H, Davies B, Horazdovsky B, Verreault A, et al. Acetylation of histone H3 lysine 56 regulates replication-coupled nucleosome assembly. Cell. 2008 Jul 25;134(2):244–55.

93. Loyola A, Bonaldi T, Roche D, Imhof A, Almouzni G. PTMs on H3 Variants before Chromatin Assembly Potentiate Their Final Epigenetic State. Mol Cell. 2006 Oct 20;24(2):309–16.

94. Han J, Zhang H, Zhang H, Wang Z, Zhou H, Zhang Z. A Cul4 E3 ubiquitin ligase regulates histone hand-off during nucleosome assembly. Cell. 2013 Nov 7;155(4):817–29.

95. Liu CP, Yu Z, Xiong J, Hu J, Song A, Ding D, et al. Structural insights into histone binding and nucleosome assembly by chromatin assembly factor-1. Science. 2023 Aug 25;381(6660):eadd8673.

96. Sauer PV, Gu Y, Liu WH, Mattiroli F, Panne D, Luger K, et al. Mechanistic insights into histone deposition and nucleosome assembly by the chromatin assembly factor-1. Nucleic Acids Res. 2018 Nov 2;46(19):9907–17.

97. Shibahara K, Stillman B. Replication-dependent marking of DNA by PCNA facilitates CAF-1-coupled inheritance of chromatin. Cell. 1999 Feb 19;96(4):575–85.

98. Zhang K, Gao Y, Li J, Burgess R, Han J, Liang H, et al. A DNA binding winged helix domain in CAF-1 functions with PCNA to stabilize CAF-1 at replication forks. Nucleic Acids Res. 2016 Jun 20;44(11):5083–94.

99. Smith DJ, Whitehouse I. Intrinsic coupling of lagging-strand synthesis to chromatin assembly. Nature. 2012 Mar;483(7390):434–8.

100. Chafin DR, Vitolo JM, Henricksen LA, Bambara RA, Hayes JJ. Human DNA ligase I efficiently seals nicks in nucleosomes. EMBO J. 2000 Oct 16;19(20):5492–501.

101. Huggins CF, Chafin DR, Aoyagi S, Henricksen LA, Bambara RA, Hayes JJ. Flap Endonuclease 1 Efficiently Cleaves Base Excision Repair and DNA Replication Intermediates Assembled into Nucleosomes. Mol Cell. 2002 Nov 1;10(5):1201–11.

102. Devbhandari S, Jiang J, Kumar C, Whitehouse I, Remus D. Chromatin Constrains the Initiation and Elongation of DNA Replication. Mol Cell. 2017 Jan;65(1):131–41.

103. Gali VK, Dickerson D, Katou Y, Fujiki K, Shirahige K, Owen-Hughes T, et al. Identification of Elg1 interaction partners and effects on post-replication chromatin re-formation. PLoS Genet. 2018 Nov;14(11):e1007783.

104. Kaplan N, Moore IK, Fondufe-Mittendorf Y, Gossett AJ, Tillo D, Field Y, et al. The DNA-encoded nucleosome organization of a eukaryotic genome. Nature. 2009 Mar 1;458(7236):362–6.

105. Anderson JD, Lowary PT, Widom J. Effects of histone acetylation on the equilibrium accessibility of nucleosomal DNA target sites. J Mol Biol. 2001 Apr 6;307(4):977–85.

106. Alabert C, Barth TK, Reverón-Gómez N, Sidoli S, Schmidt A, Jensen ON, et al. Two distinct modes for propagation of histone PTMs across the cell cycle. Genes Dev. 2015 Mar 15;29(6):585–90.

107. Alvarez V, Bandau S, Jiang H, Rios-Szwed D, Hukelmann J, Garcia-Wilson E, et al. Proteomic profiling reveals distinct phases to the restoration of chromatin following DNA replication. Cell Rep [Internet]. 2023 Jan 31 [cited 2023 Dec 7];42(1). Available from: https://doi.org/10.1016/j.celrep.2023.111996

108. Reverón-Gómez N, González-Aguilera C, Stewart-Morgan KR, Petryk N, Flury V, Graziano S, et al. Accurate Recycling of Parental Histones Reproduces the Histone Modification Landscape during DNA Replication. Mol Cell. 2018 Oct;72(2):239-249.e5.

109. Sporbert A, Gahl A, Ankerhold R, Leonhardt H, Cardoso MC. DNA polymerase clamp shows little turnover at established replication sites but sequential de novo assembly at adjacent origin clusters. Mol Cell. 2002 Dec;10(6):1355–65.

110. Bhaskara S, Knutson SK, Jiang G, Chandrasekharan MB, Wilson AJ, Zheng S, et al. Hdac3 is essential for the maintenance of chromatin structure and genome stability. Cancer Cell. 2010 Nov 16;18(5):436–47.

111. Rowbotham SP, Barki L, Neves-Costa A, Santos F, Dean W, Hawkes N, et al. Maintenance of silent chromatin through replication requires SWI/SNF-like chromatin remodeler SMARCAD1. Mol Cell. 2011 May 6;42(3):285–96.

112. Mermoud JE, Rowbotham SP, Varga-Weisz PD. Keeping chromatin quiet. Cell Cycle. 2011 Dec 1;10(23):4017–25.

113. Xu B, Zeng D quan, Wu Y, Zheng R, Gu L, Lin X, et al. Tumor suppressor menin represses paired box gene 2 expression via Wilms tumor suppressor protein-polycomb group complex. J Biol Chem. 2011 Apr 22;286(16):13937–44.

114. Muramatsu D, Singh PB, Kimura H, Tachibana M, Shinkai Y. Pericentric heterochromatin generated by HP1 protein interaction-defective histone methyltransferase Suv39h1. J Biol Chem. 2016 Jul 1;291(27):14393.

115. Maison C, Bailly D, Quivy JP, Almouzni G. The methyltransferase Suv39h1 links the SUMO pathway to HP1α marking at pericentric heterochromatin. Nat Commun. 2016 Jul 18;7:12224.

116. Margueron R, Justin N, Ohno K, Sharpe ML, Son J, Drury WJ 3rd, et al. Role of the polycomb protein EED in the propagation of repressive histone marks. Nature. 2009 Oct 8;461(7265):762–7.

117. Cheng L, Zhang X, Wang Y, Gan H, Xu X, Lv X, et al. Chromatin Assembly Factor 1 (CAF-1) facilitates the establishment of facultative heterochromatin during pluripotency exit. Nucleic Acids Res. 2019 Dec 2;47(21):11114–31.

118. Ming X, Zhang Z, Zou Z, Lv C, Dong Q, He Q, et al. Kinetics and mechanisms of mitotic inheritance of DNA methylation and their roles in aging-associated methylome deterioration. Cell Res. 2020 Nov;30(11):980–96.

119. Petryk N, Bultmann S, Bartke T, Defossez PA. Staying true to yourself: mechanisms of DNA methylation maintenance in mammals. Nucleic Acids Res. 2021 Apr 6;49(6):3020–32.

120. Greenberg MVC, Bourc'his D. The diverse roles of DNA methylation in mammalian development and disease. Nat Rev Mol Cell Biol. 2019 Oct;20(10):590–607.

121. Li E, Bestor TH, Jaenisch R. Targeted mutation of the DNA methyltransferase gene results in embryonic lethality. Cell. 1992 Jun 12;69(6):915–26.

122. Zeng Y, Chen T. DNA Methylation Reprogramming during Mammalian Development. Genes. 2019 Mar 29;10(4):257.

123. Wu H, Zhang Y. Reversing DNA methylation: mechanisms, genomics, and biological functions. Cell. 2014 Jan 16;156(1–2):45–68.

124. Wang Q, Yu G, Ming X, Xia W, Xu X, Zhang Y, et al. Imprecise DNMT1 activity coupled with neighbor-guided correction enables robust yet flexible epigenetic inheritance. Nat Genet. 2020 Aug 1;52(8):828–39.

125. Chen T, Ueda Y, Dodge JE, Wang Z, Li E. Establishment and maintenance of genomic methylation patterns in mouse embryonic stem cells by Dnmt3a and Dnmt3b. Mol Cell Biol. 2003 Aug;23(16):5594–605.

126. Bostick M, Kim JK, Estève PO, Clark A, Pradhan S, Jacobsen SE. UHRF1 Plays a Role in Maintaining DNA Methylation in Mammalian Cells. Science. 2007 Sep 21;317(5845):1760–4.

127. Sharif J, Muto M, Takebayashi S ichiro, Suetake I, Iwamatsu A, Endo TA, et al. The SRA protein Np95 mediates epigenetic inheritance by recruiting Dnmt1 to methylated DNA. Nature. 2007 Dec;450(7171):908–12.

128. Berkyurek AC, Suetake I, Arita K, Takeshita K, Nakagawa A, Shirakawa M, et al. The DNA Methyltransferase Dnmt1 Directly Interacts with the SET and RING Finger-associated (SRA) Domain of the Multifunctional Protein Uhrf1 to Facilitate Accession of the Catalytic Center to Hemi-methylated DNA. J Biol Chem. 2014 Jan;289(1):379–86.

129. Li T, Wang L, Du Y, Xie S, Yang X, Lian F, et al. Structural and mechanistic insights into UHRF1-mediated DNMT1 activation in the maintenance DNA methylation. Nucleic Acids Res. 2018 Apr 6;46(6):3218–31.

130. Nishiyama A, Mulholland CB, Bultmann S, Kori S, Endo A, Saeki Y, et al. Two distinct modes of DNMT1 recruitment ensure stable maintenance DNA methylation. Nat Commun. 2020 Mar 6;11(1):1222.

131. Lyons DB, Zilberman D. DDM1 and Lsh remodelers allow methylation of DNA wrapped in nucleosomes. Amasino R, editor. eLife. 2017 Nov 15;6:e30674.

132. Spada F, Haemmer A, Kuch D, Rothbauer U, Schermelleh L, Kremmer E, et al. DNMT1 but not its interaction with the replication machinery is required for maintenance of DNA methylation in human cells. J Cell Biol. 2007 Feb 26;176(5):565–71.

133. González-Magaña A, De Opakua AI, Merino N, Monteiro H, Diercks T, Murciano-Calles J, et al. Double Monoubiquitination Modifies the Molecular Recognition Properties of p15 ^{PAF} Promoting Binding to the Reader Module of Dnmt1. ACS Chem Biol. 2019 Sep 18;acschembio.9b00679.

134. Ferry L, Fournier A, Tsusaka T, Adelmant G, Shimazu T, Matano S, et al. Methylation of DNA Ligase 1 by G9a/GLP Recruits UHRF1 to Replicating DNA and Regulates DNA Methylation. Mol Cell. 2017 Aug;67(4):550-565.e5.

135. Rothbart SB, Krajewski K, Nady N, Tempel W, Xue S, Badeaux AI, et al. Association of UHRF1 with methylated H3K9 directs the maintenance of DNA methylation. Nat Struct Mol Biol. 2012 Nov;19(11):1155–60.

136. Hervouet E, Peixoto P, Delage-Mourroux R, Boyer-Guittaut M, Cartron PF. Specific or not specific recruitment of DNMTs for DNA methylation, an epigenetic dilemma. Clin Epigenetics. 2018 Dec;10(1):17.

137. Easwaran HP, Schermelleh L, Leonhardt H, Cardoso MC. Replication-independent chromatin loading of Dnmt1 during G2 and M phases. EMBO Rep. 2004 Dec;5(12):1181–6.

138. Charlton J, Downing TL, Smith ZD, Gu H, Clement K, Pop R, et al. Global delay in nascent strand DNA methylation. Nat Struct Mol Biol. 2018 Apr;25(4):327–32.

139. Xu C, Corces VG. Nascent DNA methylome mapping reveals inheritance of hemimethylation at CTCF/cohesin sites. Science. 2018 Mar 9;359(6380):1166–70.

140. Sidhu H, Capalash N. UHRF1: The key regulator of epigenetics and molecular target for cancer therapeutics. Tumor Biol. 2017 Feb;39(2):101042831769220.

141. Patnaik D, Estève PO, Pradhan S. Targeting the SET and RING-associated (SRA) domain of ubiquitin-like, PHD and ring finger-containing 1 (UHRF1) for anti-cancer drug development. Oncotarget. 2018 May 25;9(40):26243–58.

142. Tauber M, Fischle W. Conserved linker regions and their regulation determine multiple chromatin-binding modes of UHRF1. Nucleus. 2015 Mar 4;6(2):123–32.

143. Arita K, Isogai S, Oda T, Unoki M, Sugita K, Sekiyama N, et al. Recognition of modification status on a histone H3 tail by linked histone reader modules of the epigenetic regulator UHRF1. Proc Natl Acad Sci. 2012 Aug 7;109(32):12950–5.

144. Nady N, Lemak A, Walker JR, Avvakumov GV, Kareta MS, Achour M, et al. Recognition of Multivalent Histone States Associated with Heterochromatin by UHRF1 Protein. J Biol Chem. 2011 Jul;286(27):24300–11.

145. Rajakumara E, Wang Z, Ma H, Hu L, Chen H, Lin Y, et al. PHD finger recognition of unmodified histone H3R2 links UHRF1 to regulation of euchromatic gene expression. Mol Cell. 2011 Jul 22;43(2):275–84.

146. Kori S, Jimenji T, Ekimoto T, Sato M, Kusano F, Oda T, et al. Serine 298 Phosphorylation in Linker 2 of UHRF1 Regulates Ligand-Binding Property of Its Tandem Tudor Domain. J Mol Biol. 2020 Jun 26;432(14):4061–75.

147. Avvakumov GV, Walker JR, Xue S, Li Y, Duan S, Bronner C, et al. Structural basis for recognition of hemi-methylated DNA by the SRA domain of human UHRF1. Nature. 2008 Oct;455(7214):822–5.

148. Bashtrykov P, Jankevicius G, Jurkowska RZ, Ragozin S, Jeltsch A. The UHRF1 protein stimulates the activity and specificity of the maintenance DNA methyltransferase DNMT1 by an allosteric mechanism. J Biol Chem. 2014 Feb 14;289(7):4106–15.

149. DaRosa PA, Harrison JS, Zelter A, Davis TN, Brzovic P, Kuhlman B, et al. A Bifunctional Role for the UHRF1 UBL Domain in the Control of Hemi-methylated DNA-Dependent Histone Ubiquitylation. Mol Cell. 2018 Nov;72(4):753-765.e6.

150. Foster BM, Stolz P, Mulholland CB, Montoya A, Kramer H, Bultmann S, et al. Critical Role of the UBL Domain in Stimulating the E3 Ubiquitin Ligase Activity of UHRF1 toward Chromatin. Mol Cell. 2018 Nov;72(4):739-752.e9.

151. Xie S, Qian C. The Growing Complexity of UHRF1-Mediated Maintenance DNA Methylation. Genes. 2018 Dec 3;9(12):600.

152. Fang J, Cheng J, Wang J, Zhang Q, Liu M, Gong R, et al. Hemi-methylated DNA opens a closed conformation of UHRF1 to facilitate its histone recognition. Nat Commun. 2016 Apr 5;7(1):11197.

153. Zhang ZM, Rothbart SB, Allison DF, Cai Q, Harrison JS, Li L, et al. An Allosteric Interaction Links USP7 to Deubiquitination and Chromatin Targeting of UHRF1. Cell Rep. 2015 Sep;12(9):1400–6.

154. Gelato KA, Tauber M, Ong MS, Winter S, Hiragami-Hamada K, Sindlinger J, et al. Accessibility of Different Histone H3-Binding Domains of UHRF1 Is Allosterically Regulated by Phosphatidylinositol 5-Phosphate. Mol Cell. 2014 Jun;54(6):905–19.

155. Kori S, Ferry L, Matano S, Jimenji T, Kodera N, Tsusaka T, et al. Structure of the UHRF1 Tandem Tudor Domain Bound to a Methylated Non-histone Protein, LIG1, Reveals Rules for Binding and Regulation. Struct Lond Engl 1993. 2019 Mar 5;27(3):485-496.e7.

156. Zhang H, Gao Q, Tan S, You J, Lyu C, Zhang Y, et al. SET8 prevents excessive DNA methylation by methylation-mediated degradation of UHRF1 and DNMT1. Nucleic Acids Res. 2019 Aug 10;gkz626.

157. Chen H, Ma H, Inuzuka H, Diao J, Lan F, Shi YG, et al. DNA Damage Regulates UHRF1 Stability via the SCF $^{\beta\text{-TrCP}}$ E3 Ligase. Mol Cell Biol. 2013 Mar 1;33(6):1139–48.

158. Peng Y, Liu Y, Zheng R, Ye Y, Fu Y, Yin L, et al. PLK1 maintains DNA methylation and cell viability by regulating phosphorylation-dependent UHRF1 protein stability. Cell Death Discov. 2023 Oct 3;9(1):367.

159. Rigbolt KTG, Prokhorova TA, Akimov V, Henningsen J, Johansen PT, Kratchmarova I, et al. System-wide temporal characterization of the proteome and phosphoproteome of human embryonic stem cell differentiation. Sci Signal. 2011 Mar 15;4(164):rs3.

160. Ma H, Chen H, Guo X, Wang Z, Sowa ME, Zheng L, et al. M phase phosphorylation of the epigenetic regulator UHRF1 regulates its physical association with the deubiquitylase USP7 and stability. Proc Natl Acad Sci. 2012 Mar 27;109(13):4828–33.

161. Chu J, Loughlin EA, Gaur NA, SenBanerjee S, Jacob V, Monson C, et al. UHRF1 phosphorylation by cyclin A2/cyclin-dependent kinase 2 is required for zebrafish embryogenesis. Mol Biol Cell. 2012 Jan 1;23(1):59–70.

162. Hahm JY, Kim JY, Park JW, Kang JY, Kim KB, Kim SR, et al. Methylation of UHRF1 by SET7 is essential for DNA double-strand break repair. Nucleic Acids Res. 2019 Jan 10;47(1):184–96.

163. Zhang H, Liu H, Chen Y, Yang X, Wang P, Liu T, et al. A cell cycle-dependent BRCA1–UHRF1 cascade regulates DNA double-strand break repair pathway choice. Nat Commun. 2016 Jan 5;7(1):10201.

164. Bronner C, Alhosin M, Hamiche A, Mousli M. Coordinated Dialogue between UHRF1 and DNMT1 to Ensure Faithful Inheritance of Methylated DNA Patterns. Genes. 2019 Jan 18;10(1):65.

165. Achour M, Jacq X, Rondé P, Alhosin M, Charlot C, Chataigneau T, et al. The interaction of the SRA domain of ICBP90 with a novel domain of DNMT1 is involved in the regulation of VEGF gene expression. Oncogene. 2008 Apr 1;27(15):2187–97.

166. Song J, Rechkoblit O, Bestor TH, Patel DJ. Structure of DNMT1-DNA complex reveals a role for autoinhibition in maintenance DNA methylation. Science. 2011 Feb 25;331(6020):1036–40.

167. Takeshita K, Suetake I, Yamashita E, Suga M, Narita H, Nakagawa A, et al. Structural insight into maintenance methylation by mouse DNA methyltransferase 1 (Dnmt1). Proc Natl Acad Sci. 2011 May 31;108(22):9055–9.

168. Vann KR, Kutateladze TG. Histone H3 Dual Ubiquitylation Mediates Maintenance DNA Methylation. Mol Cell. 2017 Oct;68(2):261–2.

169. Ishiyama S, Nishiyama A, Saeki Y, Moritsugu K, Morimoto D, Yamaguchi L, et al. Structure of the Dnmt1 Reader Module Complexed with a Unique Two-Mono-Ubiquitin Mark on Histone H3 Reveals the Basis for DNA Methylation Maintenance. Mol Cell. 2017 Oct;68(2):350-360.e7.

170. Ren W, Fan H, Grimm SA, Kim JJ, Li L, Guo Y, et al. DNMT1 reads heterochromatic H4K20me3 to reinforce LINE-1 DNA methylation. Nat Commun. 2021 May 3;12(1):2490.

171. Li J, Wang R, Jin J, Han M, Chen Z, Gao Y, et al. USP7 negatively controls global DNA methylation by attenuating ubiquitinated histone-dependent DNMT1 recruitment. Cell Discov. 2020 Aug 24;6(1):58.

172. De Biasio A, de Opakua AI, Mortuza GB, Molina R, Cordeiro TN, Castillo F, et al. Structure of p15PAF–PCNA complex and implications for clamp sliding during DNA replication and repair. Nat Commun. 2015 Mar 12;6(1):6439.

173. Karg E, Smets M, Ryan J, Forné I, Qin W, Mulholland CB, et al. Ubiquitome Analysis Reveals PCNA-Associated Factor 15 (PAF15) as a Specific Ubiquitination Target of UHRF1 in Embryonic Stem Cells. J Mol Biol. 2017 Dec;429(24):3814–24.

174. Yu C, Gan H, Han J, Zhou ZX, Jia S, Chabes A, et al. Strand-Specific Analysis Shows Protein Binding at Replication Forks and PCNA Unloading from Lagging Strands when Forks Stall. Mol Cell. 2014 Nov 20;56(4):551–63.

175. Felle M, Joppien S, Németh A, Diermeier S, Thalhammer V, Dobner T, et al. The USP7/Dnmt1 complex stimulates the DNA methylation activity of Dnmt1 and regulates the stability of UHRF1. Nucleic Acids Res. 2011 Oct;39(19):8355–65.

176. Cheng J, Yang H, Fang J, Ma L, Gong R, Wang P, et al. Molecular mechanism for USP7-mediated DNMT1 stabilization by acetylation. Nat Commun. 2015 May 11;6(1):7023.

177. Yamaguchi L, Nishiyama A, Misaki T, Johmura Y, Ueda J, Arita K, et al. Usp7-dependent histone H3 deubiquitylation regulates maintenance of DNA methylation. Sci Rep. 2017 Mar 3;7(1):55.

178. Miyashita R, Nishiyama A, Qin W, Chiba Y, Kori S, Kato N, et al. The termination of UHRF1-dependent PAF15 ubiquitin signaling is regulated by USP7 and ATAD5. eLife. 2023 Feb 3;12:e79013.

179. Povlsen LK, Beli P, Wagner SA, Poulsen SL, Sylvestersen KB, Poulsen JW, et al. Systems-wide analysis of ubiquitylation dynamics reveals a key role for PAF15 ubiquitylation in DNA-damage bypass. Nat Cell Biol. 2012 Oct;14(10):1089–98.

180. Mancini M, Magnani E, Macchi F, Bonapace IM. The multi-functionality of UHRF1: epigenome maintenance and preservation of genome integrity. Nucleic Acids Res. 2021 Jun 21;49(11):6053–68.

181. Liang CC, Zhan B, Yoshikawa Y, Haas W, Gygi SP, Cohn MA. UHRF1 is a sensor for DNA interstrand crosslinks and recruits FANCD2 to initiate the Fanconi anemia pathway. Cell Rep. 2015 Mar 31;10(12):1947–56.

182. Motnenko A, Liang CC, Yang D, Lopez-Martinez D, Yoshikawa Y, Zhan B, et al. Identification of UHRF2 as a novel DNA interstrand crosslink sensor protein. PLoS Genet. 2018 Oct;14(10):e1007643.

183. Mistry H, Gibson L, Yun JW, Sarras H, Tamblyn L, McPherson JP. Interplay between Np95 and Eme1 in the DNA damage response. Biochem Biophys Res Commun. 2008 Oct 24;375(3):321–5.

184. Tian Y, Paramasivam M, Ghosal G, Chen D, Shen X, Huang Y, et al. UHRF1 contributes to DNA damage repair as a lesion recognition factor and nuclease scaffold. Cell Rep. 2015 Mar 31;10(12):1957–66.

185. Hahm JY, Kang JY, Park JW, Jung H, Seo SB. Methylated-UHRF1 and PARP1 interaction is critical for homologous recombination. BMB Rep. 2020 Feb;53(2):112–7.

186. Yang C, Wang Y, Zhang F, Sun G, Li C, Jing S, et al. Inhibiting UHRF1 expression enhances radiosensitivity in human esophageal squamous cell carcinoma. Mol Biol Rep. 2013 Sep 1;40(9):5225–35.

187. Liang C, Zhang X, Song S, Tian C, Yin Y, Xing G, et al. Identification of UHRF1/2 as new N-methylpurine DNA glycosylase-interacting proteins. Biochem Biophys Res Commun. 2013 Apr 19;433(4):415–9.

188. Hopfner R, Mousli M, Jeltsch JM, Voulgaris A, Lutz Y, Marin C, et al. ICBP90, a novel human CCAAT binding protein, involved in the regulation of topoisomerase IIalpha expression. Cancer Res. 2000 Jan 1;60(1):121–8.

189. Ashraf W, Ibrahim A, Alhosin M, Zaayter L, Ouararhni K, Papin C, et al. The epigenetic integrator UHRF1: on the road to become a universal biomarker for cancer. Oncotarget. 2017 Aug 1;8(31):51946–62.

190. Jin W, Chen L, Chen Y, Xu S guang, Di G hong, Yin W jin, et al. UHRF1 is associated with epigenetic silencing of BRCA1 in sporadic breast cancer. Breast Cancer Res Treat. 2010 Sep 1;123(2):359–73.

191. Liu W, Qiao R Hong, Wang D Ming, Huang X Wei, Li B, Wang D. UHRF1 promotes human osteosarcoma cell invasion by downregulating the expression of E-cadherin in an Rb1-dependent manner. Mol Med Rep. 2016 Jan 1;13(1):315–20.

192. Jeanblanc M, Mousli M, Hopfner R, Bathami K, Martinet N, Abbady AQ, et al. The retinoblastoma gene and its product are targeted by ICBP90: a key mechanism in the G1/S transition during the cell cycle. Oncogene. 2005 Nov 1;24(49):7337–45.

193. Polepalli S, George SM, Valli Sri Vidya R, Rodrigues GS, Ramachandra L, Chandrashekar R, et al. Role of UHRF1 in malignancy and its function as a therapeutic target for molecular docking towards the SRA domain. Int J Biochem Cell Biol. 2019 Sep;114:105558.

194. Tien AL, Senbanerjee S, Kulkarni A, Mudbhary R, Goudreau B, Ganesan S, et al. UHRF1 depletion causes a G2/M arrest, activation of DNA damage response and apoptosis. Biochem J. 2011 Mar 15;435(1):175–85.

195. Guan D, Factor D, Liu Y, Wang Z, Kao HY. The epigenetic regulator UHRF1 promotes ubiquitination-mediated degradation of the tumor-suppressor protein promyelocytic leukemia protein. Oncogene. 2013 Aug 1;32(33):3819–28.

196. Chen X, Zhou Y li, Liang S yu, Shi Y chuan, Lin S, Shu M qin. Overexpression of UHRF1 promoted the proliferation of vascular smooth cells via the regulation of Geminin protein levels. Biosci Rep. 2019 Feb 26;39(2):BSR20181341.

197. Dai C, Shi D, Gu W. Negative Regulation of the Acetyltransferase TIP60-p53 Interplay by UHRF1 (Ubiquitin-like with PHD and RING Finger Domains 1) *. J Biol Chem. 2013 Jul 5;288(27):19581–92.

198. Ma J, Peng J, Mo R, Ma S, Wang J, Zang L, et al. Ubiquitin E3 ligase UHRF1 regulates p53 ubiquitination and p53-dependent cell apoptosis in clear cell Renal Cell Carcinoma. Biochem Biophys Res Commun. 2015 Aug 14;464(1):147–53.

199. Kim JH, Shim JW, Eum DY, Kim SD, Choi SH, Yang K, et al. Downregulation of UHRF1 increases tumor malignancy by activating the CXCR4/AKT-JNK/IL-6/Snail signaling axis in hepatocellular carcinoma cells. Sci Rep. 2017 Jun 5;7(1):2798.

200. Kim KB, Son HJ, Choi S, Hahm JY, Jung H, Baek HJ, et al. H3K9 methyltransferase G9a negatively regulates UHRF1 transcription during leukemia cell differentiation. Nucleic Acids Res. 2015 Apr 20;43(7):3509–23.

201. Arima Y, Hirota T, Bronner C, Mousli M, Fujiwara T, Niwa S ichiro, et al. Down-regulation of nuclear protein ICBP90 by p53/p21Cip1/WAF1-dependent DNA-damage checkpoint signals contributes to cell cycle arrest at G1/S transition. Genes Cells. 2004 Feb 1;9(2):131–42.

202. Alhosin M, Omran Z, Zamzami MA, Al-Malki AL, Choudhry H, Mousli M, et al. Signalling pathways in UHRF1-dependent regulation of tumor suppressor genes in cancer. J Exp Clin Cancer Res. 2016 Dec;35(1):174.

203. Ding G, Chen P, Zhang H, Huang X, Zang Y, Li J, et al. Regulation of Ubiquitin-like with Plant Homeodomain and RING Finger Domain 1 (UHRF1) Protein Stability by Heat Shock Protein 90 Chaperone Machinery *. J Biol Chem. 2016 Sep 16;291(38):20125–35.

204. Hoogenboom WS, Klein Douwel D, Knipscheer P. Xenopus egg extract: A powerful tool to study genome maintenance mechanisms. Dev Biol. 2017 Aug;428(2):300–9.

205. Gillespie PJ, Gambus A, Blow JJ. Preparation and use of Xenopus egg extracts to study DNA replication and chromatin associated proteins. Methods. 2012 Jun;57(2):203–13.

206. Shintomi K, Inoue F, Watanabe H, Ohsumi K, Ohsugi M, Hirano T. Mitotic chromosome assembly despite nucleosome depletion in *Xenopus* egg extracts. Science. 2017 Jun 23;356(6344):1284–7.

207. Blow JJ, Laskey RA. Initiation of DNA replication in nuclei and purified DNA by a cell-free extract of Xenopus eggs. Cell. 1986 Nov 21;47(4):577–87.

208. Gambus A, Khoudoli GA, Jones RC, Blow JJ. MCM2-7 Form Double Hexamers at Licensed Origins in Xenopus Egg Extract. J Biol Chem. 2011 Apr;286(13):11855–64.

209. Schmid JA, Berti M, Walser F, Raso MC, Schmid F, Krietsch J, et al. Histone Ubiquitination by the DNA Damage Response Is Required for Efficient DNA Replication in Unperturbed S Phase. Mol Cell. 2018 Sep 20;71(6):897-910.e8.

210. Wagner SA, Beli P, Weinert BT, Nielsen ML, Cox J, Mann M, et al. A Proteome-wide, Quantitative Survey of In Vivo Ubiquitylation Sites Reveals Widespread Regulatory Roles *. Mol Cell Proteomics [Internet]. 2011 Oct 1 [cited 2023 Oct 12];10(10). Available from: https://doi.org/10.1074/mcp.M111.013284

211. Abbas T. The Role of Ubiquitination and SUMOylation in DNA Replication. Curr Issues Mol Biol. 2021;40(1):189–220.

212. Oya E, Nakagawa R, Yoshimura Y, Tanaka M, Nishibuchi G, Machida S, et al. H3K14 ubiquitylation promotes H3K9 methylation for heterochromatin assembly. EMBO Rep. 2019 Oct 4;20(10):e48111.

213. Zhang X, Li B, Rezaeian AH, Xu X, Chou PC, Jin G, et al. H3 ubiquitination by NEDD4 regulates H3 acetylation and tumorigenesis. Nat Commun. 2017 Mar 16;8:14799.

214. Brykczynska U, Hisano M, Erkek S, Ramos L, Oakeley EJ, Roloff TC, et al. Repressive and active histone methylation mark distinct promoters in human and mouse spermatozoa. Nat Struct Mol Biol. 2010 Jun;17(6):679–87.

215. Kao HI, Campbell JL, Bambara RA. Dna2p Helicase/Nuclease Is a Tracking Protein, Like FEN1, for Flap Cleavage during Okazaki Fragment Maturation *. J Biol Chem. 2004 Dec 3;279(49):50840–9.

216. Rossi ML, Bambara RA. Reconstituted Okazaki Fragment Processing Indicates Two Pathways of Primer Removal *. J Biol Chem. 2006 Sep 8;281(36):26051–61.

217. Hu L, Li Z, Wang P, Lin Y, Xu Y. Crystal structure of PHD domain of UHRF1 and insights into recognition of unmodified histone H3 arginine residue 2. Cell Res. 2011 Sep;21(9):1374–8.

218. Das-Bradoo S, Nguyen HD, Wood JL, Ricke RM, Haworth JC, Bielinsky AK. Defects in DNA ligase I trigger PCNA ubiquitylation at Lys 107. Nat Cell Biol. 2010 Jan;12(1):74–9; sup pp 1-20.

219. Bradley D, Beltrao P. Evolution of protein kinase substrate recognition at the active site. PLoS Biol. 2019 Jun;17(6):e3000341.

220. Zhang J, Gao Q, Li P, Liu X, Jia Y, Wu W, et al. S phase-dependent interaction with DNMT1 dictates the role of UHRF1 but not UHRF2 in DNA methylation maintenance. Cell Res. 2011 Dec;21(12):1723–39.

221. Elia AEH, Wang DC, Willis NA, Boardman AP, Hajdu I, Adeyemi RO, et al. RFWD3-Dependent Ubiquitination of RPA Regulates Repair at Stalled Replication Forks. Mol Cell. 2015 Oct 15;60(2):280–93.

222. Maréchal A, Li JM, Ji XY, Wu CS, Yazinski SA, Nguyen HD, et al. PRP19 Transforms into a Sensor of RPA-ssDNA after DNA Damage and Drives ATR Activation via a Ubiquitin-Mediated Circuitry. Mol Cell. 2014 Jan 23;53(2):235–46.

223. Hedglin M, Aitha M, Pedley A, Benkovic SJ. Replication protein A dynamically regulates monoubiquitination of proliferating cell nuclear antigen. J Biol Chem. 2019 Mar 29;294(13):5157–68.

224. Liu G, Yan J, Wang X, Chen J, Wang X, Dong Y, et al. RPA-mediated recruitment of Bre1 couples histone H2B ubiquitination to DNA replication and repair. Proc Natl Acad Sci. 2021 Feb 23;118(8):e2017497118.

225. Han J, Li Q, McCullough L, Kettelkamp C, Formosa T, Zhang Z. Ubiquitylation of FACT by the cullin-E3 ligase Rtt101 connects FACT to DNA replication. Genes Dev. 2010 Jul 15;24(14):1485–90.

226. Zhang Y, Zhang Q, Zhang Y, Han J. The Role of Histone Modification in DNA Replication-Coupled Nucleosome Assembly and Cancer. Int J Mol Sci. 2023 Mar 3;24(5):4939.

227. Murawska M, Schauer T, Matsuda A, Wilson MD, Pysik T, Wojcik F, et al. The Chaperone FACT and Histone H2B Ubiquitination Maintain S. pombe Genome Architecture through Genic and Subtelomeric Functions. Mol Cell. 2020 Feb 6;77(3):501-513.e7.

7. APPENDIX

Table A 1. Replisome proteins identified by mass spectrometry from Uhrf1 immunoprecipitation and from chromatin isolated in immunodepleted extracts in the middle of S phase. *TSC: Total Spectral Counts

		IP from chromatin in mid S phase			Chromatin isolated from ID extract in mid S phase		
	Protein (kDa)	IgG	Uhrf1	Fold Change	ΔMock	ΔUhrf1	Fold Change
		TSC (coverage)			TSC (coverage)		
Replisome components	Mcm2 (100)	55 (46%)	353 (58%)	6.4	338 (61%)	279(51%)	0.8
	Mcm3 (90)	14 (12%)	316 (56%)	22.6	260 (57%)	221 (57%)	0.9
	Mcm4 (97)	39 (41%)	278 (56%)	7.1	231 (57%)	199 (52%)	0.9
	Mcm5 (82)	19 (20%)	230 (60%)	12.1	301 (59%)	220 (60%)	0.7
	Mcm6 (93)	43 (34%)	270 (49%)	6.3	233 (50%)	208 (54%)	0.9
	Mcm7 (82)	32 (38%)	227 (58%)	7.1	266 (57%)	184 (61%)	0.7
	Orc1 (100)	0	38 (26%)	-	92 (38%)	72 (32%)	0.8
	Orc2 (63)	0	12 (18%)	-	36 (22%)	20 (21%)	0.6
	Orc3 (81)	0	14 (17%)	-	38 (24%)	29 (16%)	0.8
	Orc4 (49)	0	14 (30%)	-	19 (30%)	16 (26%)	0.8
	Rpa1 (67)	24 (24%)	377 (65%)	15.7	177 (50%)	174 (61%)	1
	Rpa2 (29)	11 (21%)	47 (46%)	4.3	31 (19%)	46 (46%)	1.5
	TopIIα (179)	0	210 (24%)	-	411 (49%)	320 (44%)	0.8
	TopIIβ (177)	-	-	-	91 (15%)	20 (10%)	0.2
	TopIIIα (114)	0	10 (9%)	-	38 (20%)	34 (10%)	0.9
	TopIIIβ (97)	0	26 (22%)	-	0	8 (10%)	-
	Topbp1 (169)	-	-	-	22 (12%)	34 (15%)	1.6
	Chtf18 (113)	-	-	-	32 (22%)	24 (17%)	0.8
	Rfc2 (38)	0	16 (34%)	-	48 (58%)	26 (56%)	0.5
	Rfc3 (40)	0	25 (39%)	-	66 (58%)	35 (53%)	0.5
	Rfc4 (40)	0	11 (24%)	-	48 (45%)	25 (38%)	0.5
	Rfc5 (38)	-	-	-	37 (35%))	17 (38%)	0.5
	Pol α (165)	0	15 (11%)	-	89 (23%)	59 (24%)	0.7
	Pol ε (188)	0	11 (4%)	-	92 (22%)	77 (24%)	0.8
	Lig1 (120)	0	143 (36%)	-	23 (14%)	0	-
	Fen1 (43)	-	-	-	9	0 (17%)	-
	Dna2 (120)	0	12 (9%)	-	3 (2%)	11 (10%)	3.7

Table A 2. DNA methylation related proteins identified by mass spectrometry from Uhrf1 immunoprecipitation and from chromatin isolated in immunodepleted extracts in the middle of S phase. *TSC: Total Spectral Counts

		IP from chromatin in mid S phase			Chromatin isolated from ID extract in mid S phase		
	Protein (kDa)	IgG	Uhrf1	Fold Change	ΔMock	ΔUhrf1	Fold Change
		TSC (coverage)			TSC (coverage)		
DNA methylation	Uhrf1 (87)	29 (19%)	789 (69%)	27.2	35 (16%)	0	-
	Dnmt1 (168)	-	-	-	68 (21%)	0	-
	Usp7 (129)	0	16 (8%)	-	11 (8%)	2 (2%)	0.2
	Lig1 (120)	0	143 (36%)	-	23 (14%)	0	-

Table A 3. Proteins related with nucleosome delivery, assembly and remodelling identified by mass spectrometry from Uhrf1 immunoprecipitation and from chromatin isolated in immunodepleted extracts in the middle of S phase. *TSC: Total Spectral Counts

		IP from chromatin in mid S phase			Chromatin isolated from ID extract in mid S phase		
	Protein (kDa)	IgG	Uhrf1	Fold Change	ΔMock	ΔUhrf1	Fold Change
		TSC (coverage)			TSC (coverage)		
Nucleosome delivery, assembly and remodelling	H2A (15)	7 (28%)	19 (45%)	2.7	41 (53%)	26 (49%)	0.6
	H2B (14)	16 (52%)	45 (64%)	2.8	93 (93%)	59 (76%)	0.6
	H3.2 (15)	-	-	-	117 (74%)	52 (60%)	0.4
	H3.3 (15)	14 (24%)	35 (43%)	2.5	69 (73%)	0	-
	Spt16 (118)	5 (4.7%)	124 (37%)	24.8	141 (47%)	107 (39%)	0.8
	Ssrp1 (79)	0	45 (20%)	-	75 (41%)	62 (27%)	0.8
	Chaf1a-a (101)	-	-	-	11 (7%)	0	-
	Chaf1a-b (100)	-	-	-	10 (7%)	0	-
	Hdac1 (55)	-	-	-	29 (22%)	0	-
	Hdac2 (56)	-	-	-	35 (25%)	17 (13%)	0.5
	Smarca5 (122)	0	164 (38%)	-	282 (62%)	277 (56%)	1
	Smarca2 (183)	-	-	-	24 (9%)	0	-
	Hira (112)	0	31 (15%)	-	83 (23%)	99 (27%)	1.2
	Hells (97)	0	44 (24%)	-	62 (35%)	113 (47%)	1.8
	Hsp90α (83)	0	47 (42%)	-	13 (15%)	26 (31%)	2
	Hsp90β (83)	0	103 (50%)	-	39 (25%)	33 (33%)	0.9
	Hsc70 (71)	0	56 (36%)	-	175 (57%)	157 (56%)	0.9

Table A 4. Proteins related with DNA damage response identified by mass spectrometry from Uhrf1 immunoprecipitation and from chromatin isolated in immunodepleted extracts in the middle of S phase. *TSC: Total Spectral Counts

		IP from chromatin in mid S phase			Chromatin isolated from ID extract in mid S phase		
	Protein (kDa)	IgG	Uhrf1	Fold Change	ΔMock	ΔUhrf1	Fold Change
		TSC (coverage)			TSC (coverage)		
DNA damage response	ATR (301)	0	115 (19%)	-	28 (8%)	55 (15%)	2
	Smarcal1 (107)	0	50 (30%)	-	3 (3%)	18 (12%)	6
	WRN (161)	8 (2%)	203 (30%)	25.4	59 (21%)	99 (30%)	1.7
	Rif1 (257)	0	120 (14%)	-	242 (33%)	333 (31%)	1.4
	Fancd2 (163)	0	13 (6%)	-	57 (18%)	44 (18%)	0.8
	Fancl (43)	0	5 (15%)	-	14 (25%)	5 (15%)	0.4
	Etaa1 (90)	0	3 (2%)	-	2 (3%)	11 (12%)	5.5
	Rad50 (154)	0	22 (9%)	-	19 (8%)	46 (27%)	2.42
	Rad26 (82)	0	4 (4%)	-	0	6 (7%)	-
	Hsp90α (83)	0	47 (42%)	-	13 (15%)	26 (31%)	2

A

sp|P84233|H32_XENLA (100%), 15,388.7 Da
Histone H3.2 OS=Xenopus laevis PE=1 SV=2
9 exclusive unique peptides, 16 exclusive unique spectra, 54 total spectra, 54/136 amino acids (40% coverage)

MARTKQTARK STGGKAPRKQ LATKAARKSA PATGGVKKPH
RYRPGTVALR EIRRYQKSTE LLIRKLPFQR LVREIAQDFK
TDLRFQSSAV MALQEASEAY LVGLFEDTNL CAIHAKRVTI
MPKDIQLARR IRGERA

B

Sequence	Prob
(R)KSTGGKAPR(K)	96%
(R)KQLATK(A)	47%
(R)KQLATKAAR(K)	100%
(R)KQLATKAAR(K)	100%
(R)KQLATKAAR(K)	100%
(R)KQLATKAAR(K)	100%
(R)KQLATKAAR(K)	100%
(R)KQLATKAAR(K)	100%
(R)KQLATKAAR(K)	100%
(R)KQLATKAAR(K)	100%
(R)KQLATKAAR(K)	100%
(R)KQLATKAAR(K)	99%
(R)KQLATKAAR(K)	99%
(R)KQLATKAAR(K)	98%
(R)KQLATKAAR(K)	97%
(R)KQLATKAAR(K)	97%
(R)KQLATKAAR(K)	97%
(R)KQLATKAAR(K)	97%
(R)KQLATKAAR(K)	96%
(R)KQLATKAAR(K)	95%
(R)KQLATKAAR(K)	95%
(R)KQLATKAAR(K)	94%
(R)KQLATKAAR(K)	93%
(R)KQLATKAAR(K)	93%
(R)KQLATKAAR(K)	93%
(R)KQLATKAAR(K)	90%
(R)KQLATKAAR(K)	87%
(K)QLATKAAR(K)	99%
(K)QLATKAAR(K)	99%
(K)QLATKAAR(K)	99%
(K)QLATKAAR(K)	99%
(K)QLATKAAR(K)	99%
(K)QLATKAAR(K)	99%
(K)QLATKAAR(K)	95%
(K)QLATKAAR(K)	94%
(K)QLATKAAR(K)	82%
(K)QLATKAAR(K)	24%
(R)KSAPATGGVK(K)	100%
(R)KSAPATGGVK(K)	100%
(K)SAPATGGVKKPHR(Y)	100%
(K)SAPATGGVKKPHR(Y)	97%
(K)SAPATGGVKKPHR(Y)	31%
(K)SAPATGGVKKPHR(Y)	22%
(R)RYQKSTELLIR(K)	100%
(R)RYQKSTELLIR(K)	100%
(R)YQKSTELLIR(K)	100%
(R)YQKSTELLIR(K)	100%
(R)YQKSTELLIR(K)	100%
(R)YQKSTELLIR(K)	100%
(R)YQKSTELLIR(K)	100%
(R)YQKSTELLIR(K)	100%
(R)EIAQDFKTDLR(F)	97%
(R)EIAQDFKTDLR(F)	79%
(R)EIAQDFKTDLR(F)	47%

Figure A. 1. Peptide sequences identified ubiquitinated (with GG remnant) for Histone H3. A) Sequence of *Xenopus laevis* histone H3, with peptides found ubiquitinated marked in yellow and lysins with GG remnant in green. **B)** Peptides found ubiquitinated on histone H3. Lysins with GG remnant are shown in green.